

Regulatory genetic variation in the Flavin-  
containing monooxygenase 1 gene (*FM01*):  
detection and functional consequences

Matthew Hancock

A dissertation submitted to the Faculty of Life Sciences in partial fulfilment  
of the requirements for the degree of Doctor of Philosophy in the  
University of London.

Department of Structural and Molecular Biology  
University College London

## Abstract

The amount of both *FMO1* mRNA and protein in various human tissues has previously been shown to vary by as much as 10-fold between individuals. This is likely to be caused by genetic variation as the enzyme's expression profile is not affected by exogenous agents.

DNA sequences controlling transcription (promoter regions) have been defined upstream of the three transcriptional start sites P0, P1 and P2 within different cell lines. The use of these promoters has also been defined in various mouse tissues by real-time PCR.

A number of SNPs are present within the three defined *FMO1* promoters in addition to the 3'UTR. Sequencing of individuals from the Corriel repository consisting of individuals from Africa, Asia and Europe has revealed further variation including a CT deletion at the P1 transcriptional start site.

To test the effect of genetic variation high-throughput DNase I capillary footprinting has been used to check for the effect of SNPs on DNA-protein binding. The technique has been shown to detect the effects of mutations on DNA-protein binding but no differences have been seen for *FMO1* SNPs within promoter regions as yet. The technique has the potential to rapidly analyse regulatory polymorphism in a number of genes and the effect in different tissues without the need for cloning or cell culture.

A SNP which introduces an additional in-frame upstream translation initiation codon has been tested in-vitro for its effect on translational efficiency. The upstream ATG variation has been shown to have a 2-fold increase in protein expression over the downstream ATG and therefore individuals with this SNP are likely to produce 2-fold more *FMO1* protein resulting in different effects to drugs.

## Acknowledgements

During my PhD I have had a wonderful experience of Science and the community within it. Therefore, there are many people I wish to acknowledge for the help and support I received. I thank my supervisor Professor Elizabeth Shephard. I could not have asked for a better supervisor in terms of her help and support. I particularly appreciate the help she gave me when first starting in the lab. I had no previous lab experience before undertaking the PhD and she took the time to help me develop my practical work. I also would like to especially thank Dr. Azara Janmohamed for advice and support throughout my PhD.

I would like to thank Dr. Mina Edwards for helping me with cell culture and transfection and especially with difficult to transfect cell lines. I thank Dr. Lyndsey Houseman for helping me with experiments during the first year of my PhD. I thank all the members past and present in Lab 402 for making it a really pleasant place to work, especially to Sandra Gonzalez-Malagon who has been a great friend throughout my time at the lab.

I thank the members of my thesis committee, Professor Dallas Swallow and Dr. Kate Bowers for very constructive meetings and comments. I thank Dr. Neil Bradman for part-funding of my BBSRC-case studentship. I thank Prof. Ian Phillips for interesting and developing discussions.

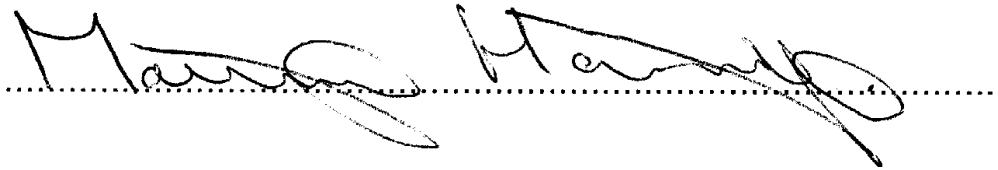
Within the department I would like to thank the members of Professor Jeremy Brockes lab for the help and support I received, especially Mr. Phil Gates for advice

in cloning and molecular biology, Dr. James Godwin for advice in developing my project, and Dr. Robert Blassberg for developing the RT-PCR strategy. I also thank all the members of the Brockes lab for creating a fantastic social environment in which to discuss science.

Lastly, I would like to thank my family who, although are not scientists, have really understood the stresses and strains of PhD life. I recommend Devon as an excellent escape from PhD life! I also thank my partner Dr. Zanna Briscoe for supporting me throughout this work. Without her help and support I do not think this could have been achieved.

I, Matthew Andrew Hancock confirm that the work presented in this thesis is my own.

Where information has been derived from other sources, I confirm that it has been indicated in the thesis.

A handwritten signature in black ink, appearing to read "Matthew Hancock", is written over a horizontal dotted line. The signature is fluid and cursive, with the first name "Matthew" and the last name "Hancock" clearly distinguishable.

## Contents

<b>Chapter 1 : Introduction .....</b>	<b>16</b>
1.1 Xenobiotic metabolism .....	16
1.2 Flavin-containing monooxygenases, background.....	16
1.3 FMO catalytic cycle and substrates .....	18
1.4 The Flavin-containing monooxygenase family.....	23
1.4.1 Human FMO chromosomal locations.....	28
1.5 Contribution of FMOs to xenobiotic metabolism.....	29
1.6 <i>FMO1</i> chemical regulation.....	33
1.7 Mechanisms of gene regulation.....	33
1.8 Chromosomal localisation and structure of the human and mouse <i>FMO1</i> genes...37	
1.9 <i>FMO1</i> expression .....	40
1.10 Alternatively spliced, non-coding exons and their function.....	43
1.11 <i>FMO1</i> Genetic Variation.....	45
1.11.1 Protein coding region variation .....	45
1.11.2 Untranslated mRNA Variants.....	49
1.11.3 Promoter Variants .....	49
1.12 <i>FMO1</i> in drug metabolism .....	51
1.13 <i>FMO1</i> and disease .....	54
1.14 Expression Profiles.....	54
1.15 How Regulatory polymorphisms and polymorphism influencing splicing cause changes in gene expression.....	59
1.16 Regulatory polymorphism and splice-site polymorphism observed in drug metabolizing enzyme genes.....	62
1.17 Methods of identifying and analysing regulatory polymorphism.....	64
1.18 Illumina second-generation sequencing and its application for regulatory polymorphism .....	68
1.19 Polymorphism effecting translation efficiency.....	70
1.20 3T3-L1 adipocytes and their use as a model for adipocyte biology .....	72
<b>1.21: Aims of this study .....</b>	<b>75</b>
<b>Chapter 2 : Materials and Methods .....</b>	<b>78</b>
2.1 <i>Escherichia coli</i> ( <i>E. coli</i> ) strains and culture conditions.....	78
2.1.1 Genotypes of <i>E. coli</i> strains .....	78
2.1.2 Culture of <i>E. coli</i> cells .....	78
2.2 Small scale isolation of plasmid DNA from <i>E. Coli</i> .....	79

2.3 Large-scale isolation of plasmid DNA from <i>E. Coli</i> .....	80
2.4 Quantification of DNA/RNA by UV spectrophotometry .....	82
2.5 Bacterial Transformation.....	82
2.6 Preparation of glycerol stocks .....	83
2.7 Restriction endonuclease digestion of DNA .....	84
2.8 Agarose gel electrophoresis of DNA fragments .....	85
2.9 Purification of DNA fragments from agarose gels.....	86
2.9.1 Purification of DNA in solution .....	87
2.10 DNA ligation .....	87
2.11 Polymerase chain reaction (PCR) .....	88
2.11.1 Bio-X-act DNA polymerase.....	91
2.12 Reverse transcriptase polymerase chain reaction .....	92
2.13 TOPO T/A cloning .....	93
2.14 Isolation of RNA from cells, mouse and human tissues.....	95
2.14.1 Tissue preparation .....	95
2.14.2 RNA isolation from tissue cultured cells.....	95
2.15 COS-7 AND 3T3-L1 cell culture .....	97
2.15.1 HK-2 cell culture.....	97
2.16 Transient transfection of cells.....	98
2.17 Isolation of Nuclear proteins from cell lines.....	99
2.18 Dual-luciferase® reporter assay and pGL3 vectors .....	100
2.19 RNA Transfection .....	103
2.20 Reporter constructs used for transfection studies.....	103
2.20.1 FMO1 promoter reporter constructs .....	103
2.20.2 FMO1 P2 leader sequence construct.....	104
2.21 Protein concentration determination .....	108
2.22 Protein Gel Electrophoresis (SDS/PAGE) .....	109
2.23 Electrophoretic Mobility Shift assay .....	110
2.24 Real-time PCR .....	112
2.24.1 Calculation of relative amounts of FMO1 transcripts within and between tissues .....	115
2.25 3T3-L1 differentiation.....	116
2.26 3T3-L1 adipocyte nucleofection.....	117
2.27 <i>In-vitro</i> RNA production .....	118
2.28 Phusion® site-directed mutagenesis .....	119
2.28.1 <i>FMO1</i> promoter mutation constructs .....	120
2.29 DNA sequencing.....	121

2.29.1 PCR for sequencing .....	122
2.29.2 Sequencing reaction .....	123
2.29.3 Cleaning the sequencing reaction.....	123
2.29.4 Phase haplotype reconstruction .....	124
2.30 DNase I capillary footprinting.....	124
2.30.1 Labelling DNA.....	124
2.30.2 Binding reaction .....	124
2.30.3 DNase I digestion .....	125
2.30.4 Capillary electrophoresis and data analysis.....	126
2.30.5 Dye terminator sequencing.....	126
2.31 Software Packages .....	127
<b>Chapter 3 : Profiling of <i>Fmo1</i> gene expression in mouse tissues and cell-lines...</b>	<b>130</b>
3.1 Quantification of the expression of <i>Fmo1</i> in different mouse tissues by real-time PCR.....	132
3.1.1 Selection of reference genes to normalise <i>FMO1</i> expression.....	132
3.1.2 Quantification of the <i>FMO1</i> global transcript in different mouse tissues.....	136
3.1.3 Quantification in different mouse tissues of the P0, P1 and P2 <i>FMO1</i> mRNA transcripts.....	138
3.1.4 The relative expression of the P0, P1 and P2 transcripts combined to that of the global expression of <i>FMO1</i> mRNA.....	138
3.2 Expression of <i>Fmo1</i> in 3T3-L1 cells undergoing differentiation to adipocytes....	143
3.2.1 <i>Fmo1</i> expression during differentiation of the EACC™, 3T3-L1 mouse fibroblast cell line.....	143
3.2.2 <i>Fmo1</i> expression during differentiation of the ATCC™ 3T3-L1 cell line .....	147
3.2.3 <i>Fmo1</i> P0, P1 and P2 transcript expression during 3T3-L1 differentiation....	151
3.2.4 <i>Fmo1</i> global expression during differentiation of the ATCC™. 3T3-L1 mouse fibroblast cell line.....	151
<b>Chapter 4 : Characterisation of different <i>FMO1</i> promoters .....</b>	<b>157</b>
4.1 Definition of human <i>FMO1</i> promoters in COS-7, HK-2, and 3T3-L1 cells .....	158
4.1.1 Reporter gene assay controls .....	158
4.1.2 Optimisation of transfection for COS-7, HK-2 and 3T3-L1 cell lines .....	160
4.1.3 COS-7 cell transfection .....	163
4.1.4 Ratio of <i>FMO1</i> promoter usage in COS-7 cells .....	163
4.1.5 Transfection of HK-2 cells with <i>FMO1</i> promoter constructs.....	166
4.1.6 Ratio of <i>FMO1</i> promoter usage in HK-2 cells.....	167
4.1.7 <i>FMO1</i> promoter usage in 3T3-L1 fibroblast cells .....	169
4.1.8 Ratio of <i>FMO1</i> promoter usage in 3T3-L1 cells.....	169



4.2 Transfection using nucleofection of 3T3-L1 differentiated into adipocytes .....	172
4.3 The <i>FMO1</i> P2 promoter region and prediction of transcription factor binding...	176
4.4 The defined P1 promoter region and potential protein binding sites .....	179
4.5 Epigenetic analysis of the human <i>FMO1</i> promoters.....	182
4.5.1 DNase I hypersensitive regions (HRs) located within and surrounding the <i>FMO1</i> gene (Fig4.10) .....	182
4.5.2 DNase I Hypersensitivity regions in different tissues surrounding the P1 and P2 promoters .....	185
4.5.3 The CTCF insulator binds upstream of the P0 promoter and may play a role in <i>FMO1</i> repression within the human liver .....	187
4.5.4 Chip-seq experiments identifying transcription factor binding within P0, P1 and P2 promoters.....	190
4.6 <i>FMO1</i> P2 promoter mutations and their influence on promoter activity .....	194
4.6.1 Mutations in the <i>FMO1</i> P1 promoter .....	194
4.6.2 A mutation introduced into the <i>FMO1</i> P2 promoter reduces reporter gene activity .....	195
4.6.3 Loss of protein binding due to a mutation within the GC box protein binding region of the P2 promoter is detected by a gel shift assay.....	198
4.7 The significance of a polymorphism, -11C>T, which potentially reduces the translational efficiency of the <i>FMO1</i> protein.....	200

<b>Chapter 5 : Dideoxy sequence analysis of the human <i>FMO1</i> P0, P1, and P2 promoters .....</b>	<b>207</b>
5.1 Experimental design: Number of individuals and regions to be sequenced.....	208
5.2 Identification of novel polymorphism within the <i>FMO1</i> P1 and P2 promoter regions.....	211
5.3 Confirmation of the -515G>A and -503C>T SNPs and genotyping in CEU, YRI and JPT/HAN populations .....	212
5.4 Construction and analysis of <i>FMO1</i> P1, P2 haplotypes in CEU, YRI and JPT/HAN populations.....	217
5.5 Construction and analysis of <i>FMO1</i> P0 haplotypes in CEU, YRI and JPT/HAN populations.....	222

<b>Chapter 6 : Optimisation and development of capillary DNase I footprinting for the detection of regulatory polymorphisms that alter DNA-protein binding events .....</b>	<b>228</b>
6.1 Labelling and detection of DNA fragments for capillary DNase I footprinting.....	229
6.2 Footprinting analysis of the Simian Virus 40 promoter (SV40) .....	230
6.2.1 Optimisation of the SV40 promoter nuclear protein binding reaction .....	233
6.2.2 DNase I digestion .....	233

6.2.3 Increasing the binding competitor does not affect the DNA-protein binding profile of the promoter .....	237
6.2.4 Increasing DNA amount increases the FAM signal and DNA-Protein binding is less specific .....	237
6.2.5 Confirmation of DNA-protein binding events .....	238
6.2.6 Analysis of digested DNA fragments .....	242
6.3 Dye terminator sequencing reactions to determine location of DNA-protein binding.....	244
6.4 Description of the SV40 DNA-protein binding profile.....	244
6.5 Normalisation of signal intensity to the LIZ marker .....	247
6.6 Footprinting analysis of the novel FMO1 P1 and P2 promoters .....	248
6.6.1 P1 Promoter.....	248
6.6.2 The <i>FMO1</i> P2 promoter footprint analysis.....	250
6.7 Loss of protein binding at the P2 promoter was visualised by DNase I capillary footprinting and therefore validates this technique for screening regulatory polymorphism <i>via</i> this method.....	252

## List of figures

### Chapter 1: Introduction

Figure 1.1 Catalytic cycle of FMOs.....	20
Figure 1.2 The predicted FAD and NADPH binding sites of mammalian FMOs .....	27
Figure 1.3 Illustration of methods of gene regulation within the cell.....	36
Figure 1.4 The 5' <i>FMO1</i> gene region of (A) human and (B) mouse.....	38
Figure 1.5. The <i>FMO1</i> gene and the location of protein coding SNPs .....	48
Figure 1.6 Mechanisms that result in differences in protein expression between individuals .....	61
Figure 1.7 Illustration of the morphological and gene regulatory changes that occur during 3T3-L1 adipocyte differentiation.....	74

### Chapter 2: Materials and methods

Figure 2.1 pCR®4-TOPO vector map (Invitrogen catalogue).....	94
Figure 2.2 Maps of pGL3 vectors and the pRL vector .....	106
Figure 2.3 Cloning of the FMO1 P2 leader sequence into the pSP-luc+NF fusion vector .....	107

### Chapter 3 : Profiling of *Fmo1* gene expression in mouse tissues and cell-lines

Figure 3.1 Selection of suitable reference genes for the normalisation of <i>Fmo1</i> expression in different mouse tissues .....	135
Figure 3.2 Global <i>Fmo1</i> expression in different mouse tissues.....	137
Figure 3.3 Relative gene expression of <i>Fmo1</i> mouse transcripts within different mouse tissues.....	139
Figure 3.4 Comparison of the total relative expression of the <i>Fmo1</i> P0, P1, and P2 transcripts with the relative expression of the <i>Fmo1</i> global transcript.....	142

Figure 3.5 Images of (A) EACC™ 3T3-L1 fibroblasts and (B) differentiated EACC™ 3T3-L1 adipocytes.....	145
Figure 3.6 <i>Fmo1</i> and adipocyte markers, LPL, FABP, and PPAR- $\gamma$ expression in 3T3-L1 (EACC™ cell line) pre-adipocyte and mature adipocytes.....	146
Figure 3.7 Comparison of the EACC 3T3-L1 differentiated cell line with the ATCC™ 3T3-L1 differentiated cell line .....	149
Figure 3.8 Expression profiling of (A) <i>FMO1</i> , (B) LPL (C) PPAR- $\gamma$ (D) FABP mRNAs during 3T3-L1 differentiation.....	150
Figure 3.9 Quantification of <i>Fmo1</i> global gene expression during 3T3-L1 differentiation (ATCC) .....	153

#### **Chapter 4 : Characterisation of different *FMO1* promoters**

Figure 4.1 Illustration of the sequences upstream of each of the <i>FMO1</i> transcriptional start sites cloned within the pGL3-Basic plasmid .....	159
Figure 4.2 Determination of DNA/LIPID ratios for optimal transfection of (A) COS-7 and (B) HK-2 cells.....	162
Figure 4.3 Reporter gene activity of PGL3-Basic constructs containing DNA sequences upstream of the three <i>FMO1</i> transcriptional start sites transfected into COS-7 cells... ..	165
Figure 4.4 Reporter gene activity of PGL3-Basic constructs containing DNA sequences upstream of the three <i>FMO1</i> transcriptional start sites transfected in HK-2 cells.....	168
Figure 4.5 Reporter gene activity of PGL3-Basic constructs containing DNA sequences upstream of the three <i>FMO1</i> transcriptional start sites transfected in 3T3-L1 cells .....	171
Figure 4.6 GFP Nucleofection of 3T3-L1 adipocytes .....	173
Figure 4.7 Illustration of human <i>FMO1</i> promoters defined by reporter gene assays ....	175
Figure 4.8 Annotation of P2 promoter.....	178
Figure 4.9 Annotation of P1 promoter.....	181
Figure 4.10 Genome wide DNase I chromatin assays outlining DNase I sensitive sites upstream of the <i>FMO1</i> P0, P1 and P2 promoter. ....	184
Figure 4.11 Illustration of DNase I hypersensitivity sites within the defined <i>FMO1</i> P1 and P2 promoter regions .....	186
Figure 4.12 Schematic representation of CTCF binding upstream and downstream of the P0 promoter, as well as DNase I hypersensitive sites within human tissues.....	189
Figure 4.13 Illustration of transcription factor binding within the <i>FMO1</i> P1 and P2 promoter regions .....	192
Figure 4.14 Schematic representation of transcription factors that bind to the P0 promoter .....	193
Figure 4.15 Illustration of mutations introduced to the P2 promoter reporter gene construct and the natural variations occurring within the P1 promoter .....	196
Figure 4.16 Reporter gene activity of the pGL3-255_128 P2 promoter construct and the pGL3-255_128* GC box mutant within COS-7 cells .....	197
Figure 4.17 Gel shift assay showing loss of protein binding at the <i>FMO1</i> P2 promoter due to a mutation within the GC binding box .....	199
Figure 4.18 Reporter gene activities of RNA produced from the pSP-ATG/ATG and the pSP-ACG/ATG vectors .....	202

#### **Chapter 5 : Dideoxy sequence analysis of the human *FMO1* P0, P1, and P2 promoters**

Figure 5.1 Location of primers used to amplify DNA from individuals for subsequent dideoxy sequence analysis .....	210
--	-----

Figure 5.2 The frequency of alleles and genotypes within (A) the <i>FMO1</i> P1 and P2 promoter and (B) the <i>FMO1</i> P0 promoter.....	214
Figure 5.3 Illustration of the HapMap consortium genotyped SNPs within the <i>FMO1</i> P1 and P2 promoter region.....	216
Figure 5.4 Predicted haplotype frequencies of the <i>FMO1</i> P1 and P2 promoter regions in different populations.....	220
Figure 5.5 (A) Illustration of the polymorphisms that reside within the P1 and P2 promoter regions of <i>FMO1</i> and (B) the high frequency haplotypes within the populations analysed.....	221

## **Chapter 6 : Optimisation and development of capillary DNase I footprinting for the detection of regulatory polymorphisms that alter DNA-protein binding events**

Figure 6.1 Annotation of the SV40 promoter sequence and PCR FAM labelling of the sequence.....	232
Figure 6.2 0.005U of DNase I is optimal to produce an evenly size-distributed set of DNA fragments.....	236
Figure 6.3 Increasing the amount of competitor DNA does not affect the DNase I footprinting trace of the SV40 promoter.....	239
Figure 6.4 Capillary DNase I footprinting of the SV40 promoter with increased amounts of SV40 DNA template.....	240
Figure 6.5 Treatment of DNA-protein binding reaction with proteinase K removes DNase I footprints within the SV40 promoter.....	241
Figure 6.6 The chromatograms above show the DNase I digested fragments from the 5'FAM labelled SV40 promoter after incubation with COS-7 nuclear protein extract...	243
Figure 6.7 Illustration of a section of the SV40 footprinted promoter aligned with dye-terminated sequencing reactions.....	246
Figure 6.8 DNase I footprinting of the human <i>FMO1</i> P1 promoter using COS-7 nuclear extract.....	249
Figure 6.9 DNase I footprinting of the human <i>FMO1</i> P2 promoter using COS-7 nuclear extract.....	251
Figure 6.10 Detection of the loss of DNA-protein binding within the <i>FMO1</i> P2 promoter.....	253

## **List of tables**

Table 1.1 Xenobiotic Metabolism.....	17
Table 1.2 Examples of some <i>FMO1</i> substrates and their sites of oxidation.....	22
Table 1.3 Expression levels of <i>FMO1</i> mRNA or protein measured in different human tissues.....	42
Table 1.4 Drugs metabolized by <i>FMO1</i> .....	53
Table 1.5 Geoprofile data which show an increase in <i>Fmo1</i> expression.....	57
Table 1.6 Geoprofiles which show a decrease in human <i>FMO1</i> or mouse <i>Fmo1</i> expression.....	58
Table 2.1 PCR cycling conditions.....	90
Table 2.2 PCR cycling used for quantitative real time PCR.....	114
Table 2.3 PCR cycling conditions for site-directed mutagenesis.....	121
Table 2.4 Amplification parameters used for dye-terminator sequencing reactions....	127

## Abbreviations

ABI	Applied Biosystems
ALS	amyotrophic lateral sclerosis
amp	Ampicillin
AP1	activator protein 1
bp	base pairs
BSA	bovine serum albumin
C/EBP	CC/AAT enhancer binding protein
CANX	Calnexin
CAT	Catalase
cDNA	complementary DNA
Chip-seq	chromatin immunoprecipitation
CYPs	cytochrome P450s
dATP	deoxyadenosine triphosphate
DMEs	drug-metabolizing enzymes
DNA	deoxyribonucleic acid
DNase I	deoxyribonuclease I
DTT	Dithiothreitol
ECACC	European Collection of Animal Cell Culture
EDTA	ethylene diaminetetracetate
EGTA	ethylene glycol-bis ( $\beta$ -aminoethyl ether)- N,N,N' tetraacetate
EIF1AX	eukaryotic translation initiation factor 1A, X-linked
EMSA	electrophoretic mobility shift assay
ENCODE	The Encyclopedia of DNA Elements
ESE	exon splicing enhancer
EST	expression sequence tag
EtBr	ethidium bromide
FAD	flavin adenine dinucleotide
FAIRE-seq	formaldehyde-Assisted Isolation of Regulatory Elements
FMO	flavin-containing monooxygenase
GAPDH	glyceraldehyde 3-phosphate dehydrogenase
HBG1	hemoglobin subunit gamma-1
HEPES	N-2-hydroxyethyl piperazine N'-2-ethanesulphonic acid
HiDi	highly deionized
HNF1 $\alpha$	hepatocyte Nuclear Factor 1
HNF4 $\alpha$	hepatocyte Nuclear Factor 4
hr	Hour
HRs	hypersensitive regions
IGF2	insulin-like growth factor 2
Kb	Kilobase
KDa	kilo Daltons
LB	Luria Bertani
LD	linkage disequilibrium
LEF1	lymphoid enhancer-binding factor 1
LPL	lipoprotein lipase

MI	myocardial infarction
MPP+	1-methyl-4-phenylpyridine
MPTP	1-methyl-4-phenyl-1,2,3,6-tetrahydropyridine
NAPDH	nicotinamide adenine dinucleotide phosphate
NF-Y	nuclear transcription factor Y
NP-40	nonidet P40
NRG1	neuregulin 1
nt	Nucleotide
ORFs	open reading frame
OTX2	orthodenticle homeobox 2
PAGE	polyacrylamide gel electrophoresis
PBS	phosphate buffered saline
PCR	polymerase chain reaction
PGC1- $\alpha$	peroxisome proliferator-activated receptor gamma coactivator 1
RACE	rapid amplification of cDNA clones
RLU	relative light units
RNA	ribonucleic acid
RNase	Ribonuclease
ROS	reactive-oxygen species
RT-PCR	real-time PCR
SDS	sodium dodecyl sulphate
SNP	single nucleotide polymorphism
SOLiD	Supported Oligo Ligation Detection
SORT1	Sortilin
SV40	Simian virus 40
TBE	tris-Borate EDTA
TE	tris-EDTA
TEMED	N,N,N',N'-Tetramethylethylenediamine
UCSC	University of California Santa Cruz
UTR	untranslated region
UV	Ultraviolet
YY1	yin yang 1

# **Chapter 1**

## **Introduction**

# **Chapter 1: Introduction**

## **1.1 Xenobiotic metabolism**

Xenobiotics are chemicals that are taken up by the body from exogenous sources. These chemicals are usually lipophilic and therefore chemical modifications are required to facilitate their removal from the body. Drug metabolising enzymes (DMEs) modify xenobiotics by bio-transformation. These bio-transformations convert the xenobiotics into inactive, more polar and more readily excretable metabolites.

Xenobiotic metabolism is divided into two phases; phase I and phase II reactions (Table 1.1). Phase I reactions bio-transform the xenobiotic in preparation for downstream phase II reactions by either unmasking or creating a functional group. Phase II enzymes conjugate the metabolite produced from the phase I reaction with a more polar chemical of endogenous origin.

Phase I reactions can be separated into three pathways. Two of these pathways function to unmask existing functional groups by either the use of hydrolytic or reductive enzymes. The third pathway consists of oxidising enzymes, which add a new functional group on to the xenobiotic. It is this group of enzymes to which the Flavin-containing monooxygenases (FMOs) belong.

## **1.2 Flavin-containing monooxygenases, background**

The flavin-containing monooxygenases (FMOs) are the second largest family of phase-1 drug-metabolizing enzymes (DMEs). The enzymes are membrane-bound



Phase I enzymes	Phase II enzymes
1. Hydrolytic enzymes	1. UDP-glucuronyl transferases
a) Amidases	2. Glutathione transferases
b) Esterases	3. Glycine N-acetyl transferases
c) Epoxide hydrolases	4. Sulfotransferases
2. Reductive enzymes	5. Acetyl CoA transferases
a) Azo reductases	
b) Disulfide reductase	
c) Aldo-keto reductases	
d) Nitro reductases	
e) Reductive dehalogenation	
3. Oxidative enzymes	
<b>a) Flavin-containing monooxygenases</b>	
b) Amine oxidases	
c) Alcohol and aldehyde dehydrogenases	
d) Cytochrome P450 monooxygenases	

### Table 1.1 Xenobiotic Metabolism

The table shows drug metabolising enzymes from the two phases of metabolism. Modified from Schenkman et al 1999.

and are located within the endoplasmic reticulum with relative molecular masses of between 59-63 kDa. The FMOs all contain a flavin-adenine dinucleotide (FAD) group and are able to catalyze, in the presence of NADPH, the oxidation of a wide range of foreign chemicals including therapeutic drugs, dietary-derived compounds and pesticides (Cashman and Zhang, 2006; Krueger and Williams, 2005; Ziegler, 1993). The xenobiotic being metabolized is said to be mono-oxygenated by the FMO enzyme as only one atom of molecular oxygen is inserted into the molecule within the xenobiotic (for reviews on this process see Ziegler, 1990; Hines et al., 1994; Phillips et al., 1995). FMO activity was first discovered in 1964 (Pettit et al., 1964) and an FMO protein was first purified in 1972 (Ziegler and Mitchell, 1972). The FMO protein was initially named after the person who isolated it, Daniel Ziegler, and was known as "Ziegler's enzyme". FMO activity has been observed and tested in human, rabbit, mouse, rat, dog, sheep and guinea pig. A prokaryotic equivalent of FMO, the cyclohexanone monooxygenase from *Acinetobacter* exists. This is described as an FMO due to its mechanistic similarities (Ryerson et al., 1982). The homology between mammalian and the prokaryotic form is only 25% (Donoghue et al., 1976). FMO-like proteins have also been observed in plants within the *Arabidopsis* species (Zhao et al., 2001). Some evidence suggests an FMO role in resistance to microbial pathogens within *Arabidopsis* (Koch et al., 2006). As the products of FMO metabolism are generally less toxic or pharmacologically active than the parent compound these proteins play an important role in detoxification.

### **1.3 FMO catalytic cycle and substrates**

The FMO catalytic cycle is unique to this family of enzymes. The cycle is based on kinetic and spectral studies with FMO protein purified from pig liver (Poulsen et al.,

1979; Beate and Ballou, 1980; Beate and Ballou, 1981). The cycle is described below.

FMOs contain a flavin adenine dinucleotide (FAD) as their prosthetic group. The FAD prosthetic group is reduced by NADPH and  $H^+$ . It is this reduced form that reacts with molecular oxygen creating a peroxyflavin intermediate defined as 4 $\alpha$ -hydroperoxyflavin (FAD-OOH) (see Fig.1.1 for catalytic cycle). This stable intermediate is capable of oxygenating any compound able to enter the active site of the FMO. This is due to the energy required for the reaction already present within the enzyme before contact with the substrate. Therefore the precise fit usually required to lower the activation energy of the reaction is not required. This is a novel characteristic for a monooxygenase enzyme (including the major DME family, the cytochrome P450s) because the substrate does not need to bind to the enzyme to activate it (Ziegler, 1993). Compounds gaining access to the active site of FMOs are generally restricted to those compounds containing a soft nucleophile. The site of FMO oxidation occurs within the electron-rich centre of the nucleophile, which is usually nitrogen, sulphur, or phosphorous heteroatom. Boron and iodide are also substrates of FMOs (Jones and Ballou, 1986). Substrates include dietary metabolites, medicinal drugs, toxins, pesticides and selenium-containing compounds.

There are many endogenous biochemicals that contain soft nucleophiles. It is thought that these chemicals are protected from FMO oxidation due to the number and position of charged groups on nucleophiles within these molecules (Taylor and

Ziegler, 1987). FMOs are able to oxidise monocationic amines or anionic sulphur compounds where the charge is localised to the sulphur atom. However, if there is

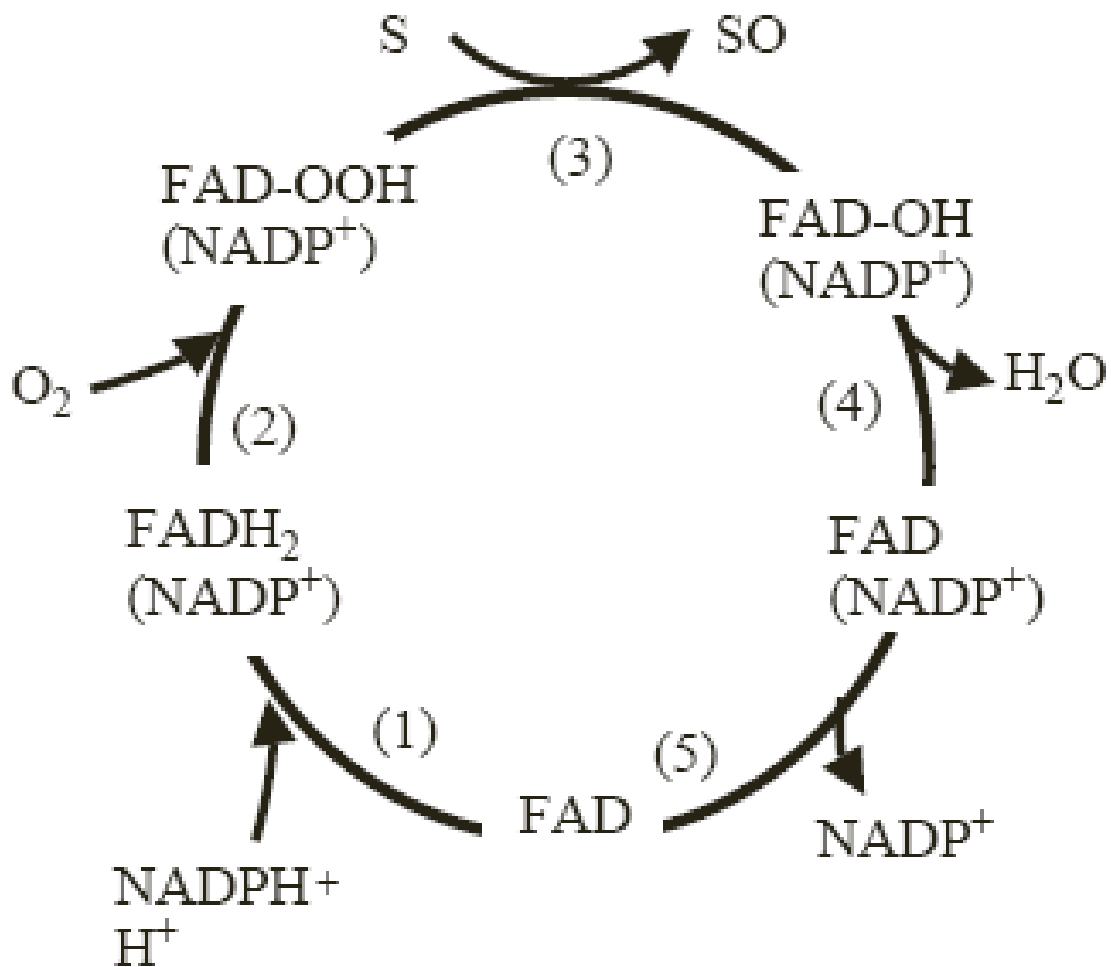


### Figure 1.1 Catalytic cycle of FMOs

NADPH reduces the flavin group, FAD, to FADH<sub>2</sub> (1). Oxygen binds to the reduced enzyme and an internal electron transfer generates the 4 $\alpha$ -hydroperoxyflavin form of the enzyme. (2) It is in this state that the substrate contacts FMO1. One atom of oxygen is attached to the substrate to form SO and one atom to form water and the product is released immediately (3). H<sub>2</sub>O and NADP<sup>+</sup> are released (4 and 5). The enzyme is then once again available for the generation of the 4 $\alpha$ -hydroperoxyflavin form of the enzyme (Krueger and Williams, 2005).

an additional charged group within the molecule the FMO enzyme does not metabolize it. All essential nucleophiles are dications (polyamines), dipolar ions (amino acids) or have one or more anionic groups distal to an electron-rich heteroatom (e.g. biotin). An exception to this is cysteamine which has been observed as a substrate for FMOs (Duffel et al., 1987). It is for this reason outlined that cellular nucleophiles are not substrates, and FMOs are able to discriminate between essential and xenobiotic soft nucleophiles.

There are a few known endogenous substrates of FMO1. As mentioned previously cysteamine can be converted to the disulphide cysteamine by pig liver FMO (Duffel et al., 1987) and the yeast FMO (Suh and Robertus, 2000). As yet, only two other endogenous substrates have been identified, cysteine S-conjugates (Elfarra, 1995; Krause et al., 2003) and methionine (Duescher et al., 1994; Krause et al., 1996). Both of these are converted to sulphoxides by FMOs. The  $K_M$  for methionine sulphoxidation (Elfarra, 1995) suggests that this reaction is only significant when toxic levels of methionine are present in the diet or in the event of a defect in methionine metabolism (Regina et al., 1993). Table 1.2 lists some of the known substrates for FMO1, the isoform that is the subject of this thesis.

Compound	Site of oxidation	Type of compound	Reference
MPTP	N	Neurotoxin	(Cashman and Ziegler, 1986)
Nicotine	N	Stimulant	(Park et al., 1993)
Cimetidine	S	Gastric ulcer drug	(Cashman et al., 1995)
Thiobenzamide	S	Hepatotoxicant	(Hodgson, 1999b)
Phorate	S	Pesticide	(Hodgson, 1999b)
Ranitidine	N/S	Gastric/ duodenum ulcer drug	(Chung et al., 2000)
Tamoxifen	N	Anti-cancer drug	(Hodgson et al., 2000)
Amphetamine	N	Behaviour stimulant	(Cashman et al., 1999)
Trimethylamine	N	Dietary derived amine	(Lang et al., 1998)
Maclobemide	N	Monoamine oxidase inhibitor (antidepressant)	(Hoskins et al., 2001)
Imipramine	N	Tricyclic antidepressant	(Narimatsu et al., 1999)
Clozapine	N	Tricyclic antidepressant	(Tugnait et al., 1997)
Brompheniramine	N	Antihistamine	(Cashman et al., 1993)
Albendazole	S	Tapeworm infection drug	(Fargetton et al., 1986)
Fonofos	P	Pesticide	(Venkatesh et al., 1991)
Methimazole	S	Anti-thyroid drug	(Kedderis and Rickert, 1985)

**Table 1.2 Examples of some FMO1 substrates and their sites of oxidation**

The first column is the compound metabolized by FMO1. The next column shows the atom that is oxygenated within the molecule by FMO, the third column shows the type of compound the FMO substrate is.

## 1.4 The Flavin-containing monooxygenase family

As mentioned previously, FMO activity was first identified in pig liver in 1964. Subsequently, FMO was identified within liver (Kimura et al., 1983), lung, and kidney of rat, mouse (Sabourin et al., 1984), rabbit (Tynes et al., 1985), guinea pig (Yamada et al., 1990), dog (Lattard et al., 2002) and sheep (Williams et al., 1989; Longin-Sauvageon et al., 1998). Characterization of FMO protein preparations suggested multiple forms of FMOs. The rate of dimethylaniline *N*-oxidation, a reaction carried out by the FMO enzyme, was shown to be effected differently within different tissues. The addition of  $\text{Hg}^{2+}$  and  $\text{Mg}^{2+}$  ions increased the rate of reaction using purified FMO from rabbit lung but decreased the rate of reaction when purified FMO was used from rabbit liver (Devereux et al., 1977). Further characterisation of the rabbit lung and liver FMO forms revealed that they are immunologically and catalytically distinct (Williams et al., 1984). It was later discovered that these proteins were products of two distinct genes.

Molecular biology techniques were used to isolate FMO cDNAs from various species by a number of different research groups. As a result of sequence analysis it was clear that the FMOs could be divided into 5 distinct groups. These groups corresponded to the different FMO isoforms. These isoforms were named FMO1, FMO2, FMO3, FMO4 and FMO5 (Lawton et al., 1994). Pig liver FMO was renamed FMO1 and the rabbit lung isoform was named FMO2. Each isoform is encoded by a different gene.

The FMOs have been well characterised within mice as mouse is an important model organism for toxicological studies. A mouse liver cDNA library was screened with the rabbit FMO3 cDNA as the probe. As a result the mouse FMO3 cDNA was isolated (Falls et al., 1997). The purified FMO3 protein has a molecular weight of 58 kDa (534 amino acids) and has 82% sequence homology with human FMO3. The mouse FMO2 cDNA was obtained from an expressed sequence tag (EST) from the IMAGE consortium (Karoly and Rose, 2001). This cDNA was also expressed within *E. coli* and encodes a protein of 61 kDa (535 amino acids) in size and shows 86% sequence homology with human FMO2. The mouse FMO1 and FMO5 cDNAs were isolated by screening a mouse liver library with rabbit cDNA sequences as probes (Cherrington et al., 1998b). Analysis of the cDNA sequences revealed the FMO1 mouse protein to have a molecular weight of 59.9 kDa and was 532 amino acids in length. It shares an 83.8% sequence similarity with human FMO1. The FMO5 protein has a molecular weight of 60 kDa and was 533 amino acids in length. It shares an 84.1% sequence similarity with human FMO5.

The human FMO1 cDNA was isolated using a pig FMO1 cDNA probe and revealed that the human protein is 532 amino acids in length (Dolphin et al., 1991). The human FMO4 cDNA was also isolated by the same research group using the newly isolated FMO1 cDNA as a probe (Dolphin et al., 1992). The paper describes the now classified FMO4 gene as the FMO2 gene. The genes were renamed at a later date, with numbers being given in order of the isolation of the purified proteins (Lawton et al., 1994). The isolated cDNA



encodes an FMO4 protein of 558 amino acids (Dolphin et al., 1992). The human *FMO3* gene was isolated using three synthetic 36-mer oligonucleotide probes which were designed from the pig FMO1 nucleic acid sequence. Analysis of the FMO3 cDNA sequence revealed a protein length of 533 amino acids (Dolphin et al., 1996). The human FMO2 cDNA was isolated from a human lung cDNA library using a PCR product from the rabbit FMO2 cDNA (Dolphin et al., 1998). The identified FMO2 protein was shown to contain a premature stop codon and contains 64 fewer amino acids compared to the orthologues of other mammals (Dolphin et al., 1998). When the human FMO2 protein was heterologously expressed, the protein produced was inactive. This premature stop codon has been shown not to occur in some African and Hispanic populations (Dolphin et al., 1998; Veeramah et al., 2008). About 28% of individuals of African descent carry at least one copy of the functional gene (Dolphin et al., 1998, Veeramah et al., 2008). The human FMO5 cDNA was isolated using the rabbit FMO5 cDNA. The cDNA encodes a protein of 533 amino acids (Overby et al., 1995).

Once isolated, the FMO cDNA clones of the different FMO isoforms were expressed heterologously in *E. coli*, yeast or in *Sf9* insect cells. This allowed the substrate for each isoform to be studied. There is a substantial amount of data comparing substrate specificity of rabbit lung FMO2 and the pig lung FMO1. It has been shown that FMO2 can oxygenate long aliphatic primary amines (e.g. n-octylamine) but the FMO1 enzyme cannot (Poulsen et al., 1986)(Nagata et al., 1990). The FMO1 enzyme metabolizes short side chain tertiary amines (e.g. imipramine) but the FMO2 enzyme does not.

Comparative studies have compared different mouse FMOs using different pesticide substrates. This study revealed specific and common substrates between the isoforms (Hodgson, 1999a). For example, the pesticide phorate is the preferred substrate of FMO1 and the pesticide fonofos is a substrate for FMO5 (Hodgson, 1999a). Methimazole, a drug used in the treatment of hyperthyroidism is oxidised by the FMO isoforms at different efficiencies (Itagaki et al., 1996). The  $K_M$  value for the oxidation of methimazole by FMO5 is very high compared to other isoforms.

The five functional FMOs share 51-57% amino acid sequence homology and >80% similarity exists between the orthologous mammalian isoforms. The conserved functional domains within the protein sequence include two GXGXXG motifs which are proposed to be binding sites for FAD (amino acids 9-14) and NADP (amino acids 191-206) (Fig.1.2). These domains are present in the five functional FMOs. The three glycine residues in the proposed FAD binding site were mutated independently in the rat FMO1 protein. The mutant proteins were expressed within yeast. This experiment revealed that all three glycines are required for a catalytically active FMO (Kubo et al., 1997).

The FAD binding site is within a fingerprint sequence which predicts a  $\beta\alpha\beta$  secondary structure known as a Rossman fold. This fingerprint sequence is predicted to be involved in the binding of di-nucleotides (Wierenga, 1985). A hydrophobic motif is conserved through the functional FMOs (F (A/T) TGY) centred around residue 330. The conservation of these residues is illustrated within Fig. 1.2. As yet no mammalian structure exists for any of the functional FMOs. However a structure exists for the yeast *Schizosaccharomyces pombe*

		FAD-binding domain		NADPH-binding domain		
FMO1	Rat liver <sup>20)</sup>	4	RVAIVGAGVSGLASIK	19	186 RVLVVMGNSGTDIIV	201
	Mouse liver <sup>a)</sup>	4	RVAIVGAGVSGLASIK	19	186 RVLVVMGNSGTDIIV	201
	Rabbit liver <sup>13, 43)</sup>	4	RVAIVGAGVSGLASIK	19	186 RVLVIGMNSGTDIIV	201
	Human liver <sup>14)</sup>	4	RVAIVGAGVSGLASIK	19	186 RVLVVMGNSGTDIIV	201
	Pig liver <sup>12)</sup>	4	RVAIVGSGVSGLASIK	19	186 SVLVVMGNSGTDIIV	201
FMO2	Rabbit lung <sup>13)</sup>	4	KVAIVGAGVSGGLISLK	19	186 RILVIGIGNSASDIIV	201
	Guinea pig lung <sup>18)</sup>	4	KVAIVGAGVSGGLISLK	19	186 RILVIGIGNSASDIIV	201
FMO3	Rabbit liver <sup>21, 44)</sup>	4	KVAIVGAGVSGGLASIA	19	186 RVLVIGLNSGEDIIV	201
	Human liver <sup>16, 17)</sup>	4	KVAIVGAGVSGGLASIR	19	186 RVLVIGLNSGEDIIV	201
FMO4	Human liver <sup>15)</sup>	4	KVAIVGAGVSGGLSSIK	19	186 RVLVIGLNTGGDIIV	201
	Rabbit liver <sup>21)</sup>	4	KVAIVGAGVSGGLTSIK	19	186 RVLVIGLNSGGDIIV	201
FMO5	Rabbit liver <sup>19)</sup>	5	RVAVIGAGVSGGLACIK	20	187 RVIVIGIGNSGGLAAV	202
Consensus sequence			GxGxxG		GxGxxG/A	

**Figure 1.2 The predicted FAD and NADPH binding sites of mammalian FMOs**

These sites are conserved and are found at a similar position in all known mammalian FMOs (reproduced from Kubo et al., 1997).

(Eswaramoorthy et al., 2006). This FMO is cytosolic and lacks an extra 85 residues from the mammalian FMOs at the C-terminus. It is thought this protein plays a role in regulating the thiol/disulfide ratios in the cell (Suh et al., 1999). Deletion of the enzyme within yeast reduces proper folding of endogenous carboxypeptidase Y by about 40%.

### **1.4.1 Human FMO chromosomal locations**

*FMO1- FMO4* genes were localised to a cluster spread out over a region of 245kb along the long arm of chromosome 1(1q24.3) (Shephard et al., 1993)(Phillips et al., 1995). *FMO5* was mapped closer to the centromere in the region 1q21 (McCombie et al., 1996). The order and position of the *FMO* genes were determined experimentally which was in agreement with the order determined by the human genome project. An additional gene was identified from the human genome project data and named *FMO6P* (<http://www.sanger.ac.uk/UGP/Chr1/>). Later Hines et al showed that *FMO6P* probably encodes a pseudogene as full-length transcripts were not identified (Hines et al., 2002). A second cluster of 5 *FMO* genes was identified from the human genome data (<http://www.sanger.ac.uk/UGP/Chr1/>) but all have shown to be pseudogenes (*FMO7P-FMO11P*) (Hernandez et al., 2004).

The five functional FMOs, through phylogenetic analysis, have been shown to have evolved around 210-275 million years ago through several gene duplications of an ancestral gene (Hernandez et al., 2004). This pre-dates the evolution of mammals and therefore it is predicted that all mammals possess the five functional FMOs.

An endogenous role for FMOs has yet to be fully determined, however, a few endogenous substrates exist as discussed earlier. Two mouse knockout lines recently developed by our laboratory, (*Fmo1* (-/-), *Fmo2* (-/-), *Fmo4* (-/-) and *Fmo5* (-/-), show evidence for a role for FMOs in energy homeostasis. The *Fmo1* (-/-), *Fmo2* (-/-), *Fmo4* (-/-) mice are as healthy as their age matched wild-types but have a significantly lower weight (Veeravalli et al., 2010). Histology of white adipose tissue has also shown reduced storage of fat (Veeravalli et al., 2010). This is a consequence of enhanced whole-body energy expenditure, due mostly to increased resting energy expenditure, attributed, partly, to increased fatty acid  $\beta$ -oxidation in skeletal muscle. The knockout mice have an increased capacity for exercise, with no evidence for an increase in adaptive thermogenesis (Veeravalli et al., 2010).

### **1.5 Contribution of FMOs to xenobiotic metabolism**

Before the discovery of the FMO family of drug-metabolising enzymes, oxygen and NADPH-dependent microsomal oxidations were attributed to the cytochrome P450 (CYP) family of monooxygenases. This is the largest family of drug metabolizing enzymes in humans containing over 50 isoforms (Danielson, 2002). Like the FMOs the CYPs catalyse the oxidation of xenobiotics and chemicals. In addition endogenous roles have been defined for many of the CYP enzymes, e.g. the metabolism of steroids (Danielson, 2002). There exists an overlap between some FMO and cytochrome P450 substrates. There are a number of substrates that can be oxidised by both the FMOs and cytochrome P450s. For example, within the mouse liver thioridizane which is an anti-psychotic drug is oxidised at two sulphur atoms

by CYP or oxidised at a nitrogen atom by FMO (Blake et al., 1995).

Tamoxifen, an estrogen receptor inhibitor, used in the treatment of mammary cancer has shown to be metabolized to its *N*-oxide form by FMOs and is metabolized to other metabolites by CYP (Mani et al., 1993).

There are cases where both CYPs and FMOs monooxygenate a substrate to produce the same product. Thiobenzamide, which is a liver toxicant, is oxygenated by both families and the contribution ratio of this compound was 1:1 to 1:4 in the mouse liver and 1:2 in the rat liver and 2:3 in the rat lung (Tynes and Hodgson, 1983).

The relative contribution of each family to the metabolism of a substrate can be determined by selectively inhibiting the activity of either FMOs or CYPs. There are no known chemical inhibitors for FMOs, but their activity can be knocked down by heating, whereas CYPs are more thermally stable (Cashman, 2008; Shephard and Phillips, 2010). There are several CYP inhibitors but all microsomal CYP activity can be inhibited by knocking out the activity of NADPH-dependent cytochrome P450 reductase with an antibody to this protein. FMO activity can be inferred by monitoring activity in the presence and absence of the FMO substrate methimazole (Kedderis and Rickert, 1985).

MPTP is metabolized in the mitochondria by monoamine oxidase type B. One of the products of this reaction is a neurotoxin, the MPP<sup>+</sup> (1-methyl-4-phenylpyridinium) ion. MPP<sup>+</sup> induces the degeneration of dopaminergic

neurons and causes Parkinson's disease-like symptoms in humans and monkeys (Langston and Irwin, 1986)(Tipton and Singer, 1993). MPTP is detoxified in the liver by MPTP *N*-oxide, by FMOs (Tipton and Singer, 1993) and to 4-phenyl-1, 2, 3, 6 tetrahydropyridine (PTP) by CYPs (Weissman et al., 1985). Before the MPTP drug was administered, mice were treated with an FMO substrate. This caused an increased level of MPP<sup>+</sup> in the mouse brain (Chiba et al., 1988) and a reduction of dopamine in the brain (Chiba et al., 1990). This suggests FMOs play an important role in MPTP detoxification.

MPTP metabolism has been studied with the house musk shrew due to the low level of FMO1 expression within this model organism (Mushiroda et al., 2000b). In contrast the house musk shrew contains a high expression of CYP enzymes. Brain homogenates from rat and *Suncus* were both able to produce the MPP<sup>+</sup> toxin. However, only the MPTP *N*-oxide was detected within rat brain homogenates. Interestingly the administration of MPTP results in the accumulation of MPP<sup>+</sup> toxins within the *Suncus* brain and not in the rat brain (Mushiroda et al., 2001). It is hypothesised that FMO expression in the small microvessels of the rat brain allows the detoxification of the MPTP toxin, preventing its entry to the brain by its conversion to the *N*-oxide.

An FMO and CYP substrate called Ranitidine is a drug used to treat gastric ulcers and Zollinger Ellison Syndrome (Zeldis et al., 1983). The drug can be metabolized to its *N*- or *S*-oxide or to desmethylrantidine. By competitively inhibiting FMOs with methimazole it was shown that FMOs are responsible for 93% of the *N*- or *S* oxidations (Zeldis et al., 1983). By using a specific CYP

inhibitor, SKF525A, it was shown that CYPs are responsible for all of the desmethylations (Zeldis et al., 1983).

FMOs exclusively carry out the *N*-oxidation of the dietary derived tertiary amine trimethylamine (TMA) (Lang et al., 1998). An inability to process this compound results in the disorder trimethylaminuria (Humbert et al., 1970).

Recently mice lacking FMOs have shown adverse effects to the drug imipramine. An *Fmo1* (-/-), *Fmo2* (-/-), *Fmo4* (-/-) mouse line was produced by using chromosomal engineering and Cre-loxP technology (Hernandez et al., 2009). Imipramine has four major metabolites, three produced by cytochromes P450 and one, imipramine *N*-oxide, solely by FMO1. When treated with imipramine, wild-type mice became sedated and produced imipramine *N*-oxide in the brain and other tissues. In contrast, knockout mice did not produce imipramine *N*-oxide, but showed exaggerated pharmacological behavioural responses, such as tremor and body spasm, and had a higher concentration of the parent compound imipramine in the serum and kidney and there was an increase in desipramine in the brain (Hernandez et al., 2009). The absence of FMO1-mediated *N*-oxidation of imipramine shows enhanced central nervous system effects of the drug.



## **1.6 FMO1 chemical regulation**

It was shown by Ziegler et al. that the short amine n-octylamine can increase the rate of oxidation of dimethylaniline by pig FMO1 (Ziegler et al., 1971). However, n-octylamine is not a substrate for FMO1 (Nagata et al., 1990). It was proposed that FMO possesses distinct catalytic and regulatory sites (Ziegler et al., 1971).

Indole-3-carbinol is a breakdown product of glucobrassicin which is a component of cruciferous vegetables (McDanell et al., 1988). The compound has been shown to inhibit the expression of the FMO1 protein by 75-90% in the rat liver (Katchamart et al., 2000). This compound is not however able to inhibit FMO1 expression within the guinea pig, mouse and the rabbit (Katchamart and Williams, 2001). The effect of nitric oxide on FMO1 was investigated within the rat. FMO1 mRNA levels were decreased to 33% of control levels when nitric oxide was over produced in the rat liver (Park et al., 1999). Within rat also, the FMO1 protein was shown to be induced by a polycyclic aromatic hydrocarbon, 3-methylcholanthrene (3MC). FMO1 mRNA level was induced by 3.5 fold and the catalytic activity was induced by 2.9 fold by 3MC (Chung et al., 1997).

## **1.7 Mechanisms of gene regulation**

The regulation of human gene expression is a highly coordinated, complex and critical process. Gene regulation determines the biological variability seen between different cell types, different developmental states, and

environmental reactions. A region of DNA crucial for gene expression is the promoter region. In protein-coding genes these regions are located upstream of the transcriptional start site. They consist of a core promoter where the RNA polymerase II and its co-factors bind forming the pre-initiation complex. This sequence is usually about 50 bp in size. The further sequence upstream is defined as the extended promoter region. Transcription factors will bind within these regions. This region is where factors may bind which allow temporal and spatial transcription of the gene. These factors interact with the RNA initiation complex to enhance or reduce the amount of transcription. This region semantically can be defined as the promoter, however regulatory sequence which affects transcription have been shown to occur megabases away from the transcriptional start site or occur downstream of the transcriptional start site and in general are defined as enhancers. Enhancers can be affected by further binding factors called insulators which bind between the enhancer and the promoter preventing their interaction. Insulators can prevent the binding of enhancers to neighbouring genes or to the native loci.

Epigenetics plays a large role in the regulation of genes. Epigenetics describes the modifications to the DNA in structure and chemistry. Methylation and acetylation of DNA, can switch genes on and off by preventing the binding of a regulatory factor or preventing that region of DNA to be structurally modified to allow regulatory factors to bind. For example the IGF2 gene is regulated differentially depending on the methylation state of an insulator (Sasaki et al., 2000). Insulators can act differently depending on

which parental allele is inherited through a phenomenon known as genomic imprinting. Due to methylation of the DNA the insulator is no longer able to bind. The paternal IGF2 allele is methylated and prevents the binding of the insulating factor CTCF whereas the mother's IGF2 allele is unmethylated and the CTCF factor can bind. This results in only the paternal allele being active (Giannoukakis et al., 1993).

A project was begun in 2004, as a collective effort of many laboratories, to identify the functional elements in 1% of the human genome (The ENCODE Project Consortium 2004). Transcriptional start sites and promoter regions were predicted for the 900 genes found within this resource. Promoter sequences were cloned into a reporter plasmid and tested for their ability to drive transcription within the environment of 16 different cell lines. Using correlative data comparing RNA expression and promoter activity, the contribution of the promoter to overall transcriptional activity was predicted for the 900 genes. It is predicted from the data that promoter regions defined as between -300 to -50 upstream of the transcriptional start site contributes to 28% of the variability seen in RNA expression (Cooper et al., 2006). This shows that the promoter region plays an important role in overall expression of the gene but also that enhancer elements outside of this region contribute to RNA expression. Extended sequence of up to 1000 bp of the transcriptional start sites were tested for 45 genes. These extended regions were shown to contain negative regulatory elements in 55% of the genes studied (Cooper et al., 2006). Fig.1.3 summarises different regulatory elements that interact with the core promoter.

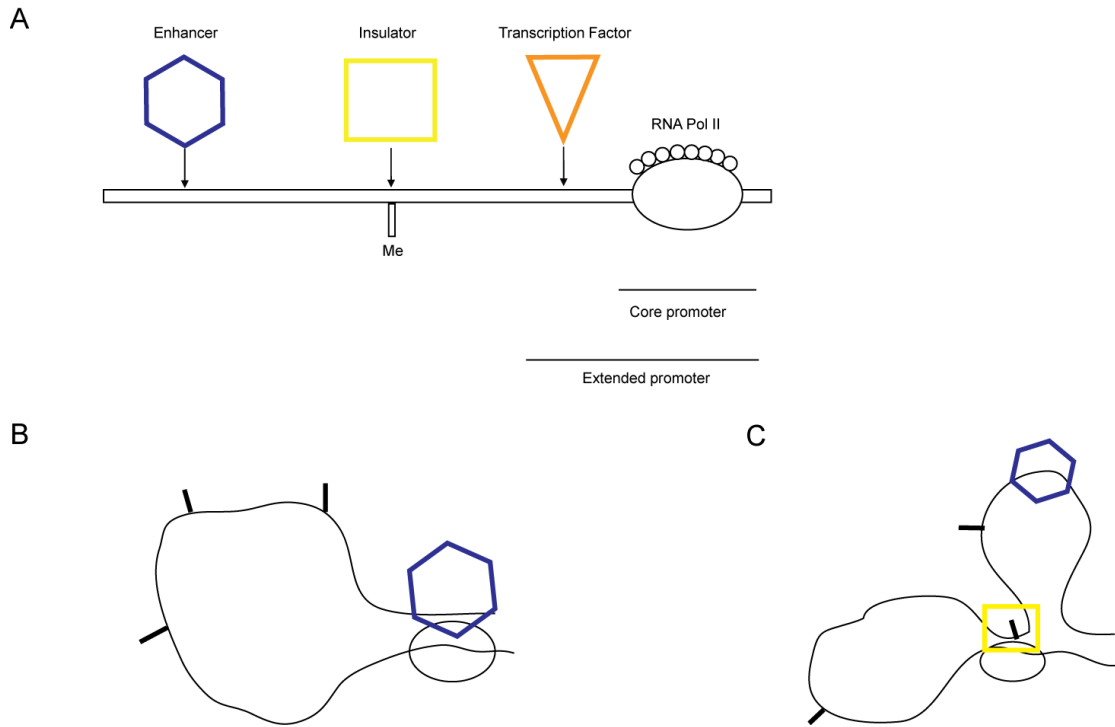


**Figure 1.3 Illustration of methods of gene regulation within the cell**

**(A)** Different types of regulatory factors illustrated positionally to the binding of RNA polymerase II and cofactors. RNA pol II and cofactors represent the core promoter. Upstream of this region, further transcription factor binding sites are present within a region defined as the extended promoter. Upstream of the promoter, further regulatory factors are present which enhance or reduce transcriptional activity. Insulators can bind to prevent the effect of enhancers.

**(B)** Illustration of how enhancers might activate transcription and **(C)** the ability of insulators to block enhancer activity. The black bars represent alterations in the methylation state of the DNA altering DNA structure and allowing insulator binding.

## 1.8 Chromosomal localisation and structure of the human and mouse *FMO1* genes

The human *FMO1* gene is 37.5 kb long and the mouse *Fmo1* gene is 37.5 kb and in both species the gene has 8 coding exons (2-9) and 2 non-coding exons (0 and 1). Translation initiation occurs within exon 2 at a weak Kozak consensus sequence. Transcription starts at promoter sites located within intron 1, or upstream of exons 0 or 1. The choice of promoter is tissue-specific. In the human, it has been discovered that transcription only begins in the foetal liver from the beginning of exon 0 from a promoter designated P0 (Shephard et al., 2007), and the mRNA is produced by a splicing event from exon 0 to exon 2 (Fig.1.4) (Hernandez et al., 2004). In the kidney, transcription also begins from P0 and the kidney mRNA is also spliced in the same way (Fig.1.4). In addition to this promoter, in the kidney the *FMO1* mRNA is transcribed from a promoter designated P2, located just upstream of exon 2 in an intronic sequence (see Fig.1.4) (Shephard et al., 2007). A cDNA that encodes a full-length protein has been found that has a transcriptional start site at the beginning of exon 1. This cDNA was found in the human small intestine (accession no. AK097039). The method of oligo-capping was used to isolate the cDNA. The P1 transcript is therefore predicted to be full length (Ota et al., 2004). This promoter has been designated P1 (see Fig.1.4). The mRNA is formed by a splicing event from the sequences derived from exon 1 to exon 2 (see Fig.1.4). Alternative promoters in the *FMO1* gene do not result in variations in protein sequence as exon 0 and 1 are non-coding exons.

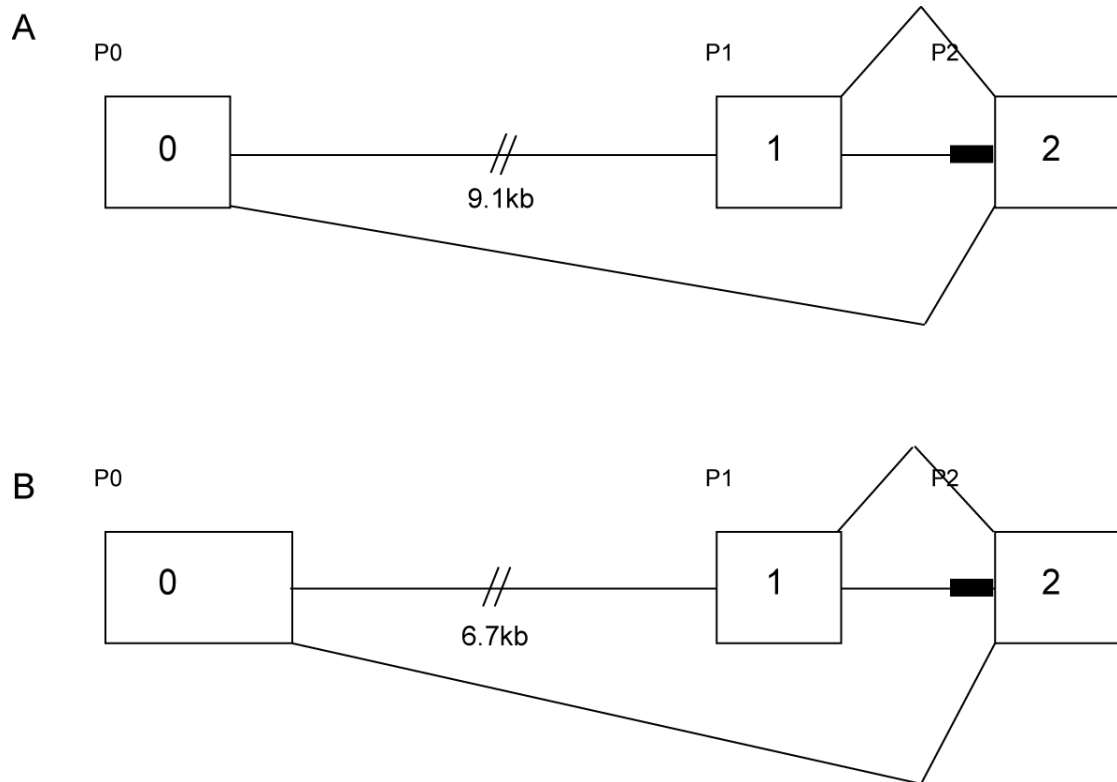


**Figure 1.4 The 5'*FMO1* gene region of (A) human and (B) mouse**  
 The illustrations show the two non-coding exons 0 and 1 that are present in both mouse and human. The translation of the *FMO1* protein occurs within and near the start of exon 2. The human and mouse both produce transcripts from the start of the non-coding exon 0 and 1. These transcripts are spliced as shown in the illustration. The P0 transcript is spliced from exon 0 to exon 2. The P1 transcript is spliced from exon 1 to exon 2. A third transcript which starts intronically from exon 2, defined as P2, has been observed in both human and mouse. Each of the transcriptional start sites are depicted in the above figure by P0, P1 or P2.

Inter-individual variation in the amount of FMO1 protein has been shown to be high. Within the foetal liver, variation is between 10-20 fold depending on gestational age (Koukouritaki et al., 2002). In the kidney, variation has been reported to be less than 4-fold (Krause et al., 2003), or less than 5-fold (Hamman et al., 2000). In the small intestine variation has been reported to be up to 5-fold (Yeung et al., 2000). As *FMO1* is rarely inducible by exogenous agents it is highly likely these variations in amount of protein are manifested by genetic polymorphism. By locating these polymorphisms, the function and impact of this enzyme in humans for drug metabolism can be assessed.

Analysis of available mouse liver cDNA clones found within the NCBI database identified (D16215, BC011229, BF532824, AI115B9, AA245076, AI255718, AA238774 and BI247068) show different lengths of cDNA, but each contain exon 0. Therefore all the cDNAs isolated from the liver are the P0 transcript. There are five available kidney cDNA clones. Three of these cDNA clones have 5'UTR sequences derived from the 3'-end of intron 1 and exon 2. RT-PCR and sequence analysis of the amplified products confirmed that, in kidney, transcription can occur from within intron 1, from a promoter designated P2 (Shephard et al., 2007). Two other cDNA clones, AI118998 and CB955318 are the products of a splicing event between exon 2 and a novel exon 1. Figure 4 show the production of the alternatively spliced transcripts seen in mouse and human.

## 1.9 FMO1 expression

In 1971 Daniel Ziegler isolated and identified a novel mixed-function oxidase which metabolized nitrogen- and sulphur- containing compounds. The enzyme is therefore sometimes referred to as Ziegler's enzyme (Ziegler et al., 1971). As described above, a cDNA for the mixed function oxidase was isolated in 1991 (Dolphin et al., 1991) and was mapped to the long arm of chromosome 1 (Shephard et al., 1993) which encodes a protein with 532 amino acid residues and a molecular weight of 60 Kda. The protein was classified as FMO1 in 1993 (Lawton et al., 1994). In the human foetal liver *FMO1* is expressed but is switched off shortly after birth and is not expressed in the adult (Koukouritaki et al., 2002). Currently it is not known what causes the silencing of the *FMO1* gene in human adult liver. There is evidence from transfection studies of HepG2 cells that repetitive elements specific to the human just upstream of the liver core promoter repress transcription from P0 in the foetal liver (Shephard et al., 2007). It is thought that continuation of expression in adult extra-hepatic tissues can be explained by the use of the alternative promoters found for kidney and small intestine. Table 1.3 summarises the amounts of FMO1 RNA or protein detected in different tissues.

*FMO1* is also expressed in mouse and rabbit foetal liver (Dolphin et al., 1996). The expression of *FMO1* in the foetus suggests a possible role for FMO1 in the metabolism of xenobiotics that the foetus is exposed to via the placenta. The FMO1 enzyme may also have an endogenous role within the foetus.



In all other mammals including mouse, rat, dog, pig and rabbit, *FMO1* remains expressed in the adult liver (Cherrington et al., 1998a; Gasser et al., 1990; Lattard et al., 2002; Lawton et al., 1990; Stevens et al., 2003). The main site of expression of *FMO1* in the adult human is the kidney (Dolphin et al., 1991; Dolphin et al., 1996; Phillips et al., 1995; Yeung et al., 2000). In the adult human kidney expression levels are not much lower than the major hepatic cytochrome P450 (CYP450) CYP3A4 (see table 1.3 for amount of expression) (Shimada et al., 1994) and greater than the total content of CYP450s in the kidney (Jakobsson and Cinti, 1973). It is therefore likely *FMO1* plays a major role in renal drug metabolism within the human. The human *FMO1* gene is also expressed, but to a lesser extent, in the small intestine (see table 1.3) (Yeung et al., 2000). In addition to the kidney and small intestine, EST profiles have shown *FMO1* to be expressed in heart, pineal gland, lymph node, mammary gland, pharynx, placenta, testis, pancreas, thymus, thyroid, medulla and muscle. EST profiles have also shown *FMO1* expression to significantly decrease in tumours. The expression of *FMO1* in numerous extra-hepatic tissues suggests a possible further as yet unknown endogenous role for this protein.

Mouse *Fmo1* has been localised in different cell types using antisense RNA probes specific to *FMO1* (Janmohamed et al., 2004). Within the liver, *FMO1* was localised to the perivenous region. In kidney it was localised to the proximal and distal tubules as well as the glomerulus. In lung it was localised to the terminal bronchiole and the alveoli and within the brain it is localised to the neurons of the cerebellum and the choroid plexus. EST profiles within the

mouse show *Fmo1* expression in the kidney, embryonic and mammary tissues, brain, lung, heart, ovaries, testis, foetal kidney and liver.

Tissue	RNA molecules per cell	Protein (pmol/mg)	Reference
Foetal Liver	945.7		(Zhang and Cashman, 2006)
Adult Liver	96		(Zhang and Cashman, 2006)
Adult Kidney	6198.2		(Zhang and Cashman, 2006)
Adult Lung	595.7		(Zhang and Cashman, 2006)
Adult Small Intestine	522.9		(Zhang and Cashman, 2006)
Adult Liver		<1	(Yeung et al., 2000)
Adult Kidney		47±9	(Yeung et al., 2000)
Adult Small Intestine		2.9±1.9	(Yeung et al., 2000)
Foetal liver		14.4±3.5	(Koukouritaki et al., 2002)
Foetal liver <15weeks		7.8±5.3	(Koukouritaki et al., 2002)
Foetal liver 15W≤26W		3.8±2.6	(Koukouritaki et al., 2002)
Foetal liver 26W≤3days		2.0±1.8	(Koukouritaki et al., 2002)
Foetal liver >3 days		0.1±0.3	(Koukouritaki et al., 2002)

**Table 1.3 Expression levels of FMO1 mRNA or protein measured in different human tissues**

The left column identifies the tissue being analysed. The second and third column give RNA and protein quantification respectively and with standard deviations.

## **1.10 Alternatively spliced, non-coding exons and their function**

The use of alternative splicing by mammalian genes allows for the expansion of transcript and protein diversity. A variety of mRNAs can be produced from a single gene to produce proteins of diverse function (Pajares et al., 2007). A number of genes display complex gene regulation due to the use of alternative promoters, which in turn produce alternative transcripts (Landry et al., 2003). Genome-wide analysis indicate that >60% of human genes use alternative splicing (Baek et al., 2007; Sun et al., 2006; Takeda et al., 2007; Kimura et al., 2006; Cooper et al., 2006). It is predicted that between 30-50% of human genes have multiple promoters (Cooper et al., 2006). ENCODE regions which are characterised promoters (representing 1% of the human genome) were analysed in 16 diverse cell lines using transient transfection reporter assays. That study identified more than 20% of genes as having functional alternative promoters (Birney et al., 2007). An independent study found that 35% of 100 erythroid genes examined had evidence of alternative first exons and promoters in humans (Tan et al., 2006). These studies indicate the common existence of alternative promoters in mammalian genomes. Although alternative promoters are common, the functional significance and their role in disease has been minimally explored, with the exception of a few genes e.g. TP53, tumor protein p53; LEF1, lymphoid enhancer-binding factor 1; GNAS, guanine nucleotide binding protein (Murray-Zmijewski et al., 2006). Alternative promoter usage allows for the diversification of gene regulation. Separate promoters allow for tissue-, developmental-, cell-, and lineage-specific regulation. For example the EIF1AX (eukaryotic translation initiation factor I, X linked) and HBG1 (haemoglobin, g A) genes both contain a TATA-

box promoter and a TATA-less promoter. The TATA box promoter is used during and after embryonic development (Davis and Schultz, 2000; Duan et al., 2002). This allows for developmental-specific factors to regulate the gene at the desired level between the different developmental states. This regulation can be very complex, for example the *NRG1* gene contains 9 alternative promoters (Steinthorsdottir et al., 2004). *NRG1* is tightly regulated during neuronal differentiation and the different promoters, which consist of non-coding and coding alterations, are believed to regulate spatio and temporal expression (Steinthorsdottir et al., 2004). Modifications of this regulation have been linked to cancer and schizophrenia (Tan et al., 2007).

The *FMO1* gene is in the category of genes that use multiple promoters that do not change the overall protein sequence. The transcripts contain different 5' regions due to alternative splicing of non-coding exons (Fig.1.4). The *FMO1* gene has three alternative promoters P0, P1 and P2 which are regulated tissue-specifically and developmentally. Alternative promoters which alter the 5' region of the transcript have been shown to alter the translational efficiency of the protein. The mRNA for the gene *RUNX1* which is initiated from the proximal promoter has a long 5'UTR which contains an internal ribosomal entry site (Levanon and Groner, 2004). This internal ribosome site mediates cap-independent translation (Pozner et al., 2000). *OTX2* (orthodenticle homeobox 2) which is associated with medulloblastoma brain tumor, like *FMO1* is transcribed from three alternative promoters which produce identical proteins (Courtois et al., 2003). The sequence characteristics within 5' UTRs, which can contain upstream translation initiation codons (AUGs), upstream

open reading frames (ORFs), secondary structure and internal ribosomal entry sites) play important roles in differential regulation of translation efficiency.

### **1.11 FMO1 Genetic Variation**

The genomic reference sequence used in this thesis is NT\_004487.19. The cDNA reference sequence used to describe protein-coding variation in this thesis is NM\_002021.1. The Adenine base of the methionine initiation codon is defined as +1. The FMO1 transcripts have been reported to start from different locations. I am therefore reporting SNPs in untranslated regions from the adenine base of the methionine initiation codon for ease of comparison.

#### **1.11.1 Protein coding region variation**

Sequencing of the *FMO1* gene in 50 unrelated individuals of African American descent identified four non-synonymous single nucleotide polymorphisms.

The dbSNP reference number is given followed by the nucleotide and protein position relative to the reference sequence.

rs56841822

NM\_002021.1: c.291C>G

NP\_002012.1: p. (His97Gln)

rs1684314

NM\_002021.1: 907A>G

NP\_002012.1: p. (Leu303Val),

rs28360418

NM\_002021.1: 908T>C

NP\_002012.1: p. (Leu303Thr)

rs606390545

NM\_002021.1: g.1504C>T

NP\_002012.1: p. (Arg502X)

(Fig.1.5) (Furnes et al., 2003). These are all rare variations except for Ile303Val. This is found within African American populations and more specifically the Yoruba population of Nigeria at a frequency of 10-15%. This variant has so far not been found in Asians and Europeans. For each of these protein-coding variants catalytic activity has been assessed using a heterologous expression system. The four substrates tested were methimazole, imipramine, fenthion, and methyl p-tolyl sulphide (Furnes and Schlenk, 2004). Three of the variants His97Gln, Ile303Thr, and Ile303Val had no significant effect on enzyme activity. Arg502X which causes a premature stop codon resulting in 31 residues missing from the FMO1 protein had variable effect on enzyme activity. On imipramine, fenthion and methyl p-tolyl sulphide there were only modest affects. Towards methimazole the variant was completely inactive. This study shows protein coding SNPs in *FMO1* may have a substrate specific affect on enzyme activity. The Arg502X variant is very rare and would therefore have little or no effect on the general population. An additional SNP is reported within dbSNP126 classified as rs16864310. There is currently no functional data on this SNP. Its prevalence

so far has been shown to be limited to a Chinese population and has only a frequency of 2% within this population and is therefore unlikely to have an effect on the general population.

There are three synonymous variants,

rs742350

NM\_002021.1:c.746C>T

NP\_002012.1: p. (Thr249Thr)

rs1126692

NM\_002021.1:c.1187A>G

NP\_002012.1: p. (Val396Val)

rs28360432

NM\_002021.1:c.1400A>G

NP\_002012.1: p. (P467P)

(See Fig.1.5) (Furnes et al., 2003), within FMO1 which have not been analysed for any possible effect on RNA secondary structure or splicing rates and efficiency.

## FMO1

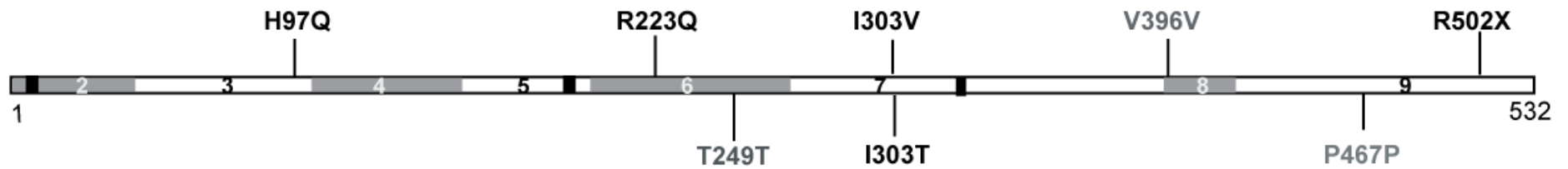


### Figure 1.5 The *FMO1* gene and the location of protein coding SNPs

The figure shows the position of the SNP relative to the amino acid position. If there is a non-synonymous change the amino acid substitution is shown, reproduced from Phillips and Shephard, 2008.



### 1.11.2 Untranslated mRNA Variants

There are four verified SNPs within the 3' untranslated region of the *FMO1* mRNA: +27590G>A (dbSNP126, rs28360435), +27578 G>A (dbSNP126, rs28360434), +27568C>T (dbSNP126, rs12954) and +27664C>T (dbSNP126, rs7877) (Hines et al., 2003). The SNP rs12954 has been verified by eight sequencing panels. Hardy Weinberg estimates of genotype frequencies suggest selection against the T/T genotype. This SNP and +27664C>T has also been associated with amyotrophic lateral sclerosis as discussed later.

### 1.11.3 Promoter Variants

There is a large amount of variation upstream of the *FMO1* transcriptional start sites (see chapter 5) which may influence the amount of transcript produced. Due to the 10-20 fold observed variation between individuals in the amount of *FMO1*, this is a strong hypothesis. This variation is also likely to be due to genetic polymorphism as *FMO1* expression has been shown not to be greatly affected by foreign chemicals as is the case for the *CYP* genes.

To date there has been limited analysis of polymorphisms within sequences upstream of the *FMO1* transcriptional start sites. The largest sequencing study was undertaken by Hines and co-workers. They sequenced and analysed *FMO1* regions in 177 individuals who collectively represented a diverse population of individuals including Northern Europeans, Africans, and East and South Asians (Hines et al., 2003). Regions flanking the P0 promoter, exons 0, 2, 9 and short flanking intronic sequences were examined for SNPs.

Four SNPs were identified upstream of P0 (g.-10361T>A, dbSNP126, g.-10330C>T, g.-10046A>G and g.-9782C>A) but none were found to be within previously defined regulatory regions (Luo and Hines, 2001). A polymorphism within exon 0 (-9536C>A relative to the ATG translation start site) lies within a conserved core binding sequence for the yin yang 1 (YY1) transcription factor. Electrophoretic mobility shift assays (EMSAs) using HepG2 cellular extracts demonstrated that the C>A transversion eliminates YY1 binding (Hines et al., 2003). However this transversion also increased the affinity for this sequence to bind to other regulatory factors Oct1, HNF1 $\alpha$  and HNF1 $\beta$  indicating a complex mechanism of gene regulation. Transfection of HepG2 cells with reporter constructs under the control of either the -9536C or -9536A alleles showed no difference in the activity of the minimal promoter (Hines et al., 2003). An extended construct caused a 2-3 fold loss of reporter gene activity expression only when the -9536A variation was present.

There is a distinct question mark over these results as *FMO1* expression data of two human foetal livers homozygous for the -9536G>A variant showed expression of *FMO1* in the upper quartile range within their age bracket. This result contradicts the reporter gene data that suggested that this variant reduces *FMO1* expression (Koukouritaki et al., 2002). Further analysis is needed to elucidate the role of other transcription factors, which may bind to this region and compensate for the loss of expression as a consequence of YY1 binding.

Two SNPs, -11T>C and +17248T>C are located within splice acceptor sites (Hines et al., 2003). However, it is unlikely they affect splicing of the FMO1 transcript and subsequently the amount of protein as both SNPs are pyrimidine to pyrimidine changes. SNPs within the P1 and P2 promoters have yet to be defined and this aspect forms part of this thesis (Chapter 4). Defining of these promoters will allow the testing of polymorphism identified upstream of the P1 and P2 transcriptional start sites for their influence on gene expression.

### **1.12 FMO1 in drug metabolism**

FMO1 metabolizes a number of therapeutic drugs (Krueger and Williams, 2005). These are generally nitrogen or sulphur (see Table 1.4) containing compounds and are used as treatments for a wide range different diseases and disorders including breast cancer (FMO1 metabolizes tamoxifen) and tuberculosis (FMO1 metabolizes thiacetazone). FMO1 substrates are, in general, also metabolized by members of the cytochrome P450 family of DMEs.

The metabolites of the two enzyme systems (the FMOs and the CYP450s) can be quite different e.g. tamoxifen metabolism CYP3A4 produces a toxic metabolite whereas FMO1 produces the *N*-oxide, which is considered to be a detoxification pathway (Parte and Kupfer, 2005). The FMO1 metabolite is also capable of being reduced back to tamoxifen by CYP3A4 (Parte and Kupfer, 2005). The role of FMOs and CYPs in the metabolism of the same drug and

the retro-reduction of FMO products is discussed in a recent review (Shephard and Phillips, 2010).

Knockout mice that are null for the *Fmo1* gene show extreme adverse affects towards the drug imipramine, which was not seen in age-matched wild type mice (Hernandez et al., 2009). The drug is also a substrate for various CYPs. The knockout mice produce no imipramine *N*-oxide (a product only of FMO1). The adverse affects of the drug, in the absence of FMO1, show that the protein is required for the detoxification of this drug *in vivo*. This study also provides evidence for a more important role for FMO1 in the metabolism of imipramine than was previously thought. To understand an individual's response to a specific drug a good understanding of the contribution of both the FMO and CYP systems is required as well as the other enzymes that may be involved in the detoxification (or activation) of a drug.

Compound	Type	Health condition	Oxidation site	Reference
Benzydamine	Nonsteroidal antiinflammatory		N	(Lang and Rettie, 2000), (Stormer et al., 2000)
Chlorpromazine	Dopamine D2 antagonist	Psychosis	N	(Kim and Ziegler, 2000)
Deprenyl	Monoamine oxidase type B inhibitor	Parkinson's disease	N	(Szoko et al., 2004)
Imipramine	5HT/noradrenalin re-uptake inhibitor	Antidepressant	N	(Kim and Ziegler, 2000)
Itopride	Dopamine D2 antagonist	Gastroprokinetic	N	(Mushiroda et al., 2000a)
Methamphetamine	Psychostimulant		N	(Szoko et al., 2004)
N-deacetyl ketoconazole*	Antifungal agent		N	(Rodriguez and Miranda, 2000)
Olopatadine	Antihistamine		N	(Kajita et al., 2002)
Orphenadrine	Anticholinergic	Parkinson's disease	N	(Kim and Ziegler, 2000)
SNI-2011	Muscarinic receptor agonist	Sjogren's Syndrome	N	(Washio et al., 2003)
Tamoxifen	Estrogen receptor modulator	Breast Cancer Therapy	N	(Parte and Kupfer, 2005)
Xanomeline	Muscarinic receptor agonist	Alzheimer's Disease	N	(Ring et al., 1999)
Ethionamide	Antibiotic	Tuberculosis	S	(Krueger and Williams, 2005)
Methimazole	Thyroperoxidase inhibitor	Hyperthyroidism	S	(Furnes and Schlenk, 2004)
S-methyl esonarimod*	Cytokine production inhibitor	Rheumatism	S	(Ohmi et al., 2003)
Tazarotenic acid**	Retinoic acid receptor modulator	Acne/Psoriasis	S	(Attar et al., 2003)
Thiacetazone	Antibiotic	Tuberculosis	S	(Qian and Ortiz de Montellano, 2006)

**Table 1.4 Drugs metabolized by FMO1**

The table above shows the compounds metabolized by FMO1, the type of compound, and the site of oxidation by FMO1.

### 1.13 FMO1 and disease

Gene expression profiling of myocardial tissue from patients with atrial fibrillation showed a significant increase in FMO1 mRNA (Kim et al., 2003). Most of the genes up-regulated in this study were involved in oxidative stress. No SNPs within *FMO1* have been associated with this disease. Expression profiling of spinal cord tissue from patients suffering from sporadic amyotrophic lateral sclerosis (ALS) showed significant decrease in FMO1 mRNA (Malaspina et al., 2001). An association study was subsequently carried out on two SNPs within the 3'UTR region of FMO1, +27568C>T (rs12954) and +27664C>T (rs7877) in a group of sporadic ALS patients and a control group (Cereda et al., 2006). They were shown to both be over-represented in female, but not male, ALS patients.

### 1.14 Expression Profiles

There are a number of expression profiles available for mouse and human FMO1 from a range of microarray data. This resource is available through the National Centre for Biotechnology Information database (<http://www.ncbi.nlm.nih.gov/GEOprofiles>). These profiles give clues to the regulation of the *FMO1* gene and support evidence for an endogenous role for the protein in energy homeostasis. The GEO profiles where *FMO1* expression changes significantly are illustrated in table 1.5 and 1.6. The fatty acid palmitate, which is a negative regulator of PGC-1 $\alpha$ , represses *Fmo1* expression (GDS2648 / 1417429\_at / Fmo1 / Mus musculus) (Crunkhorn et al., 2007). PGC-1 $\alpha$  is a transcription co-factor which plays a role in the

regulation of reactive oxygen species (ROS) metabolism (Uldry et al., 2006), thermogenesis, gluconeogenesis, brown adipose differentiation, mitochondrial biogenesis and fatty acid oxidation (Liang and Ward, 2006). These processes that are involved in energy homeostasis can be linked to the metabolic phenotype of the *Fmo1* (-/-), *2* (-/-), *4*(-/-) knockout mouse observed in our laboratory.

Expression profiles have also shown that knocking out the transcription factor HNF4 $\alpha$  results in severe down regulation of *Fmo1* within mouse embryonic liver (see GEO profile: GDS1916/1417429\_at/FMO1/Mus musculus (Battle et al., 2006). However, the absence of HNF4 has no effect on *Fmo1* expression in the foetal colon (Garrison et al., 2006). HNF4 $\alpha$  and PGC-1 $\alpha$  as a cofactor, regulate genes involved in gluconeogenesis in the liver and pancreas, but not the small intestine (Puigserver, 2005). Another transcription factor from the same family as HNF4 $\alpha$ , HNF-1 $\alpha$ , down regulates *Fmo1* in pancreatic  $\beta$ -cells (see GEO profile: GDS1916/1417429\_at/FMO1/Mus musculus) (Akpinar et al., 2005). HNF-1 $\alpha$  and HNF4 $\alpha$  have been linked to type 2 diabetes in the young (Ellard, 2000). Many other expression profiles show increased *Fmo1* expression in differentiated cells. Time course studies of myocyte and adipocyte differentiation show increased FMO1 mRNA over time. A microarray study of within 3T3-L1 adipocytes using RNA isolated from mice in which insulin receptors were knocked out to disable differentiation shows FMO1 mRNA to be significantly repressed ( $p < 0.003$ ) (Tseng et al., 2005). A number of other factors involved in cellular differentiation also seem to regulate *Fmo1* within different tissues (see table 1.4 and 1.5).

An analysis of the available *FMO1* expression data indicates transcription factor candidates that might regulate the gene and lends further evidence for a role of the FMO1 protein in regulating energy homeostasis.



Geoprofile code	Regulatory factor	Role/Function	Organism	System	Reference
GDS1473 / 101911_at/FMO1/Mus musculus	HNF1- $\alpha$	Pancreatic beta cell growth, Glucose homeostasis	mouse	Pancreatic islets	(Akpinar et al., 2005)
GDS1916 / 1417429_at/FMO1/Mus musculus	HNF4- $\alpha$	Hepatogenesis, Gluconeogenesis, Glucose homeostasis	mouse	Embryonic Liver	(Battle et al., 2006)
GDS2854 / 1417429_at / Fmo1 / Mus musculus	MYOD	Regulates myogenic differentiation	mouse	Embryonic fibroblasts	(Di Padova et al., 2007)
GDS2334 / 1417429_at / Fmo1 / Mus musculus	MYOD	Regulates myogenic differentiation	mouse	Embryonic fibroblasts	(Cao et al., 2006)
GDS2660 / Msa.63.0_s_at / Fmo1 / Mus musculus		Adipocyte differentiation	mouse	3T3-L1 differentiation	(Cheung et al., 2007)
GDS2412 / 1417429_at / Fmo1 / Mus musculus		Myotube differentiation	mouse	Myotube differentiaion	(Chen et al., 2006)

**Table 1.5 GEO profile data which show an increase in *Fmo1* expression**

The GEO profile is shown on the left column. The next column describes the regulatory factor that influences the expression of *Fmo1*. The third column describes the role of this factor and the next two columns describe the organism system used for the analysis.

Geoprofile code	Regulating factor	Role/Function	Organism	System used	Reference
GDS1384 / 205666_at / FMO1 / Homo sapiens	v-myb, c-myb transcription factors	Induces apoptosis in tumours	human	MCF7 cells	(Liu et al., 2006)
GDS1434 / 101991_at / Fmo1 / Mus musculus	P63 transcription factor	Epidermal morphogenesis	mouse	18.5 days skin layer embryo	(Koster et al., 2006)
GDS2184 / 101991_at / Fmo1 / Mus musculus	Runx2	Skeletogenesis	mouse	Embryo 14.5 days developed	(Hecht et al., 2007)
GDS2629 / 1417429_at / Fmo1 / Mus musculus	Get-1	Epidermal differentiation	mouse	Embryonic skin	(Yu et al., 2006)
GDS2648 / 1417429_at / Fmo1 / Mus musculus	Palmitate	Induces apoptosis in the Heart	mouse	CDC12 myotubes	(Crunkhorn et al., 2007)
GDS2610 / 1417429_at / Fmo1 / Mus musculus	glycerol kinase knock down	GK is at the interface of fat and carbohydrate metabolism	mouse	brown adipose	(Rahib et al., 2007)

**Table 1.6 GEO profiles which show a decrease in human *FMO1* or mouse *Fmo1* expression**

The GEO profile is shown on the left column. The next column describes the regulatory factor influencing the expression of the gene. The third column describes the Role of this factor and the next two columns describe the organism system used within the experiment.

## **1.15 How Regulatory polymorphisms and polymorphism influencing splicing cause changes in gene expression**

Many studies have shown that variation in the expression of genes is heritable. Expression profiling and genome-wide mapping studies have added to our knowledge of the extent of variation and its influence. Inter-individual variation in mRNA amounts can be accounted for in general by differences in *cis*-acting elements (such as DNA polymorphism in such an element) and the binding of trans-acting modulators (transcription factors) to these elements. It is predicted that 25-35% of inter-individual differences in gene expression are due to variation in *cis*-acting elements (Pastinen and Hudson, 2004). A DNA polymorphism changing a *cis*-acting element sequence, and as a consequence the transcript abundance, can be defined as a regulatory polymorphism. Transcript expression can be changed by a number of different mechanisms. In general, regulatory polymorphism is found outside the protein-coding region of the gene, although premature translation stop codons also influence the amount of mRNA produced (Willing et al., 1996).

Regulatory polymorphism can influence transcription by altering the binding of RNA polymerase and transcription factors to the DNA, pre-mRNA splicing, exonic splicing enhancers (ESEs), exon skipping (Gregory et al., 2007), mRNA stability (Carter et al., 2002; Sheets et al., 1990; Conne et al., 2000; Di Paola et al., 2002), mRNA trafficking, or induce epigenetic changes (Ober et al., 2003; Ober et al., 2006). Epigenetic regulatory variation can alter transcription rates by changing the methylation state of the promoter or enhancer. Alterations in methylation patterns due to regulatory polymorphism can alter the imprinting of the gene (Singh et al., 2010). Regulatory

polymorphism may also cause disruption of insulator binding (Roberts et al., 2007).

Regulatory polymorphism has been observed to alter the binding of transcription factors in a variety of ways. This can be through disruption of a binding site or modification of a binding site so that the efficiency of protein binding is altered (Taulan et al., 2007). With the advent of genome wide association studies a large number of *cis*-acting regulatory polymorphism are being shown to be associated with disease. Functional studies on these SNPs have shown *cis*-acting regulatory variation to alter transcription factor binding in novel ways. For example, a genome-wide association study identified a locus on chromosome 1p13 strongly associated with both plasma low-density lipoprotein cholesterol (LDL-C) and myocardial infarction (MI) in humans. The authors showed, through a series of studies in human cohorts and human-derived hepatocytes, that a common non-coding polymorphism at the 1p13 locus, rs12740374, creates a C/EBP (CCAAT/enhancer binding protein) transcription factor binding site and alters the hepatic expression of the SORT1 gene (Musunuru et al., 2010).

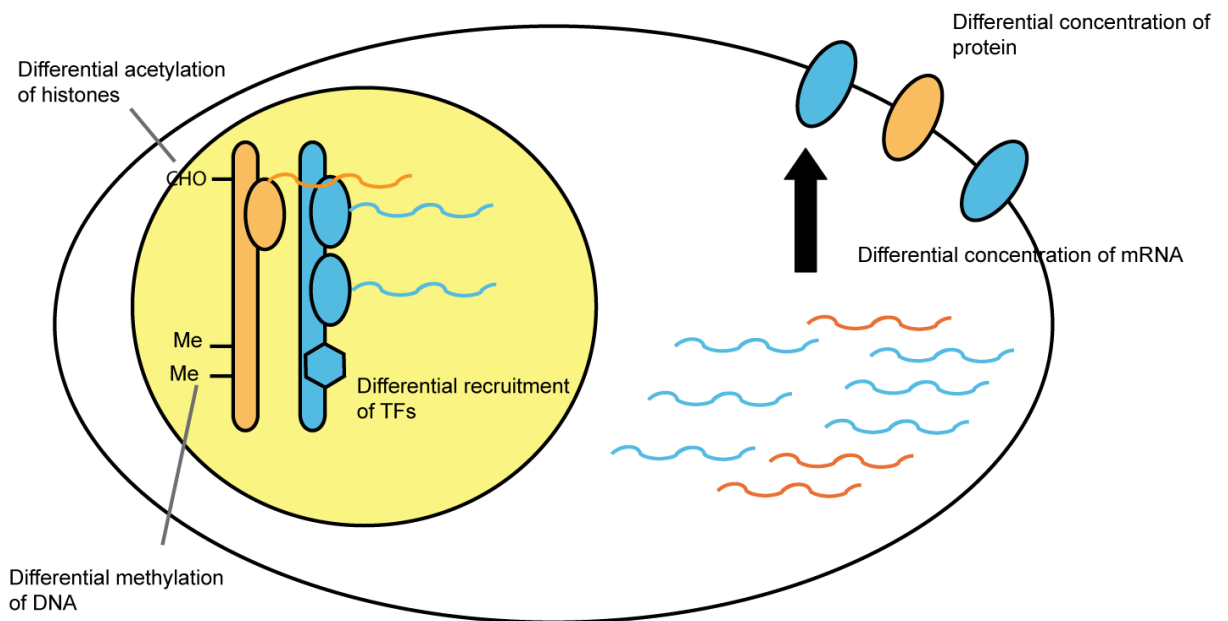


### Figure 1.6 Mechanisms that result in differences in protein expression between individuals

The diagram shows the nucleus within the cell. The two chromosomes are depicted. The chromosomes show how different mechanisms can alter the expression of genes. Epigenetic mechanisms including methylation and acetylation as shown in the diagram can lead to changes in mRNA expression. Differential recruitment of transcription factor binding can also lead to differences in mRNA expression. The processing of the transcript (splicing, transport) can also vary between individuals resulting in varied availabilities of transcripts within the cytoplasm for translation. All these factors contribute to the overall variability in protein expression between individuals.

## **1.16 Regulatory polymorphism and splice-site polymorphism observed in drug metabolizing enzyme genes**

This section outlines a number of regulatory SNPs and SNPs that influence splicing that have been identified in some important genes coding for drug metabolising enzymes. This will reinforce the importance of regulatory polymorphism in drug metabolism and outline some of the issues which make their identification difficult.

The majority of regulatory polymorphisms have been found within promoter or enhancer regions. Other SNPs that influence mRNA splicing and thus the amount of activity of the protein are also included. The CYP family have been extensively studied for regulatory polymorphism. This is the major hepatic family of drug metabolizing enzymes. I will review the literature on the CYP1A2, CYP2D6 and CYP2A6. CYP1A2, which metabolizes clozapine, paracetamol, phenacetin, theophylline, imipramine, and tacrine. Four regulatory polymorphisms have been observed in *CYP1A2* that alter transcript abundance. The SNP, -2964G>A is found within an enhancer region. Individuals with the A allele have a reduction in enzyme activity compared to individuals that possess the G allele (Nakajima et al., 1999). The SNP -163C>A was found associated with increased enzyme induction in patients given caffeine (Sachse et al., 1999). A novel SNP -730C>T was identified within an Ethiopian population. A haplotype containing the T variant showed significantly decreased enzyme activity towards the substrate caffeine. The T allele was shown to prevent the binding of the transcription factor ets (Aklillu et al., 2003). A *CYP1A2* splice donor site polymorphism, found in a single

individual, was implicated in the poor metabolism of clozapine (Allorge et al., 2003).

*CYP2D6* is the most polymorphic of the *CYP* genes and the protein constitutes 2% of total hepatic CYP protein. *CYP2D6* is involved in the oxidative metabolism of more than 70 drugs. Two SNPs alter the splicing of the gene. A G>A SNP within the consensus sequence at the splice site of the third intron causes a loss of protein in individuals with the A/A genotype. These individuals have been shown to be poor metabolizers of *CYP2D6* substrates (Kagimoto et al., 1990). The second polymorphism, a splice acceptor site found within intron 1, which causes a premature stop codon, was observed in a poor metabolizer of *CYP2D6* substrates (Marez et al., 1995). The third SNP, a regulatory polymorphism, 1584G>C, in the promoter of *CYP2D6*, was shown to be associated with *CYP2D6* activity *in vivo* (Lovlie et al., 2001) possibly due to an increase in protein expression (Zanger et al., 2001). More recent evidence suggests the -1584G>C is in linkage disequilibrium with the functional *CYP2D6*\*35 allele, which has been found in many duplication-negative "ultra rapid" metabolizers (Gaedigk et al., 2003). These are individuals which do not contain duplications of the gene and are ultra-rapid metabolizers. This outlines the difficulty in defining regulatory polymorphism based on purely associative studies.

The enzyme *CYP2A6* accounts for about 10% of all CYP expression within the liver (Pelkonen et al., 2000). The enzyme metabolizes nicotine, cotinine, and some drugs (e.g., fadrozole, halothane, losigamone, letrozole,

methoxyflurane). A SNP, -48T>G, which disrupts the TATA box of the gene, was identified in a Turkish individual. This SNP was further identified in different populations and allele frequencies (the G allele) were between 5-15%. The G/G genotype reduces reporter gene activity to 50% of the T/T genotype (Pitarque et al., 2001). A polymorphism was identified within an enhancer region of *CYP2A6* located at position -1013A>G. Reporter gene assays showed the region, between -1005 and -1019, containing the polymorphism elicited a strong enhancer effect. The *CYP2A6\*1D* allele, containing the -1013 G/G genotype showed significantly reduced reporter gene activity. An EMSA showed that the A/A genotype have higher affinity nuclear protein binding than does the G/G genotype (Pitarque et al., 2004). A novel polymorphism was identified in the 5' flanking region of the *CYP2A6* gene located at position -745A>G. This polymorphism lowers the binding efficiency of the NF-Y transcription factor to the CCAAT binding sequence. Reporter gene assays show the -745 G variant reducing promoter activity to 78% of the wild type activity (von Richter et al., 2004).

### **1.17 Methods of identifying and analysing regulatory polymorphism**

Linkage disequilibrium can be described as the non-random association of alleles. Definition of regulatory polymorphisms is complicated by linkage disequilibrium (LD) within the human genome. A variant in one individual or a population may seem like the causative polymorphism when in reality it is only in linkage disequilibrium with the causative polymorphism. To illustrate, the lactase persistence phenotype is conferred by a regulatory SNP, C>T, 14 kb upstream of the start of translation (Enattah et al., 2002). The T allele is in



complete association with lactase persistence within a Finish population (Enattah et al., 2002). Subsequent studies show, that in some individuals, there is equal contribution of expression from the C and T allele (Poulter et al., 2003). The variation has not been associated with lactase persistence within certain African populations (Mulcare et al., 2004).

In the previous section the *CYP2D6* gene polymorphism, -1584G>C, was described. This shows an *in vivo* association with reduced CYPD26 activity (Gaedigk et al., 2003). The polymorphism was shown to be in strong linkage disequilibrium with a coding region SNP associated with a poor metabolizer phenotype. Therefore the SNP could potentially only be in linkage with the causative polymorphism. To partly overcome the problem of LD, the order of polymorphisms that exist along the chromosome of an individual (known as a haplotype) can be tested for functional effect instead of testing only a single variant. This way the influence of regulatory polymorphism can be deduced by studying the effects of different genetic backgrounds. This, however, requires detailed knowledge of the regulatory sequence. Therefore there is a requirement for *in vivo* associative data to be combined with functional data to define the influence of a regulatory polymorphism.

There are many methods to analyse regulatory polymorphism and I will review both common and more recent methodologies. The most common and traditional way of identifying a regulatory polymorphism is by measuring its ability to drive transcription when attached to a synthetic reporter construct. The reporter gene produces an exogenous product allowing quantification of

this protein within transfected cells. Originally, the reporter gene used was the chloramphenicol acetyltransferase (CAT) gene. Subsequently the reporter gene luciferase was introduced due to its ability to be easily quantified by luminescence, in comparison to the quantification of radioactive acetylated products of chloramphenicol. Before regulatory polymorphisms can be tested, the promoter needs to be defined. This is achieved by refining the sequences upstream of the transcriptional start sites until the most important regulatory sequences have been established. Polymorphisms can then be studied, either by introducing the mutation by site-directed mutagenesis or by amplifying and cloning the promoter sequence from different individuals. Candidate polymorphisms can be chosen which disrupt consensus DNA binding sites for transcription factors. These are good candidates for playing a role in regulating the gene being studied. This technique is limited as the causative SNP may be in LD with the promoter SNP being analysed. Thus the influence of the causative SNP will be missed as it is not present within the promoter region that has been defined.

Additional techniques are required to observe the physical effect of the SNP on gene regulation. DNase I footprints have traditionally been used to identify the DNA-protein binding profile along the promoter. The EMSA can be used to determine if the SNP affects the binding of a trans-acting regulatory factor. There are disadvantages to analysing regulatory polymorphism *in vitro*. The regulatory variation is not found in its natural environment. The DNA is not in the natural chromatic state and the DNA will not necessarily regulate expression or influence protein binding as it does *in vivo*.

In an attempt to overcome some of the limitation of regulatory polymorphism analysis, use has been made of allele-specific markers to analyse the influence of an individual allele. First, allele-specific markers are identified. Subsequently, gene expression from each allele is measured by specific RT-PCR toward each allele (Singer-Sam et al., 1992). This technique is limited because it cannot identify differences in trans-acting-factor binding that may cause differences in gene regulation between individuals. To address the problem, allelic expression and differences in trans-acting factor binding measuring can be carried out within the same individual using the same cell type. The allelic expression can then be determined for individuals and association studies made to obtain candidate regulatory SNPs. This technique is limited to studying markers within the mRNA coding region or with SNPs that are in LD.

The development of an assay, which does not require a heterozygote marker, is that which measures the amount of RNA polymerase II phosphorylation. The phosphorylation of specific serine residues within RNA polymerase II allows its release from the initiation complex and the commencement of elongation (Knight et al., 2003). Phosphorylation is therefore directly linked to the activation of transcription. The authors showed that chromatin immunoprecipitation assays, using antibodies to phosphorylated RNA polymerase II, allows the influence of allelic differences on transcription to be assessed.

Measurements of allele-specific expression that better reflect the *in vivo* situation are a powerful and accurate tool for elucidating regulatory polymorphism. The causative SNP responsible for influencing expression must of course be identified. To identify causative regulatory SNPs, allele-specific approaches would have to be combined with techniques that can directly test the effect of individual SNPs on gene expression.

### **1.18 Illumina second-generation sequencing and its application for regulatory polymorphism**

The techniques described thus far have been based on analysing a single gene or a small group of genes. Genome-wide sequencing is now feasible with the advent of second-generation sequencing (Shendure and Ji, 2008). There are a number of different types of second-generation sequencing and I describe here the use of cyclic-array sequencing. Cyclic array sequencing has been realized in different commercial products. The 454 sequencing technology (used in the 454 Genome Sequencers, Roche Applied Science; Basel), Solexa technology (used in the Illumina (San Diego) Genome Analyzer) and the SOLiD platform (Applied Biosystems; Foster City, CA, USA), the Polonator (Dover/Harvard). All systems are based on a similar workflow. The DNA to be sequenced is fragmented. The fragments are each ligated to a linker sequencer. PCR by amplification from the linker DNA is used to generate amplicons. Within the different systems these PCR products are spatially oriented (Solexa). The amplified products are sequenced via enzymatic reaction (454) or fluorescence imaging of terminated reactions (Solexa and SOLiD).

The ability to sequence whole genomes using second-generation sequencing will lead to the rapid increase in the identification of human genetic variation. A project to sequence 1000 individual genomes from various populations is currently being undertaken which should identify novel variation (Siva, 2008). The second-generation sequencing platforms have been utilised to study not only variation but also the analysis of gene regulation on a genomic scale. Researchers are now able to analyse the epigenome using second-generation sequencing technology. The epigenome can be described as the source of variation within the genome other than the sequence itself. This includes the chromatin, methylation and acetylation state of the DNA. These modifications are extremely important in overall gene expression in altering the chromatin structure of DNA thus effecting the regulation of genes. As a result epigenetics is responsible for cell-type specificity, differentiation, development, proliferation, and the cell's environmental responses.

Analysis of the epigenome can identify regulatory regions that are specific to the condition of the cell. DNase I-seq (Song and Crawford, 2010), NA-seq (Gargiulo et al., 2009), and Formaldehyde-Assisted Isolation of Regulatory Elements (FAIRE-seq) (Giresi et al., 2007), are three epigenetic techniques which allow the identification of regulatory regions throughout the whole genome. The techniques work under the same principle. The DNA is treated with DNase I, which digests DNA that is in a relaxed state as opposed to a nucleosomal state. In the relaxed state the DNA is more liable to be digested by DNase I. These digested regions will result in many smaller fragments. These DNase I digested fragments will therefore be enriched. The DNA

fragments are transferred to an illumina sequencing machine and analysed. The sequence signal strength is correlated with the amount of DNase I digestion and areas of high signal strength are good indicators of regulatory regions. DNase I-seq has identified a substantial number of open regions within many different cell lines and tissues revealing a large number of tissue specific regulatory regions. For example the epigenome of human pancreatic islet cells has been examined by Formaldehyde-Assisted Isolation of Regulatory Elements (FAIRE-seq) analysis (Gaulton et al., 2010). By removing identified regulatory regions from other cell types, regions specific to the islet cells can be determined (Gaulton et al., 2010). By locating regulatory specific regions polymorphism can be identified and tested for their functional effect (Gaulton et al., 2010).

DNase I-seq has been undertaken at a resolution high enough to resolve the sequence to which individual proteins are bound. However the resolution required means that the number of sequence reads is extremely expensive (Hesselberth et al., 2009).

### **1.19 Polymorphism effecting translation efficiency**

A number of genetic polymorphisms have been shown to occur within the mRNA coding sequence that influences the translational efficiency of the protein. Polymorphism has been shown to alter the rate of translation and the production of protein. This can occur due to the polymorphism introducing a mutation within the Kozak sequence. A polymorphism within the Kozak

sequence of the glycoprotein *ib alpha* gene is a major determinant of plasma membrane levels of the platelet GPIb-IX-V complex (Afshar-Kharghan et al., 1999). A polymorphism within the Kozak sequence of the annexin V gene is associated with myocardial infarction in young people (Gonzalez-Conejero et al., 2002). Polymorphism has also been shown to disrupt or create ATG initiation codons. A polymorphism within the vitamin D receptor gene introduces a second upstream ATG initiation codon. This polymorphism has shown to be a risk factor associated with insulin resistance in Caucasians (Chiu et al., 2001), associated with bone mineral density and vertebral fractures in postmenopausal Italian women (Gennari et al., 1999), and associated with height (Minamitani et al., 1998). The polymorphism creates a second translation initiation site. It has been shown that individuals with this polymorphism produce two distinct proteins (Arai et al., 1997). The upstream ATG was shown to produce 1.7-fold increase in reporter gene activity than the ACG form in transfected COS-7 cells (Arai et al., 1997).

In the course of the work described in this thesis, a common polymorphism was identified within the *FMO1* gene. This results in a second ATG upstream of the defined translational start site. This polymorphism, a C>T transition, occurs in-frame, 12 base pairs upstream of the accepted ATG for *FMO1*. This is the same distance as seen between the ATG initiation sites in the vitamin D receptor gene (Zysow et al., 1995). Chapter 2 describes the experimental work carried out on the *FMO1* ATG polymorphism.

## **1.20 3T3-L1 adipocytes and their use as a model for adipocyte biology**

3T3-L1 cells were used in the experiments described in Chapters 1 and 2. Several different fibroblast cell lines exist that can be differentiated into adipocytes in culture. The 3T3 cell line was immortalised from primary embryonic stem cells from the Swiss mouse strain. These cells were originally isolated to obtain immortal cell lines suitable for viral transformation (Todaro and Green, 1963). When in culture, the cells were observed to produce foci of cells that accumulated lipid. In 1972, 3T3 cells were clonally expanded based on lipid accumulation within the cells. Different clones produced differing amounts of lipid. The 3T3-L1 line is one of the clonal expansions of the 3T3 cells that convert to cells accumulating a large amount of lipid (Green and Meuth, 1974). The cells were shown to possess a latent programme of differentiation that, when activated, converts them to adipocytes. The differentiation process was shown to have specific stages of conversion (Fig.1.7). The first stage is the accumulation of triglycerides, which could be stained with oil-red O. In the second stage the cells have extended processes. When the cells enter the third stage they become spherical and take on the morphology of young, adipose cells. The cells were shown to accumulate the enzymes and proteins responsible for the synthesis and degradation of triglyceride and hormonal regulation of lipid accumulation. 3T3-L1 cells were confirmed as containing a latent programme of adipocyte differentiation when they developed into mature fat pads after injection into athymic mice (Green and Kehinde, 1979). The 3T3-L1 adipocytes have been shown to possess most of the structural and organelle characteristics of



animal adipocytes (Novikoff et al., 1980). The formation and development of fat droplets also mimic primary adipose tissue (Green and Meuth, 1974).

Adipose conversion was shown to be more efficient when a cocktail of adipogenic factors are introduced to the culturing media. These factors are high concentrations of insulin, a glucocorticoid, usually dexamethasone, and an agent that elevates intracellular cyclic adenosine monophosphate (cAMP) levels, a signalling molecule which activates protein kinases and subsequently changes glycogen, sugar, and lipid metabolism with the cell, and foetal bovine serum (Student et al., 1980). This cocktail is added to the cells after they reach confluency when cultured in foetal bovine serum. Twenty four hours later, with the addition of the differentiation cocktail, the cells undergo a post-confluent mitosis and subsequent growth arrest (Bernlohr et al., 1985). This is followed by one round of DNA replication and cell division. At day 2, the cells complete post-confluent mitosis and enter into an unusual growth arrest called  $G_D$  (Scott et al., 1982). This has been hypothesised to happen so the DNA can unwind and allow transcription factors access to the open form of the DNA (Cornelius et al., 1994). After growth arrest the cells are committed to becoming adipocytes. The growth arrest is a requirement for subsequent differentiation. At day 3, growth-arrested cells begin to express late markers of differentiation. These late markers consist of lipogenic and lipolytic enzymes in addition to other proteins responsible for producing the mature adipocyte phenotype. At day 5-7 the cells round up, accumulate fat droplets, and become terminally differentiated adipocytes.

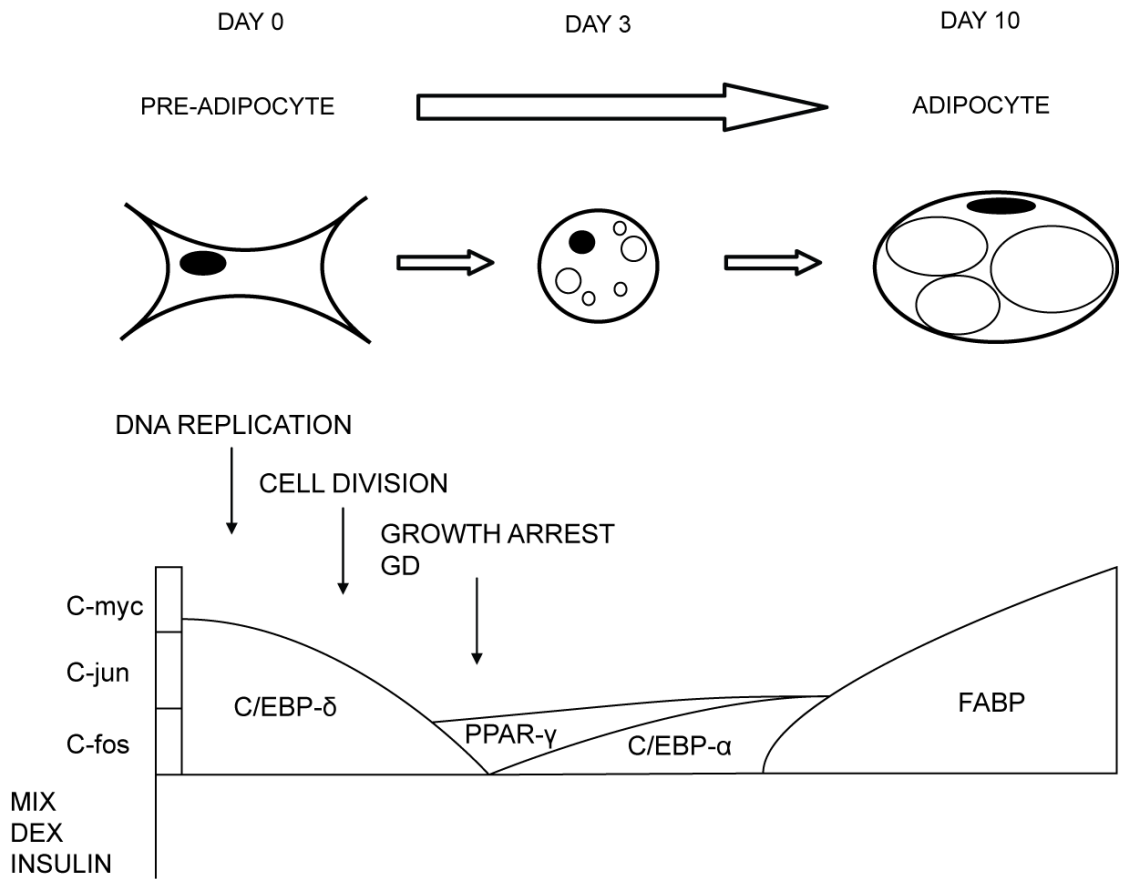


**Figure 1.7 Illustration of the morphological and gene regulatory changes that occur during 3T3-L1 adipocyte differentiation**

The diagram shows the 3T3-L1 differentiation process post addition of differentiation media (MIX (methylisobutylxanthine), DEX (dexamethasone), and INSULIN). The time course of morphological changes is shown. The illustration below shows the time course of expression of key regulators of 3T3-L1 differentiation and key changes within the cell cycle.

## 1.21: Aims of this study

1. To further investigate the usage of the *FMO1* alternative promoters in different mouse tissues and mouse cell lines.

*FMO1* has a role in drug metabolism and more recently a role in energy homeostasis has been defined. Further definition of promoter usage in different tissues and cell types will help further our understanding of the multiple promoters used and the mechanisms that regulate *FMO1* transcription. Identifying which of the *FMO1* transcripts is produced in different tissues will give context to a genetic polymorphism that may have a transcript-specific effect.

2. To define the human *FMO1* P1 and P2 promoter sequences that are responsible for transcription of *FMO1*.

This will be carried out in the context of different cell types. These promoter regions will help define regulatory polymorphism that may be responsible for the large inter-individual variation seen between individuals in the expression of *FMO1*. Data will be collated from genome-wide expression analysis to further validate the defined promoter regions.

3. To identify the amount of genetic variation within the *FMO1* P0, P1 and P2 promoters.

Re-sequencing of the *FMO1* promoters may yield novel variation that may be responsible for the high inter-individual variation seen between individuals.

Re-sequencing will also identify genotype frequencies in different populations for previously discovered polymorphism.

4. To examine the effects of *FMO1* promoter polymorphism a novel approach will be taken to improve the speed at which promoter polymorphism may be analysed by the researcher.

Recent developments in DNase I capillary footprinting will be further developed and used to analyse promoter polymorphism. This approach will also allow the effects of the polymorphism on DNA-protein binding to be visualised. The *FMO1* promoter polymorphism will ideally be examined with this method as well as the DNA-protein binding profile of the *FMO1* P1 and P2 promoters.

# **Chapter 2**

## **Materials and Methods**

## Chapter 2: Materials and Methods

General laboratory chemicals were purchased from BDH. Trizma base was purchased from Sigma. Other chemicals and materials were purchased from various companies. Company names, other than BDH, have been indicated in bracket.

### 2.1 *Escherichia coli* (*E.coli*) strains and culture conditions

#### 2.1.1 Genotypes of *E.coli* strains

XL-Blue MRA strain:  $\Delta$  (*mcrA1*) 183, (*mcrCB-hsdSMR-mrr*) 173, *endA1*, *supE44*, *thi-1*, *gyrA96*, *relA1*, *lac*) (Stratagene)

Library efficiency DH5 $\alpha$ <sup>TM</sup> competent cells [*supE44*,  $\Delta$ *lac U169* ( $\Phi$ 80 *lacZ* $\Delta$ M15), *hsdR17*, *recA1*, *endA1*, *gyr A96*, *thi-1*, *relA1*] (Invitrogen)

#### 2.1.2 Culture of *E. coli* cells

##### Materials

-Luria Bertani (LB) agar medium (10 g bacto-tryptone, 5 g yeast extract, 5 g NaCl, 15 g agar per litre) (BIO101, Anachem).

-Luria Bertani (LB) medium (10 g bacto-tryptone, 5 g yeast extract, 5 g NaCl per litre) (BIO101, Anachem).

-Ampicillin (amp), 50 mg/mL stock solution (Sigma)

##### Method

LB Medium and LB agar were both purchased in tablet form. After addition of an appropriate amount of distilled water the media were autoclaved. The

medium was cooled to 50°C in a water bath. At this temperature ampicillin was added to a concentration of 100 µg/mL. The agar was poured into 82 mm Petri dishes (20 mL/plate). The agar solidified at room temperature and plates were stored at 4°C. Bacteria (either from a glycerol stock or transformed cells) were streaked or spread on to the plates. Inverted plates were incubated at 37°C.

Ampicillin was added to LB medium to a concentration of 50 µg/mL. A single colony of bacteria from an agar plate was used to inoculate 5 mL of LB-amp media and incubated overnight at 37°C in a shaking incubator. This is referred to as a starter culture.

## **2.2 Small scale isolation of plasmid DNA from *E. Coli***

### **Materials**

-Luria Bertani (LB) medium (10 g bactotryptone, 5 g yeast extract, 5 g NaCl per litre) (BIO101, Anachem).

-Qiaprep Miniprep Kit (all solutions were provided in the kit) (QIAGEN).

### **Method**

All centrifuge steps were carried out using a Tube centrifuga 5415R.

A 4 mL starter culture was divided into two 2 mL Tube tubes and centrifuged at 4,000 rpm in a bench top centrifuge for 4 minutes (min). The supernatant was discarded and the bacterial pellet was re-suspended in 150 µL of P1

buffer. The two samples, containing the resuspended bacteria, were added together. All subsequent centrifugation steps were carried out at 13,000 rpm.

Cells were lysed by the addition of 250  $\mu$ L of lysis solution, P2 and mixed gently. The lysis solution was neutralized by the addition of 350  $\mu$ L of solution N3. This is a high salt buffer, which precipitates denatured genomic DNA and proteins leaving plasmid DNA in solution.

The precipitate was pelleted by centrifugation for 10 min. The lysate is added to the QIAprep column, which fits in a collection tube. The resin in the column selectively binds plasmid DNA at high salt concentrations and elutes at low salt concentration.

The column was centrifuged for 1 min and the eluate discarded. The column was then washed with 750  $\mu$ L of PE buffer and centrifuged for 1 min and the eluate discarded. The column was centrifuged for a further 1 min to remove any traces of buffer PE. The collection is discarded and the column is placed in a fresh 1.5 mL Tube. Plasmid DNA was eluted with 50  $\mu$ L of water followed by centrifugation for 1 min.

## **2.3 Large-scale isolation of plasmid DNA from *E. Coli***

### **Materials**

- Isopropanol
- Ethanol (70%)



- TE Buffer (10 mM Tris-HCL, 1 mM EDTA pH 8)
- QIAfilter Plasmid Midi Kit (QIAGEN). Kit includes the following solutions:
  - P1, resuspension buffer (50 mM Tris-Cl (pH 8), 10 mM EDTA, 100 U/mL RNase A).
  - P2, lysis solution (200 mM NaOH, 1% w/v SDS).
  - P3, neutralization buffer (3 M potassium acetate, pH 8).
  - QBT, equilibration buffer (750 mM NaCl, 50 mM MOPS, pH 7, 15% v/v isopropanol, 0.15% v/v Triton X-100).
  - QC, wash buffer (1 M NaCl, 50 mM MOPS pH 7, 15% v/v isopropanol).
  - QF, elution buffer (1.25 M NaCl, 50 mM Tris-CL pH 8.5, 15% v/v isopropanol).

## **Method**

100 mL of LB media was inoculated with 5 mL of an overnight starter culture. The culture was incubated 37°C overnight in a shaking incubator. The culture was centrifuged at 4000 rpm (using a Sorvall Evolution RC 728411) for 15 min. The supernatant was discarded and the bacterial pellet resuspended in 4 mL of buffer P1.

Cells were lysed with the addition of 4 mL of buffer P2. The tube was inverted 4-6 times and left to stand for 5 min. 4 mL of buffer P3 was added to neutralise the lysis solution. This results in formation of a white precipitate. The lysate was immediately poured into a filter cartridge. The cartridge was left for 10 min at room temperature to allow separation of the precipitate.

The cleared lysate was filtered into a column which had previously been equilibrated with 10 mL of buffer QBT. The resin in the column selectively binds plasmid DNA. The lysate was allowed to pass through the column. Cellular metabolites and RNA were washed off the column with the addition of 2, 10 mL washes with solution QC.

A 10 mL plastic tube was placed under the column and 5 mL of elution buffer was added to the column to elute plasmid DNA. 1.5 mL of isopropanol was added to the eluate, the sample mixed well. Plasmid DNA was pelleted by centrifugation at 4°C at 8000 rpm (Sorvall Evolution RC 728411). The supernatant was discarded and the clear pellet was transferred to a 1.5 mL tube using a pipette tip. The pellet was washed with ~1.4 mL of 70% ethanol and the sample centrifuged at 13000 rpm for 10 min (Tube centrifuga 5415R). The supernatant was removed and the pellet dried in a heat block at 50°C for 10 min. The dried pellet was re-suspended in an appropriate volume of TE buffer.

## **2.4 Quantification of DNA/RNA by UV spectrophotometry**

The concentration of DNA or RNA was determined using the Nanodrop™ 1000. After setting a blank reading (TE buffer), 1 µL of DNA sample was added directly onto the reader. The absorbance of this solution was measured at 260 nm. The machine gave a reading of ng (DNA/RNA)/µL.

## **2.5 Bacterial Transformation**

### **Materials**

- Library efficiency DH5 $\alpha$  competent cells (Invitrogen).
- SOC medium (20 g tryptone, 5 g yeast extract, 5 g NaCl, 2.5 mM KCL, per litre, pH 7.5) (Sigma).
- LB/amp plates (see 2.1)

### **Method**

Competent cells were thawed on ice. Cells (10  $\mu$ L) were mixed with 1 ng of plasmid DNA or 50  $\mu$ L of cells were mixed with 2  $\mu$ L of a ligation reaction. The mixture was incubated on ice for 30 min. The cells were subsequently heat-shocked for 60 s at 42 $^{\circ}$ C and transferred back to ice. 250  $\mu$ L of SOC medium was added and the cells were incubated at 37 $^{\circ}$ C for 1 hr in a shaking incubator. 100  $\mu$ L of the bacterial culture was placed on LB/amp plates.

## **2.6 Preparation of glycerol stocks**

### **Materials**

Glycerol (100%, autoclaved)

Overnight culture of *E.coli*.

### **Method**

For long-term storage of *E. coli* cultures, 1 mL of bacterial culture was mixed with 200 $\mu$ l of glycerol in a 1.5 mL tube. The contents were mixed well and immediately stored at -70 $^{\circ}$ C.

## 2.7 Restriction endonuclease digestion of DNA

### Materials

- Restriction enzymes (NEB). Enzyme concentration was 10,000units/mL
- 10X Reaction buffer1 (NEB) 10 mM Bis Tris Propane-HCL, 10 mM MgCl<sub>2</sub>, 1 mM dithiothreitol (pH 7.0 @ 25C).
- 10X Reaction buffer 4:50 mM potassium acetate, 20 mM Tris-acetate, 10 mM Magnesium Acetate, 1 mM Dithiothreitol (pH 7.9 @ 25°C).
- BSA (10mg/mL stock solution) (NEB).

Note: the reaction buffer was selected according to the enzyme used.

### Methods

Plasmid DNA, reaction buffer (to a final concentration of 1x) and BSA to a final concentration of 0.1 µg/µL were added to a 1.5 mL tube. Different total reaction volumes (ranging from 20 to 100 µL) were used depending on the amount of DNA being digested. The restriction enzyme was added last, at a concentration of 1 unit per µg of DNA. The sample was incubated at 37°C (the optimum temperature of the restriction enzymes used). The incubation time was at least 1 hr.

When two enzymes were used, with two different optimal buffer conditions, the most compatible buffer was chosen and the amount of enzyme added modified to allow for any loss in enzyme activity.

## 2.8 Agarose gel electrophoresis of DNA fragments

### Materials

-10x Tris borate-EDTA buffer (TBE) (0.89 M Tris-base, 0.09 M Boric acid, 20 mM EDTA (pH 8)

-Agarose (BioLine)

-6x loading buffer (0.25% bromophenol blue, 0.25% xylene cyanol, 30% glycerol), stored at room temperature.

-Ethidium Bromide (EtBr) (10 mg/mL stock solution, stored at 4°C) (Fisher)

-DNA hyperladder I and V (BioLine)

### Method

A 1% agarose gel was prepared by melting 1 g of agarose in 100 mL of 1xTBE buffer in a microwave oven. EtBr was added to the mixture to a final concentration of 0.5 µg/mL. The cooled mixture was poured into a gel mould with the appropriate comb in place. The gel was left to set for at least 30 min. Once set, running buffer (1xTBE) was poured in to the gel mould placed in the gel tank. TBE was added until the gel was completely submerged. The comb was then removed.

DNA marker (10 µL, containing loading buffer) was loaded into the first well.

Three microlitres of loading buffer (on Nesco film) was mixed with each sample prior to loading the gel. The gel was electrophoresed at 60-100 volts to separate the DNA fragments. After electrophoresis the DNA fragments were visualised on a UV transilluminator.

## **2.9 Purification of DNA fragments from agarose gels**

Isolation of DNA using QIA quick Gel extraction kit.

### **Materials**

- Agarose gel (1%, w/v, supplemented with EtBr).
- Electrophoresis buffer (1xTBE)
- 6x loading buffer
- Isopropanol
- Qiaquick Gel extraction kit (QIAGEN). All solutions were supplied with the kit.

### **Method**

DNA was mixed with the loading buffer and electrophoresed on a 1% agarose gel in TBE as described above. The separated DNA fragments were visualised on a UV transilluminator. The fragment of interest was excised using a sterile blade. The piece of agarose was transferred to a 1.5 mL tube and weighed.

Three volumes of buffer QG was added to the tube (3 volumes more than the weight of the piece of agarose gel). The agarose was melted by heating to 50°C for 10 min. 1 volume of isopropanol was added. The mixture was loaded onto a QIAquick column, which had been placed inside a collection tube. The column was centrifuged for 1 min at 13000 rpm in a bench top centrifuge for 1 min. The DNA fragment binds to the resin and the eluate was discarded. All centrifuge steps in this protocol were carried out at 13000 rpm in a bench top centrifuge for 1 min.

500  $\mu$ L of Solution QG was added the column centrifuged to remove traces of agarose. 750  $\mu$ L of Solution PE was added and the column centrifuged to remove salts. After removing the eluate the column was centrifuged for a further 1 min to remove all traces of solution. DNA was eluted by adding 30  $\mu$ L of water to the column, followed by centrifugation. The amount and quality of DNA was assessed with a nanodrop spectrophotometer by determining absorbance at 260 and 280 nm.

### **2.9.1 Purification of DNA in solution**

Additional materials from method **2.9**

Buffer PB - (supplied within the Qiagen PCR purification kit)

#### **Method**

Purification of DNA in solution (from PCR reactions or binding reactions) was carried out using the above protocol but without the need to dissolve the agarose gel in buffer QG. 5 parts buffer PB was added to one part of DNA and mixed before passing through the column.

### **2.10 DNA ligation**

#### **Materials**

-DNA ligase kit (BioLine). The kit includes the following:

-Quick-stick ligase (2000 U/ $\mu$ L)

-Quick-stick buffer

## **Method**

20 ng of vector was mixed with a 3-fold molar excess of insert in a 1.5 mL Tube. The volume was adjusted to 14  $\mu$ L using sterile water. 1  $\mu$ L of QS ligase was added. Finally 5  $\mu$ L of QS buffer (4x stock solution) was added to make a total reaction volume of 20  $\mu$ L.

The reaction sample was mixed thoroughly by pipetting and incubated at room temperature for 5 min. 2  $\mu$ L of the ligation reaction was used to transform 50  $\mu$ L of competent cells. Plasmid DNA was isolated from 5 of the resulting bacterial colonies. Plasmid DNA was analysed by restriction endonuclease digestion to confirm which colony corresponds to a recombinant plasmid, resulting from the ligation reaction.

### **2.11 Polymerase chain reaction (PCR)**

All PCR reactions were carried out in a Techne Genium PCR machine.

#### **Materials**

-BioTaq DNA polymerase (BioLine)

-10x  $\text{NH}_4$  Reaction Buffer-160 mM  $(\text{NH}_4)_2\text{SO}_4$ , 670 mM Tris-HCL (pH 8.8 at 25°C). (BioLine)

-50 mM  $\text{MgCl}_2$  (BioLine)

-100 mM dNTPs (BioLine)

-Forward and reverse primers lyophilised (MWG), resuspended and stored at 100 ng/ $\mu$ l and used at a working concentration of 10 ng/ $\mu$ l.



## **Method**

The PCR consisted of 10 ng of genomic DNA or 1 ng of plasmid DNA, 1x reaction buffer, 0.2 mM dNTP mix, 0.5  $\mu$ M reverse and forward primers, 1.5mM MgCl<sub>2</sub> made up to 24.9  $\mu$ L using sterile water. Finally 0.5 U of BioTaq polymerase was added. If multiple PCR reactions were carried out, a mastermix was made and 24.9  $\mu$ L distributed to each tube before adding the taq enzyme separately. A control reaction, with no DNA template, was used as a negative control.

Amplification parameters are shown in table 2.1. The annealing temperature was dependent on the melting temperature of the primers. The melting and annealing temperature of the primers was determined using the equation in table 2.1. The amplified products were visualised using agarose gel electrophoresis.

Programme	Cycle and temperature	Time
Programme 1	1 cycle	Time
	95°C	5min
	annealing temp	30 sec
	72°C/68°C	1min/kb
Programme 2	30 cycles	
	95°C	30 sec
	annealing temp	30 sec
	72°C/68°C	1min/kb
Programme 3	1 cycle	
	72°C/68°C	10min

B

$$T_m = 69.3 + (0.41 \times (G+C)) - 650/\text{length (nt)}$$

$$\text{Annealing temperature} = ((T_{m1} + T_{m2})/2) - 6$$

### Table 2.1 PCR cycling conditions

Extension temperature was 72°C for Taq and 68°C for BioXact. The annealing temperature is dependent on the primer pair. The  $T_m$  of each primer was calculated using the equation in (B). The  $T_m$  values of both primers were used to calculate the annealing temperature.

### **2.11.1 Bio-X-act DNA polymerase**

This is a mixture of polymerase enzymes that display 3'-5' proof reading activity in addition to 5'-3' polymerase activity. This reduces the chance of misincorporated nucleotides during primer extension. This enzyme was used to produce constructs used in reporter gene assays as accurate replication of the template was essential.

#### **Material**

BIO-X-ACT Long DNA polymerase (4 U/ $\mu$ L) (BioLine)

-OptiBuffer (10x reaction buffer) (BioLine)

-dNTP mix (100 mM) (BioLine)

-Forward and reverse primers (lyophilized) (MWG) resuspended and stored at 100 ng/ $\mu$ L and used at a working concentration of 10 ng/ $\mu$ L.

-MgCl<sub>2</sub> (50 mM) (BioLine)

#### **Method**

The PCR reaction consisted of 10 ng of human genomic DNA, 1x reaction buffer, 0.2 mM dNTP mix, 4 mM MgCl<sub>2</sub> and 0.5  $\mu$ M reverse and forward primers. The volume of the reaction was made to 24.5  $\mu$ L. Finally, 1 unit of Bio-X-Act long was added.

The amplification parameters were devised in the same way as for BioTaq polymerase, but the optimum extension temperature is 68°C rather than 72°C. The extension time is also increased to 1 min/1kb).

## 2.12 Reverse transcriptase polymerase chain reaction

### Materials

-First-Strand cDNA Synthesis Kit containing the following materials:

-Superscript II reverse transcriptase (50 U/ $\mu$ L)

-Reaction buffer (200 mM Tris-HCL (pH 8.4), 500 mM KCl)

-dNTP mix (10 mM)

-MgCL<sub>2</sub> (25 mM)

-RNase OUT (recombinant ribonuclease inhibitor (40 U/ $\mu$ L))

-Oligo (dT) 12-16 (0.5  $\mu$ g/ $\mu$ L)

-Diothiothreitol (DTT) (0.1 M)

### Method

In a 1.5 mL tube an RNA/Primer mix was made consisting of up to 5  $\mu$ g of total RNA, 1 mM of dNTPs, 1  $\mu$ L Oligo (dT) 12-18 and made up to 10  $\mu$ L with DEPC-treated water. The RNA/Primer mix was then incubated at 65°C in a heat block for 5 min. During this time the reaction mixture was prepared. This consisted of 2  $\mu$ L Reaction buffer, 4  $\mu$ L MgCl<sub>2</sub>, 2  $\mu$ L DTT and 1  $\mu$ L of RNase OUT (40 U/ $\mu$ L). Nine microlitres of reaction mixture was added to each RNA/Primer mixture which was incubated at 42°C in a heat block. Fifty units of superscript enzyme was added per tube and samples were incubated for 50 min at 42°C. The reaction was terminated by increasing the incubation temperature to 70°C for 15 min. This denatured the enzyme and therefore stopped the reaction. The samples were collected by brief centrifugation and 1  $\mu$ L of RNase H was added followed by incubation at 37°C for 20 min to

degrade any RNA. The DNA product was used as a template for PCR amplification.

## **2.13 TOPO T/A cloning**

### **Materials**

-TOPO TA cloning kit for sequencing (Invitrogen). The kit included in the following components:

-PCR4-TOPO vector (Fig.2.1) This was provided as a solution which contained 10 ng plasmid DNA/mL in 50% (v/v) glycerol, 50 mM Tris-HCL, (pH 7.4 (at 25°C)), 1 mM EDTA, 2 mM DTT, 0.1% (v/v) Triton X-100, 100 mg/mL BSA, 30 µM phenol red.

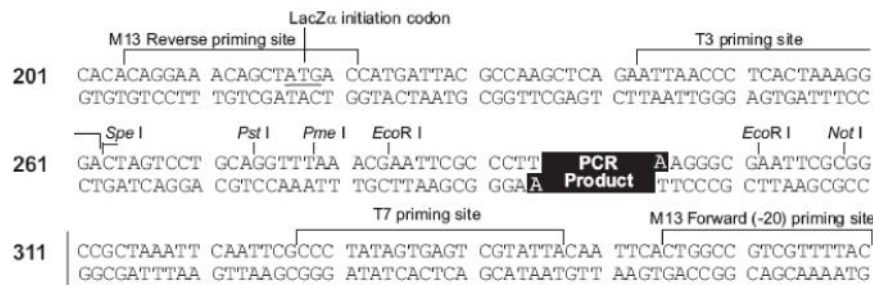
-Salt solution (1.2 M NaCl, 0.06 M MgCl<sub>2</sub>)

### **Method**

The TOPO vector is a linearised vector and possesses single thymine overhangs. The PCR products, produced by the Bio-X-act enzyme, have adenosine bases at the 3' end of each DNA strand. The adenine overhangs of the PCR product can be ligated to the thymine overhangs from the TOPO vector and the DNAs are ligated with a DNA ligase that is covalently bound to the linearised vector.

In a 1.5 mL Tube, 4 µL of a PCR product was mixed with 1 µL of salt solution and 1 µL of PCR 4-TOPO vector. The tube was incubated at room temperature for 5min. 2 µL of this reaction was used to transform 50 µL of

competent cells. DNA was isolated from bacterial colonies cultured on ampicillin agar plates.



**Comments for pCR<sup>®</sup>4-TOPO<sup>®</sup>  
3956 nucleotides**

- lac* promoter region: bases 2-216
- CAP binding site: bases 95-132
- RNA polymerase binding site: bases 133-178
- Lac repressor binding site: bases 179-199
- Start of transcription: base 179
- M13 Reverse priming site: bases 205-221
- LacZ $\alpha$ -*ccdB* gene fusion: bases 217-810
- LacZ $\alpha$  portion of fusion: bases 217-497
- ccdB* portion of fusion: bases 508-810
- T3 priming site: bases 243-262
- TOPO<sup>®</sup> Cloning site: bases 294-295
- T7 priming site: bases 328-347
- M13 Forward (-20) priming site: bases 355-370
- Kanamycin promoter: bases 1021-1070
- Kanamycin resistance gene: bases 1159-1953
- Ampicillin (*b/a*) resistance gene: bases 2203-3063 (c)
- Ampicillin (*b/a*) promoter: bases 3064-3160 (c)
- pUC origin: bases 3161-3834
- (c) = complementary strand

**Figure 2.1 pCR<sup>®</sup>4-TOPO vector map (Invitrogen catalogue)**  
 The pCR<sup>®</sup>4-TOPO vector was used to clone PCR products.

## **2.14 Isolation of RNA from cells, mouse and human tissues**

### **Materials**

- Ribopure RNA extraction kit (Ambion) containing:
- TRI reagent
- Filter cartridges
- Collection tubes (2 mL)
- 1-bromo-3-chloropropane (BCP)
- Wash solution concentrate
- Ethanol
- Elution buffer

### **2.14.1 Tissue preparation**

Adult C57BL/6 mice were sacrificed. The relevant tissues were excised and stored in RNAlater (SIGMA). To isolate RNA, 100 mg of tissue was transferred to a 1.5 mL Tube containing 1 mL of TRI reagent. Using a hand-held tissue homogeniser tissues were homogenised and then left at room temperature for 5 min. After centrifugation for 10 min at 12,000 g, insoluble material is removed from the top of the homogenate.

### **2.14.2 RNA isolation from tissue cultured cells**

Cells were grown in a monolayer to confluency in 35-mm cell culture dishes. TRI reagent was added directly to the culture dish. Cell clumps were removed by pipetting up and down several times. The mixture was then transferred to a 1.5 mL tube.

100  $\mu\text{L}$  of BCP was added per 1 mL of homogenate and vortexed at maximum speed for 15 s. This mixture was left to incubate at room temperature for 5 min. After centrifugation at 12000  $g$  for 10 min at 4°C, the mixture is separated into a lower, red, organic phase (phenol-BCP phase); an interphase; and a colourless, upper, aqueous phase.

The RNA remains in the aqueous phase while DNA and proteins are in the interphase and organic phase. The aqueous layer (around 400  $\mu\text{L}$  of 1 mL) is transferred to a new 1.5 mL tube. 200  $\mu\text{L}$  of 100% ethanol is added to 400  $\mu\text{L}$  of the aqueous phase and the sample vortexed immediately for 5 s. This avoids precipitation of RNA.

The sample was transferred to a filter cartridge, which binds RNA. The filter cartridge is placed inside a collection tube and centrifuged for 1 min at 12,000  $g$  in a bench top centrifuge. The eluate is discarded and 500  $\mu\text{L}$  of wash solution is applied to the column and centrifuged for 1 min. This is then repeated once.

The filter cartridge is then transferred to a new collection tube and 100  $\mu\text{L}$  of elution buffer is added to the cartridge and centrifuged for 1 min. The eluate contains the RNA. The RNA is then used as the template to create cDNA.



## **2.15 COS-7 AND 3T3-L1 cell culture**

### **Materials**

- COS-7, 3T3-L1 cells (Obtained from European Collection of Animal cell culture (ECACC™))
- Dulbecco's Modified Essential Medium (DMEM) (Gibco). Supplemented with 50 µg/mL of gentamycin (Gibco), 10% foetal calf serum (Gibco). Once supplemented the medium is referred to as complete medium.
- PBS (1x) (137 mM NaCl, 2.7 mM KCL, 10 mM Na<sub>2</sub>HPO<sub>4</sub>, 1.8 mM KH<sub>2</sub>PO<sub>4</sub>) (PAA).

### **Method**

COS-7 and 3T3-L1 cells were seeded into Nunclone tissue culture flasks (MG Scientific) and grown in a Heraeus incubator (Kendro), at 37°C with 5% CO<sub>2</sub> until the cells were 70-75% confluent. Cells were then washed twice with PBS, detached with 4mM EDTA in 1x PBS and pelleted by centrifugation at 1900 rpm for 2 min at room temperature in a bench top centrifuge (Sigma). The pellet was resuspended in complete medium and seeded on to 24-well plates. Cells were seeded 24 hr prior to transfection.

### **2.15.1 HK-2 cell culture**

#### **Materials**

- Defined Keratinocyte-SFM (1X) liquid (Gibco)

#### **Method**

Cells were cultured in the same conditions as COS-7 and 3T3-L1 cells.

## **2.16 Transient transfection of cells**

The chosen method of transfection of cultured cells was lipid-mediated transfection (Felgner and Ringold, 1989). The chosen lipid was LTX (Invitrogen). This is a highly efficient lipid for the transfection of cells in culture. The lipid forms vesicles that associates with DNA and is thought to aid the transfer of DNA into cells by fusion of vesicles with the cell membrane.

### **Materials**

- LTX transfection reagent (Invitrogen)
- Opti-MEM® I Reduced Serum Media without serum (Invitrogen)

### **Method**

24 hrs prior to transfection, cells were transferred into 24-well plates, so on the day of transfection the cells were 80-90% confluent. Each well represented an individual transfection experiment and each transfection was carried out in triplicate. The amount of DNA was optimised for each cell line and was therefore dependent on the cells that were transfected (section 4.1.2). COS-7 and 3T3-L1 cells were transfected with 0.4 µg of reporter construct DNA and 0.05 µg of pRL-TK (internal control plasmid). HK-2 cells were transfected with 1 µg of reporter plasmid and 0.125 µg of pRL-TK. A 1:1 ratio of transfection was shown to be suitable for COS-7, 3T3-L1, and HK-2 transfection. A mastermix solution was made for triplicate experiments. DNA was added to 300 µl of Opti-MEM® Reduced Serum Media without serum. LTX was added to this solution at a ratio of 1:1, e.g. for transfection of COS-7

cells, 0.45 µg of DNA is used for each reaction. This is multiplied by three as transfection is carried out in triplicate. This results in a total of 1.35 µg. 1.35 µL of LTX was added to the solution. The solution was gently mixed and left at room temperature for 30 min. After 30 min, 100µL of the solution was added directly into the well. Culture media was replaced after 24 hours with the growth medium and cells assayed after 48 hours.

## **2.17 Isolation of Nuclear proteins from cell lines**

### **Materials**

-PBS (1x) (137 mM NaCl, 2.7 mM KCl, 10 mM Na<sub>2</sub>HPO<sub>4</sub>, 1.8 mM KH<sub>2</sub>PO<sub>4</sub>).

-Hypotonic buffer (10 mM HEPES (pH 7.9), 10 mM KCl, 0.2 mM EDTA, 0.1 mM EGTA). Immediately before use, the buffer was supplemented with a protease inhibitor cocktail (Roche) and 1 mM DTT.

-Roche Complete Protease Inhibitor Cocktail Tablets - Mixture of several protease inhibitors with broad inhibitory specificity. For the inhibition of serine, cysteine, and metalloproteases.

-NP-40 (Sigma)

-Nuclear lysis buffer (20 mM HEPES (pH 7.9), 0.4 M NaCl, 1 mM EDTA). Immediately before use the buffer was supplemented with 1 mM DTT, protease inhibitor cocktail (Roche) and 0.02% v/v NP-40.

-Dialysis buffer (20 mM HEPES (pH 7.6), 1 mM EDTA (pH8)). Buffer was autoclaved and stored at 4°C. Immediately before use, 1 mM DTT was added to the buffer.

## **Method**

Approximately  $10^7$  cells were pelleted by centrifugation at 2500 rpm for 5 min in an Eppendorf bench centrifuge. The pellet was washed with 1x cold PBS and resuspended in 1 mL of cold hypotonic buffer. Cells were incubated on ice for 15 min. 0.4% (v/v) NP-40 was added to the cells. Cells were passaged through a 25G needle, 5-6 times to lyse the cells. The lysate was centrifuged at 10000 *g* for 2 min at 4°C. Supernatant was discarded and 300 µL of nuclear lysis buffer was added to the nuclear pellet. The samples were rolled on a denly spiramix for 30 min at 4°C. The supernatant (the nuclear extract) was transferred into another tube and was dialysed to remove excess salt. A 500 µL sample was placed in a Slide-a-Lyzer® Dialysis cassette (Pierce). The cassette was attached to a buoy and immersed in 1 litre of cold dialysis buffer in a glass beaker which contained a magnetic stirrer. The dialysis took place in the cold room and the buffer was constantly stirred. After 2 hours the buffer was replaced with fresh buffer. After an additional 2 hours of dialysis the sample was removed from the cassette and transferred into a 1.5 mL Eppendorf tube. The samples were aliquoted and stored at -70°C.

### **2.18 Dual-luciferase® reporter assay and pGL3 vectors**

The pGL3-Basic vector contains a multiple cloning site upstream of the firefly (*Photinus pyralis*) luciferase gene. FMO1 DNA sequences upstream of transcriptional start sites were cloned within the multiple cloning site upstream of the luciferase gene. The ability of these sequences to drive transcription of the reporter gene was measured. The cells were simultaneously transfected with a second vector, pRL-TK, which contains a luciferase gene sequence

from *Renilla reniformis* (Renilla) under the control of the herpes simplex virus thymidine kinase (HSV-TK) promoter.

The basis of the Dual-Luciferase reporter assay is the different substrate requirements for the firefly and the renilla luciferase proteins. The firefly luciferase activity is measured first by mixing the cell lysate (containing the expressed luciferase protein) with the Luciferase assay reagent II (LARII). To the same well, the substrate for the Renilla luciferase protein (Stop and Glo® reagent) is added and its activity measured. The Stop and Glo buffer also inhibits the firefly luciferase reaction measured previously. This allows both luciferase protein activities to be measured within the same sample. The *Renilla* reporter acts as an internal transfection control and allows for the normalisation of the firefly luciferase gene expression.

## **Materials**

-PBS (1x) (137 mM NaCl, 2.7 mM KCl, 10 mM Na<sub>2</sub>HPO<sub>4</sub>, 1.8 mM KH<sub>2</sub>PO<sub>4</sub>).

(PAA)

-Dual-Luciferase® Reporter assay System (Promega) contains

-Passive Lysis Buffer (PLB, 5x) (11.5 g Na<sub>2</sub>HPO<sub>4</sub>, 2 g KH<sub>2</sub>PO<sub>4</sub>, 80 g NaCl, 2 g KCl per litre. Final pH 7.4)

-Luciferase Assay Buffer II and substrate

-Stop and Glo® substrate and buffer

-Vectors: pGL3 basic, pGL3 control, pRL-TK

-RNA produced from the vector pSP-LUC containing the P2 FMO1 leader sequence.

## **Method**

COS-7, HK-2, 3T3-L1 fibroblasts and 3T3-L1 adipocytes were transfected with the above vectors as described previously. Cells were harvested 48 hours post transfection. This was shown to be the optimal conditions for luciferase activity. The medium was removed and cells were washed 1x with PBS. 3T3-L1 fibroblasts and adipocytes require careful removal of PBS so cells remain intact. The amount of passive lysis buffer (PLB) added depended on the area of cells to be lysed. COS-7, 3T3-L1 fibroblasts, and HK-2 cells were lysed within 24-well plates. The amount of PLB added was 100  $\mu$ L. 3T3-L1 adipocytes were grown in 18 mm dishes and 200  $\mu$ L of PLB was added. The plates were left on a rocking platform for 15 min. The lysate was removed and transferred into a 1.5 mL tube. Samples were pipette up and down and centrifuged briefly before performing the dual-luciferase assay.

One-hundred microlitres of Luciferase assay buffer was added to wells of a black 96-well plate. Twenty microlitres of cell lysate was added to each well. Luminescence was measured using the micro plate reader, PHERAstar. Timing of the addition of cell lysate ensured the luciferase reaction took place for an equal amount of time within each well. A delay in measurement of 10 s took place for each well. One hundred microlitres of the Stop and Glo reagent was added to the wells and the Renilla luciferase activity was measured in the same format as the luciferase activity. The final luciferase reading for each assay was in the form of a ratio of firefly: renilla luciferase activity.

The control plasmid, pGL3-control, contains the SV40 promoter upstream of the firefly luciferase reporter gene and an SV40 enhancer located downstream of it. Each cell line was transfected with this vector as a positive control for the transfection procedure. The vector pGL3-Basic was used as a negative control.

## **2.19 RNA Transfection**

### **Materials**

- COS-7 cells
- RNA produced in-vitro (section 2.27) from pSP-ATG and pSP ACG vectors (section 2.20.2 for cloning procedure)
- LTX lipid transfection reagent (Invitrogen)

### **Method**

Cells were transfected as shown previously (section 2.16). The amount of RNA used for each individual transfection was 1 µg. It was shown that a 2:1 ratio of LTX lipid reagent to RNA was optimal for transfection (section 4.7).

## **2.20 Reporter constructs used for transfection studies**

### **2.20.1 *FMO1* promoter reporter constructs**

The promoter fragments -255\_-128, -858\_-128, -1243\_-128, -2433\_-128 and -858\_-343, -1243\_-343, -2433\_-343 were amplified from genomic DNA (BioLine Cat.no.BIO-35025) by PCR (see section 2.11).

For cloning of promoter fragments, *HindIII* and *SacI* restriction endonuclease sites were integrated into the primer sequences (see appendix). The amplified products were cloned into the TOPO vector as described above. Upon cleavage out of the TOPO vector the fragments were purified from an agarose gel (see above) and ligated to a *HindIII/SacI* digested pGL3-Basic vector. The resulting reporter constructs are defined as pGL-255\_-128, pGL-1243\_-128, pGL-2433\_-128 and pGL-858\_-343, pGL-1243\_-343, pGL-2433\_-343.

### **2.20.2 *FMO1* P2 leader sequence construct**

The *FMO1* P2 leader sequence was cloned into the pSP-luc vector to test the significance of a polymorphism which introduces an in-frame ATG 12 bp upstream of the translational start site (Fig.2.3). The translation initiation codon of the luciferase gene is within an *NcoI* restriction site; this site and a *KpnI* site further upstream were used to clone the P2 leader sequence within the vector. This positioned the *FMO1* leader sequence directly in-frame with the luciferase gene. Due to the 3' sequence similarities between the *FMO1* sequence and the *NcoI* site, the *NcoI* site could form part of the leader sequence.

Once the leader sequence was cloned, the leader sequence contained an additional cytidine residue from the *NcoI* restriction site. This was deleted by site-directed mutagenesis (section 2.28), ligated (section 2.10) and transformed into competent cells (section 2.5). The plasmid was isolated and the upstream ATG was mutated to ACG using site-directed mutagenesis.



Both plasmids were prepared using large-scale purification and transfected into COS-7 cells. The luciferase activity was measured after 48 hr transfection using the dual luciferase assay reporter system (section 2.18).

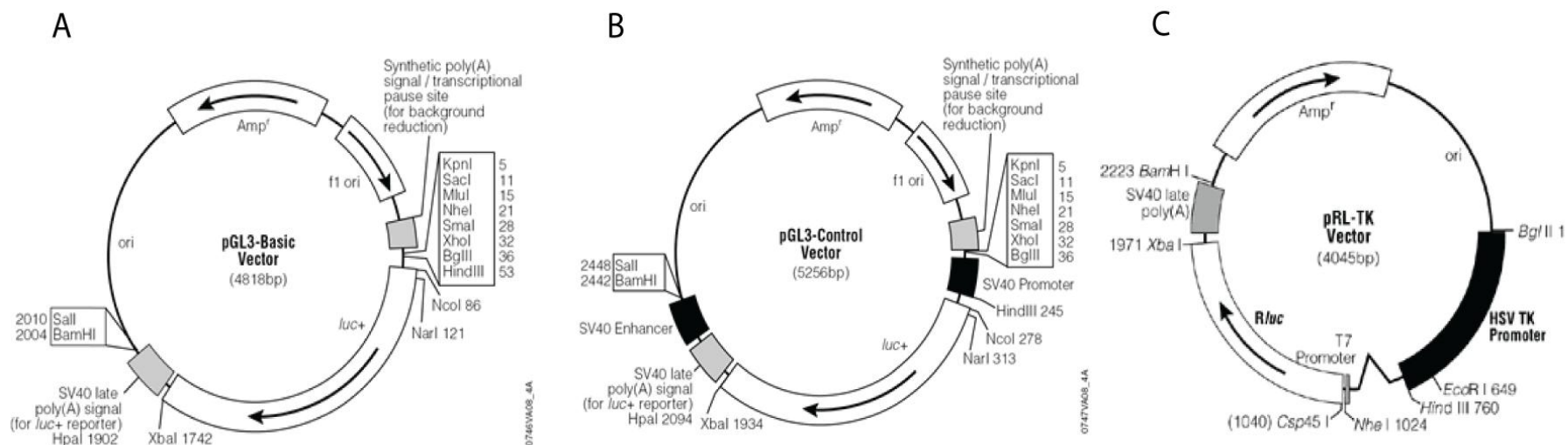


## Figure 2.2 Maps of pGL3 vectors and the pRL vector

The plasmids that were used to analyze *FMO1* reporter gene constructs in combination with the Dual-Luciferase® Reporter assay system. DNA sequences upstream of the *FMO1* transcriptional start sites were cloned adjacent to the **(A)** pGL3-Basic vector. **(B)** The pGL3-Control vector containing the SV40 promoter sequence and was used as a positive control within the reporter gene assay. The pGL3 plasmids contain a luciferase gene sequence which codes for luciferase from the firefly *Photinus pyralis*. The third plasmid **(C)** pRL-TK contains a luciferase gene sequence which codes for the luciferase protein from the *Renilla reniformis*. The pRL-TK plasmid is used to normalise the expression of firefly luciferase to control for transfection efficiency. The plasmid images are taken from the Promega catalogue.

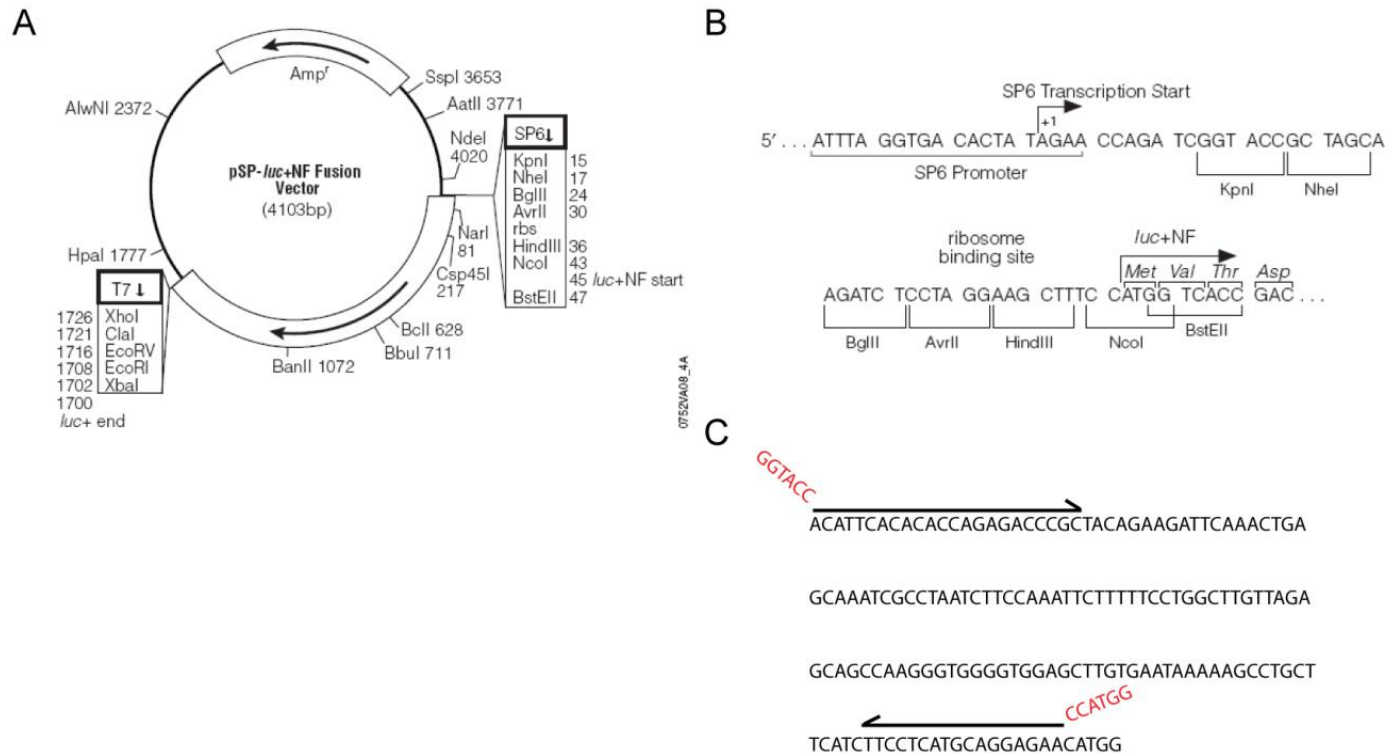


### Figure 2.3 Cloning of the FM01 P2 leader sequence into the pSP-luc+NF fusion vector

**(A)** The pSP-luc vector is shown containing a multiple cloning site upstream of the start site of luciferase and at the end of the luciferase gene. The vector contains a site for the SP6 bacterial polymerase to bind. **(B)** The sequence directly upstream of the SP6 binding region and the start of the luciferase gene. **(C)** Illustration of primers used to amplify the P2 leader sequence. The plasmid image and sequence is taken from the Promega catalogue.

## **2.21 Protein concentration determination**

### **Materials**

- DC Protein Assay (BioRad). This is a colorimetric assay for protein concentration. The reaction is based on the Lowry assay (Lowry et al., 1951). The kit is supplied as two reagents, Reagent A (alkaline copper tartrate solution) and Reagent B (Folin reagent).
- BSA (1.4 mg/mL) (BioRad).

### **Method**

BSA was used as a standard. Various amounts of BSA, ranging from 2  $\mu\text{g}$  to 20  $\mu\text{g}$ , were pipetted into test tubes. The volume of each sample was adjusted to 100 $\mu\text{L}$  with water. At the same time 10  $\mu\text{L}$  of mouse nuclear protein or cell-line protein was placed in a test tube and adjusted to 100  $\mu\text{L}$ .

Five-hundred microlitres of reagent A was added to each test tube and vortexed. Four millilitres of reagent B was added to the tube and the sample vortexed immediately. The tubes were incubated at room temperature for 30 min. During this time the samples turned blue. The absorbance of each sample at 750 nm was measured in a spectrophotometer. The standards were measured to produce a standard curve. The protein concentration of the sample was determined from the standard curve.

## 2.22 Protein Gel Electrophoresis (SDS/PAGE)

### Materials

- Protogel solution (30% w/v acrylamide, 0.8% bisacrylamide (National Diagnostics). The amount of protogel used determines the acrylamide concentration of the gel.
- TEMED (BioRad)
- Ammonium Persulfate (10%)
- SDS (0.1%, w/v)
- Tris-HCl (1.5 M, pH8.8)
- Stacking solution (0.5 M Tris-HCl, 0.4% (w/v) SDS, pH 6.8).
- Running buffer (0.025 M Trizma base, 0.192 M Glycine, 0.1% w/v SDS)
- Protein loading buffer (30% v/v glycerol, 0.2% w/v Bromophenol blue, 0.2% w/v xylene cyanol) (10x)
- SDS PAGE broad range markers (BioRad)
- $\beta$ -mercaptoethanol
- Coomassie staining solution (0.25% w/v Coomassie brilliant blue dye, 45% methanol, 10% glacial acetic acid)
- De-staining solution (45% methanol, 10% glacial acetic acid)

### Method

The integrity of the proteins from cell-line and tissue nuclear extracts was assessed by electrophoresis of the extracts on a 10% denaturing SDS-polyacrylamide gel. 50mL of gel mixture contained 16.65 mL protogel, 12.5mL Tris-HCl (pH 8.8), 0.1% (v/v) SDS and 19.8 mL water. This solution was supplemented with 0.5mL of ammonium persulfate and 50  $\mu$ L TEMED and

was poured into a gel mould and overlaid with 0.1% SDS. The gel was allowed to set overnight.

The resolving gel was overlaid by 10 mL of 3% stacking gel (1.3mL Protogel, 2.5 mL stacking buffer, 6.1 mL water, 50  $\mu$ L ammonium persulphate and 10  $\mu$ L TEMED). The stacking gel was left to set for 1 hr.

The protein samples were mixed with an equal volume of loading buffer and boiled for 3 min.  $\beta$ -mercaptoethanol was added to each sample to a final concentration of 20% (v/v). The samples were centrifuged for 2 min and loaded on a gel. The gel was electrophoresed with running buffer at 25 mA until the proteins stacked and then at 35 mA for separation.

After electrophoresis the gel was stained overnight with Coomassie blue staining solution.

## **2.23 Electrophoretic Mobility Shift assay**

### **Materials**

- Infra-red labelled forward and unlabelled reverse primers (10ng/ $\mu$ l)
- Binding buffer (50 mM hepes (pH 7.6), 2.5 mM DTT, 60% glycerol (v/v), 250 mM NaCl, 0.25% NP40 (Sigma)). Aliquots of buffer were stored at -20°C.
- Annealing buffer (10x) (0.1 M Tris-HCl (pH 8), 0.1 M  $MgCl_2$ , 0.5 M NaCl)
- Poly dl/dC (dissolved in 5 mM NaCl to a final concentration of 4 $\mu$ g/ $\mu$ L and stored in aliquots at -20°C) (Sigma).

- Protogel solution (30% w/v acrylamide, 0.8% bisacrylamide) (National Diagnostics)
- Tris borate-EDTA buffer (TBE) (10X) (0.89 M Tris-base, 0.09 M Boric acid, 20 mM EDTA (pH 8)).
- TEMED (BioRad)
- Ammonium persulfate (10%) (National Diagnostics)
- 60% glycerol
- Proteinase K (1.5 mg/mL) (Qiagen)
- SP1 competitive oligonucleotides (Eurofins MWG)

## **Method**

A 4% non-denaturing polyacrylamide gel was made. 50mL of the gel solution contained 6.66 mL of protogel, 2.5 mL of TBE (10x), 40.29 mL water, 50µl TEMED, 50 µL ammonium persulfate. The mixture was poured into a mould with a comb and the gel was allowed to set at 4°C overnight.

Nuclear extracts were thawed on ice. 10 µg of extract was mixed with 4 µL of binding buffer and 1 µL of Poly dl/dC. The volume of the binding reaction was adjusted to 20 µL with water and incubated on ice for 10 min.

10 ng of an appropriate DNA fragment, which has been labelled at the 5'end with an IR-700 dye, was added to the binding reaction. The binding reaction was incubated for a further 30 min to allow nuclear proteins to bind to the DNA. A binding reaction, without the labelled DNA, was also set-up. Also, in further reactions proteinase K (5 µg) was added to the binding reaction after the 30 min incubation. These reactions were further incubated at 37°C for 15 min, before loading on to the gel.

The samples were mixed with 2  $\mu$ L of 60% glycerol. This is to allow the sample to enter the wells efficiently. The samples were loaded on to a gel that had been pre-run for 30 min. This is to allow for the correct flow of charged ions. The gel was electrophoresed at 150V at 4°C in 0.5x TBE in a PROTEAN II xi cell-electrophoresis apparatus (Bio-Rad) for 4 hours. After electrophoresis the gel was removed with gel plates attached and imaged using an Odyssey® Infrared Imaging System.

In some instances, 100-fold molar excess of an unlabelled competitor oligo was added to the binding reaction. The competitor DNA used contained consensus binding sites for transcription factors predicted to bind within the FMO1 promoters. Competition oligonucleotides were made by annealing single stranded oligos to create a double stranded oligo. The oligos were annealed by adding equimolar amounts of each oligo in 1x annealing buffer. The oligos were annealed by heating to 95°C in a heat block for 5 minutes. The heat block was switched off and cooled to room temperature to allow the annealing of oligos.

## **2.24 Real-time PCR**

Real-time PCR was used to quantify different mouse Fmo1 transcripts. The cDNA used for real-time PCR experiments were synthesized as described previously. The Bio-Rad iCycler iQ5 Real-time PCR instrument was used to carry out all real-time PCR experiments.



## **Materials**

-mastermix (PrimerDesign)

-Forward and reverse primers at 10 ng/μL (PrimerDesign)

-cDNA (see section 2.12)

## **Method**

Real-time PCR reactions were made up of 2x master mix, 0.5μM forward and reverse primers, RNase free water, and cDNA template. A mastermix was made for each gene to be quantified. This contained 2x mastermix, 0.5 μM forward and reverse primers, and RNase free water. The mastermix was added to wells of a 96-well plate. The cDNA to be used was diluted by 10-fold prior to its production. Five microlitres of the diluted cDNA was individually added to each well. The plates were centrifuged briefly in a 5804 Eppendorf centrifuge at a speed of 1000 rpm. The samples were analysed using the Bio-Rad iCycler iQ5 Real-time PCR instrument. Amplification parameters are shown in table 2.2. The annealing temperature was set at 60°C as all primers used are designed to amplify most efficiently at this temperature. After amplification, a melt curve was undertaken to determine the number of products being formed within the PCR reaction.

<b>Programme</b>	<b>Cycle and temperature</b>	<b>Time</b>
<b>Programme 1</b>	<b>1 cycle</b>	
	95°C	10 min
	annealing temp/extension	1 min
<b>Programme 2</b>	<b>40 cycles</b>	
	95°C	15 sec
	annealing temp/extension	1 min
<b>Programme 3</b>	<b>80 cycles</b>	
	60°+0.5°C	10 sec

**Table 2.2 PCR cycling used for quantitative real time PCR**

Cycling reactions shown above were used for all real-time PCR experiments. Cycling conditions for a DNA melt curve are shown as Programme 3.

### **2.24.1 Calculation of relative amounts of FMO1 transcripts within and between tissues**

The quantities obtained from the Bio-Rad iCycler iQ5 Real-time PCR instrument are ct values. A ct value is the cycle number at which the exponential phase of the amplified product is observed. The point at which the  $C_t$  value is taken is manually determined. The  $\Delta\Delta C_t$  method was used to calculate fold differences between samples and relative differences in amount. The  $\Delta\Delta C_t$  makes the assumption that the number of amplicons doubles after each cycle. This assumption can be made in these real-time PCR experiments as the primers have been pre-determined to be close to 100% efficient. The data can be expressed in fold difference or relative quantities. I have used both throughout my research.

To determine fold difference between samples, the ct value is normalised to the reference gene ct value for that sample. This gives a relative  $C_t$  value. This  $C_t$  value is then converted from a logarithmic function to a linear function. This value will represent the relative number of molecules of the transcript within the sample. This value, which comparisons would be made to, is converted to 1 and all other values will be relative to this.

To determine the relative difference the  $C_t$  value is linearly converted before being normalised to the reference gene. The linear function of the sample is normalised by the linear function of the reference gene by dividing the sample into the reference value. This gives a sample value relative to the reference gene.

## 2.25 3T3-L1 differentiation

### Materials

-3T3-L1 cells were purchased from the ECACC™ and ATCC™®

-3T3-L1 pre-adipocyte medium -DMEM with 4 mM L-glutamine adjusted to contain 1.5 g/L sodium bicarbonate and 4.5 g/L glucose [ATCC™®; Cat. No. 30-2002], 90%; calf bovine serum, and 10% [ATCC™®; Cat. No. 30-2030]

-3T3-L1 Differentiation medium (ZenBio) (cat# DM-2-L1) – DMEM / Ham's F – 12 medium (1:1, v/v), HEPES pH 7.4, Foetal bovine serum (FBS), biotin, pantothenate, human Insulin, dexamethasone, penicillin, streptomycin, amphotericin B, isobutylmethylxanthine, PPAR $\gamma$  agonist.

-3T3-L1 Adipocyte medium (ZenBio) (cat# AM-1-L1) - DMEM / Ham's F – 12 medium (1:1, v/v), HEPES pH 7.4, foetal bovine serum (FBS), biotin, pantothenate, human insulin, dexamethasone, penicillin, streptomycin, amphotericin B.

### Method

Upon arrival from the supplier, 3T3-L1 cells were plated and grown in 3T3-L1 pre-adipocyte medium to a low density (30-50%) and then were stored in DMSO within liquid nitrogen. This is to ensure the cells do not contact each other, as this will result in differentiation being compromised. A new stock of cells was used every time a differentiation experiment was undertaken. Cells were seeded into Nunclone T75 tissue culture flasks (MG scientific) and grown in a Heraeus incubator at 37°C. At 50% confluency, cells were washed twice with PBS, detached with 0.25% trypsin-EDTA in 1x PBS and pelleted by centrifugation at 1900 rpm for 2 min, at room temperature, in a bench top centrifuge (Tube). The pellet was resuspended in pre-adipocyte medium and seeded into either Nunc T75 flasks or 24-well tissue culture

plates depending on the amount of adipocytes required. Cells were grown to 100% confluency in 1mL of pre-adipocyte media (24-well plate) or 20mL (T75 flask) and left for a further two days. The pre-adipocyte media was removed and replaced with 3T3-L1 differentiation media. This remained on the cells for 3 days. A percentage of the 3T3-L1 differentiation media was removed (0.6 mL for 24-well format, 12 mL for T75 format) and replaced with 3T3-L1 maintenance media (0.8 mL for 24-well format, and 16 mL for T75 format). The cells were left for at least a further seven days before cells were used for experiments. The media was changed every 2-3 days depending on media coloration.

## **2.26 3T3-L1 adipocyte nucleofection**

### **Materials**

-3T3-L1 adipocytes (see section 1.20)

-Nucleofector solution L (Lonza)

-DMEM [ATCC™®; Cat. No.30-2002], 10% foetal bovine serum [ATCC™®; Cat. No. 30-2020]

-Plasmid DNA

### **Method**

3T3-L1 adipocytes were differentiated as described previously. Cell-culture medium was removed from the adipocytes. The cells were washed once with PBS and subsequently trypsinised using 0.25% Trypsin-EDTA. Cells were incubated for 10 minutes at 37°C. Cells were removed and the solution within the flask moved around the cell to help cells to become detached. Once cells were detached, the trypsin was neutralised using post-differentiation medium. The cells were pipetted up and down to remove clumps of cells. The culture media was pipetted into Falcon tubes and

centrifuged at 90 *g* for 10 minutes at room temp. Cell media was removed completely. 100  $\mu$ L of nucleofector solution L was added to the cell pellet and pellets gently resuspended by pipetting up and down. Once resuspended, the DNA for transfection was added to the cell/solution L sample and mixed gently by pipetting. This solution was then transferred to a cuvette and placed in the nucleofector. The nucleofection conditions have been pre-optimised; by the manufacturer, for 3T3-L1 adipocytes and the program used is A-033. After nucleofection the cells were transferred directly into an 18 mm gelatin-coated culture dish, which had been pre-incubated at 37°C, and contained post-differentiation media. The cells were gently placed into the incubator and left overnight. The next day the media was changed to remove dead cells (caused as a result of the nucleofection). Reporter gene assays were carried out after 48 hr using the dual reporter luciferase assay (described in section 2.18).

## **2.27 *In-vitro* RNA production**

### **Materials**

- Plasmid template
- mMESSAGE mMACHINE® kit (Ambion) containing:
  - SP6 Enzyme mix – buffered 50% glycerol containing RNA polymerase, RNase inhibitor, and other components
  - 10x Reaction buffer
  - 2xNTP/CAP – neutralised buffer solution containing 10 mM ATP, CTP, UTP and 2 mM GTP and 8 mM cap analogue
  - TURBO DNase I (2U/ $\mu$ l)

-Ammonium acetate stop solution – 5 M ammonium acetate solution, 100 mM EDTA

-Lithium chloride precipitation solution - 7.5 M lithium chloride, 50 mM EDTA

## **Method**

RNA was transcribed *in vitro* from the pSP-luc plasmid containing the FMO1 P2 leader sequence (see section 2.20.2 for cloning protocol). The plasmid was first linearised with restriction digest (see section 2.7) and was purified by being passed through a Qiagen silica based column (see section 2.9.1). The DNA was quantified spectrophotometrically (see section 2.4).

1 µg of DNA was added to a microfuge tube. 10 µl of 2xNTP/CAP, 2 µL 10x reaction buffer and 2 µL of enzyme mix was added to this and made up to a total reaction volume of 20 µL. The reaction mixture was incubated for 2h at 37°C. 1 µL of turbo DNase I was added and the reaction was incubated for a further 15 min to digest the template DNA. The RNA produced from the reaction was purified by lithium chloride precipitation. Thirty microlitres of nuclease free water and 30µl of lithium chloride precipitation solution. This solution is chilled for 1 hour at -20°C. The solution is centrifuged at 13,000 rpm in a benchtop centrifuge for 15 min. The solution was decanted and ~1.4 mL of 70% ethanol added to the RNA pellet. The solution was centrifuged for 1 min at 13,000 rpm. The RNA pellet was air dried and resuspended in 20 µL of nuclease free water.

## **2.28 Phusion® site-directed mutagenesis**

### **Method**

The Phusion describes the enzyme used in the mutagenesis protocol. It is a highly efficient, accurate, hot-start DNA polymerase. Site-directed mutagenesis occurs through replication of the template DNA. Primers were designed to replicate the plasmid template and to introduce the desired mutation in the replicated products. The primers are designed back to back so to replicate the whole plasmid template resulting in linear PCR products representing the whole plasmid sequence.

To introduce a single point mutation the middle of the forward primer contains the desired point mutation. The reverse primer is designed back to back to this primer. To create deletions, primers are designed back to back surrounding the DNA sequence that you wish to delete. This results in the amplified products of the template containing the desired point mutation or removing the sequence which is not amplified.

### **2.28.1 *FMO1* promoter mutation constructs**

The *FMO1* pGL3 reporter constructs pGL-255\_-128 and pGL-858\_-343 was used as templates to create mutant reporter constructs. Two reporter gene constructs, containing point mutations within the pGL-255\_-128, were made. Three reporter gene constructs, two of which contained point mutations and a third with a deletion was created (see results chapter 4.7 for location).

The site-directed mutagenesis reaction was set-up with 5x Phusion high fidelity buffer (10 $\mu$ L), 10 mM dNTPs, forward and reverse primers (0.5  $\mu$ M) and the template DNA (1 ng). The reaction was made up to 50  $\mu$ L with nuclease free water.



Amplification parameters are shown in table 2.3. The annealing temperature is recommended from 65-72°C and was arbitrarily chosen at 65°C. This was successful for all mutagenesis reactions.

The products of the replication are linear. The primers used were 5' phosphorylated. The two linear strands were ligated to form circular DNA. The ligation reaction contained 25 ng of the mutagenesis product, 5 µL of 2x T4 Quick-stick ligation buffer mix. 0.5µl of quick T4 DNA ligase, and the reaction was made up to 5 µL. The reaction was left at room temperature for 5 minutes then transformed into competent cells (see section 2.5 for transformation protocol).

<b>Programme</b>	<b>Temperature</b>	<b>Time</b>
<b>Programme 1</b>	<b>1 cycle</b>	
	95°C	10 min
	65°C	30 sec
	72°C	10 min
<b>Programme 2</b>	<b>25 cycles</b>	
	95°C	10 sec
	annealing temp	30 sec
	72°C	10 min
<b>Programme 3</b>	<b>1 cycle</b>	
	72°C	10min

**Table 2.3 PCR cycling conditions for site-directed mutagenesis**

## 2.29 DNA sequencing

### Materials

-ABI BigDye Terminator v3.1 Cycle Sequencing Kit (cat no. 4336917)

-2/3rds HM-MC (40% PEG-8000), 1 M NaCl, 2 mM Tris-HCl pH9, 0.2mM EDTA, 3.5 mM MgCl<sub>2</sub>).

-HM Better Buffer, 200 mM Tris-HCl pH9, 5 mM MgCl<sub>2</sub>

## **Method**

### **2.29.1 PCR for sequencing**

DNA was first amplified by PCR in 96-well plates (see 2.11). The PCR products were cleaned within the 96-well plate. 3x volume (30 µL) HM-MC was added to each PCR reaction (10 µL), a lid applied to each plate, and the contents were thoroughly mixed. The plates were centrifuged at 4000 rpm within a Centra 4b centrifuge to pellet the DNA. The lids were removed, and the plates inverted on tissue paper and placed back into the centrifuge. The plates were centrifuged at 20 g for 30 s and inverted on tissue paper to remove the HM-MC along with free nucleotides and other reagents from the PCR reaction. One-hundred and fifty microlitres of ethanol was added to the pelleted DNA, the lid replaced, and the samples centrifuged for 25 min at 4000 rpm in the Centra 4b centrifuge. The plates were removed from the centrifuge, inverted on to tissue paper, and centrifuged at 20 g for 30 sec. This removes salts from the DNA. The lids were removed and the plate left to stand for the pellets to dry. 10 µL of nuclease-free water was added to the DNA pellets and samples were left for 15 min to allow DNA to resuspend.

### **2.29.2 Sequencing reaction**

The amount of DNA to be used within the sequencing reaction was determined by electrophoresis of 1  $\mu\text{L}$  of cleaned PCR product. If a strong band was visualised, 2  $\mu\text{L}$  of the PCR product would be used in the sequencing reaction. Two separate master mixes were made, one for a forward sequencing reaction, and one for a reverse sequencing reaction. These reactions were made up of 5 x ABI buffer (2  $\mu\text{L}$  per reaction), Big Dye v3.1 (0.5  $\mu\text{L}$ ), primers (1  $\mu\text{L}$  each at 1.6  $\mu\text{M}$ ). The reaction is made up to 8  $\mu\text{L}$  with water. For a 96-well plate this was scaled up to 100 reactions per sequencing reaction. 8  $\mu\text{L}$  of the mastermix is added to each PCR product. The sequencing reactions are carried out with the conditions set out in table 4.

### **2.29.3 Cleaning the sequencing reaction**

The sequence reactions are mixed with 2.5  $\mu\text{L}$  of 125  $\mu\text{M}$  EDTA and then 30  $\mu\text{L}$  of 100% ethanol was added to each well. The contents of the wells are thoroughly mixed and centrifuged at 4000 rpm for 60 min. The plates were removed and inverted on tissue paper and centrifuged at 100 rpm for 1 min. 30  $\mu\text{L}$  of 70% of ethanol was added to the wells and the samples centrifuged for 20 min at 4000 rpm. The plates were inverted on to tissue paper and centrifuged at 100 rpm for 1 min. The lids of the plate were removed and the samples air-dried for 15 min at room temperature. The samples were analysed using the Applied Biosystems Genetic Analyzer 3730.

#### **2.29.4 Phase haplotype reconstruction**

The programme Sequencher was used to identify genetic polymorphism in individuals within the sequenced promoter regions. A database was created in Microsoft Excel of genotype data of the individuals sequenced. The genotypes of each individual were ordered as they appear along the chromosome in a text document. Haplotypes were constructed for each population studied (see chapter 5 for populations and analysis) using PHASE software (Stephens et al., 2001).

#### **2.30 DNaseI capillary footprinting**

The development of a method for analysing regulatory polymorphism is described in chapter 6. The method describes the use of capillary DNase I footprinting to test the effects of regulatory polymorphism. The main method is set out within this chapter. The method for DNase I digestion, the binding reaction and dideoxy termination sequencing is set out below.

##### **2.30.1 Labelling DNA**

The template used for footprinting was labelled using PCR. The 5' primer contained a fluorescent protein FAM. The amplified products from the PCR therefore contained the 5' FAM label. The PCR method is set out in section 2.11.

##### **2.30.2 Binding reaction**

###### **Materials**

-FAM labelled forward and unlabelled reverse primers (10 ng/μl)

-Binding buffer (50 mM hepes (pH 7.6), 2.5 mM DTT, 60% glycerol (v/v), 250 mM NaCl, 0.25% NP40 (Sigma)). Aliquots of buffer were stored at -20°C.

-Poly dl/dC (dissolved in 5 mM NaCl to a final concentration of 4 µg/µl and stored in aliquots at -20°C) (Sigma).

### **Method**

- A 50 µL total reaction volume was used. The Binding buffer (5x), primers (1 µL of each), 1 µL of poly dl-dC and dH<sub>2</sub>O was added to a chilled tube on ice for 5 minutes. Fifty ng of template DNA was added and the mixture was gently mixed using a pipette tip. The binding reaction was left for 30 min to allow for DNA-Protein binding to take place.

### **2.30.3 DNase I digestion**

#### **Materials**

DNase I, 2000U/ µl (NEB)

1X DNase I Reaction Buffer: 10 mM Tris-HCl, 2.5 mM MgCl<sub>2</sub>0.5 mM CaCl<sub>2</sub> (NEB)

#### **Method**

After 30 minutes of the binding reaction 50 µL of DNase1 reaction buffer is gently added. 0.005 U of DNase I enzyme is added and the sample is left for 5 min at room temperature. The reaction is terminated by the addition of 100 µL of 0.5 M EDTA.

Once terminated the DNA is purified as described in section 2.9.

## 2.30.4 Capillary electrophoresis and data analysis

The materials and methods are set out in section 6.2.5.

## 2.30.5 Dye terminator sequencing

### Materials

-Plasmid DNA (template).

-Thermo Sequenase Dye Primer Manual Cycle Sequencing Kit (USB CORP)

containing:

-Reaction Buffer (concentrate): 150mM Tris-HCl pH9.5, 35mM MgCl<sub>2</sub>

-ddA Term Mix: 300 μM each of dATP, dCTP, dTTP & 7-deaza-dGTP, 3 μM ddATP

-ddC Term Mix: 300 μM each of dATP, dCTP, dTTP & 7-deaza-dGTP, 3 μM ddCTP

-ddG Term Mix: 300 μM each of dATP, dCTP, dTTP & 7-deaza-dGTP, 3 μM ddGTP

-ddT Term Mix: 300 μM each of dATP, dCTP, dTTP & 7-deaza-dGTP, 3 μM ddTTP

-Thermo Sequenase DNA polymerase: 20 U/μL with 0.03 U/μL Thermoplasma

Acidophilum inorganic pyrophosphatase in 50 mM Tris-HCl pH 8.0, 1 mM EDTA,

1 mM DTT, 0.5% Tween-20, 0.5% Nonidet™ P-40, 50% glycerol.

### Method

The Dye termination sequencing reactions were setup as follows: A mastermix was made containing 200 ng plasmid DNA (template), 2.2 μL of reaction buffer, 1 μL

labelled primer (FAM), this is made up to a volume of 19 μL with nuclease free water.

1 μL of the Thermosequenase enzyme is added to the mastermix. 4 μL of the mix is aliquoted into 4 tubes (kept on ice), one tube for each of the terminating nucleotides.

Each nucleotide termination mix is added to the appropriate tube. The tubes are

mixed and dye terminator sequencing reactions are carried out using the amplification procedure shown in the table below.

Programme	Temperature	Time
Programme 1	40 cycles	
	95°C	30 sec
	55°C	30 sec
	72°C	60 sec

**Table 2.4 Amplification parameters used for dye-terminator sequencing reactions**

### 2.31 Software Packages

Transcription factor binding prediction tools

-PROMO v3.0 (Messeguer et al., 2002),

[http://algggen.lsi.upc.es/recerca/menu\\_recerca.html](http://algggen.lsi.upc.es/recerca/menu_recerca.html)

A virtual laboratory for the study of transcription factor binding sites in DNA sequences

-Ali Baba v2.1, <http://www.gene-regulation.com/pub/programs/alibaba2/index.html>

-MatInspector 8.0 (Cartharius et al., 2005),

[http://www.genomatix.de/online\\_help/help\\_matinspector/matinspector\\_help.html](http://www.genomatix.de/online_help/help_matinspector/matinspector_help.html)

-ApE plasmid editor v2.0

Sequence alignment and primer design

-ApE plasmid editor v2.0

Haplotype phase construction

-PHASE (Stephens et al., 2001)

Di-deoxy sequence analysis

-Sequencher® v4.10.1

-geNORM [http://medgen.ugent.be/~jvdesomp/genorm/geNorm\\_manual.pdf](http://medgen.ugent.be/~jvdesomp/genorm/geNorm_manual.pdf)



## **Chapter 3**

# **Profiling of *Fmo1* gene expression in mouse tissues and cell-lines**

## Chapter 3: Profiling of *Fmo1* gene expression in mouse tissues and cell-lines

### Introduction

Several studies have shown an inter-individual variation of FMO1 protein and mRNA levels of between 10-20 fold (Koukouritaki et al., 2002). The expression of *FMO1* differs in different tissues of both human (Koukouritaki et al., 2002; Yeung et al., 2000; Zhang and Cashman, 2006) and mouse (Janmohamed et al., 2004). *FMO1* mRNA and protein levels are not known to be affected in response to exogenous agents and therefore differences in *FMO1* expression are likely to be due to genetic variation. The genetic variations that cause changes in *FMO1* expression will potentially be good indicators of an individual's response to drugs metabolized by *FMO1*. Locations of SNPs in regions of DNA that are critical for gene expression are predicted to alter the amount of *FMO1* available for drug metabolism.

Previously it has been shown that the gene encoding *FMO1* in human and mouse has three promoters and transcriptional start sites, resulting in three distinct transcripts (Figure 3.1). The promoters have been defined as P0 (upstream of exon 0), P1 (upstream of exon 1) and P2 (starting within intron 1, upstream exon 2). The transcripts differ in their 5' untranslated leader sequences. Exon 0 splices to exon 2; exon 1 splices to exon 2; or, part of intron 1 forms the leader sequence when transcription begins from P2 upstream of exon 2. For each transcript, translation initiation begins at the ATG located in exon 2.

An examination of the region upstream of the three transcriptional start sites shows a number of SNPs in the human gene (see chapter 5: Sequencing of human *FMO1*

promoters). This variation suggests that differences in promoter base sequence may be a source of the variability, observed in the amount of FMO1, in different individuals. A number of studies have shown the effect of polymorphisms within promoter regions that affect mRNA production of genes for other drug metabolizing enzymes (Johnson et al., 2005).

As mentioned above, the expression of the gene for FMO1 is different in different tissues. We would therefore like to know which of the three promoters is used in different tissues. SNPs shown to affect a tissue-specific promoter may influence expression of the protein in a single tissue or a limited number of tissues. This chapter describes promoter usage of the *Fmo1* gene in different tissues of the mouse and in selected cell lines.

*Fmo1* (-/-), *Fmo2* (-/-), *Fmo4* (-/-) mice show a phenotype of altered energy homeostasis (Omar, 2009; Veeravalli et al., Unpublished). The knockout mice have less fat than age-matched, wild-type mice and the ratio of pre-adipocytes to adipocytes is altered. To further understand the role of FMO1 in fat, and to understand the regulation of the gene in this tissue, we have used 3T3-L1 fibroblast cells that have been differentiated *in vitro* into adipocytes (see Chapter 1: Introduction). Each of the three *Fmo1* transcripts has been quantified at different stages of 3T3-L1 cell differentiation.

### **3.1 Quantification of the expression of *Fmo1* in different mouse tissues by real-time PCR**

Figure 3.1 shows the different splicing events that produce the three different transcripts of the *FMO1* gene. The same splicing events occur in both human and mouse. Previously P0 has been shown to be active in mouse liver, and P1 and P2 in mouse kidney (Shephard et al., 2007). Primer pairs were designed to amplify regions specific to each of the three alternatively spliced transcripts (see Figure 1.4). In addition to the quantification of each individual transcript in a tissue, the total *FMO1* transcript was also quantified using primers designed to amplify the protein-coding region. The primers used are given in the appendix. Quantifying each individual transcript and the total *FMO1* transcript amounts in a tissue/cell line will reveal, for example, if there are additional, unknown transcripts or if there is attenuation of transcription from different promoters.

#### **3.1.1 Selection of reference genes to normalise *Fmo1* expression**

To normalise the quantity of *Fmo1* transcripts produced in different tissues, reference genes were co-amplified in the PCR reaction. The reference gene is one that is expressed at the same level in the different tissues tested, and controls for differences in the amount of RNA in each sample to be amplified. There are a number of reference genes that are classically chosen for this purpose. However, the expression of these traditionally chosen genes can vary between samples depending on the tissue or biological context. Because *FMO1* mRNA expression levels were to be quantified in six different tissues, a selection of reference genes was tested for their expression variability between the different mouse tissues to be analysed. This

would ensure accurate quantification of *Fmo1* expression within the different mouse tissues.

A published algorithm called geNorm was used to choose the most stably expressed genes in each tissue (Vandesompele et al., 2002). The geNorm algorithm functions by comparing the expression profile of each reference gene with all other reference genes tested. The reference genes with the most similar profile to the other reference genes will be those whose expression is most constant in a tissue. The algorithm ranks the stability of the reference genes. This is achieved by calculating the standard deviation between the logarithmically transformed expression ratios (Figure 3.1A). The average standard deviation (M) is calculated for each reference gene compared to the other reference genes. The lower the value of M, the more stable the expression of the gene between different tissues. The most stably expressed genes between the different mouse tissues were found to be  $\beta$ -actin and calnexin (CANX), a gene that encodes a member of the calnexin family of molecular chaperones (Figure 3.1B).

The geNorm algorithm calculates the pairwise variation between the reference genes in different tissues. The number of reference genes to use to normalise gene expression is dependent on the amount of variation observed between the different reference genes. The amount of pairwise variation between the reference genes analysed in different mouse tissues is high (Figure 3.1C). This is to be expected as a number of diverse tissues were tested. Thus, to define gene expression accurately, between the different tissues, a number of reference genes need to be analysed. This will ensure accurate gene expression comparisons between different tissues.

The algorithm predicts higher accuracy of gene expression when three reference genes are used compared to two. The three most stably expressed reference genes were *elf4e*, *CANX*, and  $\beta$ -actin. These genes were chosen to normalise *Fmo1* gene expression in the different mouse tissues. The data given throughout the thesis has been normalised to *CANX*.

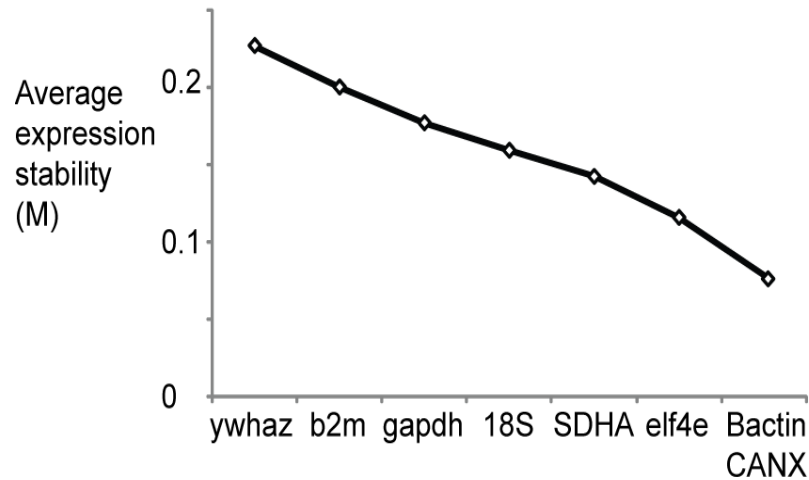
The primers for quantifying *Fmo1* transcripts were designed by the company Primer Design (<http://www.primerdesign.co.uk/>) to be 100% efficient in their amplification and therefore the quantity of each *Fmo1* transcript can be compared to each-other. When primer efficiencies are not comparable it can lead to differences in amplification and therefore the amounts of different mRNAs cannot be compared accurately.

The tissues analysed for *Fmo1* expression by quantitative real-time PCR were kidney, liver, white and brown fat, brain, lung and muscle. Kidney and liver were chosen as these tissues are known to express *Fmo1* and are key tissues in drug detoxification. The other extra-hepatic tissues which were examined play roles in energy homeostasis. In mouse kidney, *FMO1* cDNAs have been observed starting from the P0, P1 and P2 transcriptional start site. Only the P0 transcript is observed in the liver. It has not yet been determined which transcripts are produced in the other tissues to be investigated.

A

TISSUE	GAPDH	$\beta$ -ACTIN	ELF4E	CANX	SDHA	18S	B2M	YWHAZ
KIDNEY	0.05	0.24	0.33	0.55	0.31	0.84	0.81	0.01
LIVER	0.32	0.64	0.33	1	0.93	0.13	0.33	0.08
BROWN FAT	0.02	0.31	0.11	0.22	0.57	0.24	0.5	0.84
WHITE FAT	0.02	0.07	0.03	0.08	0.84	0.38	0.02	0.03
MUSCLE	0.93	0.15	0.87	0.42	0.61	0.62	0.03	0.02

B



C

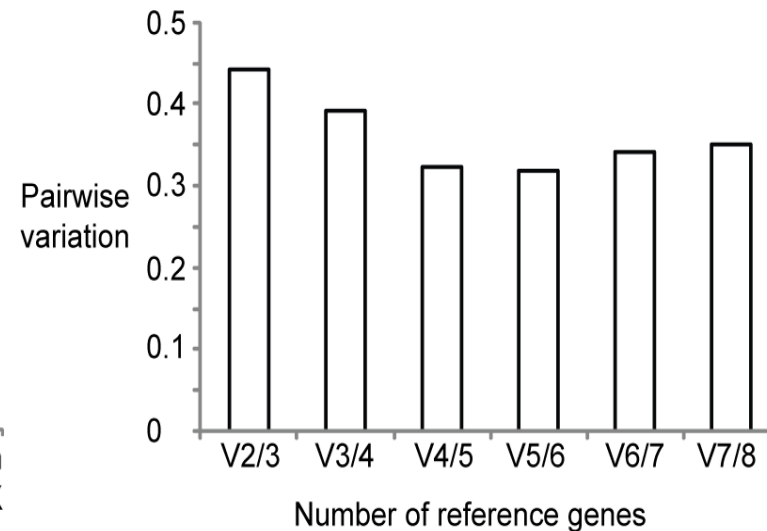


### Figure 3.1 Selection of suitable reference genes for the normalisation of *Fmo1* expression in different mouse tissues

**(A)** The table shows the expression of each reference gene relative to each other in different mouse tissues. **(B)** The average expression stability of each reference gene. This is calculated from the pairwise variation of each reference gene when compared to other reference genes. **(C)** The optimal number of reference genes to be used to accurately define gene expression. CANX and  $\beta$ -actin are shown to be equally stable. The data throughout the thesis is normalised to CANX.

### 3.1.2 Quantification of the FMO1 global transcript in different mouse tissues

Using primers designed within the protein-coding region the total transcript amount for FMO1 was determined (Figure 3.2). This is referred to as the global expression. *Fmo1* expression is highest in the kidney, where global expression in this tissue, relative to the reference gene CANX, is  $6.2 \pm 4.4$ . Global expression was measured in lung ( $3.7 \pm 0.71$ ), brown fat ( $3.7 \pm 1.59$ ), white fat ( $1.6 \pm 0.44$ ) muscle ( $0.55 \pm 0.15$ ) and brain ( $0.06 \pm 0.01$ ). The high standard error shown in kidney was due to the variation in expression between triplicate mice.

It has previously been shown by protein and mRNA quantification methods that *Fmo1* is expressed highly in the kidney. This validates the data obtained by RT-PCR. It has previously been shown that FMO1 is expressed in brown and white fat. The RT-PCR data confirms and extends this data. Because *Fmo1* is highly expressed within these tissues it seems probable that the enzyme plays some role in fat. FMO1 is known to be expressed in lung, and the RT-PCR data show that the amount is high and similar to that found in white and brown fat. *Fmo1* is expressed in muscle at about 10% of the amount present in kidney. In brain, the *Fmo1* global transcript is expressed at a low level compared to the reference gene.



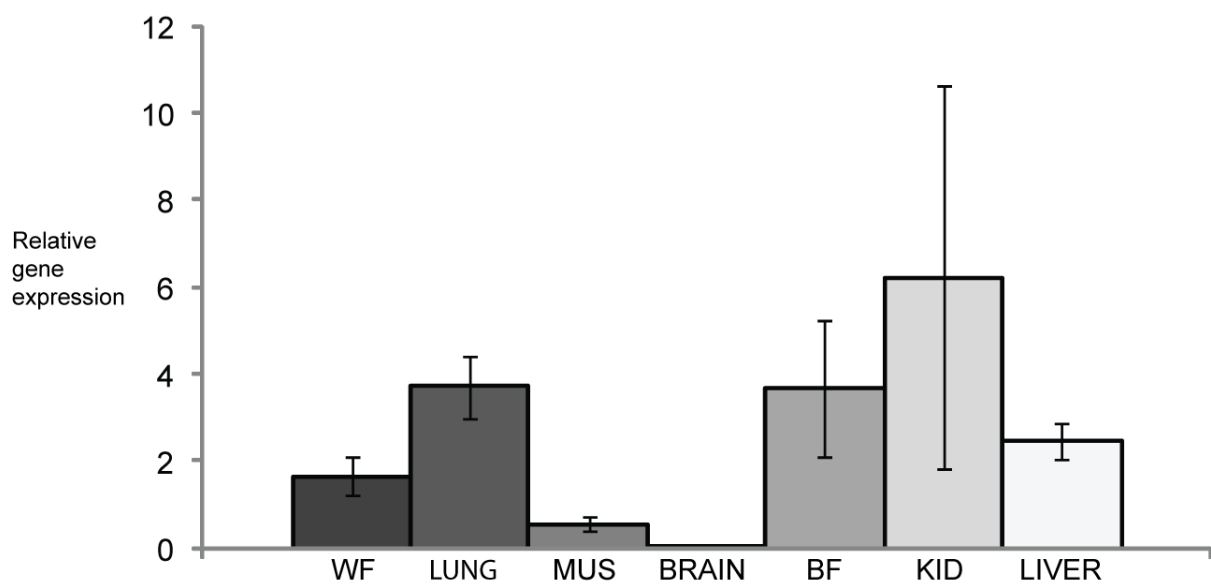


**Figure 3.2 Global *Fmo1* expression in different mouse tissues**

The bar graph shows *Fmo1* global expression levels relative to the CANX reference gene in different tissues. From left to right: white fat (WF), lung, muscle (MUS), brain, brown fat (BF), kidney (KID) and liver. All experiments were done in triplicate and the error bars represent the standard error.

### **3.1.3 Quantification in different mouse tissues of the P0, P1 and P2 FMO1 mRNA transcripts (Figure 3.3).**

In kidney the P1 transcript is the most highly expressed, while the transcripts from P0 and P2 are both low and only represent about 1% of the transcript produced from the P1 promoter (Figure 3.3). Therefore the P1 transcript constitutes the majority of FMO1 transcripts in mouse kidney. P1 is also the predominant transcript found in brown fat, brain and muscle (Figure 3.3). In brown fat the P1 transcript is about 80% higher than the P0 and P2 transcripts. In brain, the P1 transcript is about 95% more abundant than each of the P0 and P2 transcripts. In white fat and muscle the P1 transcript is about 90% more abundant than the P0 and P2 transcripts. In contrast, in the lung, both P0 and P1 transcripts are abundantly expressed at similar levels (Figure 3.3). The P2 transcript makes up only about 1% of the FMO1 transcripts in the lung. The P0 transcript is the only transcript present within the liver.

### **3.1.4 The relative expression of the P0, P1 and P2 transcripts combined to that of the global expression of FMO1 mRNA (Figure 3.4)**

The P0, P1 and P2 transcripts were each quantified by amplification of transcript specific sequences. This was achieved by using an upstream, leader-specific, forward primer. The global FMO1 transcript was quantified using primers located within the protein-coding region that is present within transcripts that are expected to be translated into FMO1 protein.

In brown fat, kidney, and liver the global transcript amount is similar to that of the combined P0, P1, P2 transcripts. The expression of the P0, P1 and P2 transcripts in

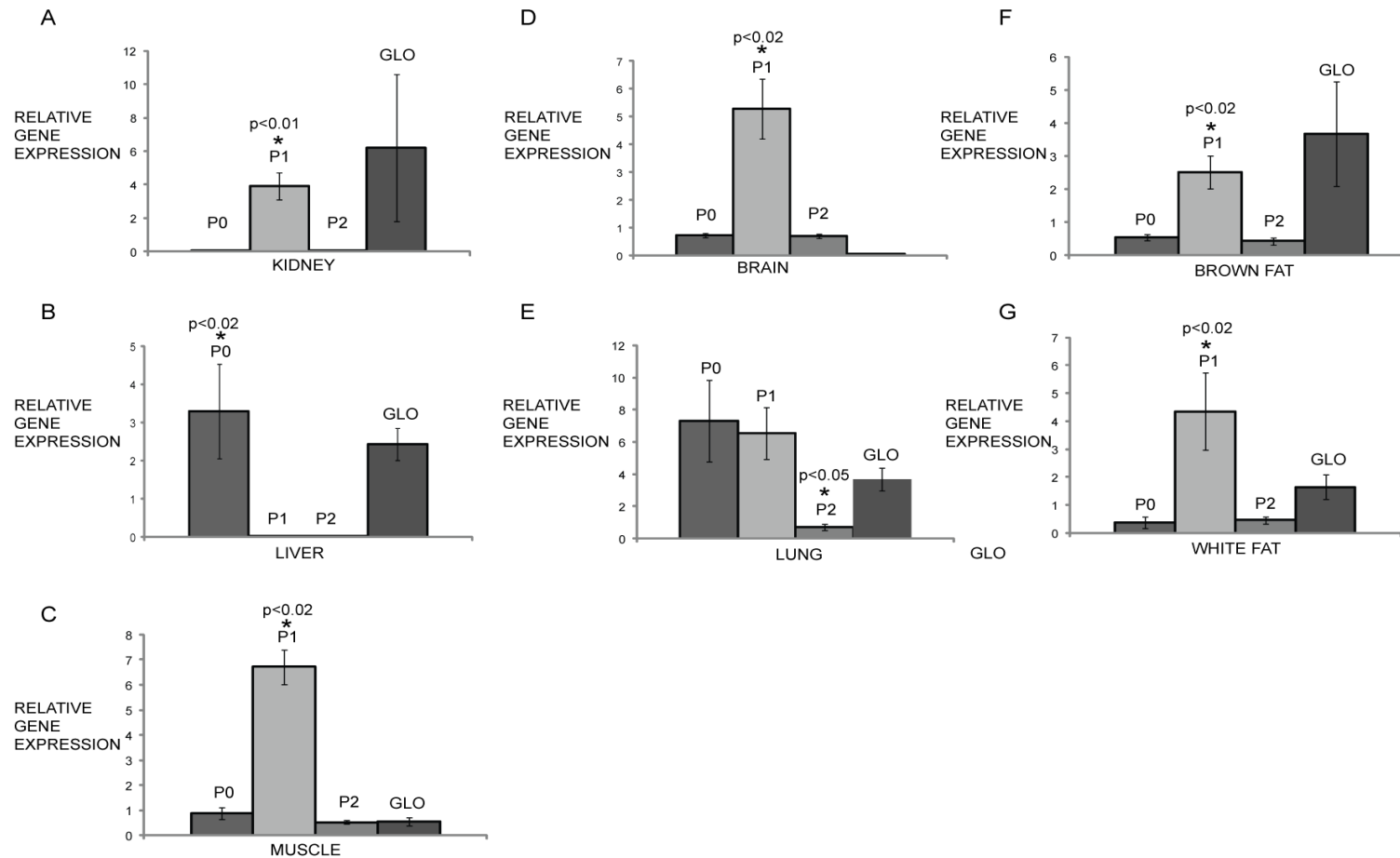


### Figure 3.3 Relative gene expression of *Fmo1* mouse transcripts within different mouse tissues

P0, P1 and P2 and global (shown as GLO) relative expression in (A) Kidney (B) Liver (C) Muscle (D) Brain (E) Lung (F) Brown fat (G) White fat. *Fmo1* expression is normalised to the mRNA levels of CANX. All experiments were done in triplicate and the error bars represent the standard error. The P1 transcript is significantly more highly expressed than the P0 and P2 transcript in the kidney (p<0.01), brain, brown fat, white fat and muscle (p<0.02). In liver, the P0 transcript is significantly higher than the P1 and P2 transcript (p<0.02). In lung the P0 and P1 transcript is significantly higher than the P2 transcript (p<0.05).

kidney is  $1.65 \pm 0.64$  higher than the global expression. In brown fat, the expression of P0, P1 and P2 added together is  $1.27 \pm 0.58$  times higher than the global expression. In liver, the expression of P0, P1 and P2 added together is  $1.32 \pm 0.2$  higher than the global expression. These differences are not significant and therefore it is likely that the P0, P1 and P2 transcripts account for the overall *Fmo1* global expression within these tissues.

In the lung, white fat, brain, and muscle, the expression of P0, P1 and P2 added together is significantly different from the global expression. In the lung the P0, P1 and P2 transcripts added together are  $4.13 \pm 0.29$  times higher than the global expression. These differences are significant ( $p < 0.02$ ). In white fat, the expression of P0, P1 and P2 added together is  $3.07 \pm 0.27$  times higher than the global expression. This expression difference is significant ( $p < 0.03$ ). In brain, the expression of P0, P1 and P2 added together is  $116.9 \pm 21.42$  times higher than the global expression. This expression difference is significant ( $p < 0.006$ ). In muscle, the expression of P0, P1 and P2 added together is  $16.1 \pm 4.4$  times higher than the global expression. This expression difference is not significant ( $p < 0.08$ ).

It seems likely that these differences are due to the production of shorter, attenuated transcripts. These transcripts may contain only the 5' region of the mRNA and would be detected only when primers are used that amplify from within the 5' leader sequence. The relative expression data of P0, P1 and P2 transcripts (Figure 3.4) indicate that attenuated transcription is most likely from the P1 promoter.

In whole brain, *Fmo1* global expression is  $0.06 \pm 0.01$  fold higher than the reference gene and shows very little variation between mice. This is a relatively low amount of

expression relative to the other mouse tissues quantified for *Fmo1* expression. However, the brain is a complex tissue and the expression of *Fmo1* is localised to neurons of the cerebrum and in the choroid plexus (Janmohamed et al., 2004). The combined P0, P1 and P2 transcript amount in brain is about 100-fold higher than that of the global FMO1 mRNA amount. Each individual transcript is present in amounts greater than that of the global transcript. Therefore, it seems that in the brain, transcription is attenuated from each of the three promoters. FMO1 protein is, however, present in mouse brain (Hernandez et al., 2009; Itoh et al., 1997). The results suggest that the amounts of protein produced might be tightly regulated via an as yet unknown mechanism of transcription attenuation.

In muscle *Fmo1* global expression is  $0.55 \pm 0.15$  relative to the reference gene. The total, combined, relative expression of the P0, P1 and P2 transcripts is  $8.1 \pm 0.98$ . This represents a 15-fold higher expression of the individual transcripts than that of the global transcript. This increase is mostly due to the abundance of P1 transcripts. As with other tissues, transcription from P1 seems highly active, but transcription seems to be attenuated.

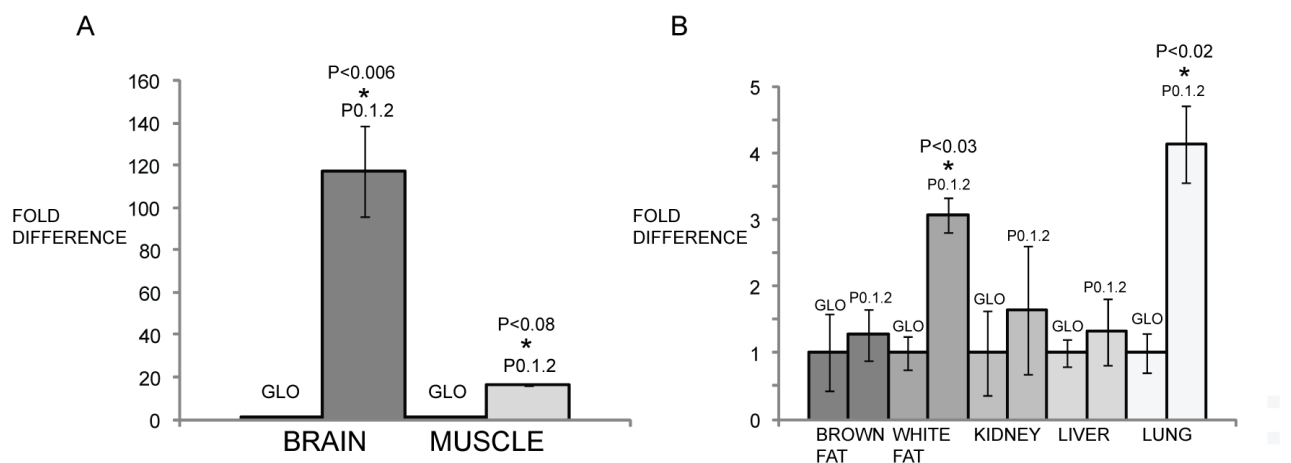


**Figure 3.4 Comparison of the total relative expression of the *Fmo1* P0, P1, and P2 transcripts with the relative expression of the *Fmo1* global transcript**

**(A)** Relative expression of the P0, P1 and P2 transcripts next to the *Fmo1* global expression for ease of comparison in brain and muscle. **(B)** Relative expression of the P0, P1 and P2 transcripts next to the *Fmo1* global expression for ease of comparison in brown fat, white fat, kidney, liver and lung. All transcript expression was normalised to the expression of the CANX gene. All values shown are relative to CANX gene expression within each tissue. All experiments were done in triplicate and the error bars represent the standard error.

## **3.2 Expression of *Fmo1* in 3T3-L1 cells undergoing differentiation to adipocytes**

A *Fmo1* mouse knock-out line has led to advances in understanding an endogenous role for FMO1. The phenotype of the mouse indicates that FMO1 plays a role in the regulation of energy homeostasis. The mice have decreased body weight and decreased amounts of white adipose tissue. The mouse transcriptome microarray (Su et al., 2002) and quantitative real-time data generated in our laboratory confirm the expression of FMO1 mRNA within white adipose tissue. Initial experiments carried out in undifferentiated 3T3-L1 cells show no expression of FMO1 mRNA. However, when differentiated into adipocytes, *Fmo1* expression is switched on. The results are described in the next section. The rationale for examining *Fmo1* expression in differentiated cells is several-fold. 1. We will be able to identify the *Fmo1* promoter used and activated in this cell type. 2. This will provide an experimental model for determining the transcription factors involved in regulating *Fmo1* expression in adipocytes. 3. Any SNPs identified within the promoter region used in adipocytes can be introduced by site-directed mutagenesis and their influence on transcription tested using a reporter gene assay.

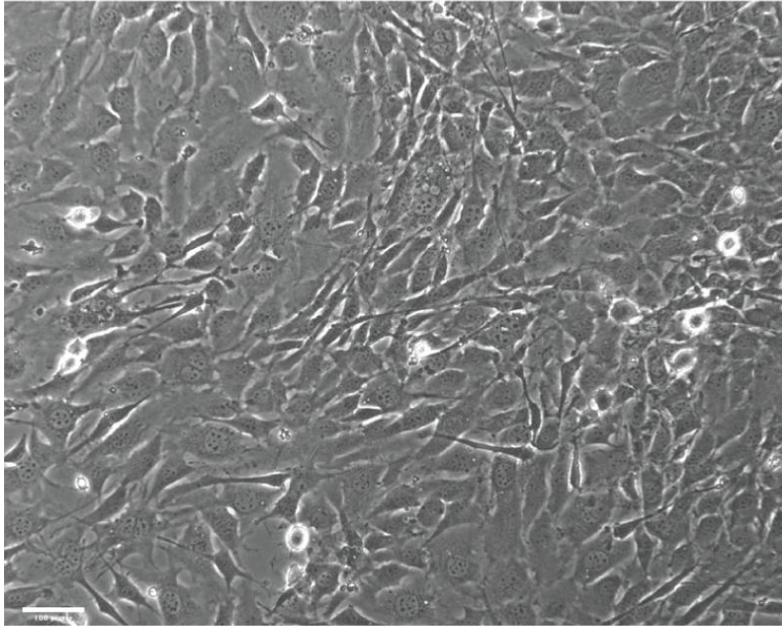
### **3.2.1 *Fmo1* expression during differentiation of the EACC™, 3T3-L1 mouse fibroblast cell line**

The cell line that was used for our initial analysis of *Fmo1* expression was obtained from the EACC™. The cell line is able to differentiate into adipocytes, but we encountered some problems with this line. The cells are able to differentiate into adipocytes but the efficiency is low. Only 30-40% of the cells differentiate due to the cells' loss of ability to be contact inhibited (Figure 3.5). Contact inhibition of cells is a

key process in the differentiation process. The cells that did differentiate required more than ten days to appear visually as adipocyte-like cells. Quantification of adipocyte markers by RT-PCR was carried out to ensure adipocyte differentiation had occurred. GAPDH was chosen as the house-keeping gene as it was previously shown to be one of the most stable genes during adipocyte differentiation (Gorzelnik et al., 2001). The 3T3-L1 cells did express Lipoprotein Lipase, PPAR- $\gamma$ , and FABP which are markers of mature adipocytes (Figure 3.6). The adipocyte markers PPAR- $\gamma$  and LPL expression is 200-fold higher in 3T3-L1 adipocytes compared to 3T3-L1 pre-adipocyte expression. The adipocyte marker FABP expression is 800-fold higher in 3T3-L1 adipocytes compared to 3T3-L1 pre-adipocytes. *Fmo1* expression is 200 fold higher in 3T3-L1 adipocytes compared to 3T3-L1 fibroblasts. Experiments on *Fmo1* transcript expression during differentiation was initially carried out within these cells. However, because the differentiation of these cells was not consistent, a 3T3-L1 cell line was purchased from the ATCC™™. This cell line is able to be contact inhibited when differentiated. These cells were very consistently and efficiently differentiated with 95-100% efficiency (Figure 3.7). The experiments on the quantification of *Fmo1* mRNA transcripts during differentiation were repeated in this cell line and are described below.



A



B

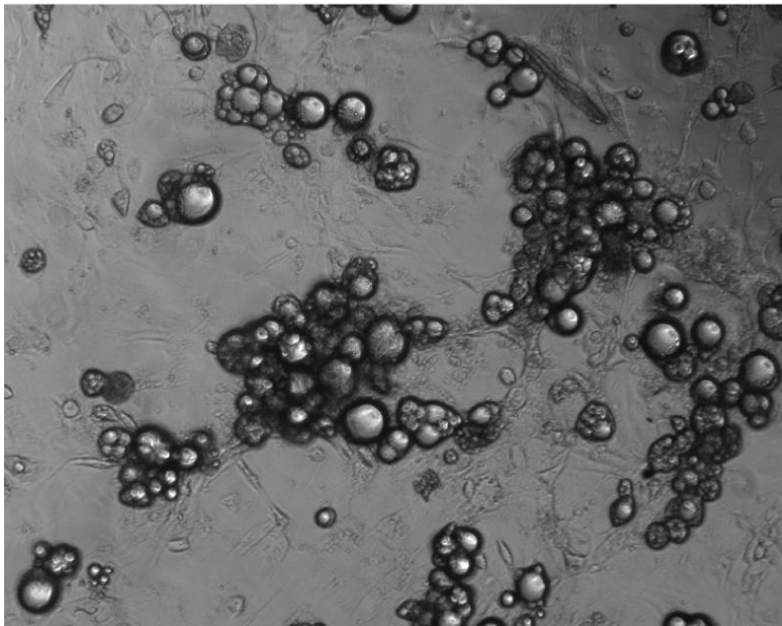


**Figure 3.5 Images of (A) EACC™ 3T3-L1 fibroblasts and (B) differentiated EACC™ 3T3-L1 adipocytes**

The round vesicles are fat globules within the cells. Note that 3T3-L1 fibroblasts can still be visualised within the background of panel B.

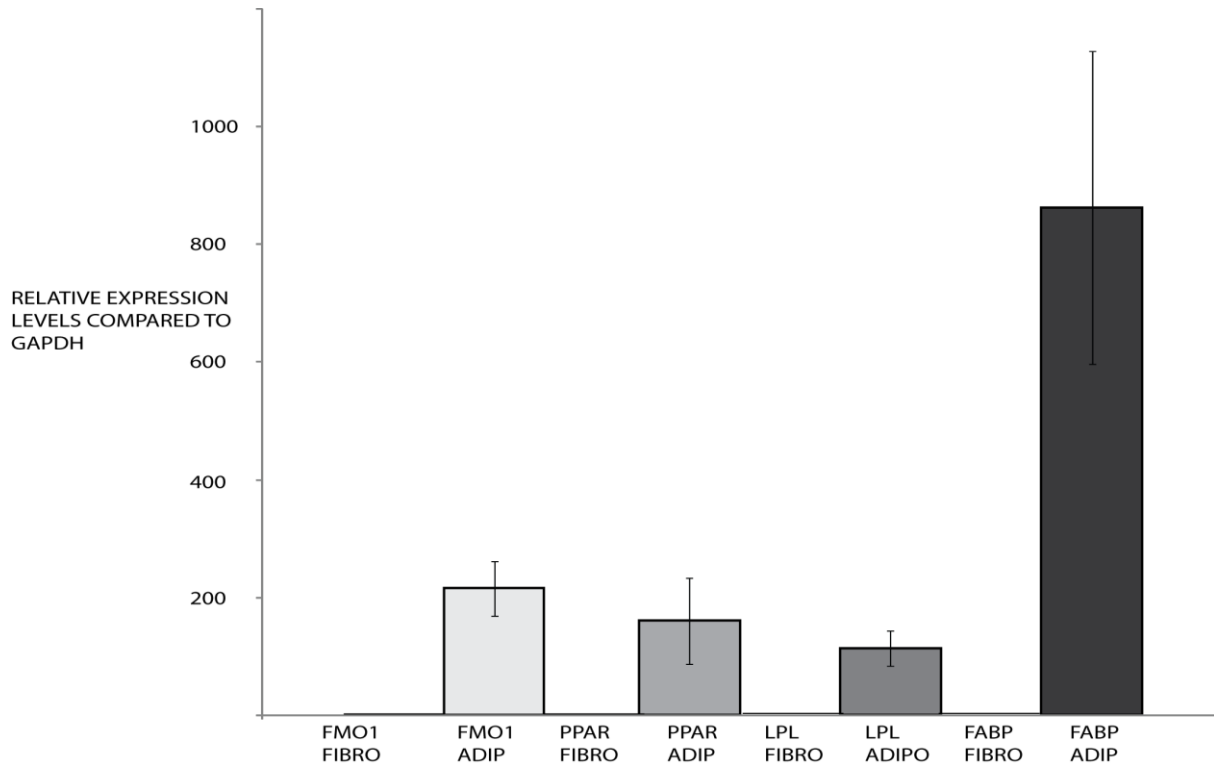


**Figure 3.6 *Fmo1* and adipocyte markers, LPL, FABP, and PPAR- $\gamma$  expression in 3T3-L1 (ECACC™ cell line) pre-adipocyte and mature adipocytes**

Markers of adipocytes and 3T3-L1 adipocytes were quantified to test the differentiated state of the 3T3-L1 cells. Differences are shown in fold difference. The data was obtained from triplicate wells of 3T3-L1 cells. The markers tested are PPAR- $\gamma$  (peroxisome proliferator-activated receptor), LPL (lipoprotein lipase), and FABP (fatty-acid binding protein). Fibroblast = 3T3-L1 fibroblast, ADIP = 3T3-L1 adipocyte.

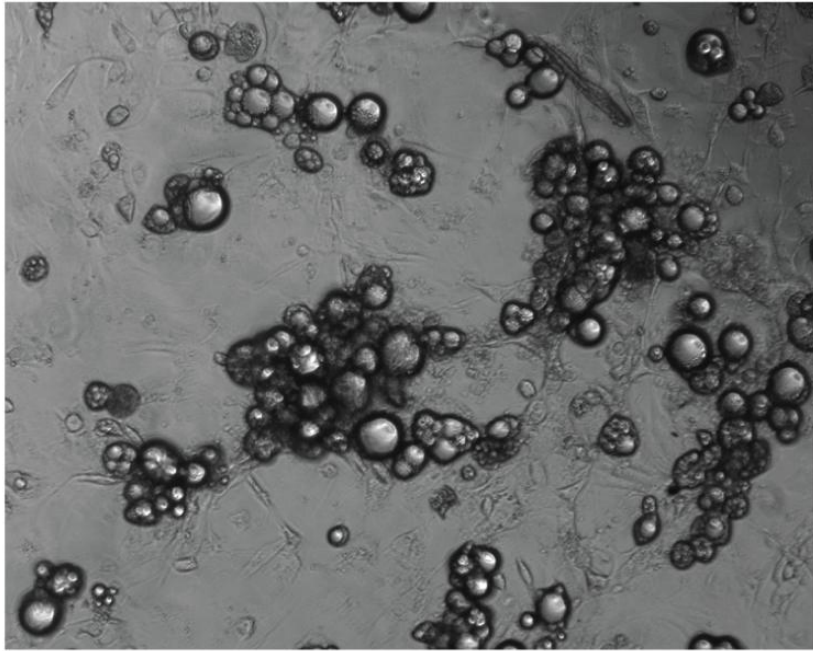
### **3.2.2 *Fmo1* expression during differentiation of the ATCC™ 3T3-L1 cell line**

When grown to full confluency, the 3T3-L1 ATCC™ cells stop growing. This is because the cells are contact inhibited. This is a requirement for efficient differentiation. Differentiation of 3T3-L1 ATCC™ cells as explained previously, is 95-100% efficient compared to 30-40% for the European cell line. The morphology of the 3T3-L1 ATCC™ cells is different from the 3T3-L1 European cell line (Figure 3.7). *Fmo1* and three adipocyte markers (PPAR- $\gamma$ , FABP and LPL) expression was measured in the 3T3-L1 pre-adipocytes and at a number of time-points after the addition of the media that allows the cells to differentiate into adipocytes. RNA was isolated from the cells at confluency and 3 hours, 1 day, 3 days, and 10 days after the addition of differentiation media. FMO1, LPL, PPAR- $\gamma$ , and FABP mRNAs were quantified at each of these time-points.

FMO1 mRNA is 200-fold higher in the ATCC™ 3T3-L1 adipocytes compared to the pre-adipocytes (Figure 3.8). This is comparable to the FMO1 mRNA fold difference seen when the EACC 3T3-L1 cells are differentiated. *Fmo1* expression is increased 10-fold, 1 day after the addition of differentiation media (Figure 3.8) and is reduced at day 3 back to pre-adipocyte levels. This may be due to a direct response to one of the hormones within the differentiation media. The majority of the increase in *Fmo1* expression is seen after 10 days and it is therefore defined as a late marker of adipocyte differentiation. The LPL adipocyte marker in the ATCC™ 3T3-L1 cell line is expressed in 3T3-L1 pre-adipocytes and throughout the time-points measured after addition of differentiation media. In comparison the LPL adipocyte marker is not expressed in the EACC 3T3-L1 pre-adipocyte and is only expressed after 3T3-L1

adipocyte differentiation. PPAR- $\gamma$  and FABP are increased through the period of 3T3-L1 differentiation. This is comparable to the observations in the 3T3-L1 EACC cell line.

A



B

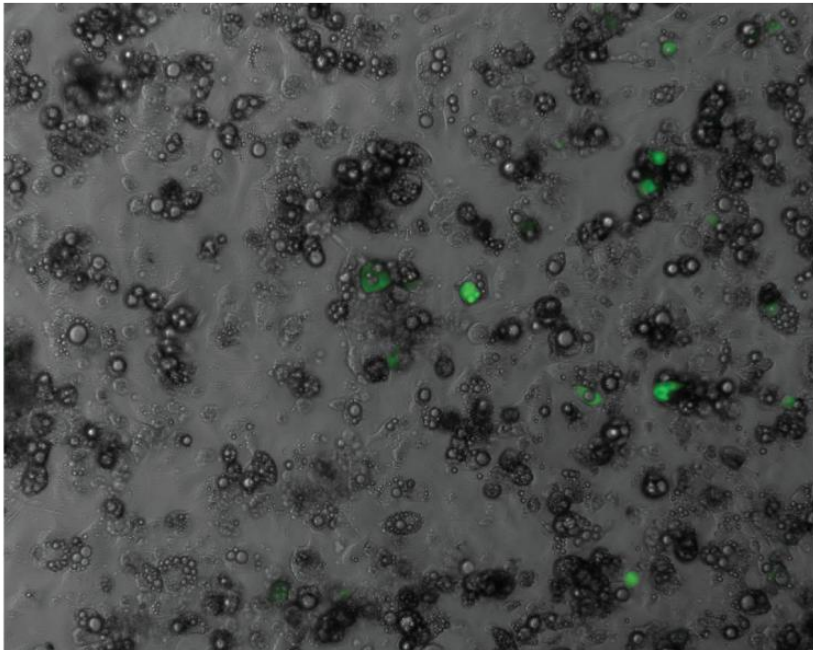


**Figure 3.7 Comparison of the EACC 3T3-L1 differentiated cell line with the ATCC™ 3T3-L1 differentiated cell line**

**(A)** Differentiated EACC 3T3-L1 cells imaged at 10 days post addition of differentiation media. **(B)** Differentiated ATCC™ 3T3-L1 cells.

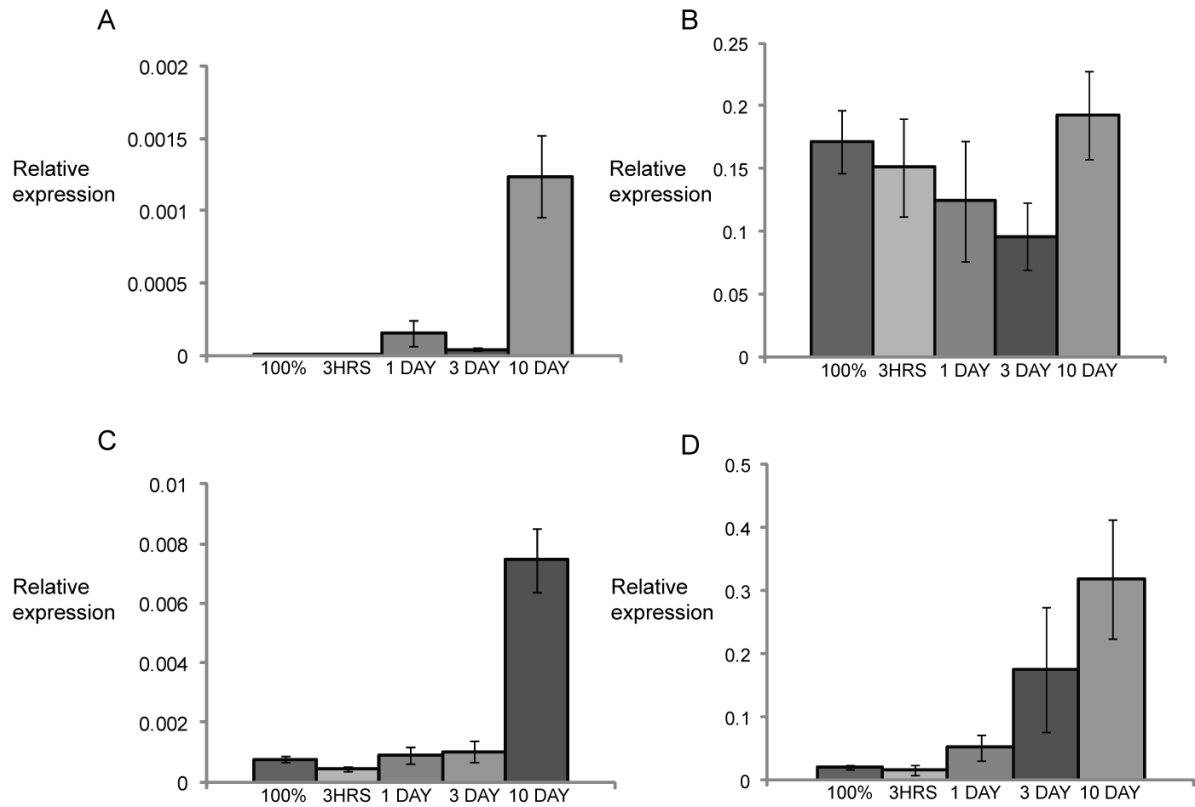


**Figure 3.8 Expression profiling of (A)FMO1, (B) LPL (C) PPAR- $\gamma$  (D) FABP mRNAs during 3T3-L1 differentiation**

Each graph shows the expression of the gene relative to the expression of GAPDH. Each bar represents a different time-point through 3T3-L1 differentiation. From left to right, in each graph, the time points are 3T3-L1 cells at 100% confluent, 3 hours, 1 day, 3 days, and 10 days after the addition of differentiation media. All experiments were done in triplicate and the error bars represent the standard error.

### **3.2.3 *Fmo1* P0, P1 and P2 transcript expression during 3T3-L1 differentiation**

In 3T3-L1 fibroblasts the three *Fmo1* transcripts (P0, P1, and P2) are expressed at a low amount relative to GAPDH. The P0 transcript is expressed at background levels. The P1 transcript is expressed at 0.00000036 the level of GAPDH. The P2 transcript is expressed at 0.000000077 the level of GAPDH. The global FMO1 transcript is expressed at 0.000006 the level of GAPDH.

*Fmo1* transcripts were quantified at a number of time points throughout the differentiation period of the 3T3 cells into adipocytes (Figure 3.9). We decided to measure transcripts at day 6, as opposed to day 3, to identify the earliest time point when *Fmo1* transcripts are significantly increased. The global *Fmo1* transcript was measured at the same time points as the individual transcripts. The P1 and P2 *Fmo1* transcripts are increased significantly (9 -fold) after 1 day post addition of differentiation media. At day 6 post differentiation the P1 transcript was increased a further 9-fold and the P2 transcript a further 15-fold. At day 10, the P1 transcript increased a further 3-fold and the P2 transcript increased a further 4-fold.

### **3.2.4 *Fmo1* global expression during differentiation of the ATCC™. 3T3-L1 mouse fibroblast cell line**

The global *Fmo1* transcript is expressed at 0.000003 relative to the reference gene (GAPDH) within undifferentiated 3T3-L1 fibroblasts. On day 1, post addition of differentiation media, the *Fmo1* transcript increases to 0.000025 relative to GAPDH. This is an 8-fold increase in the amount of *Fmo1* transcript. After 6 days post addition of differentiation media the *Fmo1* transcript increases to 0.000082. This is a

further 3-fold increase from 3 hours post addition of differentiation media. After 10 days, when the cells are visibly differentiated and express adipocyte markers. *Fmo1* expression relative to GAPDH is 0.0015.

When compared to the P1 and P2 transcripts the global *Fmo1*-transcript is on average 10-fold higher throughout the differentiation process. Within fibroblasts the total relative expression of the P1 and P2 transcripts are present at 8% of the global transcript. After 1 day post differentiation, P0 and P2 transcripts constitute 6% of the global *Fmo1* transcript. At day 6, the P1 and P2 transcripts are expressed at 20% of the global *Fmo1* transcript. At day 10, the P1 and P2 transcripts are expressed at 11% of the global *Fmo1* transcript (Figure 3.9C).

The global transcript is present in greater abundance than the combined P1 and P2 transcripts. It is possible that there is another promoter active in the 3T3-L1 cells and we are measuring the mRNA from this promoter in the global transcript expression. In the mouse the combined expression of P0, P1 and P2 in white adipose tissue is greater than that of the global transcript amount. As the 3T3-L1 cells are a cell line, there may be different mechanisms of *Fmo1* regulation than seen within adipose tissue. Mouse adipose tissue contains other cell types e.g. those of the immune system including macrophages. The non-fat cell types may have an increase in P0, P1 and P2 transcripts over the global transcript. This could obscure the true transcript ratio of adipocytes.



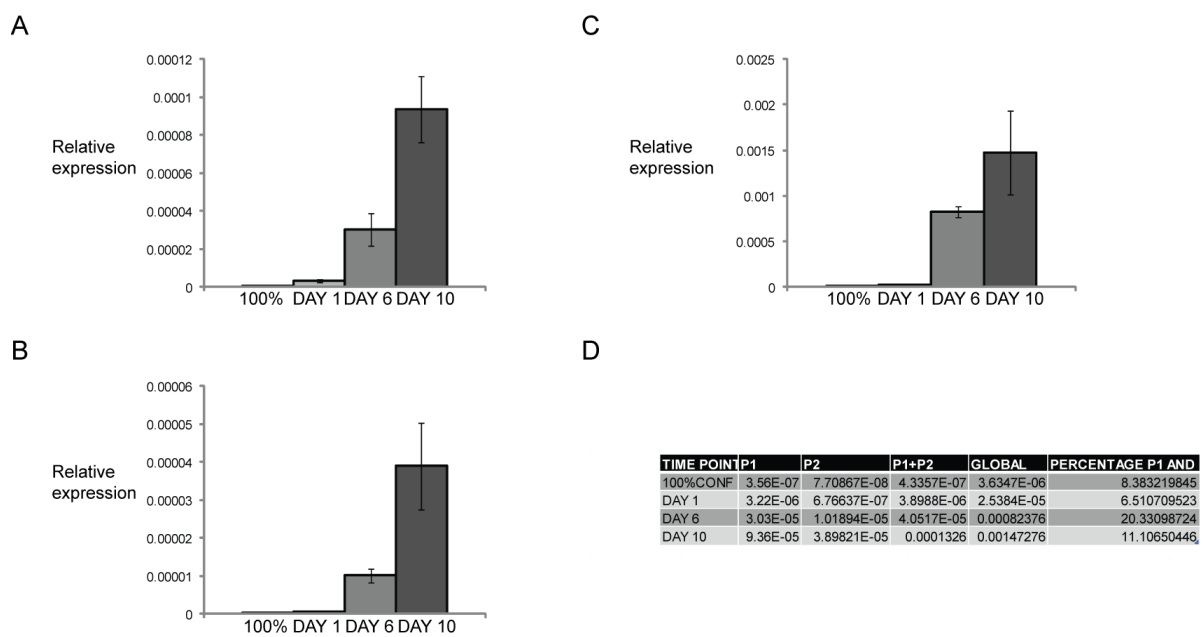


### Figure 3.9 Quantification of *Fmo1* global gene expression during 3T3-L1 differentiation (ATCC)

Relative expression of **(A)** the *Fmo1* P1 transcript **(B)** *Fmo1* P2 transcript and **(C)** global *Fmo1* transcript at different stages of 3T3-L differentiation. The different stages are undifferentiated cells at 100% confluency (100% CONF) and at 1 day, 6 days and 10 days post addition of differentiation media. *Fmo1* gene expression is normalised to the reference gene GAPDH. All experiments were done in triplicate and the error bars represent the standard error. **(D)** The relative amount of P1+P2 *Fmo1* transcript as a percentage of relative global *Fmo1* transcript.

## Discussion

The work described above is the first report of the quantification of global *Fmo1* expression in white fat, muscle, brain and brown fat. Global FMO1 mRNA amounts in white and brown fat is comparable to that found in kidney and liver, where *Fmo1* is expressed at a high level. These data provide support for a role for FMO1 in additional tissues previously not known to express the mRNA (or protein). *Fmo1* expression level in muscle is low relative to other tissues, but expression is high when compared to the reference gene. There may be a role for FMO1 in this tissue. Previously it was not known to what extent each of the alternatively spliced transcripts of *Fmo1*, the P0, the P1, and P2 transcript are produced in different tissues. The experimental data presented within this chapter show the relative amounts of each transcript produced within different tissues. The expression of each transcript has been compared to each of the other transcripts and to the global FMO1 mRNA. This has identified promoter usage in the different tissues and indicated that attenuation of transcription may take place from some promoters in some tissues. The expression of the P1 and P2 *Fmo1* transcripts were quantified during 3T3-L1 differentiation and demonstrate that the mRNAs are increased as cells differentiate from fibroblasts into adipocytes.

The results show that, in the mouse, the P1 promoter is used in all extra-hepatic tissues and that the P1 transcript is abundant in all tissues analysed. The P0 and P2 promoters are active to a similar level in kidney, muscle, brain, brown fat, and white fat. This suggests a common regulatory mechanism between these two promoters within these tissues. In the liver however, only the P0 promoter is used.

In some tissues, the combined amount of the three transcripts does not always equal that of the global *Fmo1*. This suggests that transcription from, in particular, the P1 promoter, is attenuated and that shorter transcripts might be produced. These shorter transcripts would not be detected using the primers designed in the protein-coding region of the mRNA. In the differentiated 3T3-L1 cells, global *Fmo1* expression is much greater than that of the individual transcripts. This may represent the presence of a promoter that is switched on only during the differentiation process and that we have yet to identify. Both the P1 and P2 promoters are used in 3T3-L1 cell differentiation.

**Chapter 4**

**Characterisation of different *FM01***

**promoters**

## Chapter 4: Characterisation of different *FMO1* promoters

### Introduction

The human *FMO1* gene has three known transcriptional start sites (Hernandez et al., 2004). These start sites are homologous to those used in the mouse *Fmo1* gene (Hernandez et al., 2004). In both species three different transcripts are produced, P0, P1 and P2. Previous work has shown that promoter P0 is used predominantly in the human foetal liver. The human P0 promoter has previously been characterized using reporter gene assays (Shephard et al., 2007). The reporter gene construct was transfected into HepG2 cells, which were derived from an adult human hepatoma cell line. The P1 and P2 promoters have yet to be characterised. This chapter will outline the defining of the human *FMO1* P1 and P2 promoters.

A number of genetic polymorphisms are present upstream of both the P1 and P2 transcriptional start sites. These polymorphisms may be present within regulatory sequences and therefore affect the amount of transcript produced. It is desirable to identify polymorphisms that influence transcription. These could be used as markers to identify individuals for whom drug metabolism of *FMO1* substrates might be altered because of production of lower or higher amounts of the protein.

The P1 and P2 promoters have previously not been defined, and the factors that regulate transcription from each, is not known. This chapter describes the experiments carried out to define the regions that comprise the *FMO1* P1 and P2 promoters in different cell types. Subsequently, a bioinformatics approach was used to predict factors that may regulate the activity of the promoters.

Recent advances in genome wide epigenetic analysis has given rise to a large public resource of epigenetic data. We have reviewed these resources which identify open chromatin regions within the *FMO1* gene and identify binding locations of regulatory factors. These data have been used to further justify the experimental data of defining the P1 and P2 promoters.

#### **4.1 Definition of human *FMO1* promoters in COS-7, HK-2, and 3T3-L1 cells**

The *FMO1* promoters have been defined by quantifying the activity of a reporter gene under the control of upstream sequences of each transcriptional start site. Sequences of increasing size, each starting from the transcriptional start site, are introduced to a vector where they act as the promoter responsible for the expression of a luciferase reporter gene (Figure 4.1). The *FMO1* transcripts are known to be expressed at different levels in different tissues (Dolphin et al., 1996; Yeung et al., 2000; Zhang and Cashman, 2006). Therefore I have transfected a number of different cell lines to allow for the tissue-specificity of *FMO1* expression. COS-7 is a monkey kidney fibroblast, HK-2 is a human kidney proximal tubule cell line, and 3T3-L1 is a fibroblast which can be differentiated into adipocytes in culture.

##### **4.1.1 Reporter gene assay controls**

To determine the amount of background activity in the transfected cells, the parent plasmid, used to prepare the reporter gene constructs, is used as a negative control. The negative control is the pGL3-Basic vector, which contains the luciferase gene from the firefly *Photinus pyralis*. The vector is identical to the plasmid containing *FMO1* sequences except that it does not contain a promoter sequence upstream of

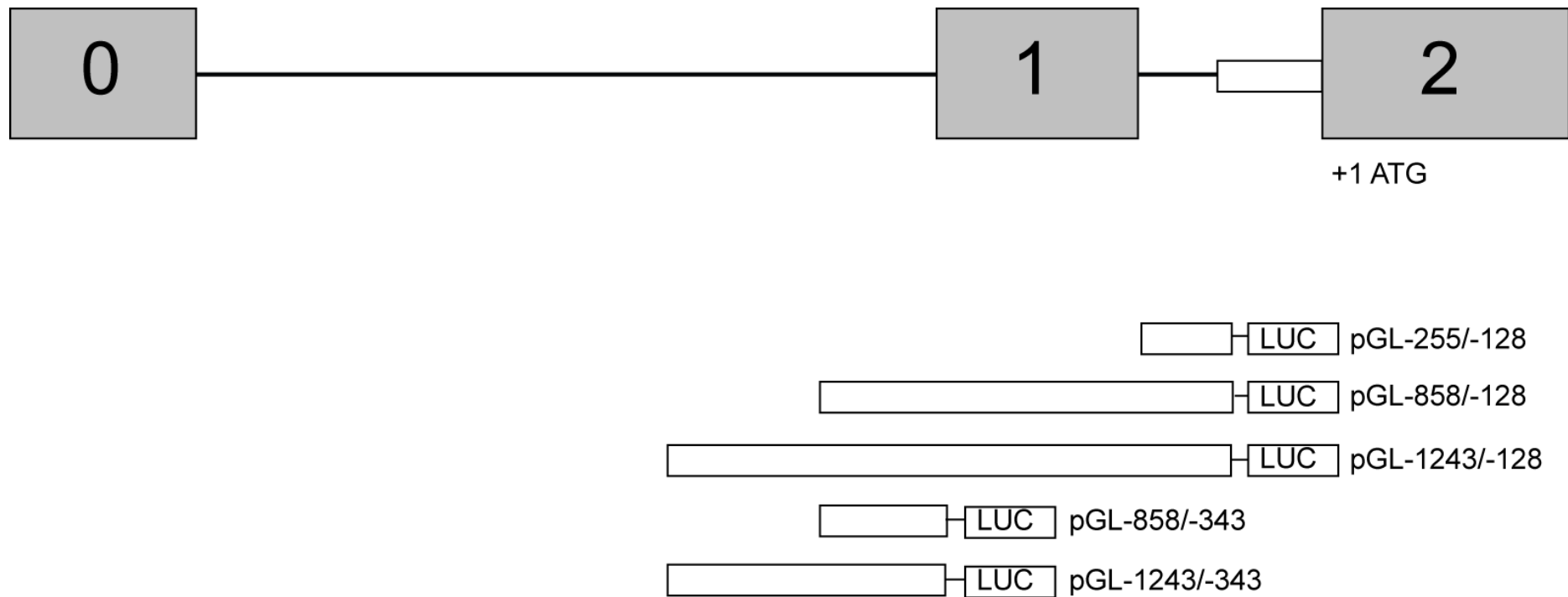


**Figure 4.1 Illustration of the sequences upstream of each of the *FMO1* transcriptional start sites cloned within the pGL3-Basic plasmid**

The figure shows the three regulatory exons of *FMO1*. These are exon 0, exon 1, and exon 2. Within exon 2 translation begins. The location of *FMO1* DNA sequences cloned into luciferase constructs are outlined by the open boxes. The numbers designate the location of the DNA region inserted into the plasmid. The numbers are relative to the A of the ATG translation initiation codon. Constructs were designed from the P2 transcriptional start site which is at location -128 and upstream of the P1 transcriptional start site which starts at position -343.

the transcriptional start site. Therefore any activity detected from the pGL3-Basic vector can be considered as the background activity. A positive control is required to assess the experimental conditions. The positive control used for the reporter gene assays is the pGL-SV40 plasmid, which also contains the luciferase gene from the firefly *Photinus pyralis*. This plasmid contains the SV40 viral promoter and produces high luciferase reporter gene activity within transfected mammalian cells. A third control is required to control for the transfection efficiency of mammalian cells by each plasmid construct. A plasmid is used that contains a coding sequence and is capable of expressing a luciferase protein from a different organism to the firefly *Photinus pyralis*. The plasmid pRL-TK contains a luciferase gene from the sea pansy *Renilla reniformis* and is co-transfected along with the experimental plasmids. The reporter gene activity of the pRL-TK plasmid can be measured separately from the firefly luciferase and is used to normalise the firefly luciferase expression.

#### **4.1.2 Optimisation of transfection for COS-7, HK-2 and 3T3-L1 cell lines**

DNA and lipofectamine reagent (LTX) amounts were optimised for reporter gene activity within COS-7 and HK-2 cell lines. The optimised conditions for 3T3-L1 cell transfection were obtained from the supplier, Invitrogen. Transfection was optimised using a reporter gene construct under the control of the SV40 promoter, pGL-SV40. The SV40 promoter is used as this is a highly efficient viral promoter and will produce a high reporter gene activity within mammalian cell lines. COS-7 and HK-2 cell lines were transfected with 0.6 µg, 0.8 µg and 1 µg of reporter plasmid. Each pGL-SV40 concentration was transfected into the cells using 1 µL, 1.5µL or 2 µL of LTX reagent to determine the amount of lipid required for optimal transfection.

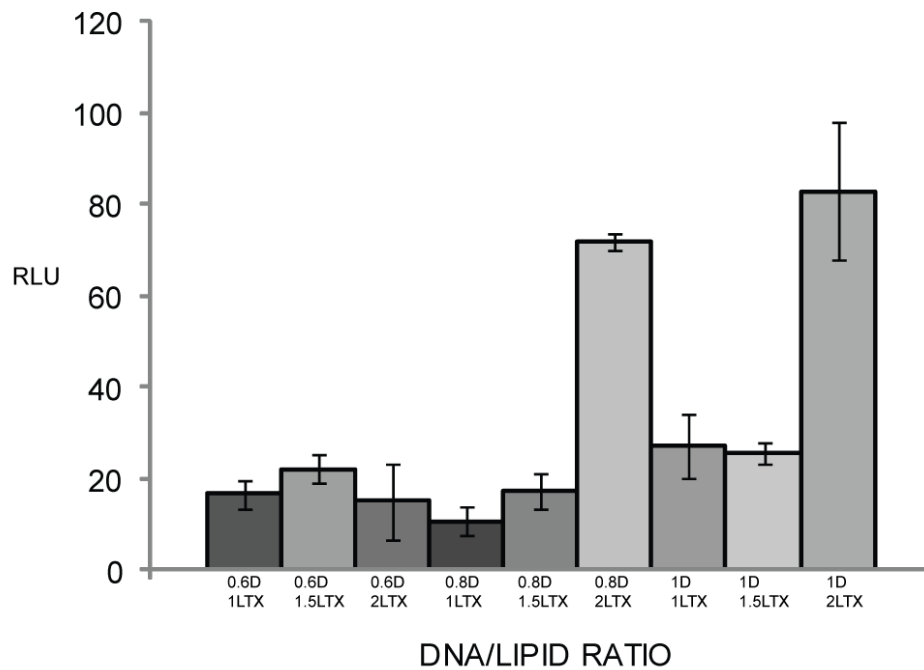


COS-7 (Figure 4.2A) cells transfected with 0.6 µg PGL3-SV40 reporter gene activity using 1 µL, 1.5 µL and 2 µL produced reporter gene activity of about 20 RLU.

Transfection of COS-7 cells with 0.8 µg DNA using 1 µL, 1.5 µL or 2 µL showed no significant improvement in RLU. When the amount of pGL3-SV40 DNA was increased to 1 µg and 2 µL of LTX was used, reporter gene activity increased to 60 RLU.

HK-2 cells (Figure 4.2B) transfected with 0.6 µg, 0.8 µg, and 1 µg of pGL-SV40 DNA using 1 or 1.5 µL of LTX reagent all produced activity averaging 20 RLU. When 0.8 µg and 1 µg of pGL-SV40 DNA was transfected into the HK-2 cells using an increased amount of LTX of 2 µL, reporter gene activity was increased to about 80 RLU. As reporter gene activity of the pGL3-SV40 construct was slightly higher when transfecting 1 µg of reporter plasmid and 2 µL of LTX it was decided these conditions would be used for transfection of *FMO1* reporter constructs into HK-2 cells.

A



B

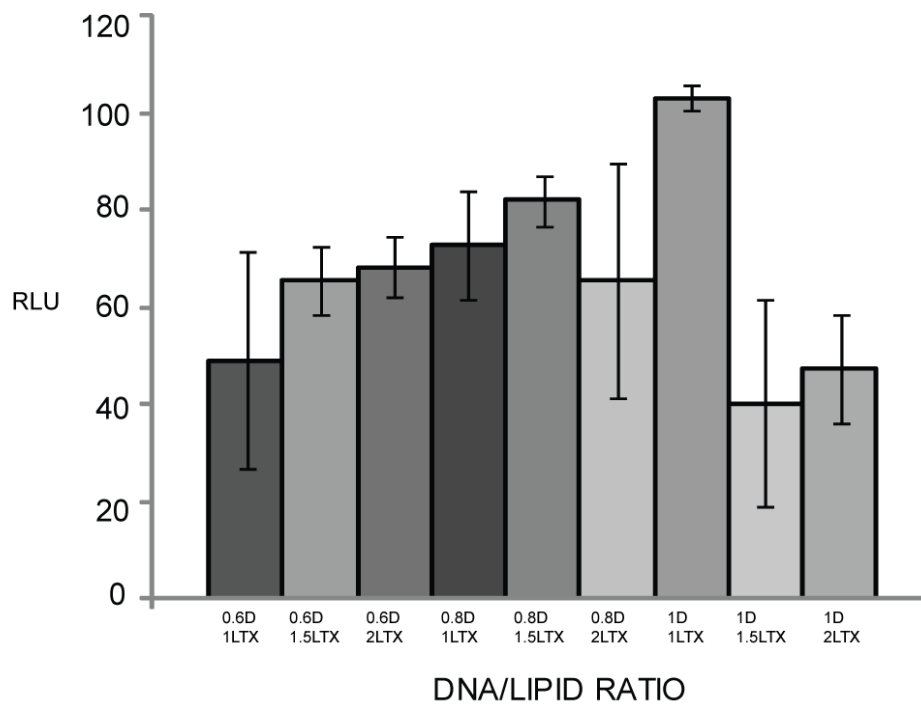


**Figure 4.2 Determination of DNA/LIPID ratios for optimal transfection of (A) COS-7 and (B) HK-2 cells**

The pGL-SV40 plasmid was transfected into both cell types at different DNA concentrations. These were 0.6 µg, 0.8 µg and 1 µg. Each DNA concentration was transfected using 1 µL, 1.5 µL and 2 µL of lipid reagent. The conditions used are shown in the figure. Cells were transfected with pRL-TK vector to control for transfection efficiency. The RLU values are pGL-SV40 light units relative to the pRL-TK light units. All experiments were done in triplicate and the error bars represent the standard deviation.

### 4.1.3 COS-7 cell transfection (Figure 4.3)

The construct pGL-255\_-128 which contains the sequence directly upstream of the *FMO1* P2 transcriptional start site produces an average of  $37 \pm 13.7$  RLU of reporter gene activity within COS-7 cells. The construct pGL-858\_-128 containing additional further sequence upstream of the P2 transcriptional start and continuing through the P1 transcriptional start site produces  $87 \pm 22.4$  RLU. This is a nearly 3-fold increase in reporter gene activity from the pGL-255\_-128 construct. The construct pGL-858\_-343 containing sequence directly upstream of the P1 transcriptional start site produces an average of  $217 \pm 63.3$  RLU. This is about 4-fold higher than the pGL-255\_-128 construct and over 2-fold higher than the pGL-858\_-128 construct. The constructs pGL-1243\_-128 and pGL-1243\_-343, which contains additional upstream sequence produce only 1 RLU. The sequence -1243\_-858 must contain a sequence that negatively regulates the reporter gene activity. Reducing the length of the pGL-858\_-343 construct to contain the sequence between -600\_-343 results in loss of reporter gene activity to 1 RLU. Therefore the sequence -858\_-600 of the *FMO1* gene upstream of the P1 promoter is responsible for the reporter gene activity observed within COS-7 cells. The reporter gene construct (Pgl-521\_+50) which defines the P0 promoter was transfected into COS-7 cells but showed low reporter gene activity.

### 4.1.4 Ratio of *FMO1* promoter usage in COS-7 cells

COS-7 cell transfection results defined the P1 promoter region as the sequence between -858\_-343 upstream of the *FMO1* translation initiation start site. This is because the pGL-858\_-343 construct when transfected into COS-7 cells gave the highest luciferase activity. The activity was reduced when additional upstream

sequence was included (pGL-1243\_-343 construct). The P2 promoter region active within COS-7 cells was defined as the region between -255\_-128. This is because the construct, pGL-255\_-128 (upstream of the P2 transcriptional start site) produced the highest reporter gene activity. The promoter was not defined further upstream as these sequences would overlap with the P1 transcriptional start site.

Comparison of reporter gene activity from P1 and P2 was made by normalising reporter gene construct activity to the activity of the P2 promoter construct. The activity of pGL-255\_-128 is set to 1. The reporter gene activity of the P1 promoter construct shows a significant 5-fold increase in reporter gene activity compared with the P2 promoter. The P1 promoter is therefore a stronger promoter in COS-7 cells than is P2. To understand the ratio of promoter usage between the P1 and P2 construct the reporter gene activity of the pGL-858\_-128 needs to be considered. The reporter gene activity of this construct will identify in which ratio the promoters are being used. When reporter gene activities are normalised to the P2 construct the pGL-858\_-128 construct is, significantly, 2.35-fold more active than this. When the pGL-858\_-128 and the P1 promoter construct relative activity to P2 are compared the pGL-858\_-128 construct is significantly 2.5-fold lower than the P1 promoter construct. Therefore the reporter gene activity of the construct containing both P1 and P2 shows intermediate activity between the P1 and P2 constructs alone. It is likely that within COS-7 cells the two promoters are being used equally but that the P1 promoter is the stronger promoter.

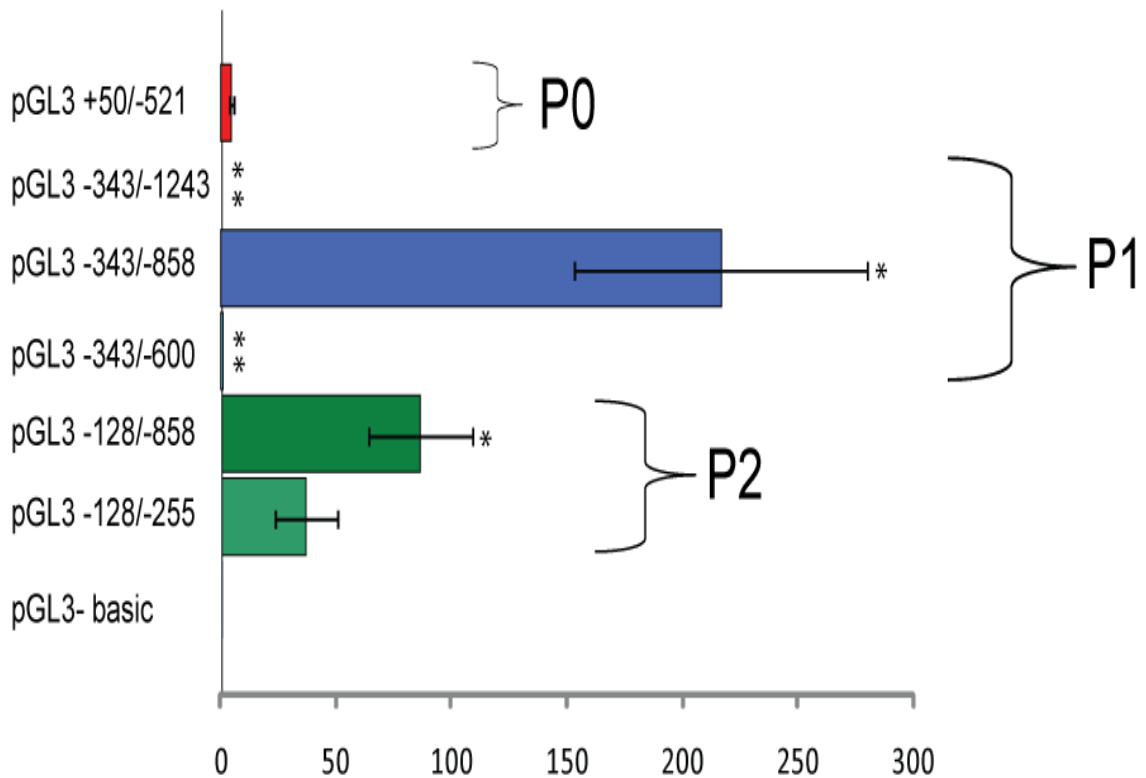


**Figure 4.3 Reporter gene activity of PGL3-Basic constructs containing DNA sequences upstream of the three FMO1 transcriptional start sites transfected into COS-7 cells**

COS-7 cells were transfected with pGL3 constructs containing *FMO1* sequences upstream of each of the three *FMO1* transcriptional start sites. The sequence location is shown next to each bar and the co-ordinates are relative to the *FMO1* mRNA translation start codon. The constructs are grouped based on which transcriptional start site they are directly upstream of. The P0 construct is labelled red. Constructs upstream of P1 are labelled blue and constructs upstream of P2 are labelled green. The pGL3 basic plasmid was transfected as a negative control. All experiments were done in triplicate and the error bars indicate the standard deviation. The construct pGL-858\_-128 is significantly different from pGL-255\_-128 and pGL-858\_-343 ( $p < 0.03$ , \*). The construct pGL-1243\_-343 and pGL-600\_343 are significantly different from pGL-858\_-343, ( $P < 0.009^{**}$ ).

#### 4.1.5 Transfection of HK-2 cells with FMO1 promoter constructs (Figure 4.4)

The HK-2 cell line was derived from human proximal tubule kidney cells and was used to test reporter gene activity because FMO1 mRNA has been localised to these cells in the mouse kidney using *in-situ* hybridization experiments (Janmohamed et al., 2004).

The P0 promoter construct (pGL-521\_+50) produces reporter gene activity of  $4.5 \pm 0.9$  RLU. The construct pGL-255\_-128 which contains the sequence directly upstream of the P2 transcriptional start site produces an average of  $3 \pm 0.1$  RLU of reporter gene activity. The construct pGL-858\_-128, containing additional further sequence upstream of the P2 transcriptional start and continuing through the P1 transcriptional start site produces  $2.7 \pm 0.4$  RLU. This is similar to that of the activity of the P2 reporter gene construct. The construct pGL-858\_-343 containing sequence directly upstream of the P1 transcriptional start site produces an average of  $8 \pm 1.1$  RLU, which is higher than obtained with both the P2 and P0 reporter gene constructs. The constructs pGL-1243\_-128 and pGL-1243\_-343 which contain additional upstream sequence produce  $1 \pm 0.1$  RLU. The sequence -1243\_-858 within the construct is negatively regulating the reporter gene activity as was seen also in COS-7 and 3T3 cells (see below). Reducing the length of the pGL-858\_-343 construct to -600\_-343 results in loss of reporter gene activity to  $1 \pm 0.3$  RLU. The FMO1 sequence between -858\_-600 is therefore responsible for the reporter gene activity within HK-2 cells upstream of the P1 promoter.

#### **4.1.6 Ratio of FMO1 promoter usage in HK-2 cells (Figure 4.4)**

Transfection of HK-2 cells with the series of *FMO1* promoter constructs define the P1 promoter region in these cells as the sequence -858\_-343 upstream of the *FMO1* translational start site. As within COS-7 cells, but in contrast to 3T3-L1 cells (see below), the sequence -1243\_-858 significantly reduces reporter gene activity. The P2 promoter region within HK-2 is defined as the region -255\_-128 as was the case for transfected COS-7 cells. The construct, pGL-255\_-128 (upstream of the P2 transcriptional start site) produces the highest reporter gene activity. The promoter is not defined further as upstream sequence as this overlaps with the P1 transcriptional start site. The ratio of promoter activity was determined as previously explained for COS-7 cell transfections. The activity of the pGL-255\_-128 is set to 1. The reporter gene activity of the P1 promoter is significantly higher, 3-fold, than the P2 promoter. The P1 promoter is therefore a stronger promoter within HK-2 cells than the P2 promoter. The reporter gene activity of the construct containing the P1 and P2 promoter (pGL-858\_-128) is equal to the P2 promoter construct. Within HK-2 cells it is likely that the P2 promoter is favoured over the P1 promoter.

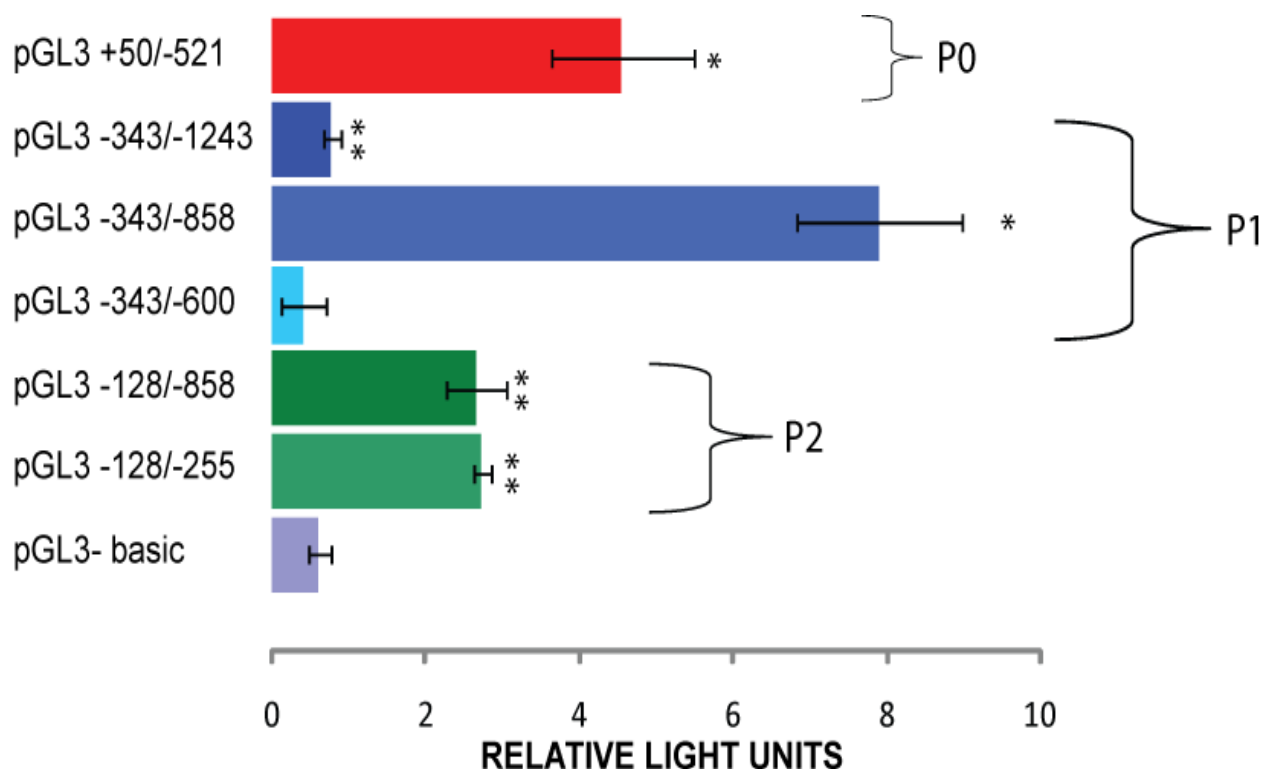


**Figure 4.4 Reporter gene activity of PGL3-Basic constructs containing DNA sequences upstream of the three *FMO1* transcriptional start sites transfected in HK-2 cells**

HK-2 cells were transfected with pGL3 constructs containing *FMO1* sequences upstream of each of the three *FMO1* transcriptional start sites. The sequence location is shown next to each bar and the co-ordinates are relative to the *FMO1* mRNA translation start codon. The constructs are grouped based on which transcriptional start site they are directly upstream of. The P0 construct is labelled red. Constructs upstream of P1 are labelled blue and constructs upstream of P2 are labelled green. The pGL3 basic plasmid was transfected as a negative control. All experiments were done in triplicate and the error bars indicate the standard deviation. The construct pGL-858\_-343 is significantly different from pGL-255\_-128, pGL-858\_-128, pGL-1243\_-343 and pGL-858\_-600 ( $p < 0.002$ , \*\*). The construct pGL-+50/521 is significantly different from the pGL-255\_-128 and the construct pGL-858\_-343 ( $p < 0.03$ , \*) and pGL-600\_-343 are significantly different from pGL-858\_-343,  $P < 0.009$ .



#### **4.1.7 *FMO1* promoter usage in 3T3-L1 fibroblast cells (Figure 4.5)**

The 3T3-L1 cell line is a mouse fibroblast cell line. It is possible to differentiate these cells into white adipocytes. The reporter construct pGL-255\_-128, which contains the sequence directly upstream of the P2 transcriptional start site produces an average of  $11 \pm 2.2$  RLU of reporter gene activity in transfected 3T3-1 cells. The pGL-521\_+50 construct containing the previously defined P0 promoter shows an average reporter gene activity of  $14 \pm 0.33$  RLU. This is comparable to the P2 reporter gene activity.

The construct pGL-858\_-128 containing additional further sequence upstream of the P2 transcriptional start and continuing through the P1 transcriptional start site produces a reduced amount of reporter gene activity of  $7 \pm 0.4$  RLU. The construct pGL-858\_-343 containing sequence directly upstream of the P1 transcriptional start site produces an average of  $7 \pm 0.16$  RLU. The constructs pGL-1243\_-128 and pGL-1243\_-343, which both contain additional upstream sequence, produce  $4 \pm 0.16$  RLU. As seen in COS-7 cells the sequence -1243\_-858 also reduces reporter gene activity in 3T3-L1 cells, although the reduction is not as great as that observed in transfected COS-7 cells. When the pGL-858\_-343 construct length is reduced to -600\_-343 reporter gene activity is reduced further, to 2 RLU. Therefore, as was observed in transfected COS-7 cells the *FMO1* sequence between -858\_-600, upstream of the P1 promoter, is responsible for the reporter gene activity observed in 3T3-L1 cells.

#### **4.1.8 Ratio of *FMO1* promoter usage in 3T3-L1 cells**

Transfection of 3T3-L1 cells with various *FMO1* promoter constructs define the P1 promoter region as the sequence -858\_-343 upstream of the *FMO1* translational start site. In comparison to the results obtained from transfected COS-7 cells the sequence -1243\_-858 does not reduce reporter gene activity as much in 3T3-L1

cells. This sequence region does not however increase reporter gene activity and can therefore be disregarded as contributing to the P1 promoter. The P2 promoter region within 3T3-L1 cells is defined as the region -255\_-128 as was the case in transfected COS-7 cells. The ratio of *FMO1* promoter activity in 3T3-L1 cells was determined as explained above for COS-7 cells. Comparison of reporter gene activity was made by normalising reporter gene construct activity to the activity of the P2 promoter construct for ease of comparison with other cell lines tested for promoter activity. The activity of the pGL-255\_-128 is set to 1. The reporter gene activity of the P2 promoter is 1.6-fold higher than that of the P1 promoter and it is significantly stronger ( $p < 0.03$ ). The reporter gene activity of pGL-858\_-128 containing the P1 and P2 promoters is 6.75 fold higher than the P2 promoter. It is not significantly different from the P1 promoter reporter gene activity. Extension of the promoter from -255\_-128 to -858\_-128 shows that the P1 promoter, when present with the P2 promoter, is favoured.

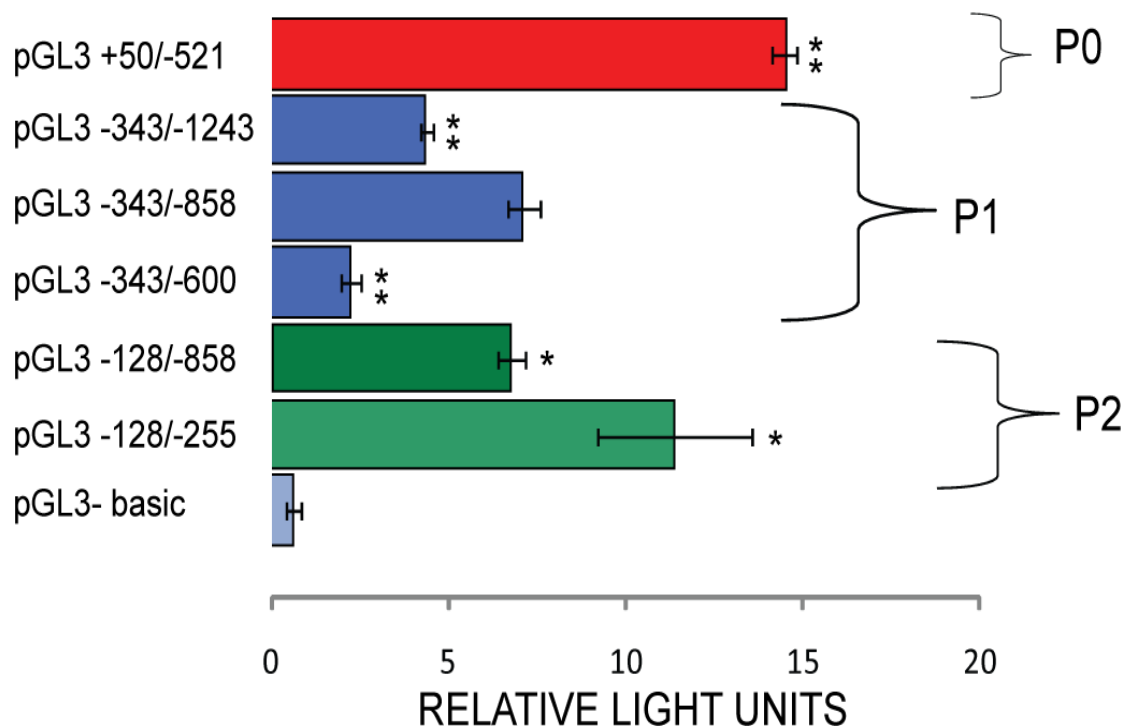


**Figure 4.5 Reporter gene activity of PGL3-Basic constructs containing DNA sequences upstream of the three *FMO1* transcriptional start sites transfected in 3T3-L1 cells**

3T3-L1 cells were transfected with pGL3 constructs containing *FMO1* sequences upstream of each of the three *FMO1* transcriptional start sites. The sequence location is shown next to each bar which is relative to the *FMO1* translation start codon. The constructs are grouped based on which transcriptional start site they are directly upstream of. The P0 construct is labelled red. Constructs upstream of P1 are labelled blue and constructs upstream of P2 are labelled green. The pGL3 basic plasmid was transfected as a negative control. All experiments were done in triplicate and the error bars indicate the standard deviation. The construct pGL-255\_-128 is significantly different from pGL-858\_-128 and pGL-858\_-343 ( $p < 0.03$ ). The construct pGL-858\_-343 is significantly different from the pGL-1243\_-343 and pGL-600\_-343 constructs ( $p < 0.0006$ , \*\*). The construct pGL-521\_+50) is significantly different from the pGL-858\_-343 ( $p < 0.00002$ , \*\*).

## 4.2 Transfection using nucleofection of 3T3-L1 differentiated into adipocytes

We now know that FMO1 is highly expressed in white adipose tissue (Omar, Ph D thesis, 2009; Veeravalli et al., Unpublished). In the previous section I described the poor expression of *FMO1* promoter constructs in undifferentiated 3T3-L1 cells. In this section the transfection of 3T3-L1 cells differentiated into adipocytes is described. 3T3-L1 cells differentiated into adipocytes are notoriously difficult to transfect. Transfection has been achieved previously using lenti-viruses (Inoue et al., 2010) and electroporation (Rolland et al., 1995; Rolland et al., 1996). Lenti-viral methods have safety implications and require a dedicated category 3 laboratory. Electroporation methods require high amounts of optimisation and yield a very limited transfection efficiency of 10-20%. Cationic-lipid methods of transfection which were used to transfect cell lines previously to a high efficiency are not effective at transfecting 3T3-L1 adipocytes.

Recent advances in electroporation have resulted in companies producing electroporation units with optimised conditions for different cell lines. This includes optimisations for 3T3-L1 adipocytes. To test the transfection efficiency of 3T3-L1 adipocytes a plasmid encoding the enhanced green fluorescent protein eGFP was nucleofected into the adipocytes and the percentage of GFP expressing cells was determined. Transfection efficiency was observed to be 30-40% (Figure 4.6). The PGL-SV40 construct which was used in previous experiments as a positive control was nucleofected into 3T3-L1 adipocytes. This plasmid produced luciferase activity of between 50-100000 RLU. Therefore the 3T3-L1 adipocytes could be used to test

human *FMO1* promoters in the context of expression of the gene in white fat. The *FMO1* P2 promoter was transfected into the 3T3-L1 adipocytes and showed a high

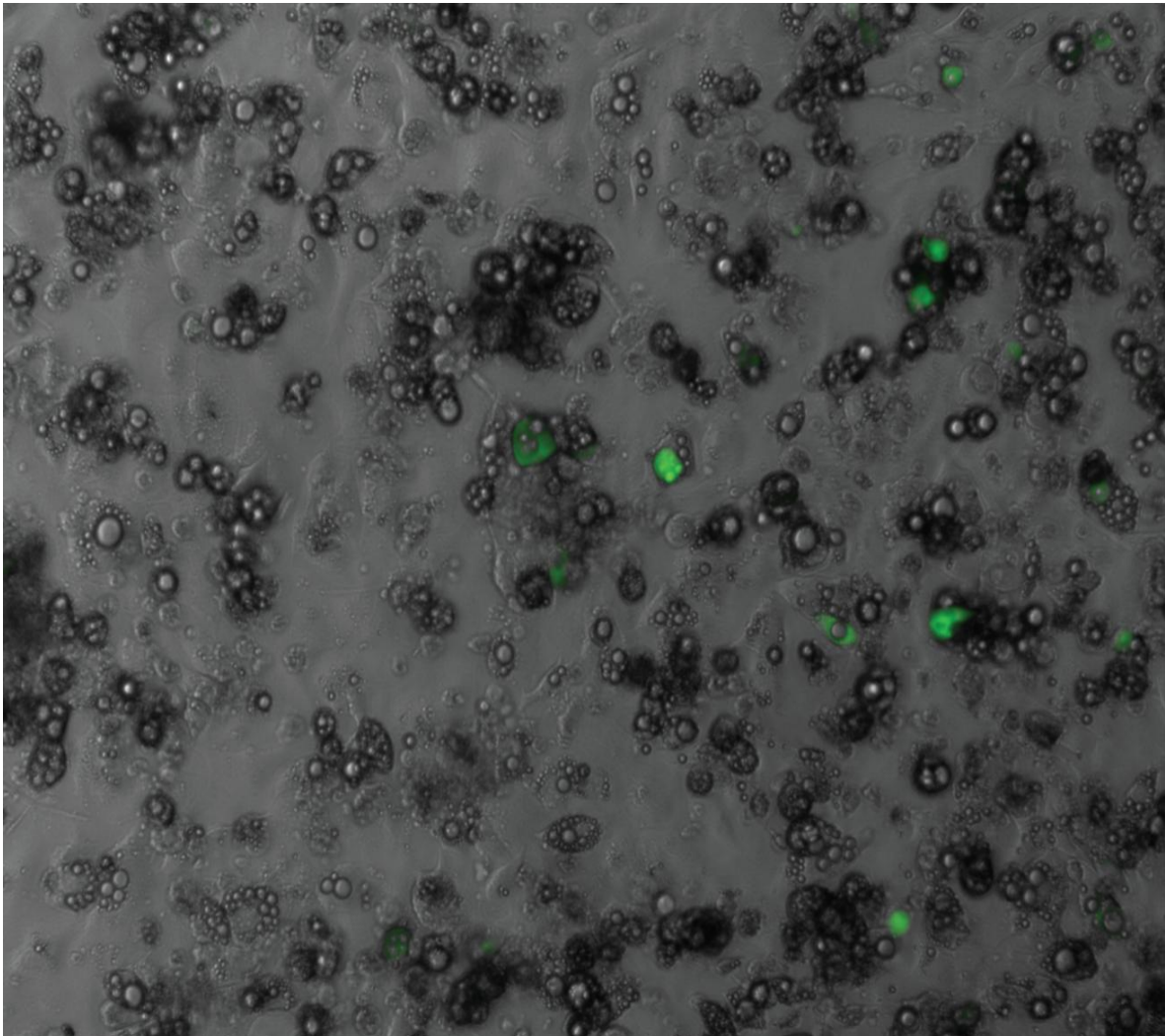


**Figure 4.6 GFP Nucleofection of 3T3-L1 adipocytes**

2  $\mu\text{g}$  of pmaxGFP® Vector (*Lonza*) was nucleofected using  $1 \times 10^7$  3T3-L1 adipocytes. Cells were plated onto 18mm dishes and imaged using fluorescence microscopy. Transfection efficiency was predicted to be 30%.

activity of between 20-30000 RLU. This data is not normalised as the pRL-TK construct used to normalise the transfection efficiency shows low or no activity in the differentiated cells. Therefore this activity could not be compared to the results obtained for undifferentiated 3T3-L1 cells described in the previous section. However, the increase in firefly luciferase activity is orders of magnitude greater than that obtained in undifferentiated 3T3-L1 cells. It seems reasonable to assume that *FMO1* promoter activity has increased due to differentiation of the cells into adipocytes. This conclusion is supported by our findings that *FMO1* mRNA is not expressed in 3T3-L1 fibroblasts, but is expressed in the differentiated cells (see chapter 1).

In future these promoter sequences identified as being responsible for the increase in transcription of *FMO1* P1 and P2 transcripts can be used to observe any differences in transcription amounts caused by SNPs.

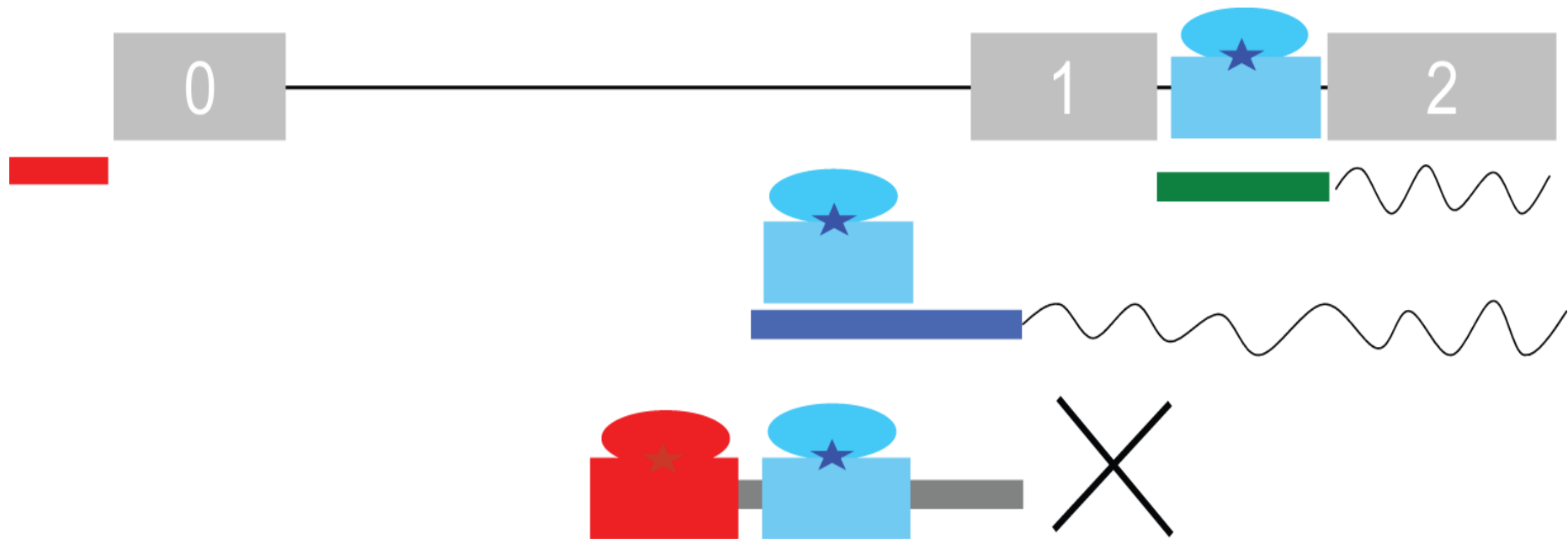


**Figure 4.7 Illustration of human *FMO1* promoters defined by reporter gene assays**

The numbered grey boxes above represent exons within human *FMO1*. The P0 transcriptional start site begins at the start of exon 0. Upstream of this represents the previously defined promoter within HepG2 cells. The P2 promoter is represented between exon 1 and exon 2 which is active in all 3 cell lines (shown in blue). The P1 promoter has a positive promoter element directly upstream of P1 (shown in blue). Increasing the length of this construct results in repressed luciferase activity (shown in red). This repression is seen in both primate cell lines (COS-7 and HK-2) but less repression is seen within the mouse cell line (3T3-L1).

### **4.3 The *FMO1* P2 promoter region and prediction of transcription factor binding**

The human P2 promoter has been defined as the region of DNA between exon 1 and exon 2, which is located between -255\_-128 upstream of the ATG translation start site. Different bioinformatics programs were used to predict binding of transcription factors to the P1 and P2 promoter regions including MatInspector, PROMO, and AliBaba. The human P2 promoter region was aligned with the mouse sequence directly upstream of the P2 transcriptional start site (Figure 4.8). This revealed large regions of sequence conservation. The human promoter region was then examined for transcription factor binding motifs. The mouse sequence was also examined in this way. This is to account for conservation in transcription factor binding between mouse and human as well as for sequence homology.

A number of different factors were predicted to bind to the P2 promoter. The promoter contains no TATA box which is a common motif found within the core promoter of several genes. The human *FMO1* P2 promoter can therefore be described as TATA-less promoters. The most conserved transcription factor binding motif within the P2 promoter is a GC box binding motif which is predicted to bind SP1, a constitutively expressed transcription factor (Figure 4.8). This is within a conserved region with the mouse, however the mouse does not contain a GC box as there is a C>T transition within this motif (Figure 4.8). The transcription factor E2F is predicted to bind upstream of SP1 but does not show conservation when aligned to the mouse sequence (Figure 4.8). Further downstream there is a large region of conservation and contains a sequence which is predicted to bind a nuclear hormone receptor. It could be a potential binding site for a number of proteins including the



estrogen, thyroid, progesterone, or vitamin D receptors, PPAR- $\gamma$  or RXR-alpha (Figure 4.8).

Previous observations (described in chapter 3) showed an increase in P2 transcripts when 3T3-L1 fibroblasts are differentiated into adipocytes. The factors predicted to bind to the P2 promoter which could be responsible for this effect are RXR-alpha and PPAR- $\gamma$  or the thyroid hormone receptor (T3R alpha). PPAR- $\gamma$  and RXR-alpha form a heterodimer to regulate genes during adipocyte differentiation. PGC1-alpha, a transcriptional co-activator also interacts with both RXR-alpha and PPAR- $\gamma$  to activate transcription. PGC1-alpha's possible role in the regulation of *FMO1* will be discussed later.



#### **4.4 The defined P1 promoter region and potential protein binding sites**

Transfection experiments of three different cell lines cell lines have identified a region in the human *FMO1* gene between -858\_-343 that positively regulates reporter gene transcription. A number of transcription factor binding sites are predicted in this region and correlate with the expression profiles revealed for *FMO1*. The muscle specific transcription factors, HEB, MyoD, and myogenin are predicted to bind within the P1 promoter within conserved regions with mouse (Figure 4.9). Previously, it was shown by RT-PCR that the predominant *FMO1* transcript in muscle is from the P1 promoter (see chapter 3). Expression data from microarrays show mouse *Fmo1* being upregulated during C2C12 myotube differentiation (Cam et al., 2006). When treated with a p73 inhibitor the myoblast cell line increases the expression of *FMO1* to the level observed within the differentiated myotubes (Cam et al., 2006). Additional expression profiles suggest this is due to direct or indirect regulation by the transcription factor MyoD (a transcription factor required for muscle cell differentiation). When MyoD is overexpressed within a fibroblast cell line *FMO1* mRNA is significantly upregulated (Di Padova et al., 2007). When a mutant form of MyoD is overexpressed the amount of *FMO1* mRNA upregulation is reduced by 50% (Di Padova et al., 2007).

Additional expression profiles give clues that *Fmo1* may be regulated by PGC1-alpha, a co-activator of many factors including PPAR-gamma. Palmitate treatment which inhibits PGC1-alpha also knocks down *Fmo1* expression in muscle. In comparison in mouse brown fat, when PGC1-alpha is knocked down, *Fmo1* expression is increased. It therefore seems that the effect of PGC1-alpha on

*Fmo1* expression may be tissue specific and may be involved in the use of multiple promoters for *Fmo1*.

A number of consensus DNA binding sites for the thyroid hormone receptor are predicted by MatInspector, Ali baba, and Promo transcription factor prediction tools. This hormone receptor has been shown to interact with the co-factor PGC1-alpha and subsequently activate transcription (Wu et al., 2002). This could be responsible for *Fmo1* activation in brown fat and muscle. PGC1 alpha is not expressed in white fat and therefore the thyroid hormone receptor may be upregulating *Fmo1* independently within this tissue. Other transcription factors that may be responsible for the increase in *Fmo1* P1 transcript are PPAR-gamma and CCAAT binding proteins. There are 3 predicted sites for CCAAT transcription factor binding within the P1 promoter (Figure 4.9).

The CCAAT binding protein and PPAR-gamma transcription factors are predicted to bind within the P1 promoter. These transcription factors are responsible for the increase in transcription of many genes during adipocyte differentiation and may be involved in *Fmo1* upregulation during 3T3-L1 differentiation.

A number of sites for a neuro-developmental factor (hen-1) are predicted within the P1 promoter region. This transcription factor was observed to be significantly over-represented in the promoter of genes which are upregulated during adipocyte differentiation. The same study also showed the upregulation of *Fmo3* during adipocyte differentiation (Kim et al., 2007).

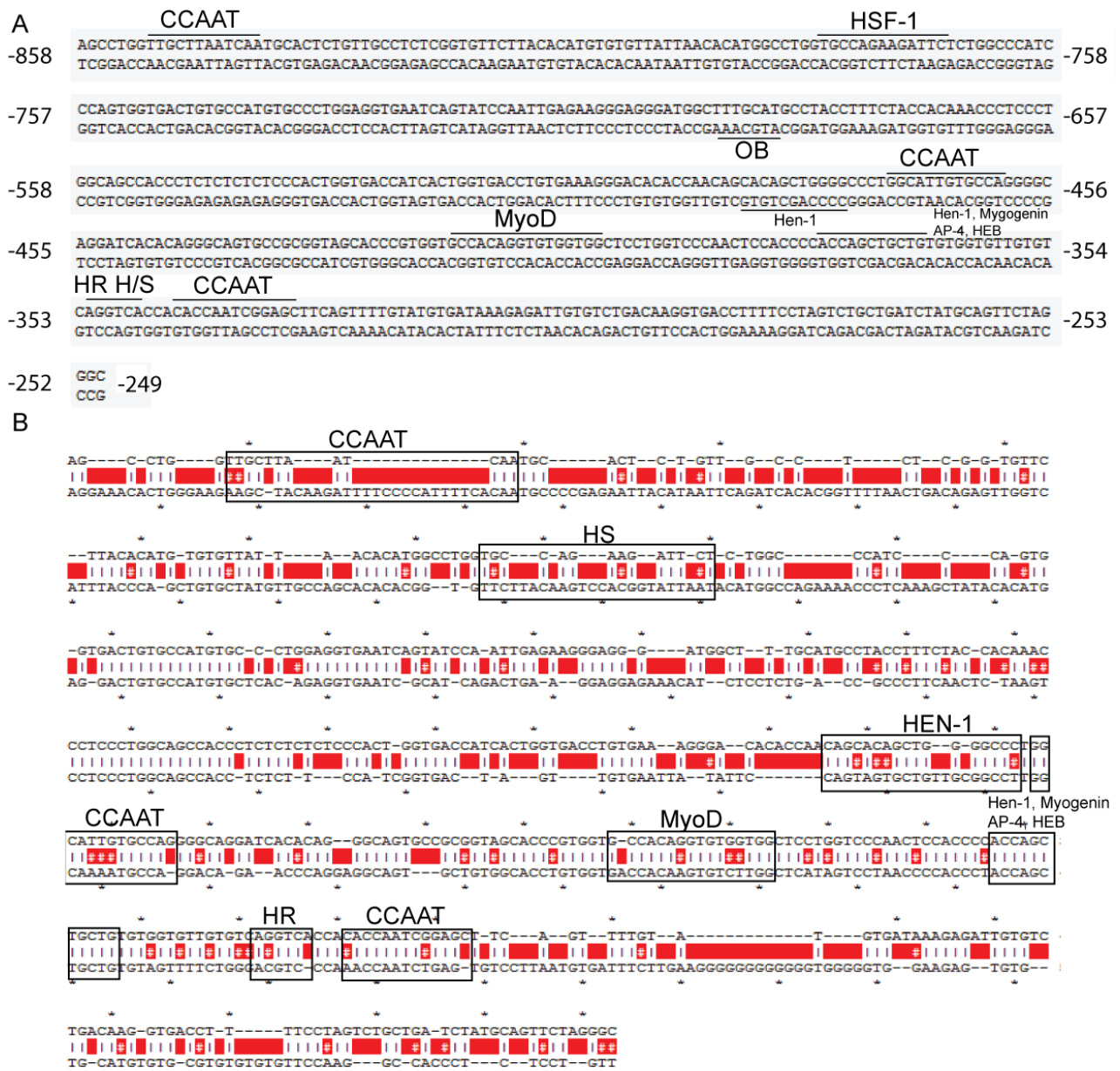


**Figure 4.9 Annotation of *FMO1* P1 promoter**

**(A)** Predicted binding locations of transcription factors within the defined *FMO1* P1 promoter. **(B)** Alignment of the *FMO1* human and mouse P1 promoters. Three CCAAT protein binding regions are outlined in the above figure. Their conservation with mouse is shown below. The figure outlines further predictions for binding sites for muscle specific factors myogenin and myoD. Within the same region Hen1, AP-4, and HEB are predicted to bind. Downstream of these sites a half-site for a nuclear hormone receptor is illustrated.

## **4.5 Epigenetic analysis of the human *FMO1* promoters**

Recent advances in epigenomics have led to genome-wide studies of chromatin analysis becoming available to the researcher. Two sources of data could tell us more about potential regulatory regions of *FMO1*. These are epigenetic studies undertaken in different human tissues and genome-wide DNase I hypersensitive (HR) assays undertaken in both cell lines and tissues. The data are obtained from The University of California, Santa Cruz (UCSC) genome browser (Kent et al., 2002) using the UCSC Genome Browser database (Rhead et al., 2010) <http://genome.ucsc.edu/>. This is an open resource which provides genome annotation for examining and comparing the genomes of organisms, aligning sequence to genomes, and displaying and sharing users' own annotation data. The data showing DNase I-seq data from different human tissues were obtained from the Epigenomics Data Analysis and Coordinating Centre (EDACC) <http://nihroadmap.nih.gov/epigenomics/>. Chip-seq data was produced within the UCSC genome browser from data obtained from the Myers Lab at the Hudson Alpha Institute for Biotechnology and by the labs of Michael Snyder, Mark Gerstein and Sherman Weissman at Yale University; Peggy Farnham at UC Davis; and Kevin Struhl at Harvard.

### **4.5.1 DNase I hypersensitive regions (HRs) located within and surrounding the *FMO1* gene (Fig. 4.10)**

The Figure (Figure 4.10) shows a schematic diagram of DNase I HR sites in multiple human foetal tissues. These tissues are adrenal gland, brain, heart, kidney and lung. A DNase I hypersensitive region (HR) is present roughly -2000 bp upstream of the

P0 transcriptional start site (Figure 4.10). This HR is present within the adrenal gland and heart but not present within the kidney, brain, and lung. A second DNase I HR is present 3500 bp downstream of the P0 transcriptional start site (Figure 4.10). This HR is seen in all tissues analyzed. The tissue-specific HR is highlighted within Figure 4.10(\*). In all tissues analysed DNase I HRs are present within the P1 and P2 promoter regions defined earlier within this chapter. However, differences are seen in the size and signal of these HRs between different tissues.

## FMO1 TRANSCRIPTS

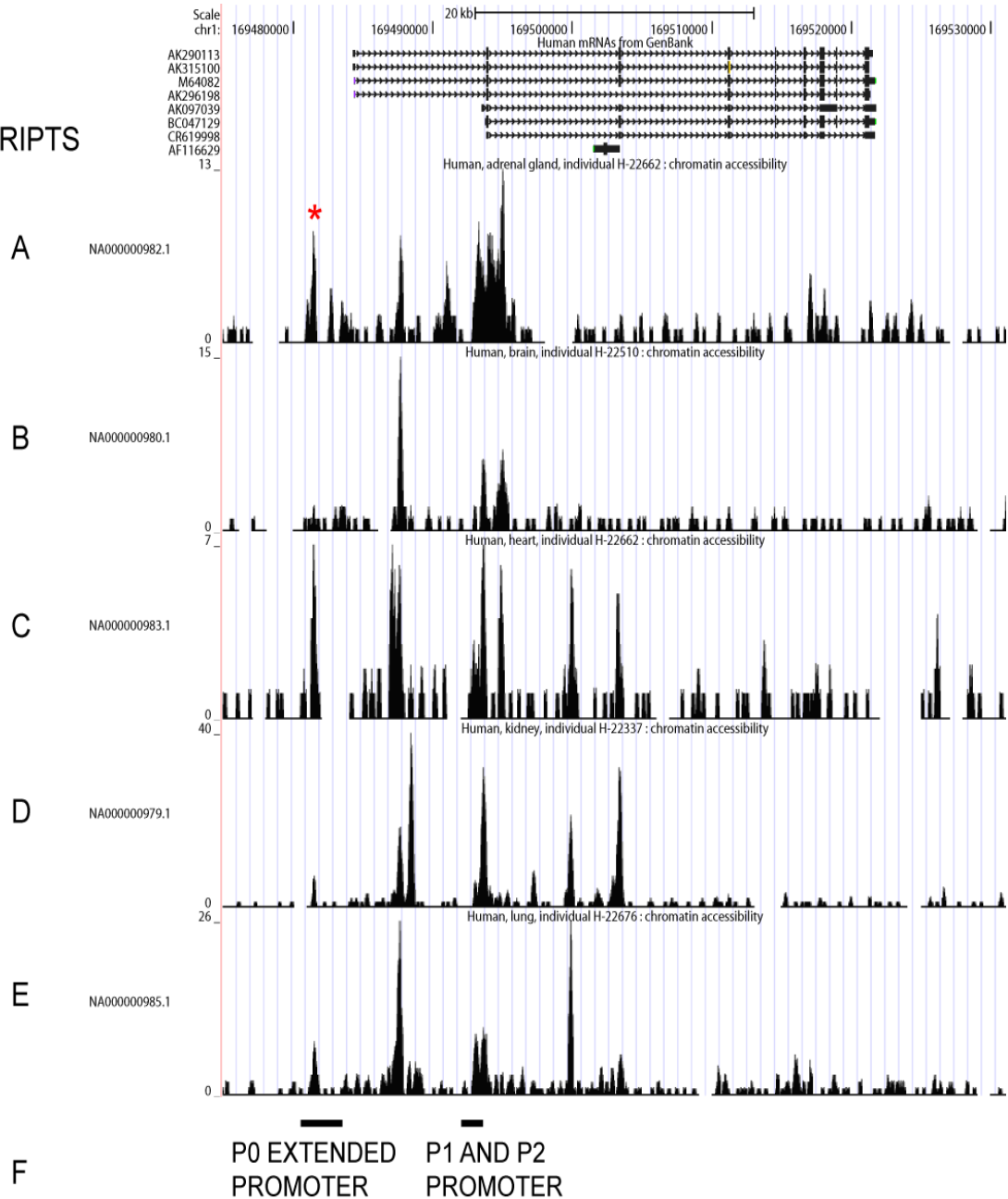


**Figure 4.10 Genome wide DNase I chromatin assays outlining DNase I sensitive sites upstream of the FMO1 P0, P1 and P2 promoter.**

DNase I sensitivity assay in human tissue (A) foetal adrenal (B) foetal brain (C) foetal heart (D) foetal kidney (E) foetal lung and (F) Location of the defined FMO1 P0, P1 and P2 promoters. DNase I hypersensitivity sites occur within the different human tissues for the previously defined P0, P1 and P2 promoters further validating their existence. The asterisk represents DNase I hypersensitive sites that change dramatically between different tissues. The above figure shows data obtained from the UCSC genome browser. The individuals who contributed to this work are cited at the beginning of this section (4.5).



## **4.5.2 DNase I Hypersensitivity regions in different tissues surrounding the P1 and P2 promoters (Figure 4.11)**

As discussed in the introduction DNase I-seq is a technique which identifies regions of DNA susceptible to DNase I digestion. These regions are good predictors of regulatory regions as the chromatin is in an open conformational state. When whole genomic DNA is treated with DNase I and fragments are sequenced, the DNase I sensitive regions will be enriched. This is illustrated as a peak within the schematic diagrams shown below. The stronger the peak the more sensitive that region is to DNase I digestion.

There are two prominent DNase I HRs within the P1 and P2 promoter region. The HR region closest to the start of *FMO1* translation is present between the start of exon 1 and ends at the start of exon 2. This region overlaps the P2 promoter -255\_-128 defined previously (Figure 4.7). The second DNase I HR is present 500/600bp upstream of exon 1 and ends at the beginning of exon 1. This region overlaps the P1 promoter -858\_-343 defined previously (Figure 4.7). The sequence upstream of this region is not sensitive to DNase I digestion. This indicates that the DNA within this region is conformationally not available for transcription factors to bind. It is therefore likely that the sequence within this region shown to reduce reporter gene activity within the pGL-1243\_-343 (Figure 4.7) would not have this effect within a cellular context. The DNase I HRs overlapping the promoter regions defined previously gives further evidence for their existence.

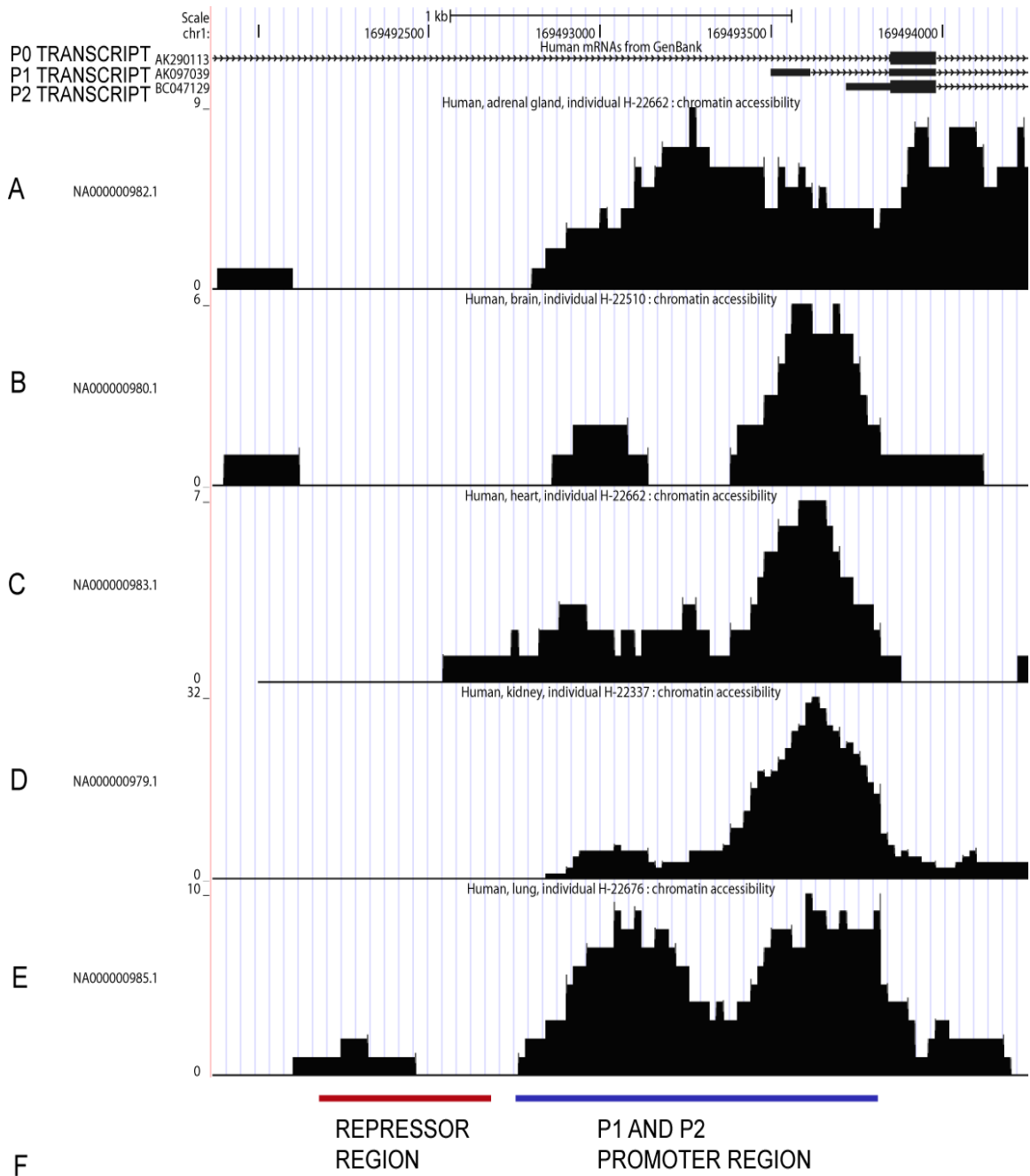


**Figure 4.11 Illustration of DNase I hypersensitivity sites within the defined *FMO1* P1 and P2 promoter regions**

The *FMO1* transcripts are shown at the top of the illustration, the first being the P0 transcript, the next being the P1 transcript and below this the P2 transcript. Below are the DNase I Hypersensitivity regions present within human (A) foetal adrenal (B) foetal brain (C) foetal heart (D) foetal kidney (E) foetal lung. (F) The regions of the P1 and P2 promoter are outlined in blue. The region shown to reduce reporter gene activity is highlighted in red. The above figure shows data obtained from the UCSC genome browser. The individuals who contributed to this work are cited at the beginning of this section (4.5).

### **4.5.3 The CTCF insulator binds upstream of the P0 promoter and may play a role in FM01 repression within the human liver (Figure 4.114.11)**

Chip-seq experiments on the whole genome are carried out by first fixing proteins to DNA within the cells or tissue. A specific antibody is used to isolate regions of DNA that are bound to specific proteins. The DNA attached to this complex is then sequenced. The sequences will be enriched where a protein has been bound. These enriched regions are illustrated as peaks in the following figures.

Chip-seq experiments in HepG2 cells show binding of the CCCTC-binding factor (CTCF) to the DNase I sensitive regions. CTCF is an 11 zinc-finger protein which has a diverse regulatory function. It has been shown to be involved in the activation/repression of transcription, insulation, imprinting and X-chromosome inactivation (Phillips and Corces, 2009). The two CTCF-binding regions align to previously described sequences that are sensitive to DNase I digestion within the human tissues analysed.

The sequence containing the CTCF-binding factor present -2000 bp upstream of the P0 transcriptional start site shows tissue-specific DNase I sensitivity. The sequence is sensitive to DNase I digestion in heart and adrenal gland. It is not sensitive in kidney and brain. There is low sensitivity in lung. The tissue-specific differences in chromatin conformation may result in tissue-specific differences in CTCF binding. The sequence containing the CTCF binding region located further downstream shows sensitivity to DNase I digestion within all tissues analysed.

In human liver the FMO1 mRNA and protein is not expressed after birth (Dolphin et al., 1996). Reporter gene assays have shown sequences upstream from the promoter that negatively regulate reporter gene activity (Shephard et al., 2007). The construct which negatively regulates the human P0 minimal promoter contains the CTCF binding region. The CTCF binding may be responsible for the loss of *FMO1* expression within the human adult liver.

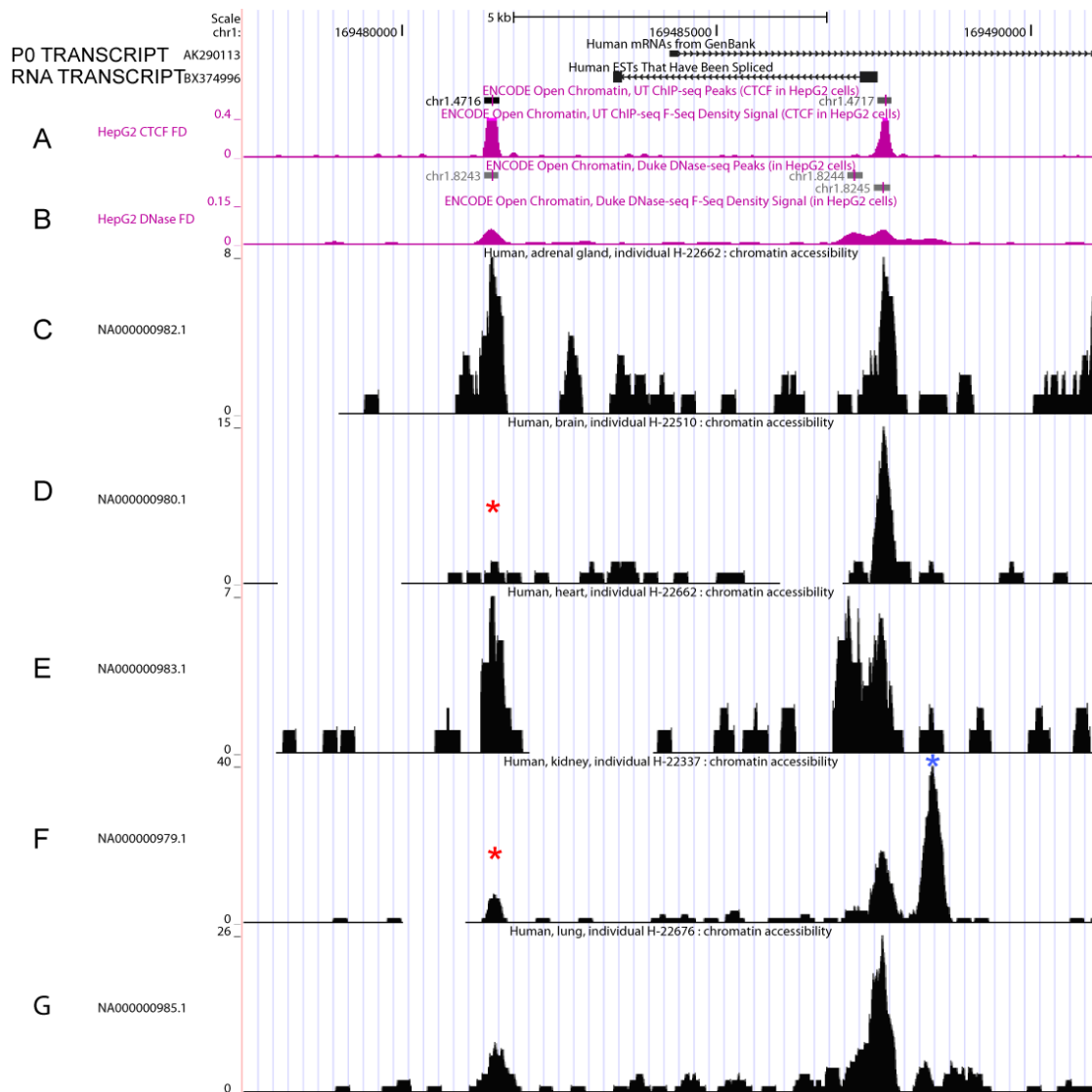


**Figure 4.12 Schematic representation of CTCF binding upstream and downstream of the P0 promoter, as well as DNase I hypersensitive sites within human tissues**

The P0 transcript is located at the top of the page. **(A)** CTCF chip-seq experiment showing the location of CTCF binding within the *FMO1* gene. **(B)** DNase I-seq experiment within HepG2 cells. **(C-G)** represent DNase I-seq experiments within (C) adrenal gland, (D) brain, (E) heart, (F) kidney and (G) lung. The asterisks represent the tissues where regions of DNase I sensitivity are lowered. The above figure shows data obtained from the UCSC genome browser. The individuals who contributed to this work are cited at the beginning of this section (4.5).

#### **4.5.4 Chip-seq experiments identifying transcription factor binding within P0, P1 and P2 promoters (Figure 4.13 and Figure 4.14)**

Genome-wide chip-seq experiments have identified transcription factors binding within the P0, P1 and P2 promoters. The transcription factors CEBP- $\beta$  and Ini1 bind within the defined P1 promoter. CEBP- $\beta$  bound to the P1 promoter within HepG2 cells. The Ini1 factor was bound to the P1 promoter within Hela cells.

Ini1 is a component of the SW1/SNF chromatin remodelling complex. It is present within this complex as a core sub-unit defined as SNF5/INI1 (Ae et al., 2002). This complex physically and functionally interacts with transcriptional activators and repressors (Sullivan et al., 2001). The complex is involved in a variety of cellular processes by regulating cell growth and differentiation specifically myeloid, erythropoietic, adipogenic, neuronal or myogenic differentiation pathways (Caramel et al., 2008). The SNF5/Ini1 sub-unit is a tumor suppressor gene. It is observed to always be inactivated in a group of highly aggressive cancers of unknown cellular origin termed malignant rhabdoid tumours (MRT) (Muchardt and Yaniv, 1999). When the SNF5/INI1 complex is re-expressed within these cancerous cells the cells show adipocyte characteristics (Caramel et al., 2008). Knock down experiments using shRNA has shown the SNF5/Ini1 is required for the differentiation of 3T3-L1 adipocytes (Caramel et al., 2008).

The second transcription factor binding within the *FMO1* P1 promoter, CEBP- $\beta$ , is a critical regulator of adipocyte differentiation (Lane et al., 1999). Bioinformatic analysis has shown a number of CCAAT binding sequences within the P1 promoter.

CEBP- $\beta$  is able to activate transcription through binding to these sequences. The FMO1 P1 transcript is also increased during differentiation. It is therefore possible that CEBP- $\beta$  could be activating the expression of the FMO1 P1 transcript. CEBP- $\beta$  and Ini1 have been shown to synergistically regulate PPAR- $\gamma$ . Transient transfection assays have shown upregulation of the PPAR- $\gamma$  promoter dependent on both the upregulation of CEBP- $\beta$  and the SNF5/INI1 (Caramel et al., 2008). Chip-seq has confirmed the presence of both factors within the promoter (Caramel et al., 2008).

It has therefore been observed that the SNF/INI1 complex upregulates genes during adipocyte differentiation and it is this mechanism that could be responsible for the upregulation of FMO1 mRNA during adipocyte differentiation.

Chip-seq experiments within HepG2 cells have shown the insulating factor CTCF binding within the P0 extended promoter region. Within the P0 extended region Chip-seq experiments carried out in multiple cell lines have revealed other transcription factor binding events. These are a second insulating factor, Rad21, which can co-regulate genes with the CTCF factor and NF $\kappa$ B also binds within a region of the P0 extended promoter.

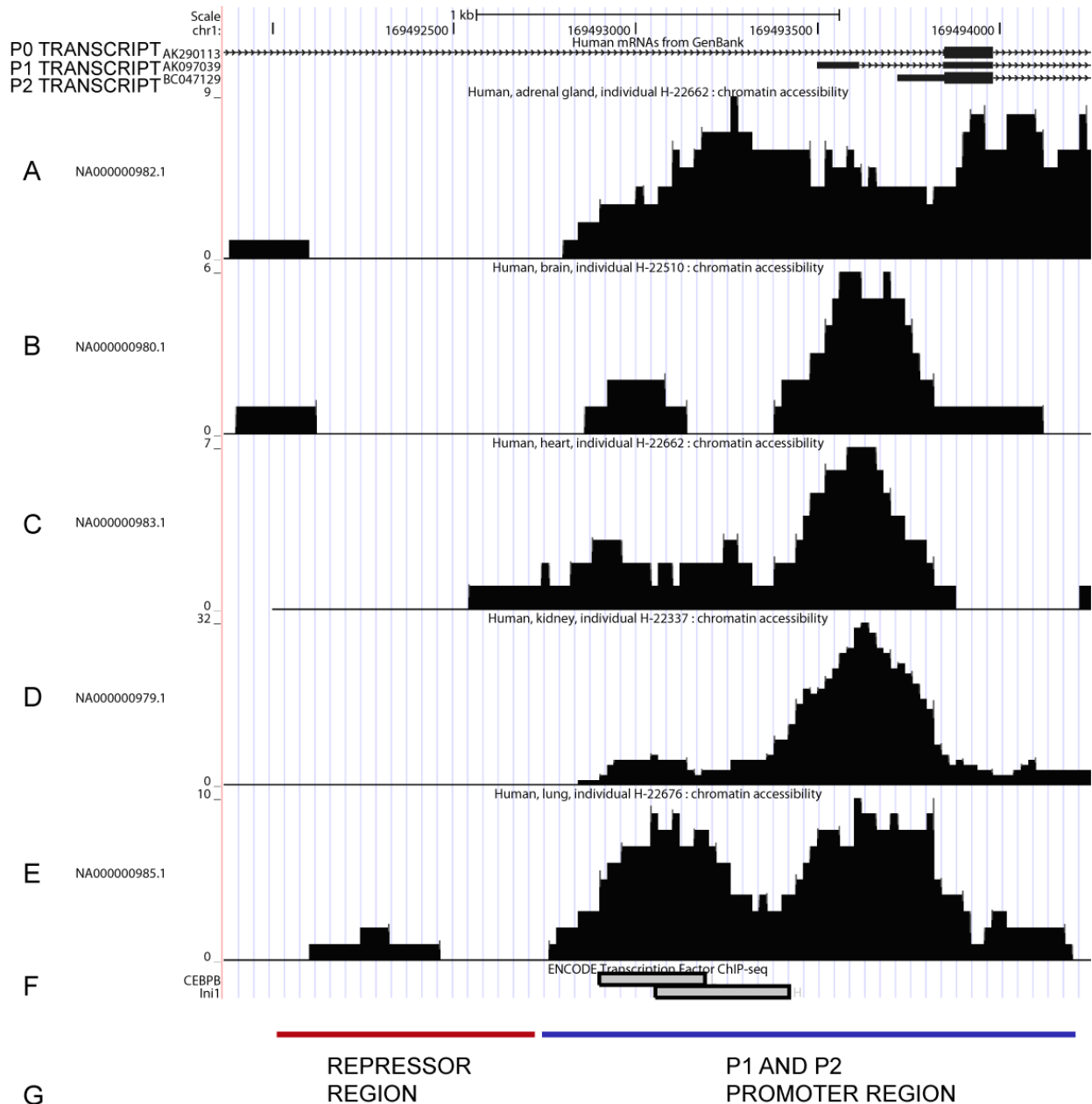


### Figure 4.13 Illustration of transcription factor binding within the *FMO1* P1 and P2 promoter regions

The *FMO1* transcripts are shown at the top of the illustration, the first being the P0 transcript, the next being the P1 transcript and below this the P2 transcript. Below are the DNase I Hypersensitivity regions for human (A) foetal adrenal (B) foetal brain (C) foetal heart (D) foetal kidney (E) foetal lung, (F) Illustration of the chip-seq signal for the binding of the transcription factors Ini1 and C/EBP- $\beta$  (grey bars), (G) The regions of the P1 and P2 promoter are outlined in blue. The above figure shows data obtained from the UCSC genome browser. The individuals who contributed to this work are cited at the beginning of this section (4.5).



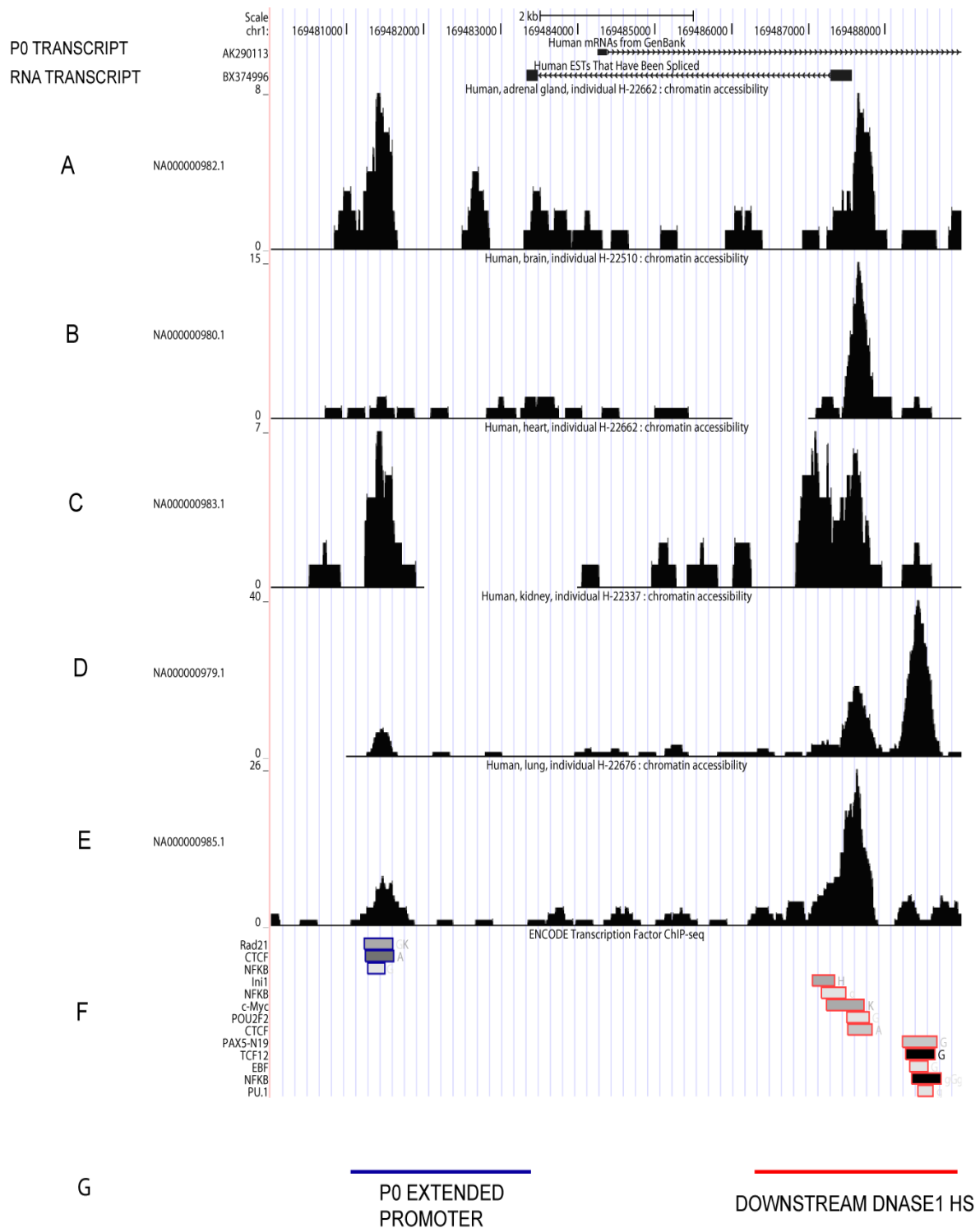


### Figure 4.14 Schematic representation of transcription factors that bind to the P0 promoter

A-E represent DNase I-seq experiments within (A) adrenal gland, (B) brain, (C) heart, (D) kidney and (E) lung, (F) illustration of ChIP-seq signals showing binding of transcription factors to the P0 extended promoter region and a downstream DNase I hypersensitive region. The above figure shows data obtained from the UCSC genome browser. The individuals who contributed to this work are cited at the beginning of this section (4.5).

The region downstream shown to be sensitive to DNase I digestion in all tissues examined and HepG2 cells binds the CTCF factor. In addition chip-seq experiments in multiple cell lines has shown the binding of additional transcription factors including Ini1, c-myc, POU2F2, PAX5-N19, TCF12, EBF and PU.1 (Figure 4.14).

#### **4.6 *FMO1* P2 promoter mutations and their influence on promoter activity**

*FMO1* sequences with mutations were created to help define protein factors that regulate the expression of the gene. Mutations were created within protein-binding regions predicted by bioinformatics and conserved between human and mouse. Two independent mutations were created within the defined human *FMO1* P2 promoter (-255\_-128) (Figure 4.15). The first mutation to be examined lies within the GC-box sequence predicted to bind SP1 (Figure 4.8). Site-directed mutagenesis was used to change the sequence from GGGGCGGG to GGGTTGGG. This mutant plasmid is defined as pGL3-255\_128\* in section **4.6.2**. This change is known to inhibit SP1 binding (Santa Cruz Biotechnology). The second mutant sequence was created by mutating a predicted half site for a nuclear receptor. In this case the sequence was changed from AGGTCA to AGCACA. This change is known to inhibit nuclear-receptors which bind to this motif (Santa Cruz Biotechnology). This mutant plasmid is defined as pGL3-255\_128\*\* in section **4.6.2**.

##### **4.6.1 Mutations in the *FMO1* P1 promoter**

A natural variation, -809G>A, is observed within the P1 promoter active region which was defined as the region -858\_-600 (see chapter 3). A second natural variation, -338\_-337CTdel occurs at the start of exon 1. The -809G>A is not predicted to be

present within a DNA-Protein binding region. However, it has been shown that that polymorphism can effect gene expression from further distances than directly to the DNA sequence to which the transcription factor binds. Separate PGL3 reporter gene constructs were made containing the two natural variations using site-directed mutagenesis.

#### **4.6.2 A mutation introduced into the FM01 P2 promoter reduces reporter gene activity**

Luciferase activity driven by the P2 promoter GC box mutant (pGL-255\_-128)\* sequence was reduced to that of the negative control indicating that the mutation abolishes P2 promoter activity (Figure 4.16). However, when the mutant pGL3-255\_-128\*\*, which is present further downstream was transfected into COS-7 cells there was no significant change in reporter activity compared with that of the wild-type sequence.

The P1 mutants were unable to be tested as when COS-7 cells were transfected with the P1 promoter the activity of the promoter was severely reduced. Therefore comparisons to the mutants would not be as informative.

Many variables had been tested to find the reason for this loss of activity. The construct containing both the P1 and P2 promoter sequences also lost reporter gene activity which is suggestive of a transcriptional response within the cells rather than the DNA being the cause of the loss of activity. Even though, DNA was remade on independent occasions and tested for subsequent activity. New cell stocks were grown to test if the cells had biochemically changed due to increased numbers of passages. The promoter activity still remained low.



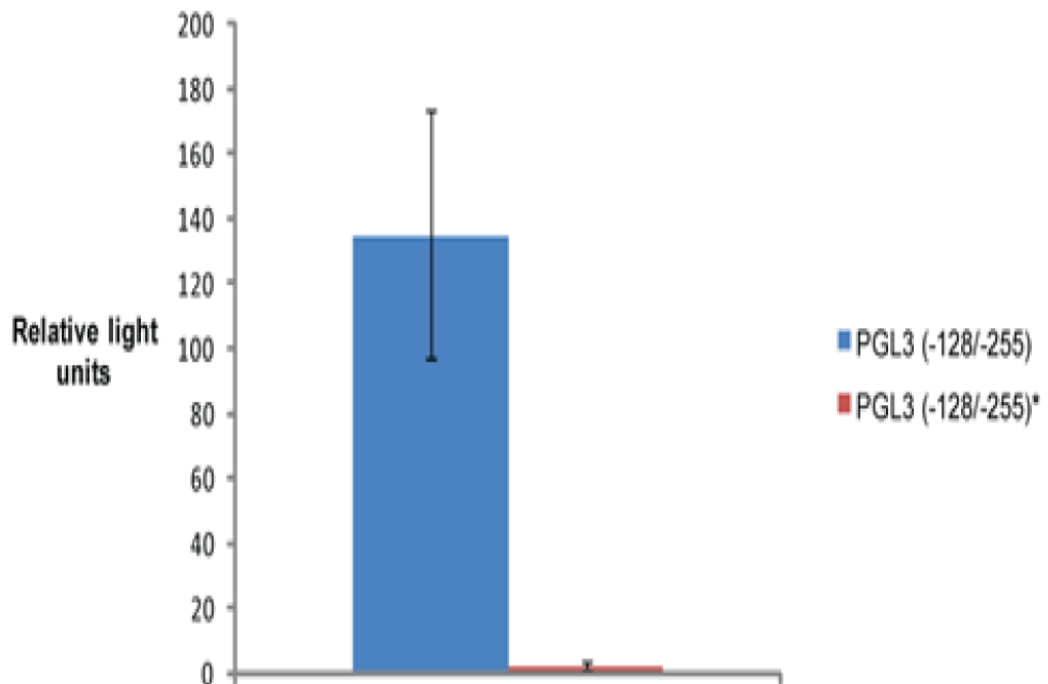


**Figure 4.16 Reporter gene activity of the pGL3-255\_128 P2 promoter construct and the pGL3-255\_128\* GC box mutant within COS-7 cells**

COS-7 cells were transfected with pGL3 constructs. The sequence location is shown within the legend. The co-ordinates are relative to the FMO1 translation start codon. The pGL3 basic plasmid was transfected as a negative control. All experiments were done in triplicate and the error bars indicate the standard deviation.

Bioinformatic analysis was undertaken and heat shock factor was predicted to bind within the P1 promoter. This factor has been shown to regulate genes in combination with the insulating factor lin1. Lin1 has been shown to bind within the FMO1 P1 promoter through chip-seq experiments (Figure 4.14).

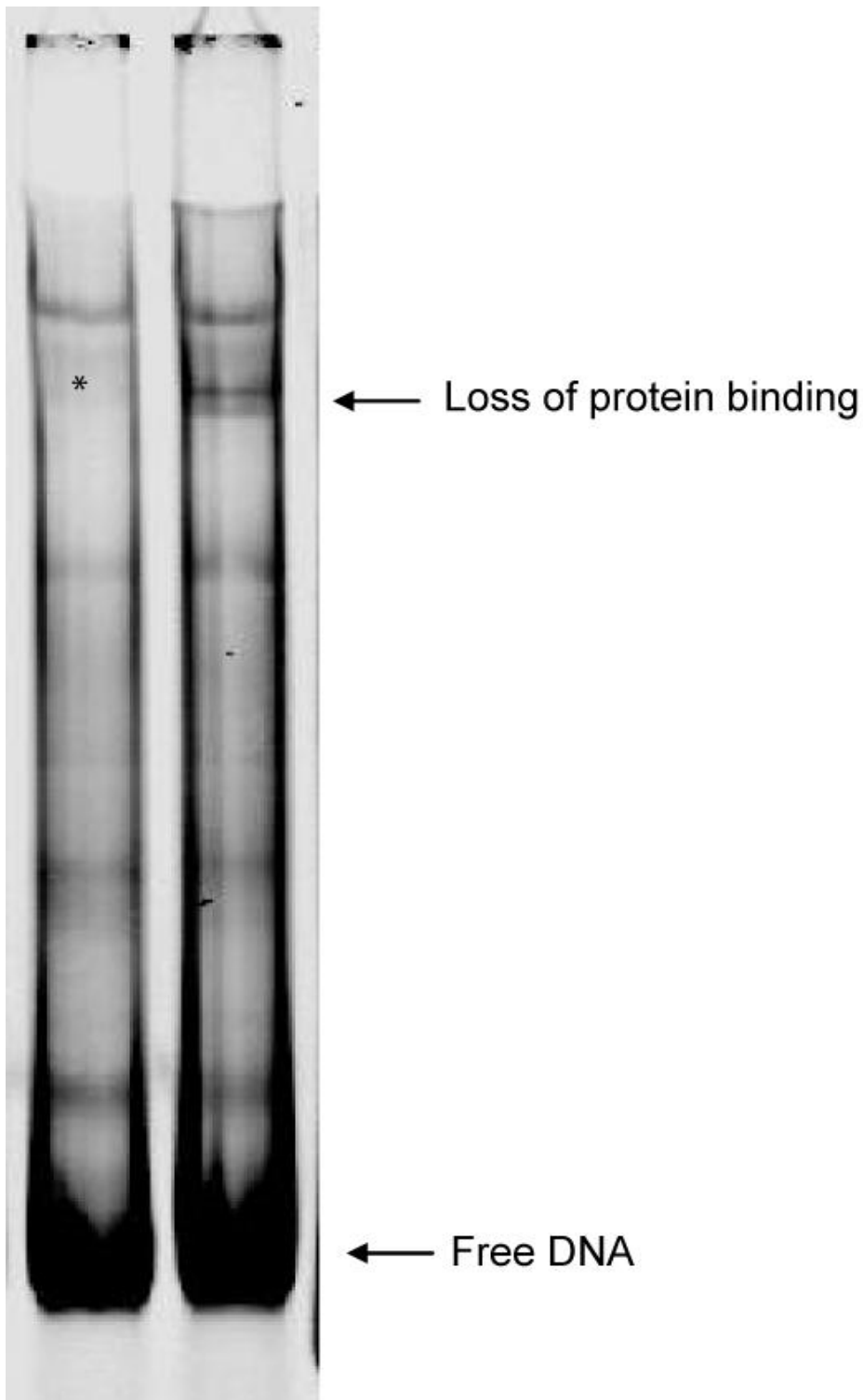
Therefore media were and incubation conditions were changed (incase of stress or oxygen changes in regulation). This did not result in a change in reporter gene activity. Future experiments could produce a second shorter construct to identify the possible negative transcriptional regulator. Activity has currently not been achieved again for the P1 promoter within COS-7 cells.

#### **4.6.3 Loss of protein binding due to a mutation within the GC box protein binding region of the P2 promoter is detected by a gel shift assay**

To determine whether protein binding had been affected, a gel-shift assay was undertaken. The probe which contained the P2 promoter (-255\_-128) was amplified from the PGL3-BASIC (-255\_-128) vector and the PGL3-BASIC (-255\_-128)\* vector. This probe was incubated with 10 µg of COS-7 protein and subsequently passed through a 4% native polyacrylamide gel.

The wild-type probe (-255\_-128) resulted in a number of shifted bands representing different DNA-protein binding events. When the mutant form of the probe (-255\_-128)\* is analysed with the same conditions, two of these bands are removed.

Therefore mutation of the GC box binding region of the FMO1 P2 promoter removes binding of a protein within this region in addition to reducing reporter gene activity (Figure 4.17).



-255\_-128 -255\_-128\*

**Figure 4.17 Gel shift assay showing loss of protein binding at the FMO1 P2 promoter due to a mutation within the GC binding box**

The lowest band represents the unbound (free) DNA, and above this, bands represent DNA-protein complexes. Comparing the GC box sequence wild-type (-255\_-128) and mutant (-255\_-128\*) shows the loss of a DNA-protein complex. The asterisk shows the loss of protein-DNA complexes with -255\_-128 DNA compared with the complexes formed with -255\_-128\*.

#### **4.7 The significance of a polymorphism, -11C>T, which potentially reduces the translational efficiency of the FMO1 protein**

The effect of polymorphism on translational efficiency was discussed in chapter 1.18 and several examples were discussed where secondary ATG translation initiation sites exist, and have affected translational efficiency, and as a result play roles in disease.

In the course of the work described in this thesis, a common polymorphism was identified within the *FMO1* gene. This results in a second ATG upstream of the defined translational start site. This polymorphism, a C>T transition, occurs in-frame, 12 base pairs upstream of the accepted ATG for FMO1. This is the same distance as seen between the ATG initiation sites in the vitamin D receptor gene (Zysow et al., 1995).

Two constructs were made using the vector pSP-luc, containing the FMO1 P2 5'UTR sequence. The making of this vector is outlined in the methods section (2.20.2 *FMO1* P2 leader sequence construct). This vector contains an SP6 bacterial RNA polymerase binding site which allows RNA to be made in-vitro using a viral vector as a template. The RNA contains the luciferase gene, the upstream FMO1 P2 5'UTR sequence, and the FMO1 3'UTR. RNA can be made in-vitro and translational efficiency of different constructs can be observed in cells using the dual luciferase reporter gene assay.

As with the pGL3 reporter gene constructs, the pSP-luc vector contains the luciferase reporter gene and therefore expression of the protein product can be



monitored. Both constructs to be tested for translational efficiency contain the accepted FMO1 translational start codon. Within the upstream ATG region a polymorphism is observed. Some individuals contain an ATG, and others an ACG (see chapter 3 for frequencies). One of the constructs contains the ATG form and the other the ACG form. The variation was introduced using PCR site-directed mutagenesis (2.28).

The amount of lipid was optimised for 1µg of RNA. The lipid ratios of 1:1 and 2:1 were tested. Transfection of RNA produced from the ATG plasmid was transfected with a RNA:lipid ratio of 1:1 and 2:1. The RNA lipid ratio of 2:1 produced significantly higher reporter gene activity.

Preliminary data (Figure 4.18) suggest that the construct containing the ATG/ATG form produces a significantly larger amount of protein than the ACG/ATG construct. This polymorphism would only have an effect within P2 transcripts as it occurs within the P2 leader sequence for translation. Individuals containing the upstream ATG may therefore produce more protein and, as a result, may process drugs at an increased rate.

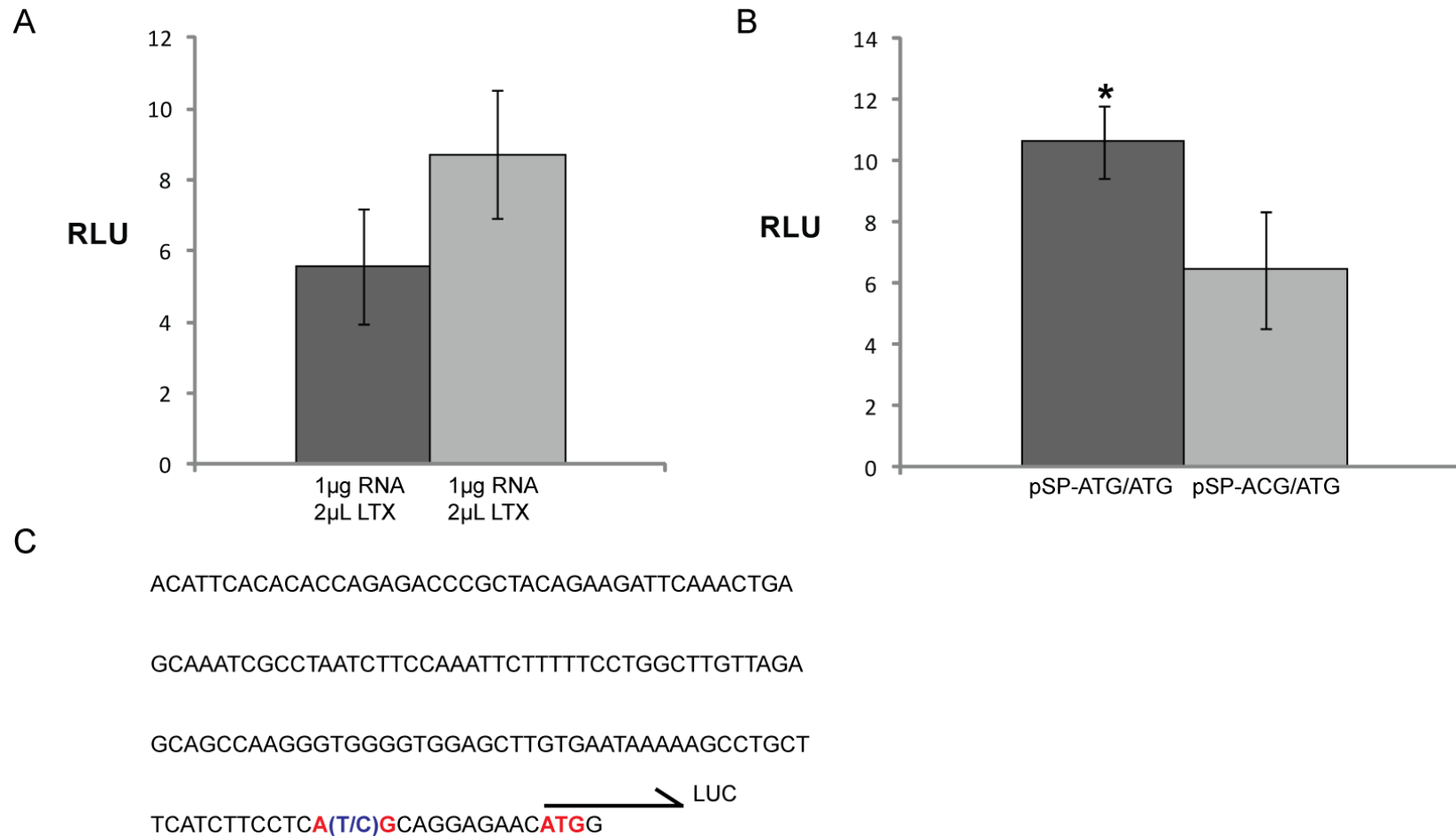


**Figure 4.18 Reporter gene activities of RNA produced from the pSP-ATG/ATG and the pSP-ACG/ATG vectors**  
**(A)** The amount of lipid-reagent (LTX) used to transfect RNA was optimised. **(B)** The relative reporter gene activity of the RNA produced from the pSP-ATG/ATG and the pSP-ACG/ATG vectors. The asterisk indicates that RNA produced from the pSP-ATG/ATG produces significantly more reporter protein than RNA produced from the pSP-ACG/ATG vector. **(C)** The FMO1 5'UTR of the P2 transcript illustrating the two ATG translation sites and the location of the -11T>C polymorphism.

## Discussion

Chapter 1 describes the quantification of *Fmo1* expression in multiple mouse tissues. The results reveal the high expression of the gene in extra-hepatic tissues and in particular in tissues that are fundamental in energy homeostasis. This gives support for a role for FMO1 in energy homeostasis. This chapter aim was to identify the regulatory regions controlling the transcription of the different FMO1 transcripts. These regions could then be used to identify and test genetic variation for effects on transcription.

Transfection of the three different cell lines with reporter gene constructs has identified novel promoter regions upstream of the P1 and P2 transcriptional start sites. Chromatin analysis within multiple human tissues gives evidence for both promoters also being within open chromatin regions. Selective use for the P1 and P2 promoter has been observed in the three cell lines. In the human kidney cell line HK-2 the P2 promoter is favoured and within the mouse cell line 3T3-L1 the P1 promoter is favoured. Several cDNA clones have been isolated from mouse that correspond to P1 transcripts. However, only a single cDNA clone has been reported that arises from the P1 promoter in humans (Shephard et al., 2007). In contrast, several cDNAs corresponding to transcripts from the P2 promoter have been reported in humans. The real-time quantitative PCR data from mouse tissues shows a preference for the P1 promoter over the P2 promoter. The data suggests the P2 promoter is favoured within human and the P1 promoter is favoured within mice. This would explain the lack of polymorphism within the human P2 promoter and the presence of a number of SNPs for the human P1 promoter. The mouse contains polymorphism within the homologous P2 promoter region.

Analysing the *FMO1* P1 and P2 promoters reveals transcription factor binding sites that could be responsible for increases in both transcripts. CCAAT binding regions are predicted within the P1 promoter. Chip-seq data also gives evidence for CCAAT binding protein (CEBP- $\beta$ ) binding within the defined promoter. As the P1 and P2 transcripts are both elevated when 3T3-L1 cells undergo differentiation to adipocytes it is possible that CEBP- $\beta$  binding could be responsible. The thyroid hormone receptor is also predicted to bind within the P1 and P2 promoter. This is a good candidate in the future to analyse its effect on *Fmo1* expression due to its role in energy homeostasis in the mouse.

Transfection of differentiated 3T3-L1 adipocytes was successful and reporter gene activity was high. In future experiments, regulatory polymorphism could be analysed in the context of these cells with further optimisation of controls. Protein extracts can also be isolated and gene expression analysis can be analysed using these extracts to further understand *Fmo1* gene regulation within brown and white adipose tissue. The insulating factor CCTF has been shown to bind in two locations surrounding the *FMO1* P0 transcriptional start site. One site is -2700 bp upstream of the human P0 promoter. This region has been shown to down regulate reporter gene activity when attached to either the human or mouse P0 minimal promoter. Comparative analysis between mouse and human sequences show the binding regions of CCTF are not conserved between mouse and human. Down regulation of the human P0 promoter in the liver shortly after birth could be due to CTCF binding within the P0 promoter.

A second CCTF binding region is present downstream of exon 0. This could play a role in the regulation of the downstream P1 and P2 promoters, although this is purely

speculative without experimental evidence. Further experiments to repress the CTCF binding factor and development of an assay to measure *FMO1* expression would determine the effects of the CTCF binding.

Observing *Fmo1* expression increasing in 3T3-L1 adipocyte differentiation (see chapter 1) gives an opportunity to understand *Fmo1* regulation in fat. Transcription-factor binding consensus sites are present within the P1 and P2 promoter regions that are good candidates for upregulating FMO1 during 3T3-L1 differentiation.

## **Chapter 5**

# **Dideoxy sequence analysis of the human *FMO1* P0, P1, and P2 promoters**

## Chapter 5: Dideoxy sequence analysis of the human *FMO1* P0, P1, and P2 promoters

### Introduction

In the previous chapter, two *FMO1* promoters, P1 and P2 were defined using reporter gene assays. Genetic polymorphism located within these promoter regions may alter the binding of cis-acting regulatory elements and influence transcription efficiency. Therefore it is desirable to identify polymorphism present within these regions as well as the previously defined P0 promoter (Shephard et al., 2007). In addition to the sequence analysis of the two novel *FMO1* promoters carried out as part of this thesis, the NIEHS (National Institute of Environmental Health Sciences) based in Washington University has sequenced these regions from 90 individuals of unknown origin (Zaitlen et al., 2005). The SNPs discovered in the NIEHS study have subsequently been genotyped by investigators within the HapMap consortium using samples obtained from the Coriel repository (2003). These individuals were originally genotyped within 4 populations and subsequently genotyped for a percentage of the SNPs within additional populations. The original populations genotyped are the **CEU**: Utah residents with Northern and Western European ancestry from the CEPH collection, **CHB**: Han Chinese in Beijing, China, **CHD**: Chinese in Metropolitan and the **YRI**: Yoruban in Ibadan, Nigeria, The additional populations genotyped for only a limited number of SNPs are the **GIH**: Gujarati Indians in Houston, Texas, **JPT**: Japanese in Tokyo, Japan, **LWK**: Luhya in Webuye, Kenya, **MEX**: Mexican ancestry in Los Angeles, California, **MKK**: Masai in Kinyawa, Kenya, **TSI**: Tuscan in Italy, **ASW**: African ancestry in Southwest USA, Denver, Colorado. It was decided that re-sequencing of these regions may reveal new genetic polymorphism in the *FMO1* promoter regions as DNA from only 90 individuals, of unknown origin, had

been sequenced by NIEHS. In addition, SNPs found at low frequency by the NIEHS have not been genotyped by the HapMap consortium. The project described in this thesis can confirm the existence of these polymorphisms and extend our knowledge on *FMO1* variation. The four populations with the most complete genotype data were available to us to be re-sequenced for the P1 and P2 *FMO1* promoter regions.

### **5.1 Experimental design: Number of individuals and regions to be sequenced**

Once genetic polymorphisms within the *FMO1* promoter regions are identified they subsequently need to be tested for functional consequences and for association with drug response to *FMO1* substrates. If *FMO1* genetic polymorphism is to be used as an indicator for drug response it is desirable that the polymorphisms are common. A common polymorphism will have a frequency of more than 5% within the population. This would be predicted to occur within 1 in 20 chromosomes. Individuals contain two alleles of the gene. Therefore the genetic variation should be apparent on average by sequencing 10 individuals.

The availability of individual DNA samples from the different populations is a limiting factor. We had available to us only 11 individuals from the YRI population and 11 from each of the JPT and HAN populations. Therefore all available YRI, JPT and HAN population DNA samples were chosen for sequencing. The JPT and HAN populations were combined as the populations have shown similar haplotypes in previous studies. There were many CEPH samples to choose from and these initially were all sequenced in 40 individuals within one region of the *FMO1* 5' flanking sequence, +53 and -629. The number of samples was then reduced to 19 individuals when subsequent regions of the upstream *FMO1* gene were sequenced. The



regions to be analysed were the P0, P1 and P2 promoter regions. The human P0 promoter was defined as between -521\_+50 upstream and downstream of the P0 transcriptional start site (Shephard et al., 2007) and P0 SNPs are throughout this chapter SNPs and sequenced regions are defined from the P0 transcriptional start site. The P1 and P2 promoter regions are located at -255\_-128 and -858\_-128 as defined in chapter 2. In the case of the P1 and P2 promoters the sequence is numbered from the 'A' of the ATG translation initiation codon. For the P0 promoter, primers were designed to encompass the -521 to +50 region, which would encompass the currently known SNPs within this region (Fig.5.1A). The region of sequence which encompassed the P1 and P2 promoter regions was too large to be sequenced within one sequencing run. As a result primer pairs were designed for two overlapping regions (Fig.5.1). The first region was between -629 and +53 and the second region was between -1158 and -527 (see Fig.5.1B). The first region was amplified to include the nucleotide at +53. This was to ensure the SNP -11T>C would be genotyped. This SNP introduces a potential upstream ATG translation initiation codon. The region between the P1 and P2 promoters was also sequenced as this contains an exon, defined as exon 1, which contains the 5'UTR sequence of the P1 transcript.

A

GCCCCCTGGCAG**CCACTCGATCATGCCTATTT**TAAATTGAGGAACTAAAGCTGAGAAAAG  
TTATACAATTTTTTCCAACATGACTCTGATAATAGCTGGTGAACGCAATACTCGAACCCAG  
GACTTGTGATTCCTCAAGATCAGACTCCTCCCATATACCTGTCTTTTATTTCCCAAGTGCT  
TGGGCAATCAGCTGCACTTAAAAAGCCTTTACAAATTGAGTTTACTAATGTGAGTAATAT  
ATGATTTTTTAAAAATAATAATTGTCCCTAAAGGTGAAATGGATCAAAGCCCTTAAAAGT  
GAATCTGTGGTGTAGTAACGTTAACATAATTGTCTTATTTTATTCTCATCCCCTTAAAG  
AATAAACTGATGAACAAGTGAGGATGCTGGTGTAACTCCCTAACTTAGTTTATAGTCTG  
TAAGCAGAAGAGTGAGTCTAAAGTACATATCACCAGACAGTGTCTCCTTAGCATTTCGC  
TGTTGCATTAATCAACAAGTAAAATATAAACAACGGCTAACCTTGGGTTTCAAATTTAA  
CATTCCTTATCTCTTAGACC**AGGTTTATCCACTGTGCTGGGGACTCCCAAGCCAGCACTG**  
**GCTCATACTGATTCATTTTGATCTCTGCTAATACCAGAGTCCTGCGTGGCAGAGCCATTG**  
**GCACCAGAAATTACAAGTACGTAAA**

B

GGGGGAAAAGCTAACATCACATAATTTAGTGA**CAAATGTGTGTGCTACTGACC**AGAAATG  
CTATAGGAATTTAAAGAACAGAGGCTCATTGATGTGAAAGGCAGATACCAATTCTTGGAA  
ATGCTTTTTAAAGTTTCAATAACTTACAGCTACTGAGCACTTACTATGTGCCAGGAGCTAT  
TCTGAGACGCCTTACATTTAATACTCACTTATTCTCACAGAACACTTCAAGGAAGCTAC  
TATTGTTTTCTTTATATTTGTGATGCACAGAAGGGTTAATCTGTCCAAGATTACACTGTC  
GTAACGATAGAGCCGCGCTTTATCTCAGGCAGCCTGGATCCAGAGCCTGGTTGCTTAAT  
CAATGCACTCTGTTGCCCTCTCGGTGTTCTTACACATGTGTGTTATTAACACATGGCCTGG  
TGCCAGAAGATTCTCTGGCCCATCCCAGTGGTACTGTGCCATGTGCCCTGGAGGTGAAT  
CAGTATCCAATTGAGAAGGGAGGGATGGCTTTGCATGCCTACCTTTCTACCACAAACCTT  
CCCTGGCAGCCACCCTCTCT**CTCTCCCCTGGTGACCATC**ACTGGTGACCTGTGAAAGGG  
ACACACCAACAGCACAGCTGGGGCCCTGGCATTGTGCCAGGGG**CAGGATCACACAGGGCA**  
**GTG**CCGCGGTAGCACCCGTGGTGGCAGGTGTGGTGGCTCCTGGTCCCAACTCCACCCC  
ACCAGCTGCTGTGTGGTGTGTGTGTCAGGTACCACCAATCGGAGCTTCAGTTTTGTAT  
GTGATAAAGAGATTGTGTCTGACAAGGTGACCTTTTTCTAGTCTGCTGATCTATGCAGT**T**  
**CTAGGGCCACAGAATGGAGACTAGAGGCAGCAGCTCAGTCTGAAGTGCAAGACTTTATCC**  
**AGTAAAAGGTCCAATTCCAGCAGCTCTGCCAGAAGCTACAGCCTTGACAAGT**GTACGAAC  
ATTTGGCACTGGTGTGCTGCATGAGGGGCGGGAACATAACCAAGCACAGGGTTAACCAGTGAC  
CTGAACATTTTCTTCTCACATTCACACACCAGAGACC**CGCTACAGAAGATTCAAAGTGA**  
**GCAAATCGCCTAATCTTCAAATTTCTTTTTCTGGCTTGTTAGAGCAGCCAAGGGTGGGG**  
**TGGAGCTTGTGAATAAAAAGCCTGCTTCATCTTCTCATGCAGGAGAATGGCCAAGCG**  
**AGTTGCCATTGTGGGAGCTGGGGTCAAGCGCCTGGCCTCCATCAAGTGCTGTCTGGAAGA**  
**AGGACTGGAGCCCACCTGCTTTGAGAGGAGCGATGACCTTGGGGGGCTGTGGAGATTAC**  
**C**

### Figure 5.1 Location of primers used to amplify DNA from individuals for subsequent dideoxy sequence analysis

(A) The P0 promoter region. The sequence in red defines exon 0. The primer locations are in bold and underlined. (B) The P1 and P2 promoter region. The sequence in red defines the exons 1 and 2. The black primers represent the primer pairs used to amplify the first region (-629\_+53) for sequencing. The blue primers represent the primer pairs used to amplify the second region for sequencing (-1158\_-527).

## 5.2 Identification of novel polymorphism within the *FMO1* P1 and P2 promoter regions (Fig.5.2)

Sequencing of the *FMO1* P0, P1 and P2 promoters has revealed two novel polymorphisms. A 2 base pair deletion was observed at the start of exon 1 (-338\_-337delCT). The two bases deleted were CT and are identified within Fig.5.5. This SNP is situated at the start of transcription for the P1 transcript. It therefore could affect the binding of the RNA polymerase at this site. The SNP was observed only within the European population (CEU). It is not present within the YRI and JPT and HAN populations. It was observed within 4 individuals in a heterozygote state. This meant that the individuals had one copy of the deletion and one copy with no deletion. The frequency of this variant within the European population is calculated to be 5%. The chances of an individual being homozygous for the polymorphism are 0.0025 or 1/400. This is therefore defined by the original criteria as a common polymorphism within the European population.

A second novel polymorphism was observed at position -497C>T and was observed within one European individual. The SNP was observed in the heterozygote state. The SNP allele frequency was 1.25%. The chances of an individual being homozygote are 0.0001% or 1/6400. The -497C>T is therefore a low frequency polymorphism.

### **5.3 Confirmation of the -515G>A and -503C>T SNPs and genotyping in CEU, YRI and JPT/HAN populations**

The HapMap project selectively genotyped SNPs within the *FMO1* gene and surrounding non-coding region. SNPs previously defined at low frequency by the NIEHS were not chosen for genotyping. Therefore the SNP -515G>A was not chosen for genotyping. Using HapMap samples, a second SNP -503C>T was genotyped, within the CEU, JPT and HAN populations, by the Sanger Centre, UK. The YRI population was not genotyped. The P1 and P2 sequence with the HapMap genotyped SNPs are illustrated in Fig.5.3. The figure also shows the HapMap frequencies of the SNPs genotyped within this study and their resulting haplotypes within the three populations.

The polymorphism -515G>A had only previously been identified to be heterozygous within 1 out of 90 individuals (180 haplotypes) sequenced. This individual was identified from the NIEHS sequencing of 90 individuals with an unknown identity. The SNP has not been genotyped by HapMap or any other genotyping project. Within the European population (CEU) the genotype frequency of the common G/G genotype was 0.83 and the frequency of heterozygotes was 0.17 (Fig.5.2). This frequency is higher than that of 0.01 previously observed from the NIEHS sequencing project. Within the YRI population, the A allele has a much higher frequency than in Europeans. The frequency of G/G homozygotes is 0.45 and the frequency of heterozygotes was 0.55. There were no observed A/A homozygotes (Fig.5.2). This is due likely to only 11 individuals being sequenced from within this population group. Within the JPT and HAN populations the SNP is not polymorphic from the 19

samples sequenced. We have therefore shown that the -515G>A SNP is at a higher frequency than previously observed and is common within the YRI population.

A SNP located at -503C>T, 12 base pairs downstream of -515G>A, is present within the samples sequenced. This SNP has been observed within the samples sequenced by the NIEHS project. The frequency of the C/C genotype is 0.644. The heterozygote frequency is 0.267 and the T/T genotype frequency is 0.089. This SNP is recorded as being genotyped within the Ensembl database ([www.ensembl.org](http://www.ensembl.org)) in individuals used within the HapMap project. The populations genotyped are CEPH and JPT and HAN. No variation is observed within these individuals and all individuals have the genotype C/C. This seems to be a reporting error. The C/C data was obtained outside of the HapMap consortium by the Sanger Institute, UK. The error may be due to the automated analysis of the sequence data. Within the CEPH population, the genotype frequencies are 0.72 for the C/C genotype and 0.28 are heterozygote for this SNP (Fig.5.2). There are no T/T homozygotes within the CEPH individuals sequenced. In the YRI population the frequency of the C/C genotype is 0.18, the C/T genotype is 0.45, and the T/T genotype is 0.36 (Fig.5.2). This is very different from the CEPH individual genotypes as the T allele is common in the YRI. In the JPT and HAN populations sequenced, there was no variation at this locus and all individuals had the C/C genotype.

The SNPs -809G>A, -513G>A, -312A>T and -11T>C were genotyped within this study in the CEU, YRI and JPT/HAN populations. The frequencies obtained from this study are given in Fig.5.2. Individuals from these populations have also been genotyped by the HapMap consortium. The SNPs from the HapMap consortium

A

## P1 AND P2 POLYMORPHISM FREQUENCIES

SNP ID (dbSNP)	POSITION (ATG)	BASE CHANGE	CEU SNP FREQ	YRI SNP FREQ	HAN/JPT FREQ
rs6670639	-809	G>A	G:0.86 A:0.14 G/G:0.72 G/A:0.28 A/A:0	G:0.45 A:0.55 G/G:0.18 G/A:0.55 A/A:0.27	G:0.97 A:0.03 G/G:0.94 G/A:0.06 A/A:0
rs28384855	-515	G>A	G:0.91 A:0.08 G/G:0.83 G/A:0.17 A/A:0	G:0.625 A:0.375 G/G:0.45 G/A:0.55 A/A:0	G:1 A:0 G/G:1
rs10912672	-513	G>A	G:0.85 A:0.15 G/G:0.74 G/A:0.26 A/A:0	G:0.5 A:0.5 G/G:0.27 G/A:0.45 A/A:0.27	G:1 A:0 G/G:1
rs10912673	-503	C>T	C:0.86 T:0.14 C/C:0.72 C/T:0.28 T/T:0	G:0.41 A:0.59 G/G:0.18 G/A:0.45 A/A:0.36	C:1 T:0 C/C:1
NOVEL	-497	C>T	C:0.99 T:0.01 C/C:0.98 C/T:0.02 T/T:0	C:1 T:0	C:1 T:0
NOVEL	-338	CT/-	CT:0.95 -0.05 CT/CT:0.9 CT/-:0.1 -/-:0	CT:1 -0	CT:1 -0
rs10798296	-312	A>T	A:0.99 T:0.01 A/A:0.98 A/T:0.02 T/T:0	A:0.82 T:0.18 AA:0.64 AT:0.36 TT:0	A:1 T:0
rs10912675	-11	T>C	T:0.72 C:0.28 T/T:0.51 T/C:0.41 C/C:0.08	T:0.15 C:0.85 T/T:0 T/C:0.3 C/C:0.7	T:0.71 C:0.29 T/T:0.5 T/C:0.42 C/C:0.08

B

## P0 POLYMORPHISM FREQUENCIES

SNP ID (dbSNP)	POSITION (ATG)	BASE CHANGE	CEU SNP FREQ	YRI SNP FREQ	HAN/JPT FREQ
rs2064078	-452	G>A	G:0.63 A:0.37 G/G:0.42 G/A:0.42 A/A:0.16	G:1 A:0	G:0.55 A:0.45 G/G:0.36 G/A:0.36 A/A:0.27
rs17350523	-188	C>T	C:0.68 T:0.32 C/C:0.53 C/T:0.29 T/T:0.18	C:0.32 T:0.68 C/C:0 C/T:0.63 T/T:0.36	C:0.42 T:0.58 C/C:0.15 C/T:0.54 T/T:0.3
rs12720462	+58	C>A	C:0.91 A:0.32 C/C:0.43 C/A:0.57 A/A:0	C:0.81 A:0.19 C/C:0.43 C/A:0.57 A/A:0	C:0.71 A:0.29 C/C:0.43 C/A:0.57 A/A:0

**Figure 5.2 The frequency of alleles and genotypes within (A) the *FM01* P1 and P2 promoter and (B) the *FM01* P0 promoter**

From left to right: The first column shows the polymorphism (SNP) identifier which can be found within the dbSNP database ([www.ncbi.nlm.nih.gov/projects/SNP/](http://www.ncbi.nlm.nih.gov/projects/SNP/)). The second column shows the position of the SNP relative to the A of the ATG translation initiation codon. The third column shows the base change for the polymorphism. The fourth column shows in order, the frequencies of the two alleles and subsequently the frequency of the genotypes within the CEU population. The fifth column shows the allele and genotype frequencies within the YRI population. The last column shows the allele and genotype frequencies within the HAN/JPT populations.

show similar allele and genotype frequencies (see figure 5.3C for HapMap SNP frequencies) and therefore the frequencies are not discussed here.

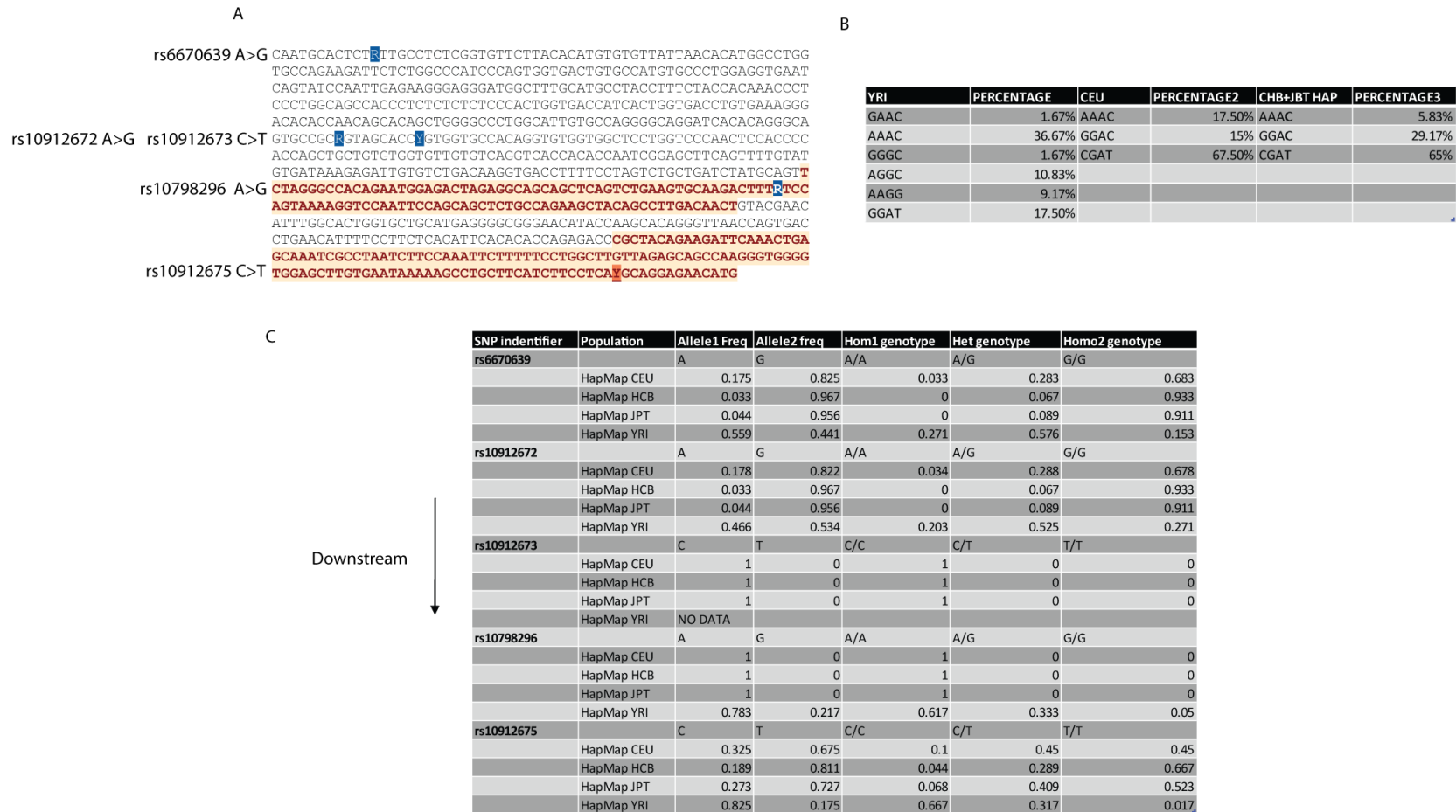


**Figure 5.3 Illustration of the HapMap consortium genotyped SNPs within the *FMO1* P1 and P2 promoter region**

**(A)** The P1 and P2 promoter region with the HapMap genotyped SNPs highlighted in blue. The red blocks illustrate exon 1 and exon 2 of the *FMO1* gene. **(B)** The haplotypes constructed by the HapMap consortium and their frequencies within the YRI (Yoruban), CEU (European) and CHB/JPT (Japanese and Han Chinese) populations. **(C)** The original frequencies of the alleles and genotypes are shown for each SNP in the order they appear along the gene.



## **5.4 Construction and analysis of *FMO1* P1, P2 haplotypes in CEU, YRI and JPT/HAN populations**

Within the following section the terms linkage and linkage disequilibria will be used.

The term linkage is used to define loci that are present on the same chromosome.

The term linkage disequilibrium is used to define the non-random association of alleles.

Haplotypes, which are how polymorphisms occur along the chromosome, give a profile of how polymorphism is inherited and physically linked. This gives the researcher an ability to study the effect of multiple SNPs and how they might act together. As I have previously defined the *FMO1* P1 and P2 promoters it would be desirable to study the SNPs within this region as they appear within the individuals sequenced as part of this project and by the sequence consortia. This analysis allows us to identify the highest frequency haplotypes. These could then be tested for their functional effect in downstream experiments. Studying haplotypes also gives us the opportunity to identify the inherited genetic unit, and differences in this unit, between different populations.

Sequencing data does not tell us on which of the two chromosomes the variation occurs. Therefore to determine the phase of the haplotypes (which chromosome they lie on) the genotypes have to be reconstructed. An alternative to haplotype reconstruction is to phase haplotypes from family pedigrees. In this study phasing haplotypes is achieved through haplotype reconstruction using statistical methods. The haplotype reconstruction was undertaken using the software Phase (Stephens and Donnelly, 2003). Phase software uses a Bayesian statistical method to

determine predicted haplotype frequencies and recombination rates. The method identifies known haplotypes (homozygous loci) and uses the assumption that the unknown haplotypes (due to heterozygosity) will be similar to the known haplotypes. The predicted haplotype frequencies and their standard deviations within the different populations are shown in Fig.5.4 and the most highly frequent haplotypes and their standard deviations are shown within Fig.5.5. The haplotypes are written in order of how the SNPs are observed along the chromosome (see Fig.5.5 for annotation). The first SNP will be the most 5' and the last SNP the most 3'. Some populations are not polymorphic for some of the SNPs. The locus will still be present within the haplotype shown for ease of comparison.

The YRI population has a larger number of predicted haplotypes compared to the other two populations. This is due to the larger variability seen between the individuals within this population. For example for the SNPs, -809G>A and -513C>A, the YRI population contain homozygote individuals for both alleles. This is not seen in the other population groups. Therefore there is more variability within the YRI population and as a result a larger number of predicted haplotypes is seen. The CEPH haplotypes are more variable than the JPT and HAN population due to a number of loci not being polymorphic within the JPT and HAN populations. The SNPs that are not polymorphic within the JPT and HAN population are -515G>A, -513G>A and -503C>T.

Examining the frequency of common haplotypes within the different populations identifies large differences between the populations. The predominant haplotype within the CEPH population is the GGGCC(CT)AT haplotype and occurs at a

predicted frequency of 53% within this population (Fig.5.5). Each SNP within the haplotype string is identified within the sequence annotation in Fig.5.5. The second most predominant haplotype is GGGCC(CT)AC and occurs at a frequency of 17% (Fig.5.5). The rest of the predicted haplotypes are of very low frequency. Therefore 70% of individuals have the same first seven 5' to 3' polymorphisms within the *FMO1* P1 and P2 promoter region (GGGCC(CT)A) and only the last SNP location is polymorphic. This polymorphism is -11T>C. The polymorphism introduces a potential second ATG initiation codon in those individuals with the T allele. The P1 and P2 polymorphisms upstream of this may have occurred on the background of this polymorphism.

The highest frequency haplotype within the YRI population is the AGATC(CT)AC haplotype which has a predicted frequency of 18% (Fig.5.5). The second most frequent haplotype is GGGCC(CT)AC at a frequency of 10% (Fig.5.5). This haplotype is also seen at a high frequency within the CEPH population. The most frequent predicted haplotype within the YRI population contains 4 out of 9 variations different from the two most frequent CEPH haplotypes. The high frequency YRI haplotypes also do not contain the T allele of the polymorphism -11C>T.

The most highly frequent haplotypes seen within the JPT and HAN populations are the GGGCC(CT)AT haplotype at a frequency of 67% and the GGGCC(CT)AC haplotype at 29% (Fig.5.5). These two haplotypes are also the highest frequent haplotypes within the European population.

A YRI HAPLOTYPES

haplotype	E(freq)	S.E
AGATC(CT)AC	0.19	0.04
GGGCC(CT)AC	0.10	0.06
GAGTCC(CT)AC	0.07	0.05
GGTC(CT)AC	0.06	0.05
GAGCC(CT)AC	0.06	0.05
AGATC(CT)TC	0.05	0.01
AGGCC(CT)AC	0.05	0.04
AGGT(CT)AC	0.05	0.04
GAATC(CT)AC	0.04	0.04
AGGCC(CT)TT	0.03	0.04
GGATC(CT)AC	0.03	0.04
GAAC(CT)AC	0.02	0.03
GGGCC(CT)TT	0.02	0.03
GGAC(CT)AC	0.01	0.03
AGACC(CT)AC	0.01	0.02
AAATC(CT)AC	0.01	0.02
AGGCC(CT)AT	0.01	0.03
AGGCC(CT)TC	0.01	0.02
AAGTC(CT)AC	0.01	0.02
GGCC(CT)TC	0.01	0.02
GGCC(CT)AT	0.01	0.02
GAGC(CT)TT	0.01	0.02
AGACC(CT)TT	0.01	0.02
AAGCC(CT)AC	0.01	0.02
AAACC(CT)AC	0.01	0.02
GAAC(CT)TT	0.00	0.02
AAGCC(CT)AT	0.00	0.01
AAACC(CT)TT	0.00	0.01
GAACC(CT)AT	0.00	0.01
GGAC(CT)TC	0.00	0.01
GAGCC(CT)TC	0.00	0.01
GAAC(CT)TC	0.00	0.01
AAGCC(CT)TC	0.00	0.01
AAGCC(CT)TT	0.00	0.01
AGGT(CT)TT	0.00	0.01
GGAC(CT)AT	0.00	0.01
AGATC(CT)TT	0.00	0.01
AGACC(CT)AT	0.00	0.01
GAGCC(CT)AT	0.00	0.01
AGACC(CT)TC	0.00	0.01
AAACC(CT)TC	0.00	0.01
AGATC(CT)AT	0.00	0.01
AAACC(CT)AT	0.00	0.01
GGAC(CT)TT	0.00	0.01
GAATC(CT)TC	0.00	0.01
GGATC(CT)TC	0.00	0.01
GAATC(CT)AT	0.00	0.01
GGATC(CT)TT	0.00	0.01
AAATC(CT)TT	0.00	0.01
AGGT(CT)AT	0.00	0.01
AAGTC(CT)AT	0.00	0.01
GGATC(CT)AT	0.00	0.01
GAATC(CT)TT	0.00	0.01
GAGTC(CT)TT	0.00	0.01
GAGTC(CT)AT	0.00	0.01
GAGTC(CT)TC	0.00	0.01
AAATC(CT)AT	0.00	0.01
AAGTC(CT)TT	0.00	0.01
AGGT(CT)TC	0.00	0.01
AAGTC(CT)TC	0.00	0.01
GGTC(CT)TT	0.00	0.01
AAATC(CT)TC	0.00	0.01
GGTC(CT)TC	0.00	0.01

B CEPH HAPLOTYPES

haplotype	E(freq)	S.E
GGGCC(CT)AT	0.53	0.04
GGGCC(CT)AC	0.18	0.04
GGGCC-AT	0.09	0.01
AAATC(CT)AT	0.06	0.03
AAATC(CT)AC	0.04	0.03
AAACC(CT)AC	0.03	0.01
GGGCT-AT	0.01	0.01
GGGCT(CT)AT	0.01	0.01
AGGT(CT)TC	0.01	0.01
AGGT(CT)TT	0.01	0.01
GGTC(CT)TT	0.00	0.01
AGGCC(CT)AC	0.00	0.01
GGTC(CT)AT	0.00	0.01
GGGCC(CT)TC	0.00	0.01
AGGT(CT)AT	0.00	0.01
GGTC(CT)TC	0.00	0.01
AGGCC(CT)AT	0.00	0.01
GGTC(CT)AC	0.00	0.01
AGGCC(CT)TT	0.00	0.01
GGGCC(CT)TT	0.00	0.01
AGGT(CT)AC	0.00	0.01
AGGCC(CT)TC	0.00	0.00
AAACC(CT)AT	0.00	0.00

C JPT/HAN HAPLOTYPES

haplotype	E(freq)	S.E
GGGCC(CT)AT	0.68	0.05
GGGCC(CT)AC	0.29	0.05
AGGCC(CT)AT	0.03	0.00

**Figure 5.4 Predicted haplotype frequencies of the *FM01* P1 and P2 promoter regions in different populations**

The haplotypes are made up of the 8 known SNPs and the novel SNP identified in this study. They are shown in order of how they appear from the 5' to the 3' end of the gene (see Fig.5.5 for annotation). The location of the SNPs can be visualised in Fig.5.3. Haplotype frequencies are shown for the (A) YRI (Yoruban) (B) CEU (European) (C) JPT/HAN (Japanese and Han Chinese). The haplotypes highlighted in red have higher standard deviations than their predicted frequency. They are therefore likely to be inaccurate.

A

CAATGCACTCT (A/G) TTGCCTCTCGGTGTTCTTACACATGTGTGTTATTAACACATGGCCTGGTGCCAGAAGAT  
TCTCTGGCCCATCCCAGTGGTGACTGTGCCATGTGCCCTGGAGGTGAATCAGTATCCAATTGAGAAGGGAGGGAT  
GGCTTTGCATGCCTACCTTTCTACCACAAACCCTCCCTGGCAGCCACCCTCTCTCTCTCCCCTGGTGACCATCA  
CTGGTGACCTGTGAAAGGGACACACCAACAGCACAGCTGGGGCCCTGGCATTGTGCCAGGGGCAGGATCACACAG  
GGCAGTGCC (A/G) C (A/G) GTAGCACC (T/C) GTGGT (A/G) CCACAGGTGTGGTGGCTCCTGGTCCCAACTCC  
ACCCACCAGCTGCTGTGTGGTGTGTGTCAGGTCACCACACCAATCGGAGCTTCAGTTTTGTATGTGATAAAGA  
GATTGTGTCTGACAAGGTGACCTTTTCCTAGTCTGCTGATCTATGCAGTT (CT/DEL) AGGGCCACAGAATGGAG  
ACTAGAGGCAGCAGCTCAGTCTGAAGTGCAAGACTTT (A/G) TCCAGTAAAAGGTCCAATTCAGCAGCTCTGCC  
AGAAGCTACAGCCTTGACAACGTACGAACATTTGGCACTGGTGCTGCATGAGGGGCGGGAACATAACCAAGCACA  
GGGTTAACCAGTGACCTGAACATTTTCCTTCTCACATTCACACACCAGAGACC CGCTACAGAAGATTCAAACCTGA  
GCAAATCGCCTAATCTTCAAATCTTTTTCTGGCTTGTAGAGCAGCCAAGGGTGGGGTGGAGCTTGTGAATA  
AAAAGCCTGCTTCATCTTCTCA (T/C) GCAGGAGAACATG

B

YRI HAPLOTYPE		
Haplotype	E(freq)	S.E
AGATC(CT)AC	0.19	0.04
GGGCCC(CT)AC	0.1	0.06
CEU HAPLOTYPE		
Haplotype	E(freq)	S.E
GGGCC(CT)AT	0.53	0.04
GGGCC(CT)AC	0.18	0.04
JPT/HAN HAPLOTYPE		
Haplotype	E(freq)	S.E
GGGCC(CT)GT	0.68	0.05
GGGCC(CT)GC	0.29	0.05

**Figure 5.5 (A) Illustration of the polymorphisms that reside within the P1 and P2 promoter regions of *FMO1* and (B) the high frequency haplotypes within the populations analysed**

**(A)** Exon 1 and exon 2 are highlighted in red. The SNPs are highlighted in blue. The novel SNP identified within this study is highlighted at the start of exon 1 (CT/DEL). **(B)** The predominant haplotypes and their frequencies and standard deviation are shown for the YRI (Yoruban), CEU (European) and JPT/HAN (Japanese and Han Chinese) populations. The eight base pair string of the haplotype corresponds to the 8 SNPs shown in **(A)** ordered from the 5' to 3' of the sequence.

## 5.5 Construction and analysis of *FMO1* P0 haplotypes in CEU, YRI and JPT/HAN populations

Sequencing of the P0 promoter has revealed no new novel variation. In total 3 SNPs have been identified which are -452G>A, -188C>T and +58C>A (Fig.5.2). The frequency of the SNPs can be observed in figure 5.2. The frequencies are similar to those shown for these SNPs by HapMap. A further 2 SNPs previously identified within the NIEHS project were not identified in the present study. These are rs28384812 located at position -10C>T and rs17515666 located at +22T>C. The two SNPs were identified within the NIEHS project and are at low frequency. The C allele of the -10C>T SNP occurs at a frequency of 0.994 and the T allele 0.006. The T allele of the +22T>C SNP occurs at a frequency of 0.994 and the C allele at a frequency of 0.006. The two SNPs are low frequency polymorphism.

Haplotypes were constructed from the three genotyped SNPs using the phase software. The CEPH and JPT/HAN populations show a higher number of haplotypes than the YRI population (Fig.5.6). This is due to the -452G>A A allele being fixed within the YRI population. In both the CEPH and JPT/HAN populations this is polymorphic.

The most frequent haplotype within the YRI population is the ATC haplotype at a frequency of 54% (Fig.5.6). The second most frequent haplotype is the ACC haplotype at a frequency of 26% and the third is ATA at a frequency of 16% (Fig.5.6). Within the CEU and JPT/HAN populations the highest frequency haplotype is GCC at a frequency of 53% and 33% respectively (Fig.5.6). Therefore the most frequent haplotype within these populations contains the G allele of the -452G>A

which is in contrast to the YRI individuals which contain the A allele. The second most frequent haplotype within the CEU and JPT/HAN populations is the ATC

**A** YRI HAPLOTYPE

Haplotype	E(freq)	S.E
ATC	0.55	0.07
ACC	0.26	0.05
ATA	0.16	0.07
ACA	0.04	0.04

**B** CEU HAPLOTYPE

Haplotype	E(freq)	S.E
GCC	0.57	0.02
ATC	0.23	0.02
ACC	0.11	0.02
GTA	0.05	0.005
ATA	0.02	0.01
ACA	0.01	0.01
GTC	0.005	0.01
GCA	0.004	0.01

**C** JPT/HAN HAPLOTYPE

Haplotype	E(freq)	S.E
GCC	0.33	0.07
ATC	0.24	0.07
ATA	0.2	0.08
GTC	0.12	0.05
GCA	0.04	0.05
GTA	0.03	0.04
ACC	0.02	0.04
ACA	0.01	0.02

**Figure 5.6 Predicted haplotype frequencies of the *FM01* P0 promoter region in different populations**

The predominant haplotypes and their frequencies and standard variation are shown for **(A)** the YRI (Yoruban), **(B)** CEU (European) and **(C)** JPT/HAN (Japanese and Han Chinese) populations. The three SNPs used in the haplotype string are - 452G>A, -188C>T and +58C>A.

haplotype at a frequency of 23% and 24% respectively (Fig.5.6). The third most frequent haplotype in the CEU is ACC at 11% and the third most frequent haplotype within the JPT/HAN population is the ATA haplotype at a frequency of 20% (Fig.5.6). This reflects the higher frequency of the A allele at the +58C>A locus.

## **Discussion**

The identification of regulatory variation within human *FMO1* gene is important as it may be linked to the efficiency of drug metabolism. These SNPs could therefore act as indicators of drug metabolism efficiency within individuals. Re-sequencing of the defined promoter regions is therefore desirable in identifying SNPs within the wider population. Upon discovery of SNPs, they can be tested functionally for their effects on transcription or cis-acting regulatory binding.

Re-sequencing the *FMO1* promoters has yielded two newly identified polymorphisms. One of which occurs at a relatively high allele frequency of 5%. This polymorphism, -337\_338CTdel is a deletion that occurs at the start of exon 1. This is the transcriptional start site for the P1 transcript. The P1 transcript, as shown in chapter 1, is the predominant transcript in most extra-hepatic tissues. The polymorphism could have an effect on transcription as it is a 2 base pair deletion within the start region of transcription. This could affect the binding efficiency of RNA polymerase II and therefore influence the amount of the P1 transcript produced. The second identified SNP, -497A>T is predicted to occur in 1/6400 individuals. This is a low frequency polymorphism and as such is not useful as a diagnostic of drug metabolism.



Haplotype construction within the three different populations has revealed differences in the abundance of haplotypes and revealed high frequency haplotypes within each population for both the P0, P1 and P2 promoters. This haplotype construction will be useful in further *in-vitro* analysis of promoter activity or protein binding. Instead of testing each individual SNP for effects on transcription, the haplotype can be tested. This will reduce the number of SNPs to analyse and also the effects of SNPs will be studied as they appear on the chromosome.

Analysing haplotypes of the P1 and P2 promoter regions indicate the C and T allele of the -11C>T variation have distinct haplotypes. Seventy-percent of the predicted haplotypes for the CEU population and 95% for the JPT and HAN population only vary at this polymorphism. The most frequent haplotype contains the T allele and the second most frequent contains the C allele. Within the YRI population the -11C>T allele has a more predictable haplotype than the other two populations. The two most frequent haplotypes contain the C allele. The variation between the two most common YRI haplotypes occur further upstream at the -809G>A and -513G>A. The most frequent being the haplotype with the A alleles.

These data suggest the P1 and P2 promoter haplotypes containing the T allele of the -11C>T variation originated within Africa and became more frequent as individuals migrated out of Africa. This may be due to the haplotypes conferring an advantage to those individuals. FMO1 is a drug-metabolising enzyme and it may have given the individual an advantage in metabolising new compounds found outside of Africa. Alternatively, the T allele may also be more frequent in other African populations and the CEPH and JPT/HAN may have similar ancestry to these populations. It would

therefore be desirable to test the effect of the -11C>T SNP functionally as it may confer a selective advantage.

## **Chapter 6**

# **Optimisation and development of capillary DNase I footprinting for the detection of regulatory polymorphisms that alter DNA-protein binding events**

# Chapter 6: Optimisation and development of capillary DNase I footprinting for the detection of regulatory polymorphisms that alter DNA-protein binding events

## Introduction

This chapter describes the optimisation of a high-throughput DNase I footprinting method for identifying the sequence of DNA bound to protein, and the affect of genetic polymorphism/mutation on protein-DNA interactions.

Recent advances in the methodology of DNase I footprinting allow capillaries to be used to analyze DNA fragments as opposed to the traditional method of using gel electrophoresis (Wilson et al., 2001; Zianni et al., 2006). This makes the technique safer and more reproducible as fragments to be analysed are labelled fluorescently, compared to traditional DNase I footprinting where DNA is radio-labelled.

With the use of capillary technology the DNase I footprint can be used for high-throughput applications as the DNA fragments are analyzed using the ABI prism genetic analyzer 3730, which allows 96 samples to be analyzed in a single run as opposed to a few samples traditionally analysed on a single polyacrylamide gel. The machine can analyse a maximum of 12 plates simultaneously.

We chose to incorporate this new methodology for a novel application in which human *FMO1* promoter polymorphisms could be screened for their affect on DNA-protein binding. As the *FMO1* promoters are tissue-specific (see chapter 1) it is desirable to analyse the influence of polymorphism in different tissues through the use of extracts from different tissue types. As the method allows a large number of

samples to be analysed this would be possible. Any change in DNA-protein binding observed is likely to change the amount of transcript produced and subsequently the amount of protein. Genetic polymorphisms shown to change DNA-protein binding by this method could then be used in association studies to determine polymorphisms that are associated with drug response.

For the proposed method to be applicable to the screening of promoter polymorphism it would have to identify DNA-protein binding events using an extract of proteins which represented a situation within a cell line or tissue. It would also have to be able to detect the affect of regulatory polymorphism on DNA-protein binding.

### **6.1 Labelling and detection of DNA fragments for capillary DNase I footprinting**

The DNA to be analysed is labelled with a suitable fluorescent dye that can then be detected within the capillaries during fragment analysis using the genetic analyzer 3730. DNA is labelled by PCR using a labelled oligonucleotide (see section 2.11 for method). The DNA template for the PCR can either be plasmid or genomic DNA. Screening a large number of genetic variations using a large number of individuals would ideally be carried out by directly amplifying the desired region of an individual's DNA. This would remove the need for cloning.

The dye that is incorporated on to the DNA during the PCR is quantified using the ABI PRISM 3730 Genetic Analyzer. The dye chosen to label DNA fragments was FAM. FAM is a fluorescein amidit, commonly used as 5' fluorophore for qPCR probes or as 5' labelled primer for different DNA sequencing approaches on ABI

instruments. To analyse the FAM-labelled fragments we used a genotyping program capable of analysing 5 separate dyes. This is known as the G5 dye set. The 5 dyes are FAM/VIC/NED/PET/LIZ. It has been shown previously that the dye FAM gives the strongest and most robust signal. As a small amount of DNA (50ng-200ng) is to be used the FAM label is the most appropriate.

## **6.2 Footprinting analysis of the Simian Virus 40 promoter (SV40)**

The SV40 promoter has previously been analysed using traditional DNase I footprinting. The promoter is well characterised and the DNA sequences to which various transcription factors bind are known (Dyanan and Tjian, 1983). The SV40 promoter was therefore chosen as a positive control for the optimisation of DNase I capillary footprinting.

The SV40 DNA was obtained in a linear form from the Promega corefootprinting kit. To label the SV40 promoter DNA with FAM it was necessary to clone the promoter into a TOPO vector (see section 2.13 for method). This was to ensure the template could be produced in large quantities and used for future experiments. It also allowed the promoter to be amplified upstream of the start of the SV40 promoter allowing the full promoter sequence to be analysed for DNA-protein binding. To ensure effective TA cloning the SV40 DNA was incubated at 72° C for 10 minutes with dATP and Taq polymerase. The Taq polymerase adds adenine nucleotides to the end of the linear DNA which is a requirement for TA cloning to be successful. Once cloned, the vector could be transformed (see section 2.5) and DNA prepared in a large quantity (see section 2.3).

The cloned SV40 DNA was then used as the template to produce a FAM-labelled fragment for capillary electrophoresis. PCR was carried out with a 5' FAM-labelled forward primer located at the start of the SV40 promoter and an unlabelled 3' reverse primer located just downstream of the SV40 promoter in the TOPO vector (Figure 6.1). The PCR product was separated through an agarose gel by electrophoresis (section 2.8). It is important that no DNA detection dye e.g. ethidium bromide or Sybr green be included in the gel. The gel was viewed with a fluorescent imager at the wavelength of FAM excitation and a single band representing the labelled promoter was visible (Figure 6.1). The DNA ladder was visualised by mixing with Sybr green prior to electrophoresis. The DNA was purified as described in section 2.9.1.

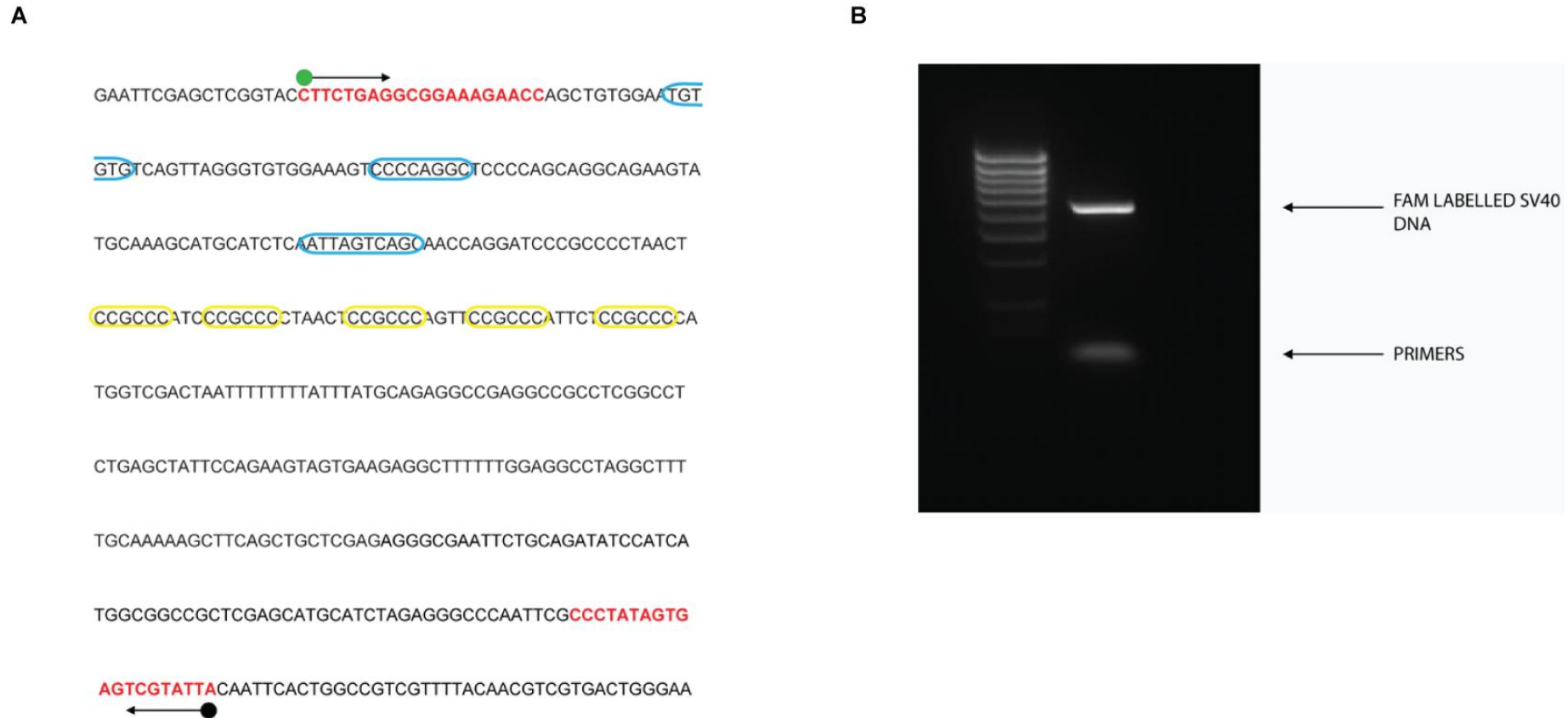


**Figure 6.1 Annotation of the SV40 promoter sequence and PCR FAM labelling of the sequence**

**(A)** SV40 positive control DNA sequence. The primers used to amplify and label the SV40 promoter sequence are indicated in red. The 5' primer is FAM labelled and the 3' primer is unlabelled. The blue and yellow regions highlight the AP1 and SP1 transcription factor binding consensus sites respectively. **(B)** The image of the labelled PCR product in lane 2, using an excitation filter for reading FAM, is shown. Lane 1 contains the BioLine hyperladder marker 4.



### **6.2.1 Optimisation of the SV40 promoter nuclear protein binding reaction**

The labelled DNA is incubated with a nuclear protein extract to allow the proteins to bind to the DNA. COS-7 (a cell line derived from African green monkey kidney fibroblasts) nuclear extract was used as this has been shown to have endogenous levels of the SP1 protein. The SV40 promoter contains several SP1 consensus binding sites for (Figure 6.1). For the binding reaction conditions see method 2.30.2 The COS-7 nuclear protein was analysed by SDS-PAGE to check protein integrity. This showed that the extracted proteins are intact and suitable for use in the footprinting experiments.

### **6.2.2 DNase I digestion**

The DNA is digested using DNase I (Section 2.30.3 for method). The concentration of the enzyme needs to be optimised so that each phosphodiester bond along the length of the fragment is cleaved. However, the conditions should be such that each fragment in the population of DNAs is ideally cleaved just once. As these cleavages occur randomly, the population of DNA strands produced by enzymatic digestion should represent all possible DNA lengths. If too much enzyme is used then a higher percentage of DNA fragments will be shorter, likewise if too little enzyme is used a higher percentage of fragments will be too long. To be able to analyse the whole promoter sequence the enzyme needs to digest randomly and evenly along the length of the fragment. Therefore a number of enzyme concentrations need to be tested. The optimal range of DNase I concentration was shown to be large (Figure 6.2). 0.05U (A) and 0.005U (B) both give an acceptable size range of DNA fragments. Footprints could be observed throughout the 350bp sequence. The higher DNase I concentration (A) does show a slight skew towards smaller DNA

fragments. I therefore chose to use 0.005U for my subsequent experiments. The result of this optimisation shows that the DNase I capillary technique could be flexible in the amount of DNase I enzyme used and would not, in most circumstances, require optimisation. This would make the technique more conducive to screening a number of different promoters. This makes the technique more applicable for high-throughput screening as a wider enzyme concentration range will make it easier to analyse a number of different promoter fragments of different length at the same time.

It was observed initially that when different nuclear protein concentrations were used that DNase I digestion would happen at different efficiencies. It was concluded that the reason for this was that as more nuclear protein was added the buffer conditions were changing and that this affected the efficiency of the DNase I enzyme. This problem was partially overcome by adding BSA to equalise the total protein content in each reaction and increasing the volume of the digestion reaction (from 20  $\mu$ L to 100  $\mu$ L). The increase in volume would help to dilute any differences in buffer conditions between samples. The DNA digestion reaction was terminated using 0.5 M EDTA which inhibits the enzyme reaction and heating to 75°C for 10 min to denature the enzyme.

Before analysing the digested DNA, it is necessary to remove the bound protein. Different methods were tested to extract the DNA from the protein. Initially the method of phenol/chloroform extraction was used. When using columns which contain a gel separating the phenol organic phase and the aqueous phase containing the DNA, the DNA extraction was shown to be much more efficient. This

was subsequently compared to the use of ion-exchange columns. Both methods were shown to work equally well, however more DNA was recovered using ion-exchange columns (see method 2.9).

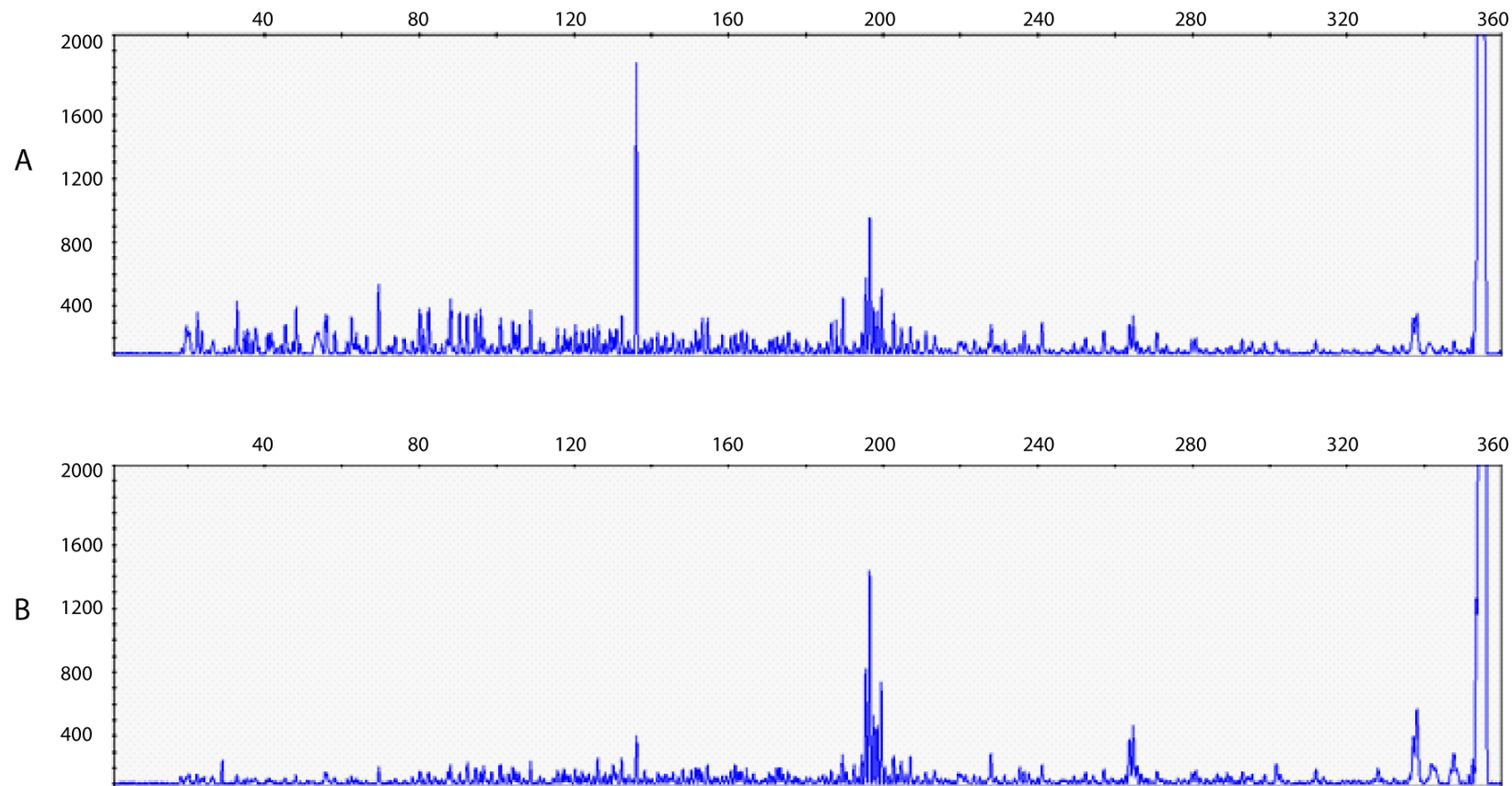


**Figure 6.2 0.005U of DNase I is optimal to produce an evenly size-distributed set of DNA fragments**

The chromatograms above show the effect of different DNase I concentrations. The chromatograms show the DNase I digested fragments from the 5' FAM labelled SV40 promoter after incubation with COS-7 nuclear protein extract. The fragments were separated through capillaries and each peak on the chromatogram represents cleavage at a phosphodiester bond by DNase 1. The x-axis represents the number of base pairs from the 5' label and the y-axis is the intensity of the peak.

### **6.2.3 Increasing the binding competitor does not affect the DNA-protein binding profile of the promoter**

The binding reaction was optimised by varying the components of the reaction. The incubation buffer used had previously been optimised within the lab for use as a general buffer which promotes binding of a high percentage of proteins to DNA (Dell et al., 1998). This buffer was also used in gel shift assays and binding was shown to be efficient (see chapter 4.19).

The amount of non-specific nucleic acid competitor was also optimised. The non-specific competitor used was Poly (deoxyinosinic-deoxycytidylic) acid sodium salt. This is a double-stranded alternating copolymer consisting of a chain of deoxyinosinic acid bound to a chain of deoxycytidylic acid. The competitor functions by mopping up nuclear protein that binds non-specifically to DNA and thus removing proteins that could interfere with proteins that bind specifically to the promoter region being analysed. By increasing the competitor concentration we can identify if proteins are binding non-specifically to the DNA being analysed. When the amount of poly (dl-dC) was increased from 4 µg to 10 µg there was no difference in the footprinting profile of the SV40 promoter when different amounts of COS-7 protein were used (Figure 6.3). We therefore decided that 4µg of competitor was sufficient to remove non-specific DNA-protein binding.

### **6.2.4 Increasing DNA amount increases the FAM signal and DNA-Protein binding is less specific**

The total amount of DNA is varied to observe how much DNA is required to visualise the labelled DNA and to test for a saturation effect which could occur if too much

DNA was added. Too much DNA may result in protein binding being undetected due to too much unbound DNA being present. Increasing the DNA template concentration from 50 ng to 200 ng resulted in the loss of DNA-protein binding specificity. The SV40 binding region is footprinted using 50 ng of template. When 200ng DNA template is used the signal is reduced non-specifically along the whole trace (Figure 6.4). A template concentration of 50ng was therefore chosen for future experiments.

### **6.2.5 Confirmation of DNA-protein binding events**

To further determine if the DNA-protein binding is specific, proteinase K was added to the incubation samples after DNA-protein binding had been allowed to proceed to completion. Proteinase K is a protease and thus digests proteins. The presence of this enzyme eliminated DNA-protein binding (Figure 6.5). This shows that the DNA-protein interactions observed are specific.

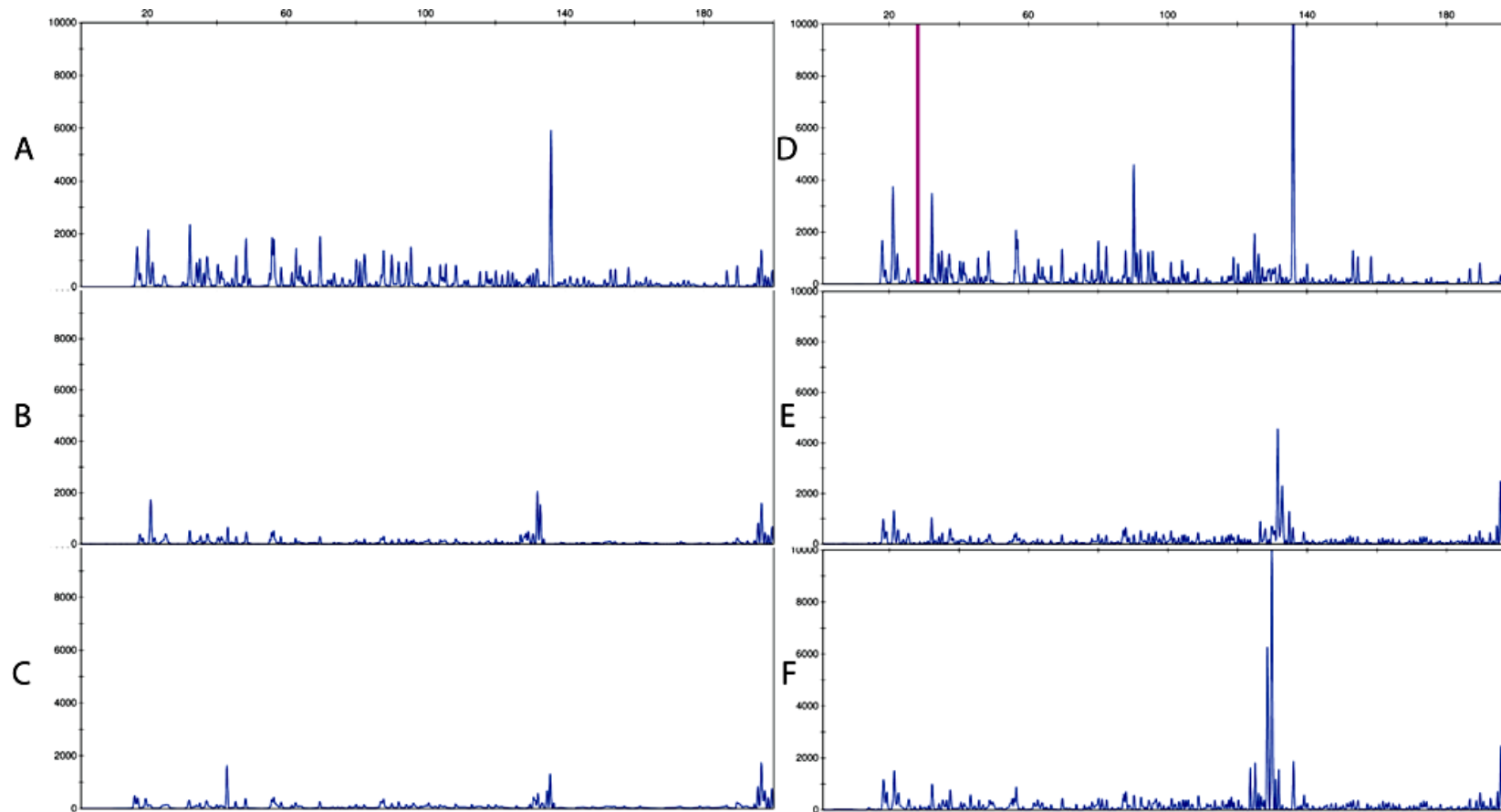


**Figure 6.3 Increasing the amount of competitor DNA does not affect the DNase I footprinting trace of the SV40 promoter**

The chromatograms above show the DNase I digested fragments from the 5'FAM labelled SV40 promoter. The fragments are separated through capillaries and each peak represents a phosphodiester bond cleavage. The x-axis represents the number of base pairs from the 5' FAM label and the y-axis represents the intensity of the peak. A to C binding reactions contained 10  $\mu\text{g}$  of competitor DNA. D to F contained 4 $\mu\text{g}$  of competitor DNA. The total COS-7 nuclear protein is **(A)** 0  $\mu\text{g}$  **(B)** 20  $\mu\text{g}$  **(C)** 40  $\mu\text{g}$  and **(D)** 0  $\mu\text{g}$  **(E)** 20  $\mu\text{g}$  **(F)** 40  $\mu\text{g}$ . The traces shown adjacent to each other contain the same amount of nuclear protein.

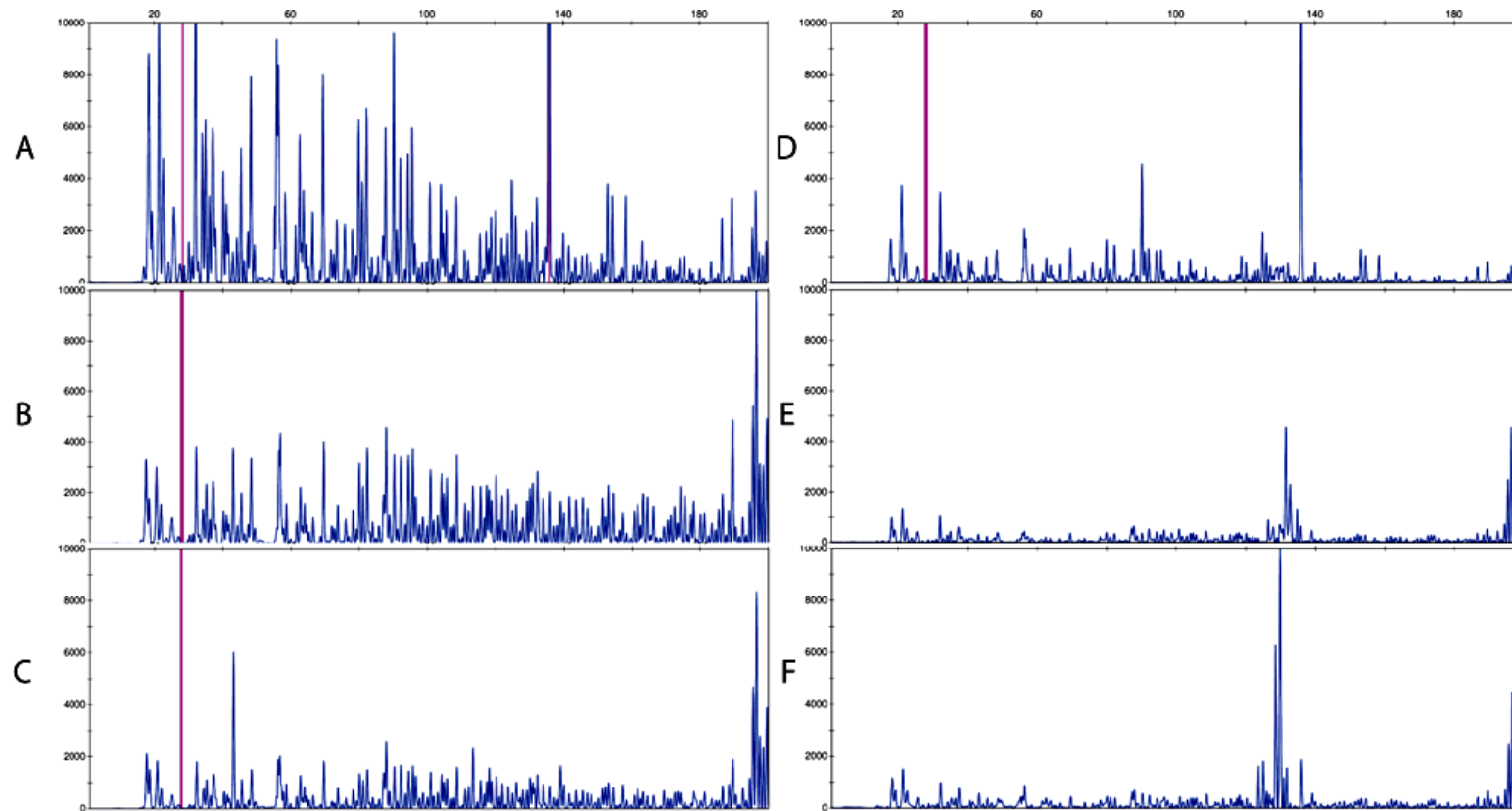


**Figure 6.4 Capillary DNase I footprinting of the SV40 promoter with increased amounts of SV40 DNA template**

The chromatograms above show the DNase I digested fragments from the 5'FAM labelled SV40 promoter after incubation with COS-7 nuclear protein extract. The fragments have been separated through capillaries and each peak represents a phosphodiester cleavage event. The x-axis represents the number of base pairs from the 5' label and the y-axis is the intensity of the peak. A to C binding reactions contained 200ng of template DNA. D to F contained 50ng of template DNA. The total COS-7 nuclear protein is **(A) 0  $\mu$ g (B) 20  $\mu$ g (C) 40  $\mu$ g** and **(D) 0  $\mu$ g (E) 20  $\mu$ g (F) 40  $\mu$ g**. The traces shown adjacent to each other contain the same amount of nuclear protein.



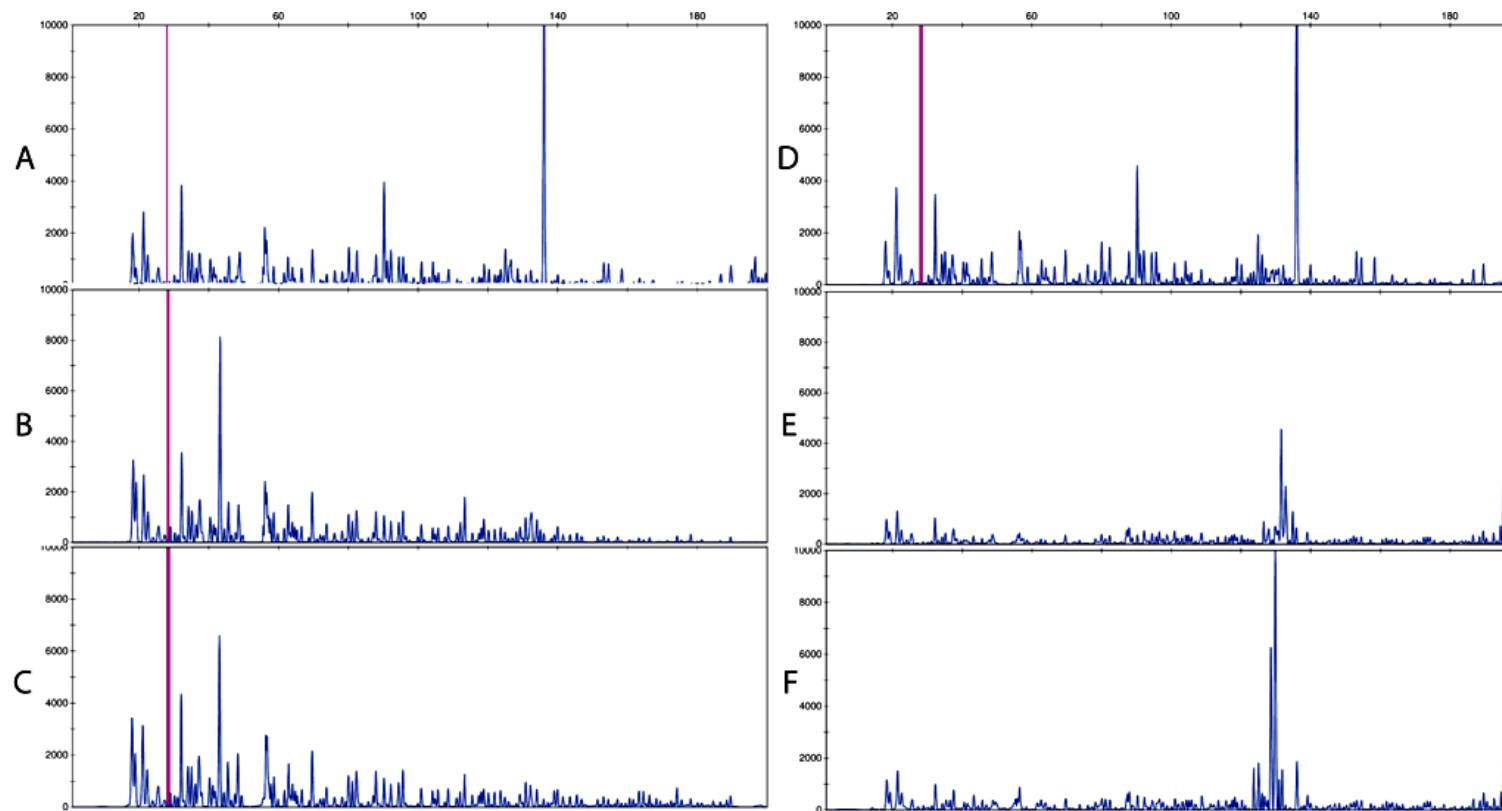


**Figure 6.5 Treatment of DNA-protein binding reaction with proteinase K removes DNase I footprints within the SV40 promoter**

The chromatograms above show the DNase I digested fragments from the 5'FAM labelled SV40 promoter. The fragments are separated through capillaries and each peak represents a phosphodiester bond cleavage. The x-axis represents the number of base pairs from the 5' FAM label and the y-axis represents the intensity of the peak. Proteinase K was added to A to C. D to F contained no Proteinase K. The total COS-7 nuclear protein is **(A)** 0  $\mu\text{g}$  **(B)** 20  $\mu\text{g}$  **(C)** 40  $\mu\text{g}$  and **(D)** 0  $\mu\text{g}$  **(E)** 20  $\mu\text{g}$  **(F)** 40  $\mu\text{g}$ . The traces shown adjacent to each other contain the same amount of nuclear protein.

### **6.2.6 The optimised conditions for capillary DNase I footprinting**

It was observed that the optimal DNA template concentration, competitor DNA concentration, and DNase I concentration was 50 ng, 4 µg, and 0.0005 U respectively. DNase I capillary footprinting using these conditions was carried out for the complete SV40 promoter. The results are shown in figure 6.6. The first 1-200 bp show significant loss of signal as more protein is added. The remaining sequence shows minimal reduction in signal. The area with reduced signal corresponds to the SV40 promoter where SP1, AP1 and AP2 transcription factors bind. The sequence further downstream shows minimal signal reduction. The technique with these optimised conditions therefore detects true DNA-protein binding events.

### **6.2.6 Analysis of digested DNA fragments**

DNase I digested DNA was eluted was recovered in a total volume of 50 µL. From this, 5µl was taken and loaded into a well of a 96-well plate. In addition samples were also diluted ten-fold and placed on the same plate. This was to ensure that any differences in protein concentration or buffer conditions would be minimal and so that signal intensities would not be affected.

Subsequently 4.9 µL of HiDi Formamide (ABI Applied Biosystems) and 0.1 µL of LIZ standard (ABI applied biosystems) were added to each sample. The LIZ standard contains DNAs of known size and is used to align the sequence traces at the end of the DNA separation. The standard contains a LIZ dye which can be detected using the G5 dye set. The samples were separated using the G5 dye set genotyping module and a voltage of 10kv using an Applied Biosystems genetic analyzer 3730.

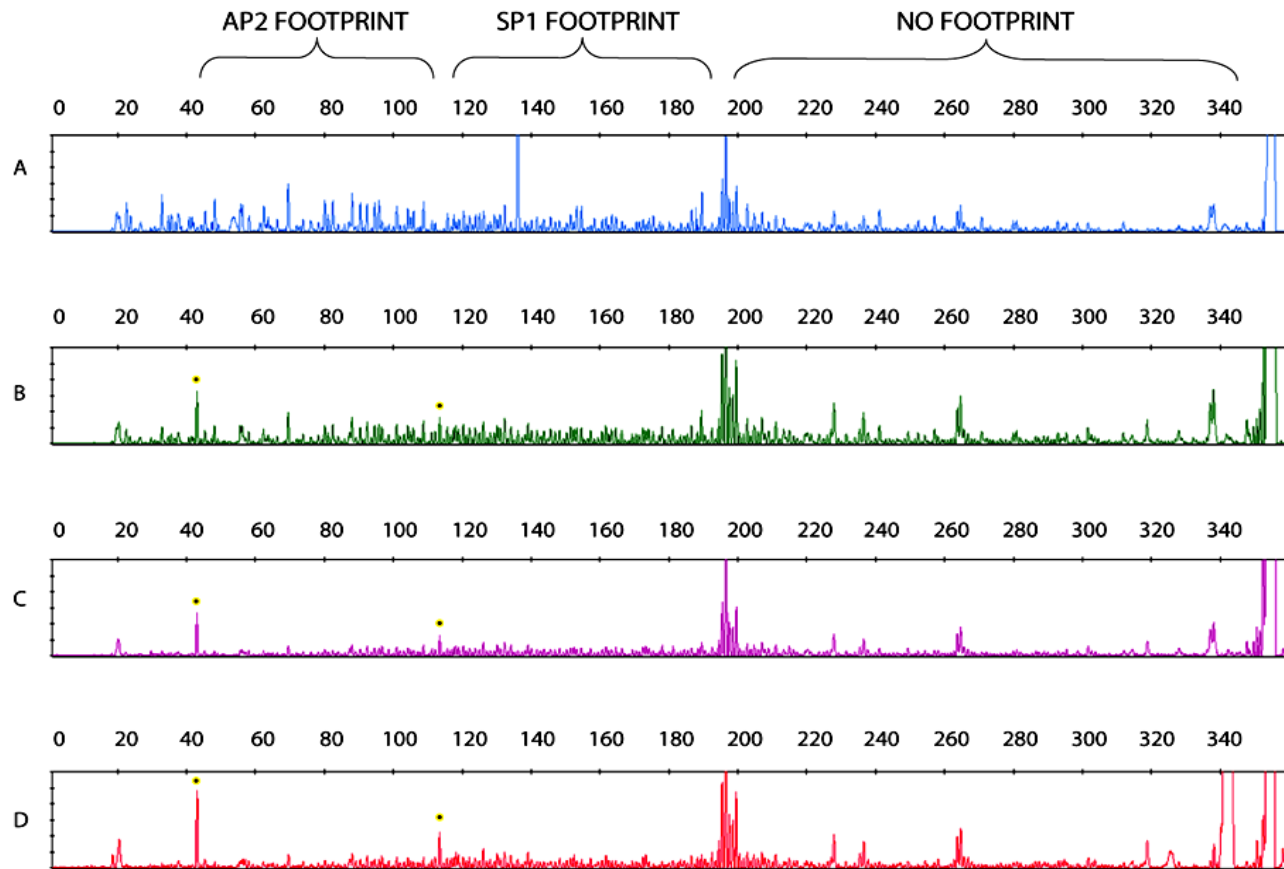


**Figure 6.6** The chromatograms above show the DNase I digested fragments from the 5'FAM labelled SV40 promoter after incubation with COS-7 nuclear protein extract

The fragments have been separated through capillaries and each peak represents a phosphodiester bond cleavage. The x-axis gives the number of base pairs from the 5' label and the y-axis is the intensity of the peak. From A to D the total COS-7 nuclear protein is increased: (A) 0  $\mu$ g (B) 10  $\mu$ g (C) 20  $\mu$ g and (D) 40  $\mu$ g. The traces were obtained using optimised conditions which were used for subsequent experiments.

### **6.3 Dye terminator sequencing reactions to determine location of DNA-protein binding**

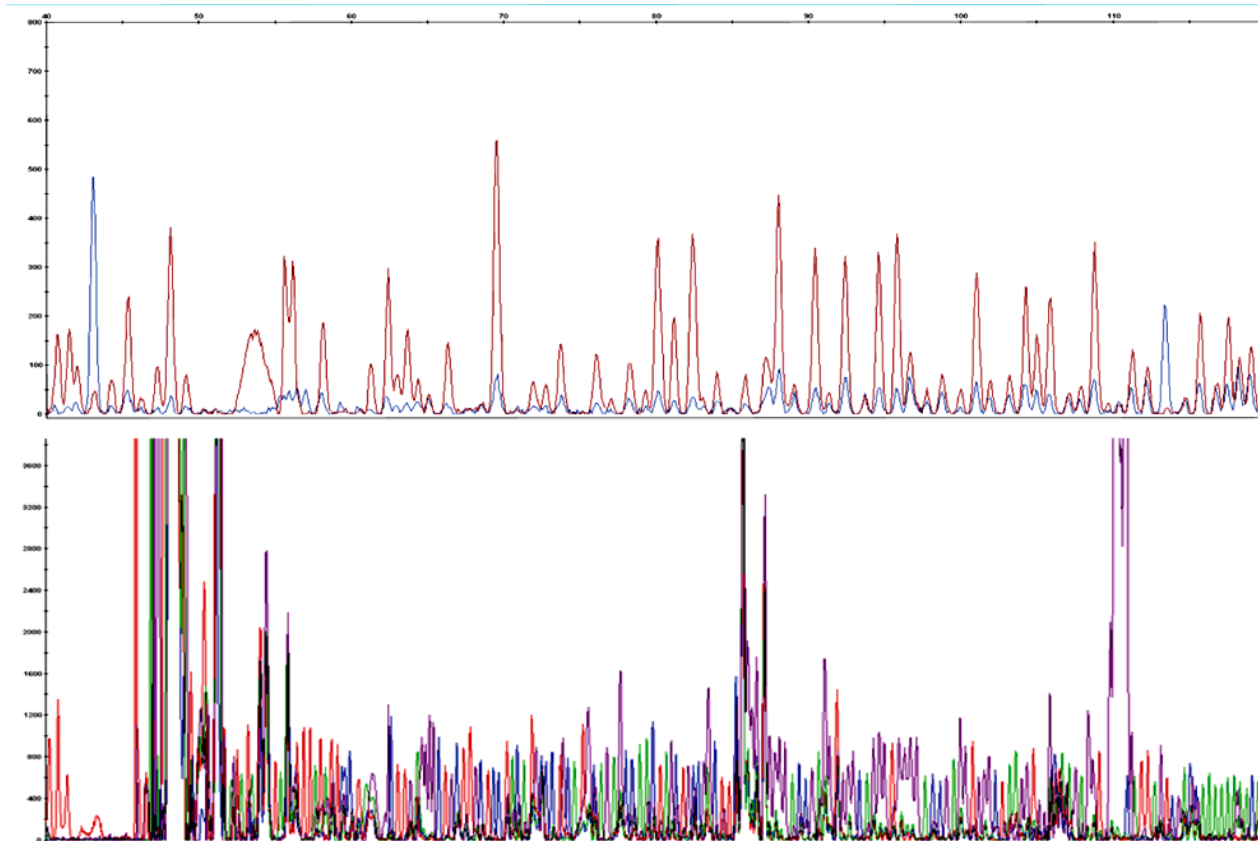
To identify the positioning of DNA-Protein interactions along the DNA fragment analysed it is necessary to also sequence the DNA fragment. Therefore dye-terminator sequencing reactions were carried out using a 5' FAM labelled primer (see section 2.30.1 for method). The dye-terminators are not labelled and therefore the dye signal will come from the 5' FAM label. The sequencing reactions were carried out with the same 5' FAM primer used to amplify the DNA sequence to be footprinted. This is essential because this allows the sequence fragment traces to be aligned (based on size) correctly with the DNase I footprint traces. The inclusion of the LIZ standard ensures that the sequence and footprinting reactions can be aligned. The software Genemapper was used to align the individual dye-terminator sequencing reactions. A different colour was applied for each dye-terminator reaction for ease of comparison (Figure 6.7B). The dye terminator sequence alignment was subsequently aligned with the DNase I footprinting traces to identify the sequence location of the DNase I footprints (Figure 6.7). This resulted in the identification of the base pairs to which protein was bound.

### **6.4 Description of the SV40 DNA-protein binding profile**

As shown in Fig.6.6 clear footprints are detected in the SV40 promoter analysed by the high throughput methodology. As a nuclear extract is used a large number of footprints are visible in the SV40 promoter DNA. The promoter region (1-200bp) is known to contain AP1, AP2 and SP1 binding consensus sites (Fig.6.1). This region of the promoter shows intense DNase I hypersensitive regions either side of the

AP1, AP2 and SP1 consensus sites. Further downstream the trace shows no footprinted regions. This area of sequence is known to contain no protein binding sites. Therefore the results of the high throughput method confirm the DNA-protein binding sites detected within the SV40 promoter by the traditional DNase I footprinting method.

**A**  
**SV40**  
**FOOTPRINTED**  
**REGION**



**B**  
**ALIGNED**  
**SEQUENCE**  
**REACTIONS**

**Figure 6.7** Illustration of a section of the SV40 footprinted promoter aligned with dye-terminated sequencing reactions

**(A)** A section of the footprinted SV40 promoter. **(B)** Dye-terminator sequencing reactions. The two chromatic traces were aligned using Genemapper software.

## **6.5 Normalisation of signal intensity to the LIZ marker**

Due to the differences in the signal intensity between samples when analyzed in the genetic analyzer 3730, the samples were normalised to the LIZ standard intensity. In a traditional footprint experiment using radioactivity and gel electrophoresis, the problem with different signal intensities between samples is solved by normalising to a region of the DNA which is predicted not to be footprinted. Using the capillary method allows us to improve the normalisation method. This is because markers which are independent of the FAM labelled DNA fragments are run within the same sample.

To normalise the FAM signal between samples 5 LIZ marker signal values are taken for all traces. For each trace an average is calculated of the 5 LIZ marker values. The trace with the smallest LIZ marker average value is divided into each trace. The value obtained is used to alter the intensity of each trace (FAM signal). The traces improved greatly in their comparable intensities between different protein concentrations.

## 6.6 Footprinting analysis of the novel *FMO1* P1 and P2 promoters

The DNase I footprinting technique optimised using the SV40 promoter was next transferred to analyse the *FMO1* P1 and P2 promoters. The areas footprinted are the P1 positive promoter region, and the P2 positive promoter region (see chapter 4 for details). Both strands of the DNA were footprinted. One strand was labelled using the 5' FAM labelled primer as the forward primer in the PCR reaction. To footprint the other strand a 3' HEX labelled reverse primer was used with an unlabelled 5' primer to amplify the DNA. The use of this primer pair allows us to visualise footprints on both DNA strands. The HEX and FAM dyes can each be read using the G5 dye set reading on the Applied Biosystems genetic analyzer 3730.

### 6.6.1 P1 Promoter (Figure 6.8)

A large footprinted area between -858 and -758 was detected in the P1 promoter. After alignment of the footprinting and sequencing termination reaction traces the footprinted areas were examined. The footprinted sequence motifs were compared to previous bioinformatic analysis used to predict the identity of transcription factors (see chapter 4). The P1 footprinted region is within sequence that is predicted to bind the CCAAT binding proteins. Having identified a footprinted region it is possible then to analyse SNPs that might change DNA-protein binding.

In addition to analysing the regions to which proteins bind that might regulate *FMO1*; the capillary footprinting method allows a high-throughput method for analysing the consequences of a genetic polymorphism.



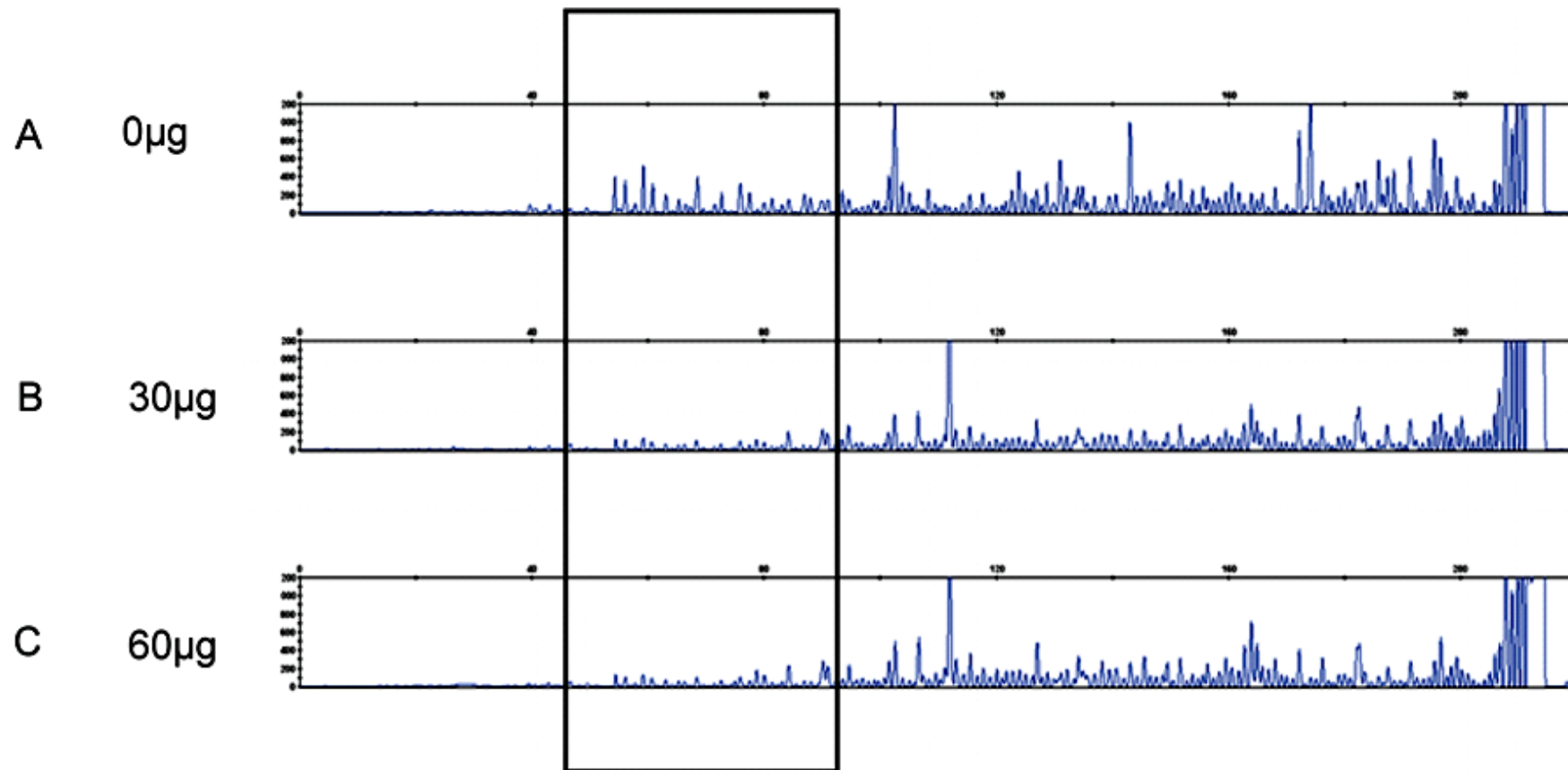


**Figure 6.8 DNase I footprinting of the human *FMO1* P1 promoter using COS-7 nuclear extract**

The chromatograms above show the DNase I digested fragments from the 5' FAM labelled *FMO1* P1 promoter. The fragments have been separated through capillaries and each peak represents a phosphodiester bond cleavage. The x-axis shows the number of base pairs from the 5' label and the y-axis is the intensity of the peak. From A to D the total COS-7 nuclear protein is increased as shown. The chromatogram shows the 5' region of the promoter contains 'footprints' as shown in the boxed region of the figure. There are also a number of smaller footprints further downstream.

### **6.6.2 The *FMO1* P2 promoter footprint analysis (Figure 6.9)**

The P2 promoter shows two predominant foot-printed regions (Figure 6.9). One footprint is within a GC box where the transcription factor SP1 is predicted to bind. The first region of DNA-protein binding overlaps with the region predicted to bind a hormone receptor between 65-100bp (see chapter 4). The second footprint is within the GC box binding site between 45-65bp.

The GC box motif was subsequently mutated to disrupt the binding of a transcription factor. This mutation was designed based on the consensus sequence for SP1 binding give sequence (Santa Cruz biotechnology manual). This mutation was analysed for its effect on function in chapter 4.

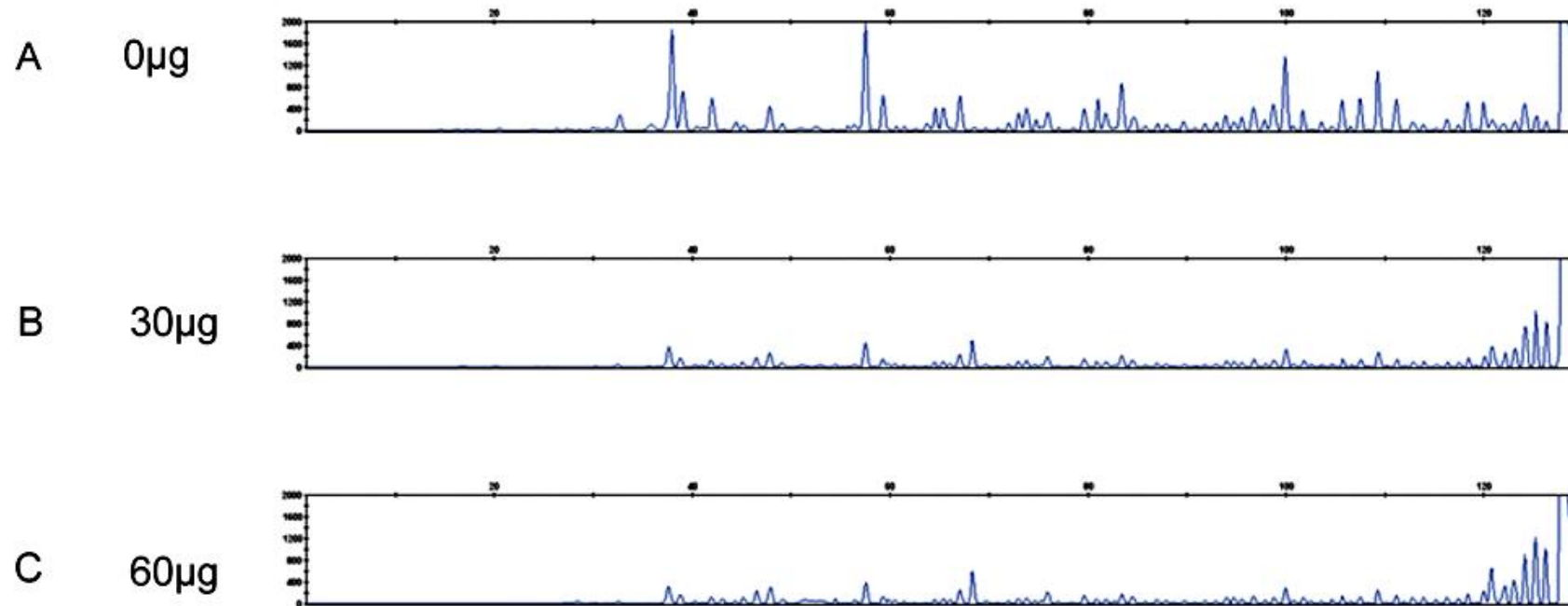


**Figure 6.9 DNase I footprinting of the human *FMO1* P2 promoter using COS-7 nuclear extract**

The chromatograms above show the DNase I digested fragments from the 5' FAM labelled *FMO1* P1 promoter. The fragments have been separated through capillaries and each peak represents a phosphodiester bond cleavage. The x-axis shows the number of base pairs from the 5' label and the y-axis is the intensity of the peak. From A to D the total COS-7 nuclear protein is increased as shown. The chromatogram shows the 5' region of the promoter contains footprints.

## **6.7 Loss of protein binding at the P2 promoter was visualised by DNase I capillary footprinting and therefore validates this technique for screening regulatory polymorphism *via* this method**

The wild type (-255\_-128) and mutant (-255\_-128)\*sequences of the *FMO1* P2 promoter were FAM labelled by PCR. These probes were then used in the DNase I capillary footprinting method using the conditions optimised previously. Protein concentrations used were 0 µg, 30 µg, and 60 µg. The chromatogram traces were aligned using Genemapper software. The termination sequencing reactions for the P2 promoter were carried out for each of the four DNA nucleotides. Each termination reaction sequencing trace was aligned and the base pair co-ordinates were noted. The co-ordinates for the *FMO1* sequences were then located within the footprinted regions of the wild-type and mutant P2 promoter sequences.

A footprint is present in the wild-type promoter and becomes more prominent as increasing amounts of COS-7 nuclear protein are added to the binding reaction. In contrast, the mutated form of the promoter shows no footprint and no loss of signal when increasing amounts of COS-7 nuclear extract is added (figure 6.7). Therefore the technique is able to identify polymorphism/ mutation that inhibit protein binding to DNA.

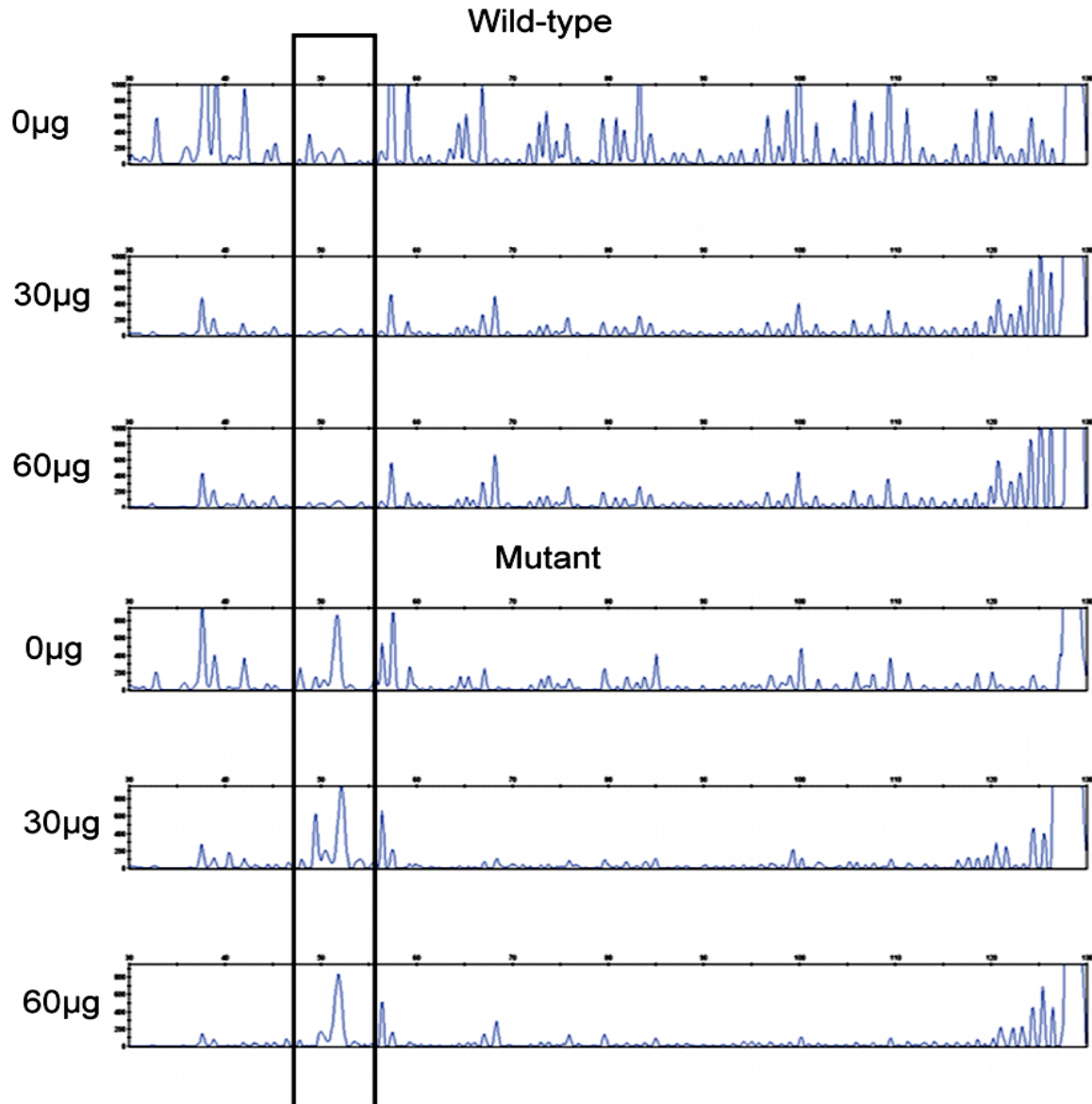


**Figure 6.10 Detection of the loss of DNA-protein binding within the *FMO1* P2 promoter**

The chromatograms above show the DNase I digested fragments of the wild type (-255\_-128) and mutant (-255\_-128)\* 5' FAM labelled *FMO1* P2 promoter. The fragments have been separated through capillaries and each peak represents a single base pair. The x-axis shows the number of base pairs from the 5' label and the y-axis is the intensity of the peak. The amount of protein added to each reaction is given adjacent to the trace. The black box highlights the region that shows loss of protein binding in the mutant sequence.

## **Discussion**

Identifying DNA regulatory regions and analysing the effects of genetic variation within these regions is currently limited. Current molecular techniques only allow us to 'easily' identify DNA regulatory regions that are proximal to the start of transcription. It is much harder to locate upstream and downstream regulatory regions that act further away from the promoter. Some DNA sequences have been shown to act tens of thousands of base pairs upstream and downstream of the promoter.

The techniques currently applied to identify regulatory regions include reporter gene assays to measure the DNA's ability to drive expression, as used throughout my project. Other techniques such as the electrophoretic mobility shift assay examine the binding of proteins to DNA and DNase I footprinting assays localise the region of DNA-protein binding and, if used in conjunction with DNA sequencing, identify the base sequence with which the protein interacts. Genetic variations can then be introduced into DNA sequences and the variants tested for their effect on gene expression or protein binding. The main caveat of these techniques is that they cannot easily be used to screen large regions of DNA.

The modification of the DNase I footprint method from polyacrylamide gels to capillary footprinting, I believe, allows the production of a technique which can be used to screen large regions of DNA. The novel application of this technique that I have shown is to screen for variations which influence DNA-protein binding. I now envisage the potential of this method to footprint tens

of thousands of base pairs upstream and downstream of a gene. Genetic variation within the regions that influence protein binding could then be analysed for their effects. Genetic variations which show a change in DNA-protein binding could then be validated by use of a reporter assay. Therefore the advantage of this approach is that important regulatory regions of DNA will be much more easily discovered.

The technique has a few caveats. The technique is being carried out *in vitro* and therefore the DNA-protein interactions observed may not be observed those observed *in vivo*. In addition, protein binding might change in different tissues or under different physiological conditions. The capillary footprint can however be carried out in a high-throughput way making it possible to examine DNA binding with different tissue tissues extracts and extracts isolated under different physiological conditions. This would not be possible using the traditional footprinting technique because of the labour-intensive nature of this method and the limited sample numbers that can easily be analysed.

The second caveat is that when amplifying from genomic DNA an individual will need to be homozygote for a genetic variant. If the individual is heterozygote the footprint signal will not be as strong and may be undetectable. However as discussed later, with the increased number of individuals now having their DNA sequenced it is likely that homozygotes will be available for most SNPs. For drug prediction results (efficacy or adversity)

then common genetic variations within a population group have greater predictive value for a health service.

The high-throughput technique will have greater application as the number of genetic variations discovered within the human genome increases. The 1000 genome project, where 1000 individuals from around the globe will be sequenced, will undoubtedly produce many new novel genetic variants. As these individuals genotypes are identified individuals can be chosen which are homozygous for an allele that one wishes to test. This would then remove the need for the researcher to sequence the gene as I have done within this project. Regions of DNA where SNPs occur can be selected and a minimal number of individuals used to test these SNPs for DNA-protein binding.

The technique also has the potential to be further developed for an *in vivo* system. The Hapmap consortium has produced cell-lines from individuals of known genotype. This therefore allows for the possibility of *in vivo* DNase I footprinting. By using a chemical reagent to digest the DNA and isolating the DNA fragments, footprinting profiles could be determined for different genotypes within *in vivo* conditions. This approach however is limited to the cellular environment and expression profile of the cell lines.

Second-generation sequencing is currently a relatively new technology. I envisage the combination of this sequencing technology with a Protein-DNA binding assay in the same context as described here. This would then allow



whole genomes to be analysed for DNA-protein binding. Combining this with a genome wide chromatin analysis would allow regulatory SNPs to be identified which would be predicted to have a significant functional consequence on the transcription of DNA.

# **Chapter 7**

## **General discussion**

## **Chapter 7: General Discussion**

The aim of this thesis was to identify and give context to regulatory SNPs within the FMO1 gene. This work was considered important due to the large variation in expression seen between individuals in FMO1 expression.

Regulatory SNPs which account for the large inter-individual variation could then be used in improving drug dosage for those drugs known to be metabolized by FMO1.

Identification of regulatory SNPs, as described in chapter 1, requires a variety of methods. The context with which the SNP influences gene expression needs to be accounted for much more than for a coding polymorphism. This is due to the plasticity of gene regulation. Genes are regulated in a tissue-, cell-, and environmentally specific manner. Therefore in order to gauge the true influence of a regulatory polymorphism these different contexts need to be examined. To identify the nature and influence of regulatory polymorphism researchers use a wide variety of techniques to show the influence of regulatory polymorphism. The range of techniques used were discussed in chapter 1.

Identification of regulatory polymorphism and its context is more difficult within genes that are regulated in a complex manner. FMO1 is an example of a gene regulated in a complex manner. It has multiple tissue-specific promoters for transcription of the gene. It is therefore crucial, it is understood which transcripts are produced in which tissues, in order to examine regulatory polymorphism in the correct context. We therefore decided that usage of the

three FMO1 promoters, P0, P1 and P2 should be examined within a number of different tissues (chapter 3). These tissues were liver, kidney, white and brown fat, brain, muscle and lung. This would allow us to study regulatory polymorphism within the correct context. It was decided a large number of extra-hepatic tissues should be included due to the identification of an endogenous role for FMO1 in energy homeostasis. The white and brown fat, muscle and brain had not previously been quantified for *FMO1* expression. The endogenous role for FMO1 also influenced us to examine the regulation of FMO1 during the differentiation of fat (chapter 3).

It was discovered in mice that *FMO1* was expressed highly in white and brown fat, comparable to levels in the kidney. The P1 transcript was much higher in most of the extra-hepatic tissues than the other two promoters outlining the importance of the P1 transcript. Examining the expression of the FMO1 transcripts during differentiation we observed the upregulation of the P1 and P2 transcripts during 3T3-L1 differentiation into adipocytes. This observation allows the 3T3-L1 adipocyte model to further understand the regulation of FMO1 within fat and further understand the endogenous role of the enzyme.

Prior to this study, promoter regions had not been defined for the P1 and P2 transcripts. Promoters were defined in the context of different cell types to account for the tissue-specificity of the promoters seen previously and during this study (chapter 4). These promoter regions in addition to the previously defined P0 promoter would therefore be candidate regions for regulatory

polymorphism. The chromatin state of the DNA was examined and the region defining the P1 and P2 promoter region were shown to be an open conformational state (chapter 4). Further upstream of the defined positive regions, a negative region was defined using reporter gene assays. This region was shown to be in a closed conformational state. It is therefore likely this region does not factor in the regulation of FMO1.

Once defined, sequences within these regions were examined for transcription factor binding. This was done by using a bioinformatics approach coupled with publicly available genome-wide gene regulation analysis data (chapter 4). This analysis showed that Chip-seq experiments undertaken within HepG2 cells showed the binding of C/EBP- $\beta$  and the insulating factor lin1. The binding is predicted to occur within the defined positive promoter region of P1. The transcription factor C/EBP- $\beta$  upregulates genes during 3T3-L1 differentiation. This factor could therefore be responsible for the upregulation of FMO1 during 3T3-L1 differentiation.

Following the defining of the P1 and P2 promoters the regions were sequenced within different populations (chapter 5). This revealed two novel SNPs. The first within the start of exon 1 which was a CT deletion, and the second downstream within the P1 promoter region. The frequency of the CT deletion was only present within the CEU (European) population. The allele frequency was 5%. This is frequent enough to be defined as a common polymorphism. Due to its location this SNP may influence the binding of RNA polymerase II. Further experiments using EMSA would confirm the changes in

DNA-protein binding within this region. Reporter gene assays would confirm its effect on transcription.

The CT deletion as well as the polymorphism further upstream of the P1 promoter were introduced and attempts were made to test their effect on reporter gene activity. The P1 promoter region reporter gene activity, when examined for comparison for mutants, showed a severely decreased activity. The reporter gene construct which contained the P1 and P2 promoter regions was also severely reduced. We deduced that as two constructs containing the same sequence had been severely down-regulated that something was now causing the repression of the reporter gene.

Bioinformatic analysis predicts the binding of heat shock factor within this region which may be affecting the reporter gene activity. The heat shock factor is also predicted to bind with the insulating factor Lin1 shown by Chip-seq to bind within the promoter region. Attempts were made to change the conditions of the cell culture to allow for the activity of the heat shock factor. Incubator and media conditions were varied and tested but the reporter gene activity did not increase. Therefore mutant activities could not be reliably examined due to the lack of a comparison.

During the defining of the FMO1 promoters, and subsequent sequencing of these regions, a method was developed to allow the testing of regulatory polymorphism on DNA-protein binding events within regulatory sequences. As discussed in chapter 1, genome-wide methods are now common in analysing

regulatory regions. DNase I-seq can be used to a resolution that allows the sequences of DNA-protein binding to be defined. These techniques allow examination of gene regulatory sequences but do not allow regulatory SNPs to be examined for their effect. This is due to the expense of examining a large number of individuals for genome wide DNA-protein binding profiles. Therefore the researcher relies on reporter gene assays and EMSAs to examine the effect of regulatory polymorphism. These techniques can be used in different contexts and are very useful at testing the effects of regulatory SNPs. However, if the researcher wishes to test a large number of regulatory polymorphism, for example, multiple SNPs within multiple promoters, or multiple genes, then these techniques can be laborious. Advances in EMSA technology, used within this thesis, allows Infra-red dyes to be used for labelling increase ease of analysis, however gel technology is still relied upon. It was therefore observed that a technique would be desirable that could deal with the ever-growing information on regulatory regions at a relatively lower cost. The technique proposed, and optimised within this thesis, was developed to address this problem.

DNase I capillary footprinting has been shown to detect the presence of DNA-protein-binding events when using purified protein and DNA labelled from a vector. This thesis describes the development of DNase I capillary footprinting with the use of whole nuclear protein extracts. This technique was further developed to show differences in DNA-protein binding could be detected using the method. A mutation created within the P2 promoter was shown within this thesis to reduce reporter gene activity and remove DNA-protein

complexes. This mutation was tested within the newly optimised technique and was able to detect the loss of protein binding within this region. The technique functions with the use of capillaries and therefore can be high-throughput. The technique is therefore validated and provides a technique for the researcher that can screen regulatory polymorphism for a large number of regulatory regions.

This technique was transferred to analyse two FMO1 P1 natural polymorphisms. These polymorphisms were shown not to influence DNA-protein binding. Further experiments would determine the influence of natural variation within the P0, P1 and P2 promoters. Ideally these SNPs can be verified within the reporter gene assay.

During the course of this thesis a SNP was observed, -11C>T that could create a second upstream ATG translation initiation codon for those individuals that have the T allele. SNPs have been shown for other genes to influence translational efficiency by the introduction of a second ATG. The translational efficiency of the two alleles were tested using reporter gene assays. The FMO1 P2 leader sequence, containing either the T or C allele was cloned upstream of the pSP-luc vector. Cloning was undertaken to replace the ATG of the luciferase reporter gene with the FMO1 downstream ATG. RNA was made from this vector in-vitro and transfected into COS-7 cells. The T allele was shown to produce more reporter gene protein than the C allele. This suggests that those individuals that have the T allele produce more FMO1 protein than individuals with the C allele. This SNP would be a



good candidate for association studies with patients with adverse drug reactions for drugs metabolized by FMO1. It could also be used in association studies with ALS patients or diseases resembling phenotypes observed within the FMO1 knock-out mice.

In summary, this thesis has further increased our understanding of how the FMO1 P0, P1 and P2 transcripts are used within mice and during 3T3-L1 differentiation. This has given context to polymorphisms found within regulatory sequences for the P1 and P2 promoter. Novel promoter sequences have been defined and characterised using different cell lines and regulatory data. These regions have been sequenced and novel SNPs identified. A novel approach and high-throughput method has been developed during this thesis and is able to screen for regulatory polymorphism in regulatory regions by detecting differences in DNA-protein binding. This approach was used to examine two FMO1 promoter polymorphisms but no differences were visualised. A regulatory SNP found -11C>T upstream of the known ATG translation initiation codon has been shown to effect translation efficiency and is a good candidate for future association studies.

# References

- (2003). The International HapMap Project. *Nature* 426, 789-796.
- Ae, K., Kobayashi, N., Sakuma, R., Ogata, T., Kuroda, H., Kawaguchi, N., Shinomiya, K., and Kitamura, Y. (2002). Chromatin remodeling factor encoded by *ini1* induces G1 arrest and apoptosis in *ini1*-deficient cells. *Oncogene* 21, 3112-3120.
- Afshar-Kharghan, V., Li, C.Q., Khoshnevis-Asl, M., and Lopez, J.A. (1999). Kozak sequence polymorphism of the glycoprotein (GP) Iba $\alpha$  gene is a major determinant of the plasma membrane levels of the platelet GP Ib-IX-V complex. *Blood* 94, 186-191.
- Aklillu, E., Carrillo, J.A., Makonnen, E., Hellman, K., Pitarque, M., Bertilsson, L., and Ingelman-Sundberg, M. (2003). Genetic polymorphism of CYP1A2 in Ethiopians affecting induction and expression: characterization of novel haplotypes with single-nucleotide polymorphisms in intron 1. *Mol Pharmacol* 64, 659-669.
- Akpinar, P., Kuwajima, S., Krutzfeldt, J., and Stoffel, M. (2005). Tmem27: a cleaved and shed plasma membrane protein that stimulates pancreatic beta cell proliferation. *Cell Metab* 2, 385-397.
- Allorge, D., Chevalier, D., Lo-Guidice, J.M., Cauffiez, C., Suard, F., Baumann, P., Eap, C.B., and Broly, F. (2003). Identification of a novel splice-site mutation in the CYP1A2 gene. *Br J Clin Pharmacol* 56, 341-344.
- Arai, H., Miyamoto, K., Taketani, Y., Yamamoto, H., Iemori, Y., Morita, K., Tonai, T., Nishisho, T., Mori, S., and Takeda, E. (1997). A vitamin D receptor gene polymorphism in the translation initiation codon: effect on protein activity and relation to bone mineral density in Japanese women. *J Bone Miner Res* 12, 915-921.
- Attar, M., Dong, D., Ling, K.H., and Tang-Liu, D.D. (2003). Cytochrome P450 2C8 and flavin-containing monooxygenases are involved in the metabolism of tazarotenic acid in humans. *Drug Metab Dispos* 31, 476-481.
- Baek, D., Davis, C., Ewing, B., Gordon, D., and Green, P. (2007). Characterization and predictive discovery of evolutionarily conserved mammalian alternative promoters. *Genome Res* 17, 145-155.
- Battle, M.A., Konopka, G., Parviz, F., Gaggl, A.L., Yang, C., Sladek, F.M., and Duncan, S.A. (2006). Hepatocyte nuclear factor 4 $\alpha$  orchestrates expression of cell adhesion proteins during the epithelial transformation of the developing liver. *Proc Natl Acad Sci U S A* 103, 8419-8424.
- Beaty, N.B., and Ballou, D.P. (1980). Transient kinetic study of liver microsomal FAD-containing monooxygenase. *J Biol Chem* 255, 3817-3819.
- Beaty, N.B., and Ballou, D.P. (1981). The oxidative half-reaction of liver microsomal FAD-containing monooxygenase. *J Biol Chem* 256, 4619-4625.
- Bernlohr, D.A., Bolanowski, M.A., Kelly, T.J., Jr., and Lane, M.D. (1985). Evidence for an increase in transcription of specific mRNAs during differentiation of 3T3-L1 preadipocytes. *J Biol Chem* 260, 5563-5567.
- Birney, E., Stamatoyannopoulos, J.A., Dutta, A., Guigo, R., Gingeras, T.R., Margulies, E.H., Weng, Z., Snyder, M., Dermitzakis, E.T., Thurman, R.E., et al. (2007). Identification and analysis of functional elements in 1% of the human genome by the ENCODE pilot project. *Nature* 447, 799-816.
- Blake, B.L., Rose, R.L., Mailman, R.B., Levi, P.E., and Hodgson, E. (1995). Metabolism of thioridazine by microsomal monooxygenases: relative roles of P450 and flavin-containing monooxygenase. *Xenobiotica* 25, 377-393.

- Cam, H., Griesmann, H., Beitzinger, M., Hofmann, L., Beinoraviciute-Kellner, R., Sauer, M., Huttinger-Kirchhof, N., Oswald, C., Friedl, P., Gattenlohner, S., et al. (2006). p53 family members in myogenic differentiation and rhabdomyosarcoma development. *Cancer Cell* 10, 281-293.
- Cao, Y., Kumar, R.M., Penn, B.H., Berkes, C.A., Kooperberg, C., Boyer, L.A., Young, R.A., and Tapscott, S.J. (2006). Global and gene-specific analyses show distinct roles for Myod and Myog at a common set of promoters. *EMBO J* 25, 502-511.
- Caramel, J., Medjkane, S., Quignon, F., and Delattre, O. (2008). The requirement for SNF5/INI1 in adipocyte differentiation highlights new features of malignant rhabdoid tumors. *Oncogene* 27, 2035-2044.
- Carter, A.M., Sachchithanathan, M., Stasinopoulos, S., Maurer, F., and Medcalf, R.L. (2002). Prothrombin G20210A is a bifunctional gene polymorphism. *Thromb Haemost* 87, 846-853.
- Cartharius, K., Frech, K., Grote, K., Klocke, B., Haltmeier, M., Klingenhoff, A., Frisch, M., Bayerlein, M., and Werner, T. (2005). MatInspector and beyond: promoter analysis based on transcription factor binding sites. *Bioinformatics* 21, 2933-2942.
- Cashman, J.R. (2008). Role of flavin-containing monooxygenase in drug development. *Expert Opin Drug Metab Toxicol* 4, 1507-1521.
- Cashman, J.R., Celestial, J.R., Leach, A., Newdoll, J., and Park, S.B. (1993). Tertiary amines related to brompheniramine: preferred conformations for N-oxygenation by the hog liver flavin-containing monooxygenase. *Pharm Res* 10, 1097-1105.
- Cashman, J.R., Park, S.B., Berkman, C.E., and Cashman, L.E. (1995). Role of hepatic flavin-containing monooxygenase 3 in drug and chemical metabolism in adult humans. *Chem Biol Interact* 96, 33-46.
- Cashman, J.R., Xiong, Y.N., Xu, L., and Janowsky, A. (1999). N-oxygenation of amphetamine and methamphetamine by the human flavin-containing monooxygenase (form 3): role in bioactivation and detoxication. *J Pharmacol Exp Ther* 288, 1251-1260.
- Cashman, J.R., and Zhang, J. (2006). Human flavin-containing monooxygenases. *Annu Rev Pharmacol Toxicol* 46, 65-100.
- Cashman, J.R., and Ziegler, D.M. (1986). Contribution of N-oxygenation to the metabolism of MPTP (1-methyl-4-phenyl-1,2,3,6-tetrahydropyridine) by various liver preparations. *Mol Pharmacol* 29, 163-167.
- Cereda, C., Gabanti, E., Corato, M., de Silvestri, A., Alimonti, D., Cova, E., Malaspina, A., and Ceroni, M. (2006). Increased incidence of FMO1 gene single nucleotide polymorphisms in sporadic amyotrophic lateral sclerosis. *Amyotroph Lateral Scler* 7, 227-234.
- Chen, I.H., Huber, M., Guan, T., Bubeck, A., and Gerace, L. (2006). Nuclear envelope transmembrane proteins (NETs) that are up-regulated during myogenesis. *BMC Cell Biol* 7, 38.
- Cherrington, N.J., Cao, Y., Cherrington, J.W., Rose, R.L., and Hodgson, E. (1998a). Physiological factors affecting protein expression of flavin-containing monooxygenases 1, 3 and 5. *Xenobiotica* 28, 673-682.
- Cherrington, N.J., Falls, J.G., Rose, R.L., Clements, K.M., Philpot, R.M., Levi, P.E., and Hodgson, E. (1998b). Molecular cloning, sequence, and expression of mouse flavin-containing monooxygenases 1 and 5 (FMO1 and FMO5). *J Biochem Mol Toxicol* 12, 205-212.

- Cheung, K.J., Tzamelis, I., Pissios, P., Rovira, I., Gavrilova, O., Ohtsubo, T., Chen, Z., Finkel, T., Flier, J.S., and Friedman, J.M. (2007). Xanthine oxidoreductase is a regulator of adipogenesis and PPAR $\gamma$  activity. *Cell Metab* 5, 115-128.
- Chiba, K., Horii, H., Kubota, E., Ishizaki, T., and Kato, Y. (1990). Effects of N-methylmercaptoimidazole on the disposition of MPTP and its metabolites in mice. *Eur J Pharmacol* 180, 59-67.
- Chiba, K., Kubota, E., Miyakawa, T., Kato, Y., and Ishizaki, T. (1988). Characterization of hepatic microsomal metabolism as an in vivo detoxication pathway of 1-methyl-4-phenyl-1,2,3,6-tetrahydropyridine in mice. *J Pharmacol Exp Ther* 246, 1108-1115.
- Chiu, K.C., Chuang, L.M., and Yoon, C. (2001). The vitamin D receptor polymorphism in the translation initiation codon is a risk factor for insulin resistance in glucose tolerant Caucasians. *BMC Med Genet* 2, 2.
- Chung, W.G., Park, C.S., Roh, H.K., and Cha, Y.N. (1997). Induction of flavin-containing monooxygenase (FMO1) by a polycyclic aromatic hydrocarbon, 3-methylcholanthrene, in rat liver. *Mol Cells* 7, 738-741.
- Chung, W.G., Park, C.S., Roh, H.K., Lee, W.K., and Cha, Y.N. (2000). Oxidation of ranitidine by isozymes of flavin-containing monooxygenase and cytochrome P450. *Jpn J Pharmacol* 84, 213-220.
- Conne, B., Stutz, A., and Vassalli, J.D. (2000). The 3' untranslated region of messenger RNA: A molecular 'hotspot' for pathology? *Nat Med* 6, 637-641.
- Cooper, S.J., Trinklein, N.D., Anton, E.D., Nguyen, L., and Myers, R.M. (2006). Comprehensive analysis of transcriptional promoter structure and function in 1% of the human genome. *Genome Res* 16, 1-10.
- Cornelius, P., MacDougald, O.A., and Lane, M.D. (1994). Regulation of adipocyte development. *Annu Rev Nutr* 14, 99-129.
- Courtois, V., Chatelain, G., Han, Z.Y., Le Novere, N., Brun, G., and Lamonerie, T. (2003). New Otx2 mRNA isoforms expressed in the mouse brain. *J Neurochem* 84, 840-853.
- Crunkhorn, S., Dearie, F., Mantzoros, C., Gami, H., da Silva, W.S., Espinoza, D., Faucette, R., Barry, K., Bianco, A.C., and Patti, M.E. (2007). Peroxisome proliferator activator receptor gamma coactivator-1 expression is reduced in obesity: potential pathogenic role of saturated fatty acids and p38 mitogen-activated protein kinase activation. *J Biol Chem* 282, 15439-15450.
- Danielson, P.B. (2002). The cytochrome P450 superfamily: biochemistry, evolution and drug metabolism in humans. *Curr Drug Metab* 3, 561-597.
- Davis, W., Jr., and Schultz, R.M. (2000). Developmental change in TATA-box utilization during preimplantation mouse development. *Dev Biol* 218, 275-283.
- Devereux, T.R., Philpot, R.M., and Fouts, J.R. (1977). The effect of Hg<sup>2+</sup> on rabbit hepatic and pulmonary solubilized, partially purified N,N-dimethylaniline N-oxidases. *Chem Biol Interact* 18, 277-287.
- Di Padova, M., Caretti, G., Zhao, P., Hoffman, E.P., and Sartorelli, V. (2007). MyoD acetylation influences temporal patterns of skeletal muscle gene expression. *J Biol Chem* 282, 37650-37659.
- Di Paola, R., Frittitta, L., Miscio, G., Bozzali, M., Baratta, R., Centra, M., Spampinato, D., Santagati, M.G., Ercolino, T., Cisternino, C., et al. (2002). A variation in 3' UTR of hPTP1B increases specific gene expression and associates with insulin resistance. *Am J Hum Genet* 70, 806-812.
- Dolphin, C., Shephard, E.A., Povey, S., Palmer, C.N., Ziegler, D.M., Ayes, R., Smith, R.L., and Phillips, I.R. (1991). Cloning, primary sequence, and

- chromosomal mapping of a human flavin-containing monooxygenase (FMO1). *J Biol Chem* 266, 12379-12385.
- Dolphin, C.T., Beckett, D.J., Janmohamed, A., Cullingford, T.E., Smith, R.L., Shephard, E.A., and Phillips, I.R. (1998). The flavin-containing monooxygenase 2 gene (FMO2) of humans, but not of other primates, encodes a truncated, nonfunctional protein. *J Biol Chem* 273, 30599-30607.
- Dolphin, C.T., Cullingford, T.E., Shephard, E.A., Smith, R.L., and Phillips, I.R. (1996). Differential developmental and tissue-specific regulation of expression of the genes encoding three members of the flavin-containing monooxygenase family of man, FMO1, FMO3 and FMO4. *Eur J Biochem* 235, 683-689.
- Dolphin, C.T., Shephard, E.A., Povey, S., Smith, R.L., and Phillips, I.R. (1992). Cloning, primary sequence and chromosomal localization of human FMO2, a new member of the flavin-containing mono-oxygenase family. *Biochem J* 287 ( Pt 1), 261-267.
- Donoghue, N.A., Norris, D.B., and Trudgill, P.W. (1976). The purification and properties of cyclohexanone oxygenase from *Nocardia globerula* CL1 and *Acinetobacter* NCIB 9871. *Eur J Biochem* 63, 175-192.
- Duan, Z.J., Fang, X., Rohde, A., Han, H., Stamatoyannopoulos, G., and Li, Q. (2002). Developmental specificity of recruitment of TBP to the TATA box of the human gamma-globin gene. *Proc Natl Acad Sci U S A* 99, 5509-5514.
- Duescher, R.J., Lawton, M.P., Philpot, R.M., and Elfarra, A.A. (1994). Flavin-containing monooxygenase (FMO)-dependent metabolism of methionine and evidence for FMO3 being the major FMO involved in methionine sulfoxidation in rabbit liver and kidney microsomes. *J Biol Chem* 269, 17525-17530.
- Duffel, M.W., Logan, D.J., and Ziegler, D.M. (1987). Cysteamine and cystamine. *Methods Enzymol* 143, 149-154.
- Dynan, W.S., and Tjian, R. (1983). The promoter-specific transcription factor Sp1 binds to upstream sequences in the SV40 early promoter. *Cell* 35, 79-87.
- Elfarra, A.A. (1995). Potential role of the flavin-containing monooxygenases in the metabolism of endogenous compounds. *Chem Biol Interact* 96, 47-55.
- Ellard, S. (2000). Hepatocyte nuclear factor 1 alpha (HNF-1 alpha) mutations in maturity-onset diabetes of the young. *Hum Mutat* 16, 377-385.
- Enattah, N.S., Sahi, T., Savilahti, E., Terwilliger, J.D., Peltonen, L., and Jarvela, I. (2002). Identification of a variant associated with adult-type hypolactasia. *Nat Genet* 30, 233-237.
- Eswaramoorthy, S., Bonanno, J.B., Burley, S.K., and Swaminathan, S. (2006). Mechanism of action of a flavin-containing monooxygenase. *Proc Natl Acad Sci U S A* 103, 9832-9837.
- Falls, J.G., Cherrington, N.J., Clements, K.M., Philpot, R.M., Levi, P.E., Rose, R.L., and Hodgson, E. (1997). Molecular cloning, sequencing, and expression in *Escherichia coli* of mouse flavin-containing monooxygenase 3 (FMO3): comparison with the human isoform. *Arch Biochem Biophys* 347, 9-18.
- Fargetton, X., Galtier, P., and Delatour, P. (1986). Sulfoxidation of albendazole by a cytochrome P450-independent monooxygenase from rat liver microsomes. *Vet Res Commun* 10, 317-324.
- Felgner, P.L., and Ringold, G.M. (1989). Cationic liposome-mediated transfection. *Nature* 337, 387-388.

- Furnes, B., Feng, J., Sommer, S.S., and Schlenk, D. (2003). Identification of novel variants of the flavin-containing monooxygenase gene family in African Americans. *Drug Metab Dispos* 31, 187-193.
- Furnes, B., and Schlenk, D. (2004). Evaluation of xenobiotic N- and S-oxidation by variant flavin-containing monooxygenase 1 (FMO1) enzymes. *Toxicol Sci* 78, 196-203.
- Gaedigk, A., Ryder, D.L., Bradford, L.D., and Leeder, J.S. (2003). CYP2D6 poor metabolizer status can be ruled out by a single genotyping assay for the -1584G promoter polymorphism. *Clin Chem* 49, 1008-1011.
- Gargiulo, G., Levy, S., Bucci, G., Romanenghi, M., Fornasari, L., Beeson, K.Y., Goldberg, S.M., Cesaroni, M., Ballarini, M., Santoro, F., et al. (2009). NA-Seq: a discovery tool for the analysis of chromatin structure and dynamics during differentiation. *Dev Cell* 16, 466-481.
- Garrison, W.D., Battle, M.A., Yang, C., Kaestner, K.H., Sladek, F.M., and Duncan, S.A. (2006). Hepatocyte nuclear factor 4alpha is essential for embryonic development of the mouse colon. *Gastroenterology* 130, 1207-1220.
- Gasser, R., Tynes, R.E., Lawton, M.P., Korsmeyer, K.K., Ziegler, D.M., and Philpot, R.M. (1990). The flavin-containing monooxygenase expressed in pig liver: primary sequence, distribution, and evidence for a single gene. *Biochemistry* 29, 119-124.
- Gaulton, K.J., Nammo, T., Pasquali, L., Simon, J.M., Giresi, P.G., Fogarty, M.P., Panhuis, T.M., Mieczkowski, P., Secchi, A., Bosco, D., et al. (2010). A map of open chromatin in human pancreatic islets. *Nat Genet* 42, 255-259.
- Gennari, L., Becherini, L., Mansani, R., Masi, L., Falchetti, A., Morelli, A., Colli, E., Gonnelli, S., Cepollaro, C., and Brandi, M.L. (1999). FokI polymorphism at translation initiation site of the vitamin D receptor gene predicts bone mineral density and vertebral fractures in postmenopausal Italian women. *J Bone Miner Res* 14, 1379-1386.
- Giannoukakis, N., Deal, C., Paquette, J., Goodyer, C.G., and Polychronakos, C. (1993). Parental genomic imprinting of the human IGF2 gene. *Nat Genet* 4, 98-101.
- Giresi, P.G., Kim, J., McDaniel, R.M., Iyer, V.R., and Lieb, J.D. (2007). FAIRE (Formaldehyde-Assisted Isolation of Regulatory Elements) isolates active regulatory elements from human chromatin. *Genome Res* 17, 877-885.
- Gonzalez-Conejero, R., Corral, J., Roldan, V., Martinez, C., Marin, F., Rivera, J., Iniesta, J.A., Lozano, M.L., Marco, P., and Vicente, V. (2002). A common polymorphism in the annexin V Kozak sequence (-1C>T) increases translation efficiency and plasma levels of annexin V, and decreases the risk of myocardial infarction in young patients. *Blood* 100, 2081-2086.
- Green, H., and Kehinde, O. (1979). Formation of normally differentiated subcutaneous fat pads by an established preadipose cell line. *J Cell Physiol* 101, 169-171.
- Green, H., and Meuth, M. (1974). An established pre-adipose cell line and its differentiation in culture. *Cell* 3, 127-133.
- Gregory, S.G., Schmidt, S., Seth, P., Oksenberg, J.R., Hart, J., Prokop, A., Caillier, S.J., Ban, M., Goris, A., Barcellos, L.F., et al. (2007). Interleukin 7 receptor alpha chain (IL7R) shows allelic and functional association with multiple sclerosis. *Nat Genet* 39, 1083-1091.
- Hamman, M.A., Haehner-Daniels, B.D., Wrighton, S.A., Rettie, A.E., and Hall, S.D. (2000). Stereoselective sulfoxidation of sulindac sulfide by flavin-containing

- monooxygenases. Comparison of human liver and kidney microsomes and mammalian enzymes. *Biochem Pharmacol* 60, 7-17.
- Hecht, J., Seitz, V., Urban, M., Wagner, F., Robinson, P.N., Stiege, A., Dieterich, C., Kornak, U., Wilkening, U., Brieske, N., et al. (2007). Detection of novel skeletogenesis target genes by comprehensive analysis of a Runx2(-/-) mouse model. *Gene Expr Patterns* 7, 102-112.
- Hernandez, D., Janmohamed, A., Chandan, P., Omar, B.A., Phillips, I.R., and Shephard, E.A. (2009). Deletion of the mouse Fmo1 gene results in enhanced pharmacological behavioural responses to imipramine. *Pharmacogenet Genomics* 19, 289-299.
- Hernandez, D., Janmohamed, A., Chandan, P., Phillips, I.R., and Shephard, E.A. (2004). Organization and evolution of the flavin-containing monooxygenase genes of human and mouse: identification of novel gene and pseudogene clusters. *Pharmacogenetics* 14, 117-130.
- Hesselberth, J.R., Chen, X., Zhang, Z., Sabo, P.J., Sandstrom, R., Reynolds, A.P., Thurman, R.E., Neph, S., Kuehn, M.S., Noble, W.S., et al. (2009). Global mapping of protein-DNA interactions in vivo by digital genomic footprinting. *Nat Methods* 6, 283-289.
- Hines, R.N., Cashman, J.R., Philpot, R.M., Williams, D.E., and Ziegler, D.M. (1994). The mammalian flavin-containing monooxygenases: molecular characterization and regulation of expression. *Toxicol Appl Pharmacol* 125, 1-6.
- Hines, R.N., Hopp, K.A., Franco, J., Saeian, K., and Begun, F.P. (2002). Alternative processing of the human FMO6 gene renders transcripts incapable of encoding a functional flavin-containing monooxygenase. *Mol Pharmacol* 62, 320-325.
- Hines, R.N., Luo, Z., Hopp, K.A., Cabacungan, E.T., Koukouritaki, S.B., and McCarver, D.G. (2003). Genetic variability at the human FMO1 locus: significance of a basal promoter yin yang 1 element polymorphism (FMO1\*6). *J Pharmacol Exp Ther* 306, 1210-1218.
- Hodgson, E. (1999a). Induction and inhibition of pesticide-metabolizing enzymes: roles in synergism of pesticides and pesticide action. *Toxicol Ind Health* 15, 6-11.
- Hodgson, E., N. J. Cherrington, R. M. Philpot and R. L. Rose (1999b). "Biochemical Aspects of Flavin-containing Monooxygenases (FMOs)". *Molecular and applied aspects of oxidative drug metabolising enzymes*, pp55-70 Ed., E. Arinc, J. B. Schenkman and E. Hodgson. Plenum publishers, New York.
- Hodgson, E., Rose, R.L., Cao, Y., Dehal, S.S., and Kupfer, D. (2000). Flavin-containing monooxygenase isoform specificity for the N-oxidation of tamoxifen determined by product measurement and NADPH oxidation. *J Biochem Mol Toxicol* 14, 118-120.
- Hoskins, J., Shenfield, G., Murray, M., and Gross, A. (2001). Characterization of moclobemide N-oxidation in human liver microsomes. *Xenobiotica* 31, 387-397.
- Humbert, J.A., Hammond, K.B., and Hathaway, W.E. (1970). Trimethylaminuria: the fish-odour syndrome. *Lancet* 2, 770-771.
- Inoue, E., Yamashita, A., Inoue, H., Sekiguchi, M., Shiratori, A., Yamamoto, Y., Tadokoro, T., Ishimi, Y., and Yamauchi, J. (2010). Identification of glucose transporter 4 knockdown-dependent transcriptional activation element on the retinol binding protein 4 gene promoter and requirement of the 20 S



- proteasome subunit for transcriptional activity. *J Biol Chem* 285, 25545-25553.
- IR Phillips, E.S. (1998). Cytochrome P450 protocols. *Methods in molecular biology*.
- Itagaki, K., Carver, G.T., and Philpot, R.M. (1996). Expression and characterization of a modified flavin-containing monooxygenase 4 from humans. *J Biol Chem* 271, 20102-20107.
- Itoh, K., Nakamura, K., Kimura, T., Itoh, S., and Kamataki, T. (1997). Molecular cloning of mouse liver flavin containing monooxygenase (FMO1) cDNA and characterization of the expression product: metabolism of the neurotoxin, 1,2,3,4-tetrahydroisoquinoline (TIQ). *J Toxicol Sci* 22, 45-56.
- Jakobsson, S.V., and Cintig, D.L. (1973). Studies on the cytochrome P-450-containing mono-oxygenase system in human kidney cortex microsomes. *J Pharmacol Exp Ther* 185, 226-234.
- Janmohamed, A., Hernandez, D., Phillips, I.R., and Shephard, E.A. (2004). Cell-, tissue-, sex- and developmental stage-specific expression of mouse flavin-containing monooxygenases (Fmos). *Biochem Pharmacol* 68, 73-83.
- Johnson, A.D., Wang, D., and Sadee, W. (2005). Polymorphisms affecting gene regulation and mRNA processing: broad implications for pharmacogenetics. *Pharmacol Ther* 106, 19-38.
- Jones, K.C., and Ballou, D.P. (1986). Reactions of the 4a-hydroperoxide of liver microsomal flavin-containing monooxygenase with nucleophilic and electrophilic substrates. *J Biol Chem* 261, 2553-2559.
- Kagimoto, M., Heim, M., Kagimoto, K., Zeugin, T., and Meyer, U.A. (1990). Multiple mutations of the human cytochrome P450IID6 gene (CYP2D6) in poor metabolizers of debrisoquine. Study of the functional significance of individual mutations by expression of chimeric genes. *J Biol Chem* 265, 17209-17214.
- Kajita, J., Inano, K., Fuse, E., Kuwabara, T., and Kobayashi, H. (2002). Effects of olopatadine, a new antiallergic agent, on human liver microsomal cytochrome P450 activities. *Drug Metab Dispos* 30, 1504-1511.
- Karoly, E.D., and Rose, R.L. (2001). Sequencing, expression, and characterization of cDNA expressed flavin-containing monooxygenase 2 from mouse. *J Biochem Mol Toxicol* 15, 300-308.
- Katchamart, S., Stresser, D.M., Dehal, S.S., Kupfer, D., and Williams, D.E. (2000). Concurrent flavin-containing monooxygenase down-regulation and cytochrome P-450 induction by dietary indoles in rat: implications for drug-drug interaction. *Drug Metab Dispos* 28, 930-936.
- Katchamart, S., and Williams, D.E. (2001). Indole-3-carbinol modulation of hepatic monooxygenases CYP1A1, CYP1A2 and FMO1 in guinea pig, mouse and rabbit. *Comp Biochem Physiol C Toxicol Pharmacol* 129, 377-384.
- Kedderis, G.L., and Rickert, D.E. (1985). Loss of rat liver microsomal cytochrome P-450 during methimazole metabolism. Role of flavin-containing monooxygenase. *Drug Metab Dispos* 13, 58-61.
- Kent, W.J., Sugnet, C.W., Furey, T.S., Roskin, K.M., Pringle, T.H., Zahler, A.M., and Haussler, D. (2002). The human genome browser at UCSC. *Genome Res* 12, 996-1006.
- Kim, S.J., Lee, K.H., Lee, Y.S., Mun, E.G., Kwon, D.Y., and Cha, Y.S. (2007). Transcriptome analysis and promoter sequence studies on early adipogenesis in 3T3-L1 cells. *Nutr Res Pract* 1, 19-28.

- Kim, Y.H., Lim, D.S., Lee, J.H., Shim, W.J., Ro, Y.M., Park, G.H., Becker, K.G., Cho-Chung, Y.S., and Kim, M.K. (2003). Gene expression profiling of oxidative stress on atrial fibrillation in humans. *Exp Mol Med* 35, 336-349.
- Kim, Y.M., and Ziegler, D.M. (2000). Size limits of thiocarbamides accepted as substrates by human flavin-containing monooxygenase 1. *Drug Metab Dispos* 28, 1003-1006.
- Kimura, K., Wakamatsu, A., Suzuki, Y., Ota, T., Nishikawa, T., Yamashita, R., Yamamoto, J., Sekine, M., Tsuritani, K., Wakaguri, H., et al. (2006). Diversification of transcriptional modulation: large-scale identification and characterization of putative alternative promoters of human genes. *Genome Res* 16, 55-65.
- Kimura, T., Kodama, M., and Nagata, C. (1983). Purification of mixed-function amine oxidase from rat liver microsomes. *Biochem Biophys Res Commun* 110, 640-645.
- Knight, J.C., Keating, B.J., Rockett, K.A., and Kwiatkowski, D.P. (2003). In vivo characterization of regulatory polymorphisms by allele-specific quantification of RNA polymerase loading. *Nat Genet* 33, 469-475.
- Koch, M., Vorwerk, S., Masur, C., Sharifi-Sirchi, G., Olivieri, N., and Schlaich, N.L. (2006). A role for a flavin-containing mono-oxygenase in resistance against microbial pathogens in Arabidopsis. *Plant J* 47, 629-639.
- Koster, M.I., Kim, S., Huang, J., Williams, T., and Roop, D.R. (2006). TAp63alpha induces AP-2gamma as an early event in epidermal morphogenesis. *Dev Biol* 289, 253-261.
- Koukouritaki, S.B., Simpson, P., Yeung, C.K., Rettie, A.E., and Hines, R.N. (2002). Human hepatic flavin-containing monooxygenases 1 (FMO1) and 3 (FMO3) developmental expression. *Pediatr Res* 51, 236-243.
- Krause, R.J., Lash, L.H., and Elfarra, A.A. (2003). Human kidney flavin-containing monooxygenases and their potential roles in cysteine s-conjugate metabolism and nephrotoxicity. *J Pharmacol Exp Ther* 304, 185-191.
- Krause, R.J., Ripp, S.L., Sausen, P.J., Overby, L.H., Philpot, R.M., and Elfarra, A.A. (1996). Characterization of the methionine S-oxidase activity of rat liver and kidney microsomes: immunochemical and kinetic evidence for FMO3 being the major catalyst. *Arch Biochem Biophys* 333, 109-116.
- Krueger, S.K., and Williams, D.E. (2005). Mammalian flavin-containing monooxygenases: structure/function, genetic polymorphisms and role in drug metabolism. *Pharmacol Ther* 106, 357-387.
- Kubo, A., Itoh, S., Itoh, K., and Kamataki, T. (1997). Determination of FAD-binding domain in flavin-containing monooxygenase 1 (FMO1). *Arch Biochem Biophys* 345, 271-277.
- Landry, J.R., Mager, D.L., and Wilhelm, B.T. (2003). Complex controls: the role of alternative promoters in mammalian genomes. *Trends Genet* 19, 640-648.
- Lane, M.D., Tang, Q.Q., and Jiang, M.S. (1999). Role of the CCAAT enhancer binding proteins (C/EBP) in adipocyte differentiation. *Biochem Biophys Res Commun* 266, 677-683.
- Lang, D.H., and Rettie, A.E. (2000). In vitro evaluation of potential in vivo probes for human flavin-containing monooxygenase (FMO): metabolism of benzydamine and caffeine by FMO and P450 isoforms. *Br J Clin Pharmacol* 50, 311-314.
- Lang, D.H., Yeung, C.K., Peter, R.M., Ibarra, C., Gasser, R., Itagaki, K., Philpot, R.M., and Rettie, A.E. (1998). Isoform specificity of trimethylamine N-

- oxygenation by human flavin-containing monooxygenase (FMO) and P450 enzymes: selective catalysis by FMO3. *Biochem Pharmacol* 56, 1005-1012.
- Langston, J.W., and Irwin, I. (1986). MPTP: current concepts and controversies. *Clin Neuropharmacol* 9, 485-507.
- Lattard, V., Longin-Sauvageon, C., Lachuer, J., Delatour, P., and Benoit, E. (2002). Cloning, sequencing, and tissue-dependent expression of flavin-containing monooxygenase (FMO) 1 and FMO3 in the dog. *Drug Metab Dispos* 30, 119-128.
- Lawton, M.P., Cashman, J.R., Cresteil, T., Dolphin, C.T., Elfarra, A.A., Hines, R.N., Hodgson, E., Kimura, T., Ozols, J., Phillips, I.R., et al. (1994). A nomenclature for the mammalian flavin-containing monooxygenase gene family based on amino acid sequence identities. *Arch Biochem Biophys* 308, 254-257.
- Lawton, M.P., Gasser, R., Tynes, R.E., Hodgson, E., and Philpot, R.M. (1990). The flavin-containing monooxygenase enzymes expressed in rabbit liver and lung are products of related but distinctly different genes. *J Biol Chem* 265, 5855-5861.
- Levanon, D., and Groner, Y. (2004). Structure and regulated expression of mammalian RUNX genes. *Oncogene* 23, 4211-4219.
- Liang, H., and Ward, W.F. (2006). PGC-1alpha: a key regulator of energy metabolism. *Adv Physiol Educ* 30, 145-151.
- Liu, F., Lei, W., O'Rourke, J.P., and Ness, S.A. (2006). Oncogenic mutations cause dramatic, qualitative changes in the transcriptional activity of c-Myb. *Oncogene* 25, 795-805.
- Longin-Sauvageon, C., Lattard, V., Lilaz-Michel, C., Buronfosse, T., and Benoit, E. (1998). Expression of two different FMOs in sheep liver. *Drug Metab Dispos* 26, 284-287.
- Lovlie, R., Daly, A.K., Matre, G.E., Molven, A., and Steen, V.M. (2001). Polymorphisms in CYP2D6 duplication-negative individuals with the ultrarapid metabolizer phenotype: a role for the CYP2D6\*35 allele in ultrarapid metabolism? *Pharmacogenetics* 11, 45-55.
- Luo, Z., and Hines, R.N. (2001). Regulation of flavin-containing monooxygenase 1 expression by ying yang 1 and hepatic nuclear factors 1 and 4. *Mol Pharmacol* 60, 1421-1430.
- Malaspina, A., Kaushik, N., and de Bellerocche, J. (2001). Differential expression of 14 genes in amyotrophic lateral sclerosis spinal cord detected using gridded cDNA arrays. *J Neurochem* 77, 132-145.
- Mani, C., Hodgson, E., and Kupfer, D. (1993). Metabolism of the antimammary cancer antiestrogenic agent tamoxifen. II. Flavin-containing monooxygenase-mediated N-oxidation. *Drug Metab Dispos* 21, 657-661.
- Marez, D., Sabbagh, N., Legrand, M., Lo-Guidice, J.M., Boone, P., and Broly, F. (1995). A novel CYP2D6 allele with an abolished splice recognition site associated with the poor metabolizer phenotype. *Pharmacogenetics* 5, 305-311.
- McCombie, R.R., Dolphin, C.T., Povey, S., Phillips, I.R., and Shephard, E.A. (1996). Localization of human flavin-containing monooxygenase genes FMO2 and FMO5 to chromosome 1q. *Genomics* 34, 426-429.
- McDanell, R., McLean, A.E., Hanley, A.B., Heaney, R.K., and Fenwick, G.R. (1988). Chemical and biological properties of indole glucosinolates (glucobrassicins): a review. *Food Chem Toxicol* 26, 59-70.

- Messeguer, X., Escudero, R., Farre, D., Nunez, O., Martinez, J., and Alba, M.M. (2002). PROMO: detection of known transcription regulatory elements using species-tailored searches. *Bioinformatics* 18, 333-334.
- Minamitani, K., Takahashi, Y., Minagawa, M., Yasuda, T., and Niimi, H. (1998). Difference in height associated with a translation start site polymorphism in the vitamin D receptor gene. *Pediatr Res* 44, 628-632.
- Muchardt, C., and Yaniv, M. (1999). The mammalian SWI/SNF complex and the control of cell growth. *Semin Cell Dev Biol* 10, 189-195.
- Mulcare, C.A., Weale, M.E., Jones, A.L., Connell, B., Zeitlyn, D., Tarekegn, A., Swallow, D.M., Bradman, N., and Thomas, M.G. (2004). The T allele of a single-nucleotide polymorphism 13.9 kb upstream of the lactase gene (LCT) (C-13.9kbT) does not predict or cause the lactase-persistence phenotype in Africans. *Am J Hum Genet* 74, 1102-1110.
- Murray-Zmijewski, F., Lane, D.P., and Bourdon, J.C. (2006). p53/p63/p73 isoforms: an orchestra of isoforms to harmonise cell differentiation and response to stress. *Cell Death Differ* 13, 962-972.
- Mushiroda, T., Ariyoshi, N., Yokoi, T., Takahara, E., Nagata, O., Kato, H., and Kamataki, T. (2001). Accumulation of the 1-methyl-4-phenylpyridinium ion in suncus (*Suncus murinus*) brain: implication for flavin-containing monooxygenase activity in brain microvessels. *Chem Res Toxicol* 14, 228-232.
- Mushiroda, T., Douya, R., Takahara, E., and Nagata, O. (2000a). The involvement of flavin-containing monooxygenase but not CYP3A4 in metabolism of itopride hydrochloride, a gastroprokinetic agent: comparison with cisapride and mosapride citrate. *Drug Metab Dispos* 28, 1231-1237.
- Mushiroda, T., Yokoi, T., Itoh, K., Nunoya, K., Nakagawa, T., Kubota, M., Takahara, E., Nagata, O., Kato, H., and Kamataki, T. (2000b). The house musk shrew (*Suncus murinus*): a unique animal with extremely low level of expression of mRNAs for CYP3A and flavin-containing monooxygenase. *Comp Biochem Physiol C Toxicol Pharmacol* 126, 225-234.
- Musunuru, K., Strong, A., Frank-Kamenetsky, M., Lee, N.E., Ahfeldt, T., Sachs, K.V., Li, X., Li, H., Kuperwasser, N., Ruda, V.M., et al. (2010). From noncoding variant to phenotype via SORT1 at the 1p13 cholesterol locus. *Nature* 466, 714-719.
- Nagata, T., Williams, D.E., and Ziegler, D.M. (1990). Substrate specificities of rabbit lung and porcine liver flavin-containing monooxygenases: differences due to substrate size. *Chem Res Toxicol* 3, 372-376.
- Nakajima, M., Yokoi, T., Mizutani, M., Kinoshita, M., Funayama, M., and Kamataki, T. (1999). Genetic polymorphism in the 5'-flanking region of human CYP1A2 gene: effect on the CYP1A2 inducibility in humans. *J Biochem* 125, 803-808.
- Narimatsu, S., Yamamoto, S., Kato, R., Masubuchi, Y., and Horie, T. (1999). Contribution of flavin-containing monooxygenase and cytochrome P450 to imipramine N-oxidation in rat hepatic microsomes. *Biol Pharm Bull* 22, 567-571.
- Novikoff, A.B., Novikoff, P.M., Rosen, O.M., and Rubin, C.S. (1980). Organelle relationships in cultured 3T3-L1 preadipocytes. *J Cell Biol* 87, 180-196.
- Ober, C., Aldrich, C.L., Chervoneva, I., Billstrand, C., Rahimov, F., Gray, H.L., and Hyslop, T. (2003). Variation in the HLA-G promoter region influences miscarriage rates. *Am J Hum Genet* 72, 1425-1435.

- Ober, C., Billstrand, C., Kuldane, S., and Tan, Z. (2006). The miscarriage-associated HLA-G -725G allele influences transcription rates in JEG-3 cells. *Hum Reprod* 21, 1743-1748.
- Ohmi, N., Yoshida, H., Endo, H., Hasegawa, M., Akimoto, M., and Higuchi, S. (2003). S-oxidation of S-methyl-esonarimod by flavin-containing monooxygenases in human liver microsomes. *Xenobiotica* 33, 1221-1231.
- Omar, B.A. (2009). Investigations into the physiological roles of the flavin-containing monooxygenases in development and homeostasis. PhD thesis.
- T. Ota, Y. Suzuki, T. Nishikawa, T. Otsuki, T. Sugiyama, R. Irie, A. Wakamatsu, K. Hayashi, H. Sato, K. Nagai, K. Kimura, H. Makita, M. Sekine, M. Obayashi, T. Nishi, T. Shibahara, T. Tanaka, S. Ishii, J. Yamamoto, K. Saito, Y. Kawai, Y. Isono, Y. Nakamura, K. Nagahari, K. Murakami, T. Yasuda, T. Iwayanagi, M. Wagatsuma, A. Shiratori, H. Sudo, T. Hosoiri, Y. Kaku, H. Kodaira, H. Kondo, M. Sugawara, M. Takahashi, K. Kanda, T. Yokoi, T. Furuya, E. Kikkawa, Y. Omura, K. Abe, K. Kamihara, N. Katsuta, K. Sato, M. Tanikawa, M. Yamazaki, K. Ninomiya, T. Ishibashi, H. Yamashita, K. Murakawa, K. Fujimori, H. Tanai, M. Kimata, M. Watanabe, S. Hiraoka, Y. Chiba, S. Ishida, Y. Ono, S. Takiguchi, S. Watanabe, M. Yosida, T. Hotuta, J. Kusano, K. Kanehori, A. Takahashi-Fujii, H. Hara, T. O. Tanase, Y. Nomura, S. Togiya, F. Komai, R. Hara, K. Takeuchi, M. Arita, N. Imose, K. Musashino, H. Yuuki, A. Oshima, N. Sasaki, S. Aotsuka, Y. Yoshikawa, H. Matsunawa, T. Ichihara, N. Shiohata, S. Sano, S. Moriya, H. Momiyama, N. Satoh, S. Takami, Y. Terashima, O. Suzuki, S. Nakagawa, A. Senoh, H. Mizoguchi, Y. Goto, F. Shimizu, H. Wakebe, H. Hishigaki, T. Watanabe, A. Sugiyama, M. Takemoto, B. Kawakami, K. Watanabe, A. Kumagai, S. Itakura, Y. Fukuzumi, Y. Fujimori, M. Komiyama, H. Tashiro, A. Tanigami, T. Fujiwara, T. Ono, K. Yamada, Y. Fujii, K. Ozaki, M. Hirao, Y. Ohmori, A. Kawabata, T. Hikiji, N. Kobatake, H. Inagaki, Y. Ikema, S. Okamoto, R. Okitani, T. Kawakami, S. Noguchi, T. Itoh, K. Shigeta, T. Senba, K. Matsumura, Y. Nakajima, T. Mizuno, M. Morinaga, M. Sasaki, T. Togashi, M. Oyama, H. Hata, T. Komatsu, J. Mizushima-Sugano, T. Satoh, Y. Shirai, Y. Takahashi, K. Nakagawa, K. Okumura, T. Nagase, N. Nomura, H. Kikuchi, Y. Masuho, R. Yamashita, K. Nakai, T. Yada, O. Ohara, T. Isogai and S. Sugano. Complete sequencing and characterization of 21,243 full-length human cDNAs. *Nat Genet* 36, 40-45.
- Overby, L.H., Buckpitt, A.R., Lawton, M.P., Atta-Asafo-Adjei, E., Schulze, J., and Philpot, R.M. (1995). Characterization of flavin-containing monooxygenase 5 (FMO5) cloned from human and guinea pig: evidence that the unique catalytic properties of FMO5 are not confined to the rabbit ortholog. *Arch Biochem Biophys* 317, 275-284.
- Pajares, M.J., Ezponda, T., Catena, R., Calvo, A., Pio, R., and Montuenga, L.M. (2007). Alternative splicing: an emerging topic in molecular and clinical oncology. *Lancet Oncol* 8, 349-357.
- Park, C.S., Baek, H.M., Chung, W.G., Lee, K.H., Ryu, S.D., and Cha, Y.N. (1999). Suppression of flavin-containing monooxygenase by overproduced nitric oxide in rat liver. *Mol Pharmacol* 56, 507-514.
- Park, S.B., Jacob, P., 3rd, Benowitz, N.L., and Cashman, J.R. (1993). Stereoselective metabolism of (S)-(-)-nicotine in humans: formation of trans-(S)-(-)-nicotine N-1'-oxide. *Chem Res Toxicol* 6, 880-888.
- Parte, P., and Kupfer, D. (2005). Oxidation of tamoxifen by human flavin-containing monooxygenase (FMO) 1 and FMO3 to tamoxifen-N-oxide and its novel

- reduction back to tamoxifen by human cytochromes P450 and hemoglobin. *Drug Metab Dispos* 33, 1446-1452.
- Pastinen, T., and Hudson, T.J. (2004). Cis-acting regulatory variation in the human genome. *Science* 306, 647-650.
- Pelkonen, O., Rautio, A., Raunio, H., and Pasanen, M. (2000). CYP2A6: a human coumarin 7-hydroxylase. *Toxicology* 144, 139-147.
- Pettit, F.H., Orme-Johnson, W., and Ziegler, D.M. (1964). The requirement for flavin adenine dinucleotide by a liver microsomal oxygenase catalyzing the oxidation of alkylaryl amines. *Biochem Biophys Res Commun* 16, 444-448.
- Phillips, I.R., Dolphin, C.T., Clair, P., Hadley, M.R., Hutt, A.J., McCombie, R.R., Smith, R.L., and Shephard, E.A. (1995). The molecular biology of the flavin-containing monooxygenases of man. *Chem Biol Interact* 96, 17-32.
- Phillips, I.R., and Shephard, E.A. (2008). Flavin-containing monooxygenases: mutations, disease and drug response. *Trends Pharmacol Sci* 29, 294-301.
- Phillips, J.E., and Corces, V.G. (2009). CTCF: master weaver of the genome. *Cell* 137, 1194-1211.
- Pitarque, M., von Richter, O., Oke, B., Berkkan, H., Oscarson, M., and Ingelman-Sundberg, M. (2001). Identification of a single nucleotide polymorphism in the TATA box of the CYP2A6 gene: impairment of its promoter activity. *Biochem Biophys Res Commun* 284, 455-460.
- Pitarque, M., von Richter, O., Rodriguez-Antona, C., Wang, J., Oscarson, M., and Ingelman-Sundberg, M. (2004). A nicotine C-oxidase gene (CYP2A6) polymorphism important for promoter activity. *Hum Mutat* 23, 258-266.
- Poulsen, L.L., Hyslop, R.M., and Ziegler, D.M. (1979). S-Oxygenation of N-substituted thioureas catalyzed by the pig liver microsomal FAD-containing monooxygenase. *Arch Biochem Biophys* 198, 78-88.
- Poulsen, L.L., Taylor, K., Williams, D.E., Masters, B.S., and Ziegler, D.M. (1986). Substrate specificity of the rabbit lung flavin-containing monooxygenase for amines: oxidation products of primary alkylamines. *Mol Pharmacol* 30, 680-685.
- Poulter, M., Hollox, E., Harvey, C.B., Mulcare, C., Peuhkuri, K., Kajander, K., Sarner, M., Korpela, R., and Swallow, D.M. (2003). The causal element for the lactase persistence/non-persistence polymorphism is located in a 1 Mb region of linkage disequilibrium in Europeans. *Ann Hum Genet* 67, 298-311.
- Pozner, A., Goldenberg, D., Negreanu, V., Le, S.Y., Elroy-Stein, O., Levanon, D., and Groner, Y. (2000). Transcription-coupled translation control of AML1/RUNX1 is mediated by cap- and internal ribosome entry site-dependent mechanisms. *Mol Cell Biol* 20, 2297-2307.
- Puigserver, P. (2005). Tissue-specific regulation of metabolic pathways through the transcriptional coactivator PGC1- $\alpha$ . *Int J Obes (Lond)* 29 Suppl 1, S5-9.
- Qian, L., and Ortiz de Montellano, P.R. (2006). Oxidative activation of thiacetazone by the Mycobacterium tuberculosis flavin monooxygenase EtaA and human FMO1 and FMO3. *Chem Res Toxicol* 19, 443-449.
- Rahib, L., MacLennan, N.K., Horvath, S., Liao, J.C., and Dipple, K.M. (2007). Glycerol kinase deficiency alters expression of genes involved in lipid metabolism, carbohydrate metabolism, and insulin signaling. *Eur J Hum Genet* 15, 646-657.
- Regina, M., Korhonen, V.P., Smith, T.K., Alakuijala, L., and Eloranta, T.O. (1993). Methionine toxicity in the rat in relation to hepatic accumulation of S-

- adenosylmethionine: prevention by dietary stimulation of the hepatic transsulfuration pathway. *Arch Biochem Biophys* 300, 598-607.
- Rhead, B., Karolchik, D., Kuhn, R.M., Hinrichs, A.S., Zweig, A.S., Fujita, P.A., Diekhans, M., Smith, K.E., Rosenbloom, K.R., Raney, B.J., et al. (2010). The UCSC Genome Browser database: update 2010. *Nucleic Acids Res* 38, D613-619.
- Ring, B.J., Wrighton, S.A., Aldridge, S.L., Hansen, K., Haehner, B., and Shipley, L.A. (1999). Flavin-containing monooxygenase-mediated N-oxidation of the M(1)-muscarinic agonist xanomeline. *Drug Metab Dispos* 27, 1099-1103.
- Roberts, J., Scott, A.C., Howard, M.R., Breen, G., Bubb, V.J., Klenova, E., and Quinn, J.P. (2007). Differential regulation of the serotonin transporter gene by lithium is mediated by transcription factors, CCCTC binding protein and Y-box binding protein 1, through the polymorphic intron 2 variable number tandem repeat. *J Neurosci* 27, 2793-2801.
- Rodriguez, R.J., and Miranda, C.L. (2000). Isoform specificity of N-deacetyl ketoconazole by human and rabbit flavin-containing monooxygenases. *Drug Metab Dispos* 28, 1083-1086.
- Rolland, V., Dugail, I., Le Liepvre, X., and Lavau, M. (1995). Evidence of increased glyceraldehyde-3-phosphate dehydrogenase and fatty acid synthetase promoter activities in transiently transfected adipocytes from genetically obese rats. *J Biol Chem* 270, 1102-1106.
- Rolland, V., Liepvre, X.L., Jump, D.B., Lavau, M., and Dugail, I. (1996). A GC-rich region containing Sp1 and Sp1-like binding sites is a crucial regulatory motif for fatty acid synthase gene promoter activity in adipocytes. Implication In the overactivity of FAS promoter in obese Zucker rats. *J Biol Chem* 271, 21297-21302.
- Ryerson, C.C., Ballou, D.P., and Walsh, C. (1982). Mechanistic studies on cyclohexanone oxygenase. *Biochemistry* 21, 2644-2655.
- Sabourin, P.J., Smyser, B.P., and Hodgson, E. (1984). Purification of the flavin-containing monooxygenase from mouse and pig liver microsomes. *Int J Biochem* 16, 713-720.
- Sachse, C., Brockmoller, J., Bauer, S., and Roots, I. (1999). Functional significance of a C-->A polymorphism in intron 1 of the cytochrome P450 CYP1A2 gene tested with caffeine. *Br J Clin Pharmacol* 47, 445-449.
- Sasaki, H., Ishihara, K., and Kato, R. (2000). Mechanisms of Igf2/H19 imprinting: DNA methylation, chromatin and long-distance gene regulation. *J Biochem* 127, 711-715.
- Schenkman, J.B., Arinc, E., Schenkman, J.B., and E, H. (1999). The fate of xenobiotics in the body. *Molecular and applied aspects of oxidative drug metabolising enzymes*, pp1-20.
- Scott, R.E., Florine, D.L., Wille, J.J., Jr., and Yun, K. (1982). Coupling of growth arrest and differentiation at a distinct state in the G1 phase of the cell cycle: GD. *Proc Natl Acad Sci U S A* 79, 845-849.
- Sheets, M.D., Ogg, S.C., and Wickens, M.P. (1990). Point mutations in AAUAAA and the poly (A) addition site: effects on the accuracy and efficiency of cleavage and polyadenylation in vitro. *Nucleic Acids Res* 18, 5799-5805.
- Shendure, J., and Ji, H. (2008). Next-generation DNA sequencing. *Nat Biotechnol* 26, 1135-1145.
- Shephard, E.A., Chandan, P., Stevanovic-Walker, M., Edwards, M., and Phillips, I.R. (2007). Alternative promoters and repetitive DNA elements define the

- species-dependent tissue-specific expression of the FMO1 genes of human and mouse. *Biochem J* 406, 491-499.
- Shephard, E.A., Dolphin, C.T., Fox, M.F., Povey, S., Smith, R., and Phillips, I.R. (1993). Localization of genes encoding three distinct flavin-containing monooxygenases to human chromosome 1q. *Genomics* 16, 85-89.
- Shephard, E.A., and Phillips, I.R. (2010). The potential of knockout mouse lines in defining the role of flavin-containing monooxygenases in drug metabolism. *Expert Opin Drug Metab Toxicol* 6, 1083-1094.
- Shimada, T., Yamazaki, H., Mimura, M., Inui, Y., and Guengerich, F.P. (1994). Interindividual variations in human liver cytochrome P-450 enzymes involved in the oxidation of drugs, carcinogens and toxic chemicals: studies with liver microsomes of 30 Japanese and 30 Caucasians. *J Pharmacol Exp Ther* 270, 414-423.
- Singer-Sam, J., LeBon, J.M., Dai, A., and Riggs, A.D. (1992). A sensitive, quantitative assay for measurement of allele-specific transcripts differing by a single nucleotide. *PCR Methods Appl* 1, 160-163.
- Singh, P., Han, L., Rivas, G.E., Lee, D.H., Nicholson, T.B., Larson, G.P., Chen, T., and Szabo, P.E. (2010). Allele-specific H3K79 Di- versus trimethylation distinguishes opposite parental alleles at imprinted regions. *Mol Cell Biol* 30, 2693-2707.
- Siva, N. (2008). 1000 Genomes project. *Nat Biotechnol* 26, 256.
- Song, L., and Crawford, G.E. (2010). DNase-seq: a high-resolution technique for mapping active gene regulatory elements across the genome from mammalian cells. *Cold Spring Harb Protoc* 2010, pdb prot5384.
- Steinthorsdottir, V., Stefansson, H., Ghosh, S., Birgisdottir, B., Bjornsdottir, S., Fasquel, A.C., Olafsson, O., Stefansson, K., and Gulcher, J.R. (2004). Multiple novel transcription initiation sites for NRG1. *Gene* 342, 97-105.
- Stephens, M., and Donnelly, P. (2003). A comparison of bayesian methods for haplotype reconstruction from population genotype data. *Am J Hum Genet* 73, 1162-1169.
- Stephens, M., Smith, N.J., and Donnelly, P. (2001). A new statistical method for haplotype reconstruction from population data. *Am J Hum Genet* 68, 978-989.
- Stevens, J.C., Melton, R.J., Zaya, M.J., and Engel, L.C. (2003). Expression and characterization of functional dog flavin-containing monooxygenase 1. *Mol Pharmacol* 63, 271-275.
- Stormer, E., Roots, I., and Brockmoller, J. (2000). Benzydamine N-oxidation as an index reaction reflecting FMO activity in human liver microsomes and impact of FMO3 polymorphisms on enzyme activity. *Br J Clin Pharmacol* 50, 553-561.
- Student, A.K., Hsu, R.Y., and Lane, M.D. (1980). Induction of fatty acid synthetase synthesis in differentiating 3T3-L1 preadipocytes. *J Biol Chem* 255, 4745-4750.
- Su, A.I., Cooke, M.P., Ching, K.A., Hakak, Y., Walker, J.R., Wiltshire, T., Orth, A.P., Vega, R.G., Sapinoso, L.M., Moqrich, A., et al. (2002). Large-scale analysis of the human and mouse transcriptomes. *Proc Natl Acad Sci U S A* 99, 4465-4470.
- Suh, J.K., Poulsen, L.L., Ziegler, D.M., and Robertus, J.D. (1999). Yeast flavin-containing monooxygenase generates oxidizing equivalents that control protein folding in the endoplasmic reticulum. *Proc Natl Acad Sci U S A* 96, 2687-2691.



- Suh, J.K., and Robertus, J.D. (2000). Yeast flavin-containing monooxygenase is induced by the unfolded protein response. *Proc Natl Acad Sci U S A* 97, 121-126.
- Sullivan, E.K., Weirich, C.S., Guyon, J.R., Sif, S., and Kingston, R.E. (2001). Transcriptional activation domains of human heat shock factor 1 recruit human SWI/SNF. *Mol Cell Biol* 21, 5826-5837.
- Sun, H., Palaniswamy, S.K., Pohar, T.T., Jin, V.X., Huang, T.H., and Davuluri, R.V. (2006). MPromDb: an integrated resource for annotation and visualization of mammalian gene promoters and ChIP-chip experimental data. *Nucleic Acids Res* 34, D98-103.
- Szoko, E., Tabi, T., Borbas, T., Dalmadi, B., Tihanyi, K., and Magyar, K. (2004). Assessment of the N-oxidation of deprenyl, methamphetamine, and amphetamine enantiomers by chiral capillary electrophoresis: an in vitro metabolism study. *Electrophoresis* 25, 2866-2875.
- Takeda, J., Suzuki, Y., Nakao, M., Kuroda, T., Sugano, S., Gojobori, T., and Imanishi, T. (2007). H-DBAS: alternative splicing database of completely sequenced and manually annotated full-length cDNAs based on H-Invitational. *Nucleic Acids Res* 35, D104-109.
- Tan, J.S., Mohandas, N., and Conboy, J.G. (2006). High frequency of alternative first exons in erythroid genes suggests a critical role in regulating gene function. *Blood* 107, 2557-2561.
- Tan, W., Wang, Y., Gold, B., Chen, J., Dean, M., Harrison, P.J., Weinberger, D.R., and Law, A.J. (2007). Molecular cloning of a brain-specific, developmentally regulated neuregulin 1 (NRG1) isoform and identification of a functional promoter variant associated with schizophrenia. *J Biol Chem* 282, 24343-24351.
- Taulan, M., Lopez, E., Guittard, C., Rene, C., Baux, D., Altieri, J.P., DesGeorges, M., Claustres, M., and Romey, M.C. (2007). First functional polymorphism in CFTR promoter that results in decreased transcriptional activity and Sp1/USF binding. *Biochem Biophys Res Commun* 361, 775-781.
- Taylor, K.L., and Ziegler, D.M. (1987). Studies on substrate specificity of the hog liver flavin-containing monooxygenase. Anionic organic sulfur compounds. *Biochem Pharmacol* 36, 141-146.
- Tipton, K.F., and Singer, T.P. (1993). Advances in our understanding of the mechanisms of the neurotoxicity of MPTP and related compounds. *J Neurochem* 61, 1191-1206.
- Todaro, G.J., and Green, H. (1963). Quantitative studies of the growth of mouse embryo cells in culture and their development into established lines. *J Cell Biol* 17, 299-313.
- Tseng, Y.H., Butte, A.J., Kokkotou, E., Yechoor, V.K., Taniguchi, C.M., Kriauciunas, K.M., Cypess, A.M., Niinobe, M., Yoshikawa, K., Patti, M.E., et al. (2005). Prediction of preadipocyte differentiation by gene expression reveals role of insulin receptor substrates and necdin. *Nat Cell Biol* 7, 601-611.
- Tugnait, M., Hawes, E.M., McKay, G., Rettie, A.E., Haining, R.L., and Midha, K.K. (1997). N-oxygenation of clozapine by flavin-containing monooxygenase. *Drug Metab Dispos* 25, 524-527.
- Tynes, R.E., and Hodgson, E. (1983). Oxidation of thiobenzamide by the FAD-containing and cytochrome P-450-dependent monooxygenases of liver and lung microsomes. *Biochem Pharmacol* 32, 3419-3428.

- Tynes, R.E., Sabourin, P.J., and Hodgson, E. (1985). Identification of distinct hepatic and pulmonary forms of microsomal flavin-containing monooxygenase in the mouse and rabbit. *Biochem Biophys Res Commun* 126, 1069-1075.
- Uldry, M., Yang, W., St-Pierre, J., Lin, J., Seale, P., and Spiegelman, B.M. (2006). Complementary action of the PGC-1 coactivators in mitochondrial biogenesis and brown fat differentiation. *Cell Metab* 3, 333-341.
- Vandesompele, J., De Preter, K., Pattyn, F., Poppe, B., Van Roy, N., De Paepe, A., and Speleman, F. (2002). Accurate normalization of real-time quantitative RT-PCR data by geometric averaging of multiple internal control genes. *Genome Biol* 3, RESEARCH0034.
- Veeramah, K.R., Thomas, M.G., Weale, M.E., Zeitlyn, D., Tarekegn, A., Bekele, E., Mendell, N.R., Shephard, E.A., Bradman, N., and Phillips, I.R. (2008). The potentially deleterious functional variant flavin-containing monooxygenase 2\*1 is at high frequency throughout sub-Saharan Africa. *Pharmacogenet Genomics* 18, 877-886.
- Veeravalli, S., Omar, B., Housman, L., Hancock, M., S, G.M., A, J., I.R, P., and E.A, S. (2010). A novel role for a flavin-containing monooxygenase in energy homeostasis.
- Veeravalli, S., Omar, B., Housman, L., Hancock, M., S, G.M., A, J., I.R, P., and E.A, S. (Unpublished). A novel role for a flavin-containing monooxygenase in energy homeostasis.
- Venkatesh, K., Levi, P.E., and Hodgson, E. (1991). The effect of detergents on the purified flavin-containing monooxygenase of mouse liver, kidney and lungs. *Gen Pharmacol* 22, 549-552.
- von Richter, O., Pitarque, M., Rodriguez-Antona, C., Testa, A., Mantovani, R., Oscarson, M., and Ingelman-Sundberg, M. (2004). Polymorphic NF-Y dependent regulation of human nicotine C-oxidase (CYP2A6). *Pharmacogenetics* 14, 369-379.
- Washio, T., Kohsaka, K., Arisawa, H., Masunaga, H., Nagatsuka, S., and Satoh, Y. (2003). Pharmacokinetics and metabolism of radiolabelled SNI-2011, a novel muscarinic receptor agonist, in healthy volunteers. *Comprehensive understanding of absorption, metabolism and excretion using radiolabelled SNI-2011. Arzneimittelforschung* 53, 80-86.
- Weissman, J., Trevor, A., Chiba, K., Peterson, L.A., Caldera, P., Castagnoli, N., Jr., and Baillie, T. (1985). Metabolism of the nigrostriatal toxin 1-methyl-4-phenyl-1,2,3,6-tetrahydropyridine by liver homogenate fractions. *J Med Chem* 28, 997-1001.
- Wierenga, W. (1985). Antiviral and other bioactivities of pyrimidinones. *Pharmacol Ther* 30, 67-89.
- Williams, D.E., Meyer, H.H., and Dutchuk, M.S. (1989). Distinct pulmonary and hepatic forms of flavin-containing monooxygenase in sheep. *Comp Biochem Physiol B* 93, 465-470.
- Williams, D.E., Ziegler, D.M., Nordin, D.J., Hale, S.E., and Masters, B.S. (1984). Rabbit lung flavin-containing monooxygenase is immunochemically and catalytically distinct from the liver enzyme. *Biochem Biophys Res Commun* 125, 116-122.
- Willing, M.C., Deschenes, S.P., Slayton, R.L., and Roberts, E.J. (1996). Premature chain termination is a unifying mechanism for COL1A1 null alleles in osteogenesis imperfecta type I cell strains. *Am J Hum Genet* 59, 799-809.

- Wilson, D.O., Johnson, P., and McCord, B.R. (2001). Nonradiochemical DNase I footprinting by capillary electrophoresis. *Electrophoresis* 22, 1979-1986.
- Wu, Y., Delerive, P., Chin, W.W., and Burris, T.P. (2002). Requirement of helix 1 and the AF-2 domain of the thyroid hormone receptor for coactivation by PGC-1. *J Biol Chem* 277, 8898-8905.
- Yamada, H., Yuno, K., Oguri, K., and Yoshimura, H. (1990). Multiplicity of liver microsomal flavin-containing monooxygenase in the guinea pig: its purification and characterization. *Arch Biochem Biophys* 280, 305-312.
- Yeung, C.K., Lang, D.H., Thummel, K.E., and Rettie, A.E. (2000). Immunoquantitation of FMO1 in human liver, kidney, and intestine. *Drug Metab Dispos* 28, 1107-1111.
- Yu, Z., Lin, K.K., Bhandari, A., Spencer, J.A., Xu, X., Wang, N., Lu, Z., Gill, G.N., Roop, D.R., Wertz, P., et al. (2006). The Grainyhead-like epithelial transactivator Get-1/Grhl3 regulates epidermal terminal differentiation and interacts functionally with LMO4. *Dev Biol* 299, 122-136.
- Zaitlen, N.A., Kang, H.M., Feolo, M.L., Sherry, S.T., Halperin, E., and Eskin, E. (2005). Inference and analysis of haplotypes from combined genotyping studies deposited in dbSNP. *Genome Res* 15, 1594-1600.
- Zanger, U.M., Fischer, J., Raimundo, S., Stuvén, T., Evert, B.O., Schwab, M., and Eichelbaum, M. (2001). Comprehensive analysis of the genetic factors determining expression and function of hepatic CYP2D6. *Pharmacogenetics* 11, 573-585.
- Zeldis, J.B., Friedman, L.S., and Isselbacher, K.J. (1983). Ranitidine: a new H<sub>2</sub>-receptor antagonist. *N Engl J Med* 309, 1368-1373.
- Zhang, J., and Cashman, J.R. (2006). Quantitative analysis of FMO gene mRNA levels in human tissues. *Drug Metab Dispos* 34, 19-26.
- Zhao, Y., Christensen, S.K., Fankhauser, C., Cashman, J.R., Cohen, J.D., Weigel, D., and Chory, J. (2001). A role for flavin monooxygenase-like enzymes in auxin biosynthesis. *Science* 291, 306-309.
- Zianni, M., Tessanne, K., Merighi, M., Laguna, R., and Tabita, F.R. (2006). Identification of the DNA bases of a DNase I footprint by the use of dye primer sequencing on an automated capillary DNA analysis instrument. *J Biomol Tech* 17, 103-113.
- Ziegler, D.M. (1990). Flavin-containing monooxygenases: enzymes adapted for multisubstrate specificity. *Trends Pharmacol Sci* 11, 321-324.
- Ziegler, D.M. (1993). Recent studies on the structure and function of multisubstrate flavin-containing monooxygenases. *Annu Rev Pharmacol Toxicol* 33, 179-199.
- Ziegler, D.M., and Mitchell, C.H. (1972). Microsomal oxidase. IV. Properties of a mixed-function amine oxidase isolated from pig liver microsomes. *Arch Biochem Biophys* 150, 116-125.
- Ziegler, D.M., Poulsen, L.L., and McKee, E.M. (1971). Interaction of primary amines with a mixed-function amine oxidase isolated from pig liver microsomes. *Xenobiotica* 1, 523-531.
- Zysow, B.R., Lindahl, G.E., Wade, D.P., Knight, B.L., and Lawn, R.M. (1995). C/T polymorphism in the 5' untranslated region of the apolipoprotein(a) gene introduces an upstream ATG and reduces in vitro translation. *Arterioscler Thromb Vasc Biol* 15, 58-64.

